ENG 307-(EQC 1995/222)

Seismic load tests on reinforced concrete beam-column joints with plain round reinforcing bars designed to pre-1970s codes

Aizhen Liu and R Park, Dept of Civil Engineering, University of Canterbury

SEISMIC LOAD TESTS ON REINFORCED CONCRETE BEAM-COLUMN JOINTS WITH PLAIN ROUND REINFORCING BARS DESIGNED TO PRE-1970S CODES

by
Aizhen Liu and R. Park

Department of Civil Engineering
University of Canterbury
Christchurch, New Zealand

EQC PROJECT No. 95/222 "Seismic Assessment and Retrofit of Existing Reinforced Concrete Building Structures"

ABSTRACT

Six as-built full-scale beam-column joints and one retrofitted exterior beam-column joint were tested under simulated seismic loading in this study. Simulated seismic load tests on as-built Units were conducted as part of an investigation of the behaviour of existing reinforced concrete structures designed to pre-1970s codes when subjected to severe earthquake forces. Simulated seismic load test on retrofitted as-built exterior beam-column joint Unit was conducted to investigate the improvement of the overall seismic performance which can be achieved by jacketing existing damaged reinforced concrete exterior beam-column joint unit using fibre-glass jacketing technique. All six as-built tests units were full-scale in size, contained plain round reinforcing bars and were replicas of parts of the moment resisting frame of an existing building in Christchurch that was constructed in the 1950s. Two of the test units were identical as-built interior beam-column joint subassemblages, and the other four were exterior beam-column joint subassemblages. The four exterior beam-column joint subassemblages were fabricated into two groups of two identical Units each. The as-built exterior beam-column joint with the beam bar hooks bent away from the joint core was retrofitted by wrapping the column parts above and below the joint core using fibre-glass jacketing after tested.

(1). For the two as-built interior beam-column joint units, the diameter of the longitudinal bars passing through the joint core was relatively larger than the code required values, the joints had no joint shear reinforcement at all, and the beams and columns had low quantities of transverse reinforcement as was typical of pre-1970s construction in New Zealand. One unit was tested with zero axial column load, and the other unit with a constant axial column load of $0.12A_g f_c^{'}$ to study the seismic behaviour of existing reinforced concrete building frames and the effect of compressive column axial load on the general seismic performance, where $f_c^{'}$= concrete cylinder compressive strength and A_g = the gross column section area.

Both units when tested displayed low available structural stiffness, low available ductility, and significant degradation of stiffness and strength during testing. The low structural stiffness could be attributed to the slip of the plain round longitudinal bars through the joint. Column bar buckling was found to initiate failure, especially when

the compressive axial load was present in the column. The utilisation of plain round bars although leading to bond slip was found to improve the joint shear strength, and to suppress the joint shear distortion, shifting the problem area from the joint shear to structural stiffness.

(2). For the four exterior beam-column joint units, the joint cores contained only limited shear reinforcement and the columns and beams had only small amount of transverse reinforcement. One of the two identical test Units in each group was tested under simulated seismic loading with zero axial column load while the other unit was tested under simulated seismic loading with a constant axial column load of about $0.25A_g f_c^{'}$ present.

(a). The as-built exterior beam-column joint Units when tested with zero axial column load demonstrated very poor force strength and stiffness behaviour, and the final failures of the as-built units were dominated by concrete tension cracking along the outer layer of column main bars adjacent to the joint core, which was initiated by the interaction between the column bar buckling and the straightening action of the beam bar hooks, irrespective of the beam bar hook details, should plain round longitudinal reinforcing bars be used. The configuration of the beam bar hooks bent into the joint core was found to result in better seismic response compared to that with the beam bar hooks bent away from the joint core in the case of zero axial column load and small amount of column transverse reinforcement provided.

(b). The as-built exterior beam-column joint Units when tested with constant compressive axial column load of about $0.25A_g f_c^{'}$ present demonstrated that the presence of compressive axial column load enhanced the force transfer by bond from the beam tension steel to the surrounding concrete, reduced the beam steel tension force needed to be transferred at the bend, improved the bond condition along the column bars, consequently totally preventing the concrete tension cracking which was associated with the interaction between the column bar buckling and the straightening action of the beam bar hooks. Consequently, the stiffness, force strength and joint shear behaviour was greatly improved, and the system energy dissipating capacity was improved due to the presence of compressive axial column load. In this case the effects of different beam bar hook details on the seismic performance of the as-built exterior beam-column joint units became very insignificant and the failure trigger

became the big beam fixed-end rotation. When compared to the test evidence observed with deformed longitudinal reinforcement, the use of plain round longitudinal reinforcement, although preventing the joint shear failure, enhanced column bar buckling and the straightening action of the beam bars in tension, thus facilitated the failure of concrete tension cracking along the outer layer of the column bars adjacent to the joint core, consequently causing significant reductions in the available shear force strength and stiffness, especially in the available stiffness. Also the adverse effects on the strength and stiffness response of the used steel type was more severe for as-built exterior beam-column joints compared to tas-built interior beam-column joints.

(3). Test on the retrofitted as-built exterior beam-column joint unit showed that fibre-glass jacketing in the column areas adjacent to the joint core, when the plain round beam bar hooks are bent away from the joint core and the axial column load is low, was very effective in improving the overall seismic performance of the system. Fibre-glass jacketing in the column areas adjacent to the joint core actuated the postulated alternative joint shear model, greatly improved the structural force strength and stiffness performance. In this case, the low flexural strength attainment resulting from bond degradation along the member longitudinal bars became of concern.

As a whole, the collapse mechanism of similar existing reinforced concrete building structures was demonstrated to be a combination of flexural failure in the beams and columns, rather than any shear failure.

ACKNOWLEDGMENTS

The financial support of the Earthquake Commission of New Zealand (Project 95/222) is gratefully acknowledged. Thanks are also due to the University of Canterbury for support, particularly to technicians Norrie Hickey and Hill, Geoff for assistance with the construction and testing of the beam-column Units.

CONTENTS

NOTATION

f_c' = concrete compressive cylinder strength (MPa)

f_y = yield strength of longitudinal reinforcement (MPa)

f_{yt} = yield strength of transverse reinforcement (MPa)

N^* = compressive axial column load (N)

A_g = gross area of column section (mm^2)

b = width of beam (mm)

d = distance from extreme compression fiber of beam to centroid of beam tension reinforcement (mm)

p = ratio of area of the top beam longitudinal bars to bd of beam

p' = ratio of area of the bottom beam longitudinal bars to bd of beam

p_t = ratio of area of the total column longitudinal bars to column gross area

ε_y = steel yield strain

d_b = diameter of longitudinal steel (mm)

s = spacing of transverse reinforcement

ϕ = the strength reduction factor, being unity here

h_b = beam depth (mm)

h_c = column depth (mm)

ϕ_u = ultimate curvature (mm^{-1})

ϕ_y = yield curvature (mm^{-1})

v_{jh} = the nominal horizontal joint shear stress (MPa)

V_{jh} = the imposed horizontal joint shear force (N)

A_j = effective joint area (mm^2)

δ_{cr} = the rigid horizontal movement due to the deformation within the test rig (mm)

V_c = the equivalent storey shear (N)

P_r = the vertical shear applied to the right beam end (N)

P_l = the vertical shear applied to the left beam end (N)

l_1 = the loading span of the left beam of 1755 mm

l_2 = the loading span of the right beam of 1755 mm

γ_j = the joint shear distortion

l_j = the initial length of the diagonal in the joint core (mm)

δ_j = the change in the length of one diagonal in the joint core (mm)

$\delta_{j'}$ = the change in the length of the other diagonal in the joint core (mm)

α_j = the angle of the diagonal to the horizontal axis

K_e = the measured initial stiffness (N/mm)

$\Delta_{y,\,test}$ = the measured first yield displacement (mm)

μ_Δ = the imposed displacement ductility factor, defined as the imposed displacement

divided by the first yield displacement

Δ_{co} = the equivalent storey deflection (mm)

Δ_{bl} = the imposed vertical displacement at the left beam end (mm)

Δ_{br} = the imposed vertical displacement at the right beam end (mm)

l_c = storey height of 3200 mm

l_b = beam span of 3810 mm

V_i = theoretical strength of the unit in terms of storey shear, based on the flexural strength of the members

V_b = theoretical strength of beam in terms of beam shear, based on the flexural strength of the beam

Δ_c = estimated storey displacement (mm)

$\Delta_{c,b}$ = contribution of beam deformation to the storey displacement (mm), referred as Beam Displacement Component (mm)

$\Delta_{c,c}$ = contribution of column deformation to the storey displacement, referred as Column Displacement Component (mm)

$\Delta_{c,j}$ = contribution of joint deformation to the storey displacement, referred as Joint Displacement Component (mm)

$\theta_{b,i}$ = rotation angle over the beam region S_i

$\theta_{c,j}$ = rotation angle over the column region R_j

${}_t\delta_i$ = measurement of the top beam curvature potentiometer over the region S_i

${}_b\delta_i$ = measurement of the bottom beam curvature potentiometer over the region S_i

${}_r\delta_j$ = measurement of the right column curvature potentiometer over the region R_j

${}_l\delta_j$ = measurement of the left column curvature potentiometer over the region R_j

${}_t\delta_1$ = the top displacement measured by beam curvature linear potentiometer at the fixed-end interface

${}_b\delta_1$ = the bottom displacement measured by beam curvature linear potentiometer at the fixed-end interface

${}_R\delta_1$ = measurement of the right column curvature linear potentiometer at the fixed-end interface

${}_L\delta_1$ = measurement of the left column curvature linear potentiometer at the fixed-end interface

${}_E\delta_{bf}$ = the flexural deformation of east beam

${}_W\delta_{bf}$ = the flexural deformation of west beam

${}_U\delta_{cf}$ = the flexural deformation of upper column

${}_B\delta_{cf}$ = the flexural deformation of bottom column

${}_b\delta_{fe}$ = the deformation due to beam fixed-end rotation

${}_c\delta_{fe}$ = the deformation due to column fixed-end rotation

$\phi_{b,i}$ = measured average curvature over the region S_i

$\phi_{c,j}$ = the measured average curvature over the region R_j

h_i = vertical distance between the top and bottom beam curvature linear potentiometers over the region S_i

s_i = longitudinal length of the region S_i

r_j = longitudinal length of the column region R_j

d_j = the horizontal distance between the right and the left column curvature potentiometers over the region R_j

l_1 = the distance from column face to the centre of west beam end pin (==1755 mm)

l_2 = the distance from column face to the centre of east beam end pin (==1755 mm)

$l_b' = l_1 = l_2$ = the distance from the column face to the centre of the beam end pin.

l' = the distance from the beam face to the pin center of the upper column

$l_c' = l'$ = the distance from the beam face to the column end pin center

x_i = the distance from column face to the centre of the region i

y_j = the distance from the beam face to the center of the region j

γ_j = the joint shear distortion

h_b = the beam depth

h_c = the column depth

$\theta_{b,fe}$ = the beam fixed-end rotation

$\theta_{c,fe}$ = the column fixed-end rotation

h_1 = the vertical distance between the two fixed-end beam curvature linear potentiometers

$\Delta_{b,fe}$ = the equivalent storey displacement due to fixed-end rotation of the beam

$\Delta_{c,fe}$ = the component of storey displacement due to column fixed-end rotations

d_1 = the horizontal distance between the two linear potentiometers over the column fixed-end zones

CHAPTER 1

INTRODUCTION

1.1 THE NEED FOR SEISMIC ASSESSMENT AND RETROFIT OF EXISTING REINFORCED CONCRETE STRUCTURES

Seismic design procedures for concrete structures have advanced significantly since about the 1970s around the world, such as in New Zealand and the United States, and the main advances have been in the understanding of the factors influencing the non-linear dynamic behaviour of structures, the introduction of capacity design philosophy and the methods for detailing reinforcement in reinforced concrete structures to achieve the structural ductile behaviour necessary to survive severe earthquakes [P1, P2, N1]. These developments have brought the realisation that many reinforced concrete structures constructed before 1970s may be deficient according to the seismic requirements of current codes.

The need for the seismic assessment of existing reinforced concrete building structures designed to outdated seismic codes, and to retrofit if necessary, has been further emphasised by the damage observed as a result of major earthquakes. Several recent earthquakes, such as the 1985 Mexico Earthquake [J2, N2] and 1989 Loma Prieta Earthquake in California, USA [B2], caused severe collapse and/or damage to existing reinforced concrete structures designed to outdated codes. The 1985 Mexico earthquake with unique ground motions resulted in huge damage to about 2300 buildings, among which about 210 existing reinforced concrete structures collapsed, and left thousands dead [N2]. Once again, the damage caused by the 1995 Hyogo-ken Nanbu Earthquake in Kobe provided renewed impetus for seismic assessment and retrofit of existing reinforced concrete building structures. In the 1995 Hyogo-ken Nanbu Earthquake, the earthquake damage to reinforced concrete buildings was much more severe for buildings built before 1981 when the most recent Japanese seismic code came into effect. Most reinforced concrete buildings built after 1981 suffered only minor damage in the 1995 Hyogo-ken Nanbu Earthquake [P7].

As a result, there have been increased activities in many countries in the seismic assessment of existing reinforced concrete buildings and retrofit where necessary to

improve their seismic performance. Several seismic assessment procedures, which are established on the basis of different principles, have been developed in many countries in recent years, a number of researches into the possible seismic behaviour of pre-1970s reinforced concrete structures have been carried out.

1.2 BACKGROUND OF THIS RESEARCH PROJECT

A research program on Seismic Assessment and Retrofit of Existing Reinforced Concrete Structures has been under way at the University of Canterbury for several years sponsored by the Earthquake Commission of New Zealand. An existing reinforced concrete frame building constructed in 1950s in New Zealand has been thoroughly investigated. Following this investigation, a number of cyclic loading tests on as-built reinforced concrete columns and beam-column joint subassemblages with reinforcing details typical of the 1950s construction in New Zealand have been conducted [R2, H1, W1]. Although the tests on the columns used plain round bars for longitudinal reinforcement [R1], the previous tests on beam-column joints used deformed bars for longitudinal reinforcement [H1, W1]. Actually, plain round bar reinforcement was used in New Zealand until about the mid 1960s when deformed bar reinforcement became widely available. The bond strength of plain bar reinforcement is low, compared with deformed bar reinforcement, particularly during cyclic loading. Conventional theory for flexure and shear was established on the basis of the assumption of perfect bond between the longitudinal reinforcement and the surrounding concrete. Plain round reinforcing bars when used for longitudinal reinforcement hence may lead to very different seismic performance from the theoretical prediction.

In addition, these previous beam-column joint tests were conducted with zero axial column load, and this was considered to be the most unfavourable condition for the joint core. It is necessary to investigate the influence of axial column load on the seismic performance of beam-column joint regions, especially on the bond performance of the beam bars passing through the joint core and the joint shear capacity. This is of particular importance when plain round bars are used for longitudinal reinforcing bars. The presence of the compressive axial column load can enhance the force transmission by bond within the joint core, introducing larger forces into the joint core and hence accelerating the joint shear failure.

1.3 OBJECTIVES OF THIS RESEARCH PROJECT

The objectives of this research project are:

(1). To identify and obtain, by tests, the information needed for the seismic assessment of pre-1970s reinforced concrete frame structures reinforced by plain round bars on the local behaviour of as-built concrete components. This is to be achieved by conducting simulated seismic loading tests on beam - column joint assemblies, which are reinforced by plain round bars and have reinforcing details typical of the pre-1970s construction in New Zealand.

(2). To testify an effective method for strengthening and repair of existing reinforced concrete building frames for earthquake loading.

(3). To develop a proper analysis method for assessing the seismic performance of existing reinforced concrete moment - resisting frame structures (pre-1970s constructions) with plain round longitudinal bars. This is to be achieved by developing a proper structural analytical model after employing the information obtained from the tests conducted in this project.

1.4 ORGANIZATION OF THE REPORT

This report consists of three parts.

In Part 1, which includes chapters 2 and 3, the available seismic procedures and the previous research projects relevant to this project conducted at the University of Canterbury are reviewed. Review of the available seismic procedures clarifies the needed information from laboratory testing on concrete components, and the review of the previous research at the University of Canterbury relevant to this project identifies what has been done in this research program and what needs to be done in this project.

In Part 2 which includes chapters 4 and 5, the test scheme proposed in this project is described first. A detailed seismic assessment of the as-built test units is then conducted based on the current New Zealand design standard NZS3101: 1995 and the realistic seismic assessment procedure, which was built on the basis of capacity philosophy, leading to the identification of critical design deficiencies. Following that, the influence of the beam bar hook details on the shear mechanism of exterior beam-

column joints is examined, and the possible retrofit methods in existing exterior beam-column joint regions are proposed.

Finally, the results from the tests on two as-built interior beam-column joint units, four as-built exterior beam-column joint units and one retrofitted existing exterior beam-column joint unit are presented and explained, with the emphasis placed on the effects of plain round bars and axial column load on the seismic behaviour of existing reinforced concrete structures reinforced by plain round bars, as well as the investigation of fibre-glass jacketing technique as a retrofit technique in improving the structural strength and stiffness properties of existing exterior beam-column joint components.

The final part reports the observed test results. Conclusions reached are given for the interior beam-column joint units and exterior beam-column joint units, respectively.

CHAPTER 2

REVIEW OF PAST RESEARCH INTO SEISMIC ASSESSMENT AND RETROFIT OF PRE-1970S REINFORCED CONCRETE STRUCTURES

2.1 INTRODUCTION

As stated in section 1.1 "THE NEED FOR SEISMIC ASSESSMENT AND RETROFIT OF EXISTING REINFORCED CONCRETE STRUCTURES", the significant developments of design procedures for concrete structures since about 1970s brought about the realisation that existing reinforced concrete structures designed to pre-1970s codes may be deficient according to the seismic requirements of current codes. Consequently, several seismic assessment procedures have been developed, and extensive laboratory studies, which aimed at obtaining the information on member strength and deformation/ductility capacities of pre-1970s reinforced concrete structures, as required by the seismic assessment procedures, have been carried out.

This chapter aims at reviewing the available seismic assessment procedures, the current methods for determining the member local behaviour and the possible retrofit methods. To achieve these aims, the typical design deficiencies present in pre-1970s reinforced concrete structures and the critical concerns in assessing the seismic performance of pre-1970s reinforced concrete structures are identified first following the review of code developments. Based on this, the reliabilities of different seismic assessment procedures are clarified. Subsequently, the current methods for determining the information required for conducting seismic assessment are outlined and the possible retrofit methods are briefly reviewed as well.

2.2 TYPICAL DESIGN DEFICIENCIES IN PRE-1970S REIFNORCED CONCRETE STRUCTURES

Code required proportions and details for reinforced concrete frame structures changed dramatically in the early 1970s. Hence many design deficiencies are present in pre-1970s reinforced concrete structures. To facilitate the identification of the possible inadequate aspects of existing reinforced concrete building structures constructed before 1970s when responding to a major earthquake, a brief review of design code development is given below.

2.2.1 Development of Seismic Codes

In New Zealand, the first code NZSS 95 to require all buildings to be subject to seismic design requirements was published in 1935 after the 1931 Hawkes Bay earthquake. Although the concept of ductility was introduced into New Zealand codes in the 1960s, no specifications were given for detailing reinforced concrete structures to achieve the ductile behaviour. The year 1976 was the milestone date when the current generation of codes for the seismic design of building structures commenced to be introduced, starting with the code for general structural design and design loadings for buildings 4203:1976. This code was followed in 1982 by NZS 3101:1982 which gave specific design provisions for concrete structures. NZS 4203 was amended and reissued in 1984 and 1992. NZS3101 was amended and reissued in 1995. These current seismic codes, which were developed based on the capacity design philosophy, took into account the seismic performance of structures during cycles of lateral loading in the post-elastic range imposed by a severe earthquake. They focused on aspects of proportioning and detailing to achieve system overall strength and ductility by means of appropriate mechanisms of post-elastic behaviour, in order to survive severe earthquakes.

Other countries, such as the United States and Japan [A2], have undergone similar evolution but a difference exists with regard to the degree of capacity design used and ductility expected from structures.

The requirements of outdated and current codes are outlined below, in order to lead to the identification of general possible problem areas in existing reinforced concrete structures constructed before 1970s:

(1). For each individual structural element, the capacity design philosophy underlying the current codes has requirements for the relative strengths of different possible failure modes of the member. Current codes not only require that the element have adequate strength (as did NZSS 95), but also that the relative strengths of its different failure modes so as to preclude the occurrence of undesirable modes of inelastic deformation, such as may result from shear or anchorage failures. This can be achieved by ensuring that the strengths of these undesirable failure modes of the element exceed the actions associated with its flexural capacity at overstrength. This latter feature, which is intended to achieve the required post-elastic mechanism and member local ductile behaviour, was not required by pre-1970s codes.

(2). For a whole reinforced concrete building frame, the capacity design philosophy underlying the current codes requires that the plastic hinge regions be well defined in order to lead to a preferred strong column-weak beam post-elastic failure mechanism where soft storey failures are precluded and regions of the structures other than plastic hinge regions remain essentially in the elastic range. For the potential plastic hinge regions, generous supply of member transverse reinforcement is needed to ensure the expected ductile behaviour. This feature is intended to achieve the required global behaviour of the whole structure; namely, adequate overall load strength, deformation and ductility capacity of the post-elastic critical deformation mechanism of the whole structure. The now outdated codes, which were based on working stress design principles, had no requirements associated with the achievement of the structural global behaviour.

Therefore it is apparent that the possible deficiencies in the seismic performance of existing (old) reinforced concrete structures designed to pre-1970s seismic codes have two major categories. One category includes the deficiencies resulting from lack of the design specifications associated with member local ductility capacity, and the other category includes the deficiencies associated with the structural global behaviour during the inelastic loading cycles. In a word, the post-elastic behaviour of existing reinforced concrete frame structures during a major earthquake is the greatest uncertainty in assessing the seismic performance of pre-1970s reinforced concrete frame structures.

2.2.2 Typical Problem Areas of Pre-1970s Existing Reinforced Concrete Structures

2.2.2.1 Beams

In existing, pre-1970s reinforced concrete frame structures, the beams often had the longitudinal bars with lap splices in the potential plastic hinge regions (see Figure 2.1). This means that yielding may concentrate over small lengths of bars outside the lap and/or slip of bars may occur at the lap, resulting in the inadequate member local ductility capacity.

Also the beams of pre-1970s reinforced concrete frame structures often had relatively sparse and inadequately-configured transverse reinforcement. This was because the design of beam transverse reinforcement according to pre-1970s codes was to resist

code-specified lateral forces rather than the shear corresponding to the development of beam flexural plastic hinges, and concrete was assumed to contribute to shear strength in plastic hinge regions. Current understanding is that transverse reinforcement in members is required not only for providing the shear force resistance but also for providing the lateral restrain against longitudinal bar buckling and the confinement of the compressed concrete. Hence the beams in pre-1970s reinforced concrete frame structures may end up with the occurrence of undesirable inelastic failure mode(s), resulting in a much reduced member local ductility capacity.

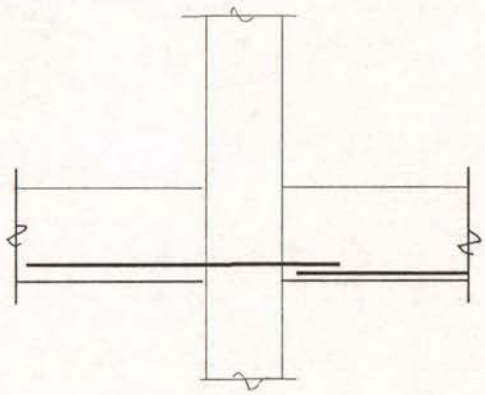

Fig.2.1 Lap splice of beam longitudinal bars in plastic hinge regions

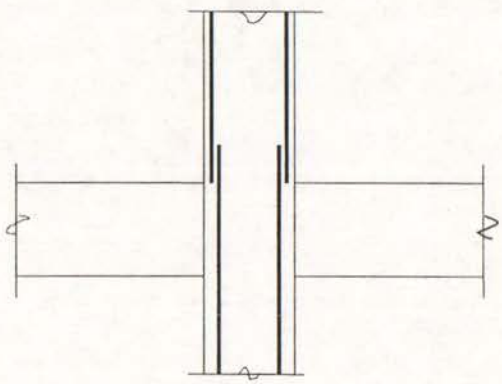

Fig.2.2 Lap splice of column longitudinal bars above joint

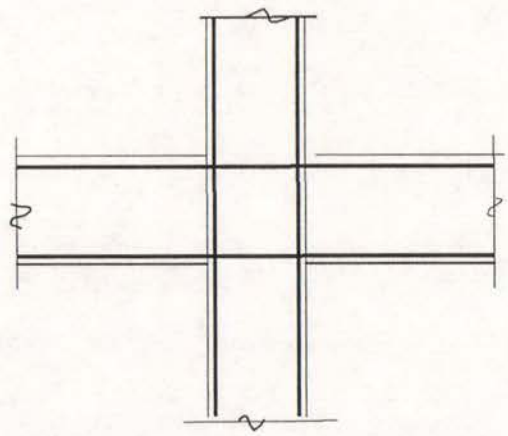

Fig.2.3 No horizontal shear reinforcement in joint

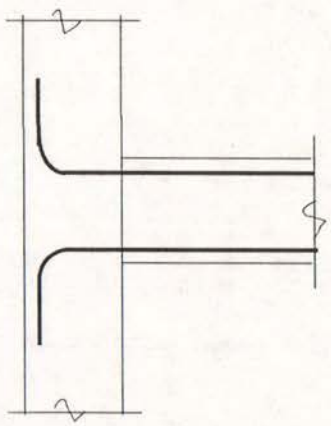

Fig.2.4 Beam bars bent away from joint in exterior columns

2.2.2.2 Columns

In existing, pre-1970s reinforced concrete frame structures, the quantity of column longitudinal reinforcement bars commonly was determined based on the bending moments obtained from code-specified lateral forces rather than the input moment strengths from the beams, as specified by current codes. The resulting columns may be weaker than the beams, possibly leading to undesirable column side sway mechanism, rather than the preferred beam sway mechanism. Consideration of the contribution of slab reinforcement to beam flexural strength in ways not originally envisioned further highlights the concern of the expected failure mechanism.

Again it is common to find column longitudinal reinforcement spliced just above the joint where the maximum moments develop, as shown in Fig.2.2. Splice lengths and transverse reinforcement along the splice were often determined assuming the splice acted only in compression, the resulting splice tensile strength and ductility are commonly inadequate for expected cyclic loadings. In this case, the column local ductility behaviour could be very inadequate.

Similar to the beams, column transverse reinforcement was spaced too widely and may be inadequately configured to act to restrain the longitudinal bar buckling and confine the compressed concrete in the potential plastic hinge regions. As a result, the columns in pre-1970s reinforced concrete frame structures may perform in a very brittle manner.

2.2.2.3 Beam-Column Joints

The greatest uncertainty when assessing the seismic performance of pre-1970s reinforced concrete frame structures is the likely behaviour of beam-column joints. Most frame structures designed before about 1970 did not have any shear reinforcement in the joint cores [P3, H1], as shown in Fig.2.3. Lack of joint transverse reinforcement may lead to reduced load strength and reduced ductility of the beam-column joint or the adjacent framing members.

It is also common to find the longitudinal beam bars of larger diameter passing through relatively small interior columns in pre-1970s reinforced concrete frame structures, resulting in high bond stresses and bar slip. This occurs as a result of seismic loading which causes the beam bar to be in compression on one side of the column and in tension on the other side, which in the limit may require twice the yield force of the bar

to be transferred to the joint core by bond. This situation would be more critical should the existing reinforced concrete frames be reinforced by plain round bars. However, current concrete design codes do not allow for the bond performance when calculating the joint shear capacity. Qualitatively, if slippage does occur, the beam bars will be in tension through the joint core and the "compression" reinforcement in the beam on one side of the column may actually be in tension. In this case, the "compression" reinforcement will not act as compression reinforcement, with a resulting loss in the available beam ductility [P1] and a possible reduction in the attained flexural strength [H5, S8]. Bond failure in interior beam - column joints will reduce the stiffness of the building but it may improve the shear strength of the joint core, since the beam compressive forces will be introduced into the joint by concrete compression rather than by bond along compression reinforcement. Hence the shear carried by the diagonal compression strut will be increased, and the diagonal tension stress introduced into the joint core by bond forces will diminish, resulting in an increase in the shear strength of the joint core due to relatively sound joint core integrity. Thus some slip of beam bars through the joint, although resulting in less ductile behaviour of the beam, will actually increase the shear strength of the joint core.

In exterior beam-column joints of pre-1970s reinforced concrete frame structures, it is not uncommon for the beam longitudinal bars to be bent away from the joint cores in the exterior columns, as shown in Fig.2.4. Such an arrangement of the beam longitudinal reinforcement in the exterior columns does not provide the best configuration to enable the tensile steel force at the bend in the bar to be transferred into the diagonal compression strut which crosses the joint core. Current design codes require the hooks to be bent into the joint core so that the bearing stresses at the inside of the bend are at the end of the diagonal compression strut.

In addition, it is also not uncommon to find that the beam bottom longitudinal reinforcement terminated a short distance into the joint, creating the possibility of bar slip (or pullout) under moment reversals and thus leading to brittle structural performance.

In many cases the presence of lap splices of beam and column longitudinal reinforcement adjacent to but outside of the joint cores in adjacent framing members will limit the input actions from those members so that joint shear failure before failure of the adjoining members will be unlikely. However, if the lap splices or inadequate

anchorage in adjacent members are strengthened as part of a seismic upgrade scheme, the joint actions may be increased to a point where the joint will require strengthening as well. This means that the investigation of structural global behaviour is necessary to preclude the occurrence of such problem shifting, instead of problem solving when the structure is to be retrofitted.

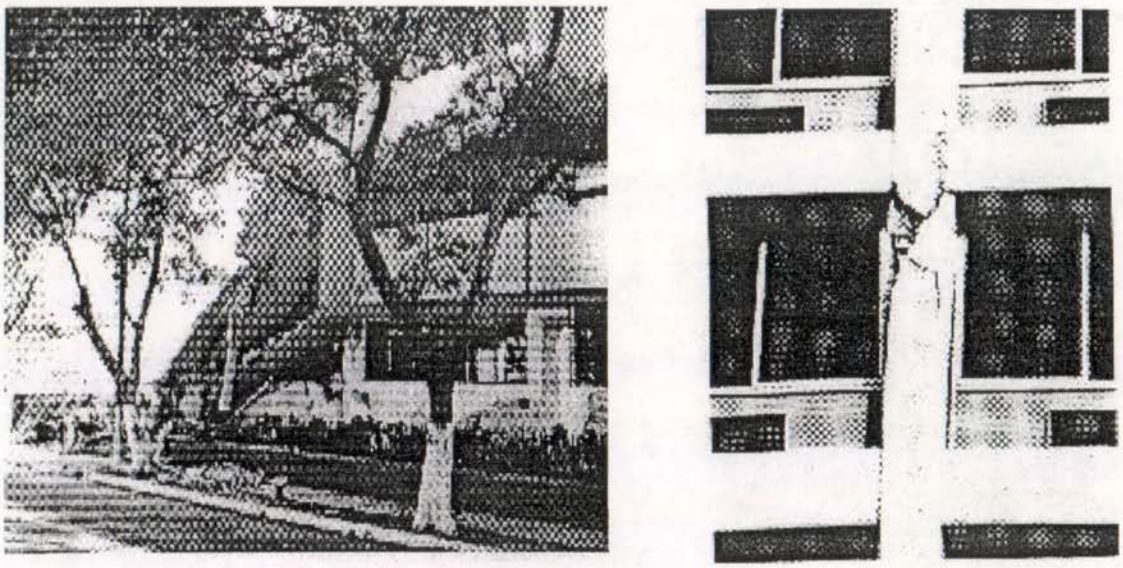

Fig. 2.5 Observed Column Failure

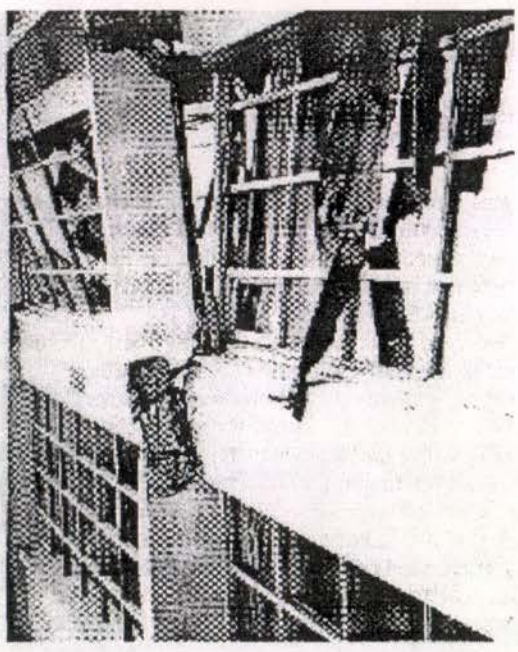

Fig. 2.6 Observed Joint Distress

2.3 OBSERVED EARTHQUAKE DAMAGE [M5, P11]

The most significant failings of existing reinforced concrete frames in past earthquakes have been attributed to failure of the columns, including column shear distress, spalling of column end regions, buckling of column longitudinal reinforcement, and formation of soft stories (Fig.2.5). Several collapses of one or more stories of buildings have been attributed to column failures.

Distress in beam-column connections has been observed following several earthquakes. In several cases, joint failure has contributed to building collapse. Fig. 2.6 shows some common examples of joint distress.

Cases of observed distress in beams have been relatively few, in comparison with failures in columns and joints. Most cases have involved splice failure, shear failure, or flexural/shear failure where beam longitudinal reinforcement was curtailed prematurely.

Reinforced concrete building frames often are characterised by their relatively low lateral stiffness. One result among many is that lateral response of the frame can be influenced strongly by the interaction with the nonstructural elements. A common interaction is between the frame and the infill elements. Several building failures in past earthquakes have been attributed to overstressing of columns that were partially restrained by nonstructural infills. Presence of the partial infill increases the column stiffness and increases the column shear-moment ratio. Interaction may occur between the frames and other nonstructural elements such as stairways. Low lateral load stiffness and the resulting lateral displacements may also lead to excessive nonstructural damage, pounding between adjacent structures, and collapse.

Apparently, the observed earthquake damage to reinforced concrete frames in past earthquakes agrees with the revealed possible problem areas, which were stated in Section 2.2.2.

2.4 REVIEW OF SEISMIC ASSESSMENT PROCEDURES

The seismic assessment of an existing reinforced concrete frame structure can be carried out under the circumstance of the known reinforcing details, the known material strengths and the known cyclic loading properties of individual members and their connections.

In recent years, several seismic assessment procedures have been developed in many countries, such as in New Zealand, the United States of American and Japan, and they

can be classified into two categories, namely check-list type of procedures and capacity design based procedures.

2.4.1 Seismic Assessment of Existing Reinforced Concrete Buildings in Japan [A1, S5]

The first complete document in Japan for the evaluation of the seismic performance of existing reinforced concrete buildings was developed in 1977 as a result of the earthquake damage observed to low rise engineered reinforced concrete buildings in the 1968 Tokachioki earthquake, and it was named as "Standard for Seismic Capacity Evaluation of Existing Reinforced Concrete Buildings". This document was revised in 1990 [A1, S5, O5].

2.4.1.1 Basic Principles

The basic principle underlying this "Standard" was that the extent of the seismic forces resisted by shear walls was the most important factor in structural responses to a major earthquake, and supply of sufficient shear capacity for structural vertical elements was the most effective way.

The basic principle established in such a way was mainly based on the observed earthquake damage as a result of the 1968 Tokachioki earthquake in Japan. The observed damage to the reinforced concrete frame structures in the 1968 Tokachioki earthquake was mainly the shear failure of columns and the earthquake damage statistics after the earthquake showed a close correlation between the load resisted by shear walls and the degree of damage.

2.4.1.2 Proposed Seismic Assessment Procedures

This Japanese procedure recommended three level screening procedures. The lower level procedure is simpler, and the result is believed to be more conservative for Japanese construction. The higher level procedure results in a less conservative conclusion, but involves more complicated analysis. The first level procedure is used to screen safe buildings while the second and third level procedures are used subsequently only for those buildings, which are found not to be satisfactory by the first level procedure. In general, the second and the third level procedures are of a similar complexity of analysis.

For all three level procedures, the safety level of the existing buildings is assessed by comparing the 'Seismic Index' I_s with the 'Seismic Protection Index' I_{so}. The 'Seismic Index' I_s is the total earthquake resisting capacity of a storey, and it includes information on the basic strength and deformation/or ductility capacity of a certain storey, the stiffness distributions in the plan and/or vertical extents of the buildings, the strength and stiffness deterioration with time and geological conditions. The 'Seismic Protection Index' I_{so} is a direct indicator of the degree of earthquake damage, and it is determined totally based on the earthquake damage observed in past earthquakes in Japan.

The main difference in determining the 'Seismic Index' I_s for different levels of screening is in the determination of basic strength and deformation/or ductility capacity of a certain storey. The first and second level procedures assess the strength of a storey by only considering the vertical lateral-resisting elements, but they have different complexities of estimation of the strength capacity of the vertical elements. The third level procedure not only considers the vertical lateral-resisting elements but also allow for the effect of the beams in determining the total strength of a certain storey. The highlight of the importance of the vertical lateral-resisting elements in determining I_s is mainly because the observation of earthquake damage proves a good correlation between the earthquake damage and the amount of walls relative to total floor area during the past earthquakes in Japan. However it need to be noted that all three level procedures assume completely rigid beam-column joint cores because of the lack of evidence of earthquake damage due to the insufficient strength of beam-column joints in Japan. This observation is most likely due to the large member sizes used in Japan.

2.4.1.3. Discussions

Evidently, the Japanese Standard above reviewed has two characteristics as follows:
Firstly, it is clear that the Standard was developed in such a way as to specifically apply to Japanese low rise reinforced concrete buildings because both the basic principles, on which the Standard was developed, and the determination of the 'Seismic Index' and the 'Seismic Protection Index' were based on the earthquake damage to the reinforced concrete buildings of Japanese construction, observed in previous earthquakes experienced in Japan. Direct application to buildings of other countries certainly may not give satisfactory prediction.

Secondly, this Standard ignores the evaluation of beam-column joints and ignores the influence of the horizontal elements on structural deformation and/or ductility capacity. Especially it has no investigation into the post-elastic critical mechanism as well as the two-level limit states, resulting in failure to identify critical areas. Basically this approach is still based on the working stress concept, and is not in accordance with the capacity design philosophy. Once the specified earthquake intensity is exceeded, how much reserve structural capacity remains is still unknown.

In addition, the damage indices were developed by relating damage levels of specific classes of structures to seismic intensity based on experience in past earthquakes, and it is inappropriate to use such damage indices in determining seismic risk of individual buildings. Also the application of a mean value from a data set with extremely wide scatter will provide little insight beyond indicating that there is a need for more detailed structural calculations.

Hence this approach could only be applied in Earthquake Disaster Preparation Projects which only require a check as to whether the investigated structure is sufficient in a given earthquake, rather than determining the available capacity of the structure. Evidently this approach could not be used in retrofit type of projects because, for retrofit projects, it is important that the retrofit schemes do not shift the problem areas to somewhere else. Hence the investigation of the post-elastic critical mechanism of the structure after retrofitting would be necessary.

2.4.2 Seismic Assessment of Existing Reinforced Concrete Buildings in USA

In the United States of America, the most comprehensive assessment methodology is based on documents prepared by the Applied Technology Corporation ATC22[A3]. ATC 22 is an ultimate limit state assessment procedure, and it provides a screening process to decide if further investigation is required. Priestley and Calvi have reviewed it in detail [P4].

2.4.2.1 Basic Principles

The basic principles on which the ATC22 method was developed are as follows:

(1). Concern is related only to life-safety: consequently, only an ultimate limit state is considered.

(2). An ultimate strength of 67% of that required by the NEHRP design recommendation is accepted.

(3). A calculation of seismic demand and seismic capacity is performed, together with checks to ensure that excess shear strength is provided, and that specially vulnerable elements are protected.

2.4.2.2 Proposed Procedures

The basic assessment procedure of the ATC22 method is to check if a series of statements is true or false. Any "false" result identifies an issue requiring further investigation. "Further investigation" means essentially applying normal design procedures for a new building with the base shear scaled to 67% of NEHRP requirements. Also, quick check relationships are suggested for the evaluation of story shear and story drift.

2.4.2.3 Discussions

Priestley [P4] pointed out a few aspects which deserve comment as follows:

(1). The use of a 67% NEHRP "new building" coefficient, which is based on historical precedent, is hard to justify on a rational basis. It is particularly inappropriate where the probability of occurrence of a major earthquake on a given fault (e.g., the Hayward fault, San Francisco) is assessed to be high.

(2). The discussion of some behaviour issues, such as the presence or absence of a strong column / weak-beam design should not be considered independent of reinforcement details.

(3). The assessment of unsatisfactory detailing is handled in a simplistic fashion, as is the issue of the significance of masonry infills.

(4). The assessment is directed towards delineation between " satisfactory " and "unsatisfactory". Although this is of prime importance to a regulatory authority, it is less complete information than may be required by a building owner.

2.4.3 Seismic Assessment of Existing Reinforced Concrete Buildings in New Zealand [N3, N4]

In New Zealand, a document "Guidelines for the Seismic Assessment of pre-1975 Reinforced Concrete Structures and Structural Steel Buildings" [N3] was prepared for the Building Industry Authority by a study group of the New Zealand National Society for Earthquake Engineering in 1994, and this document, after refined, became "The Assessment and Improvement of the Structural Performance of Earthquake Risk

Buildings, Draft for General Release" in 1996 [N4], which is referred to as "Draft" in the following.

2.4.3.1 Basic Principles

The basic principles on which the "Draft" was developed are as follows:

(1). The "Draft" concentrates on matters relating to life safety, that is to say, performance at the ultimate limit state;

(2). The "Draft" accepts a higher level of risk for pre-1975 reinforced concrete buildings, compared with those constructed to modern seismic design codes. Typically for Category IV pre-1975 reinforced concrete buildings, the risk factor is two-thirds of the corresponding risk factor for the new reinforced concrete buildings. This indicates an increase in risk for an existing reinforced concrete building of between two and three times over that of an equivalent new building for the same design life. The structural performance factor in assessing pre-1975 reinforced concrete buildings is 0.85, rather than 0.67 as given in NZS4203: 1992 for structural design. Typically for Category IV pre-1975 reinforced concrete structures, the combination of the modified risk factor and structural performance factor indicates that the numerical requirement for the assessment of a non-ductile existing reinforced concrete structure is 85% of that for designing a new structure, noting that there are offsetting factors on the resistance or strength side of the equation such as the use of probable strengths.

2.4.3.2 Proposed Procedures

The "Draft" recommends a two-stage seismic assessment procedure; that is, the rapid evaluation and the detailed assessment.

The rapid evaluation is established on the recognition and ranking of various building structure characteristics that are known to affect earthquake vulnerability, and is based on the observed damage characteristics of buildings in earthquakes. The rapid evaluation largely follows the process of ATC-21 [A4], but allowing for the features of New Zealand construction. When an existing reinforced concrete structure is assessed using the rapid evaluation method, the structural score needs to be obtained. The structural score is the sum of the indicatives of a number of potential damage parameters. The final assessment is expressed as a plot of the structural score and building area, and the decision whether or not the detailed assessment is needed is

made based on such a plot. For a given structure score, a detailed assessment is recommended if a building has an area larger than that shown in the plot.

For the detailed assessment of an existing reinforced concrete structure, "Draft" recommends two general procedures, force-based and displacement-based procedures. Both force-based and displacement-based procedures are developed based on capacity design philosophy, and the major difference between these two procedures is the end product. Whereas the force-based procedure suggests comparing the structural demand and structural capacity in terms of forces, the displacement-based procedure suggests comparing the structural demand and structural capacity in terms of displacement. The detailed review of the two capacity design based assessment procedures will be conducted in section 2.4.4.

2.4.3.3 Discussions

Basically, the rapid evaluation procedure recommended in "Draft" has similar characteristics to ATC procedure and the detailed assessment procedures recommended in "Draft" are the capacity-design based seismic assessment procedures, including the force-based and displacement-based seismic assessment procedures, which were developed and discussed by Priestley et al [P5] and Park [P6].

2.4.4 Capacity Design Based Seismic Assessment Procedures

The seismic assessment procedure based on capacity design philosophy, which has been developed in recent years, emphasises the overall (global) performance of the structure, rather than the member local behaviour only.

The capacity design based seismic assessment procedure was initially suggested by Priestley and Calvi in 1991[P4]. The procedure, when originally proposed in 1991, suggested comparing the structural demand and capacity in terms of forces, referred to as the forced-based seismic assessment procedure. In 1995, Priestley [P5] introduced into the original force-based procedure a new ideal, which was to compare the structural demand and capacity in terms of displacements, referred to as the displacement-based seismic assessment procedure. In 1997, the displacement-based seismic assessment approach [P5] was further discussed by Priestley and Calvi [P21], and by Priestley [P22].

Displacement-based approach has apparent advantages over the force-based approach. Priestley et al pointed out that failure of ductile system occurs not when the strength is reached but when the ductility capacity (i.e., the ultimate displacement) is reached and the developed strain, therefore the attained displacement, is clearly a better indicator of the structural damage level. The displacement-based approach is hence more rational than the force-based approach, especially for the seismic assessment of reinforced concrete structures. The weaknesses of the force-based approach, outlined by Priestley et al in references P5 and P21, include: (1). the improper assumption of the relationships between ductile response and elastic response of the system, namely, the use of the force reduction factor as in current forced-based seismic design codes; (2). the lack of consideration of hysteretic energy dissipation characteristics, namely, the use of the initial elastic stiffness. The use of initial elastic stiffness and the force reduction factors in the force-based approach could lead to, in terms of seismic risk, a change in probability of damage of as much as an order of magnitude, under a given event [P21]. The key element of the displacement-based assessment procedure is that a substitute structure as suggested by Shibata and Sozen [S7] is constructed and the stiffness and damping of the substitute structure are characterized by secant properties at maximum response, rather than initial elastic properties as for force-based procedure, leading to the elimination of the problems associated with the use of initial

elastic stiffness and the use of force reduction factor. Meanwhile, in 1997, Park [P6] further discussed the force-based seismic assessment procedure, and outlined, in detail, the static procedure for assessing the likely seismic performance of existing reinforced concrete moment-resisting frame structures. Park [P6] agreed that the displacement-based seismic assessment procedure has apparent advantages over the force-based approach, but pointed out [Park 1997] that since the current New Zealand design standard recommends seismic design in terms of design seismic forces and the associated ductility demand, and most engineers at present will prefer to use a force-based approach for seismic assessment of pre-1975 existing reinforced concrete structures until the New Zealand standard adopts displacement based design.

2.4.4.1 Basic Principles

The basic principles underlying the capacity design based seismic assessment procedure are as follows:

(1). Two limit states, namely serviceability limit state and ultimate limit state, are considered.

Force-based seismic assessment procedure defines the two limit states in exactly the same way as in current seismic design codes. Serviceability limit state is defined to be the state corresponding to the yield displacement (or yield curvature), -- i.e., a displacement ductility of μ_s =1. A serviceability limit corresponding to μ_s =1, while generally conservative, provides a very uneven protection against damages[P17]. Ultimate limit state is defined to correspond to the formation of the critical post-elastic failure mechanism of the structure.

Displacement-based seismic assessment procedure defines the two limit states based on strain criteria. Serviceability limit state corresponds to the concrete cracking and acceptable large residual crack widths, and is suggested by Priestley and Calvi [P21] to be a maximum concrete strain of ε_c=0.004 and a maximum reinforcement tensile strain of ε_s=0.015, whichever is reached first. Hence, unlike the force-based approach, the displacement-based approach enables a consistent level of assessment to be achieved. Ultimate limit state also is defined to correspond to the formation of the post-elastic failure mechanism of the structure.

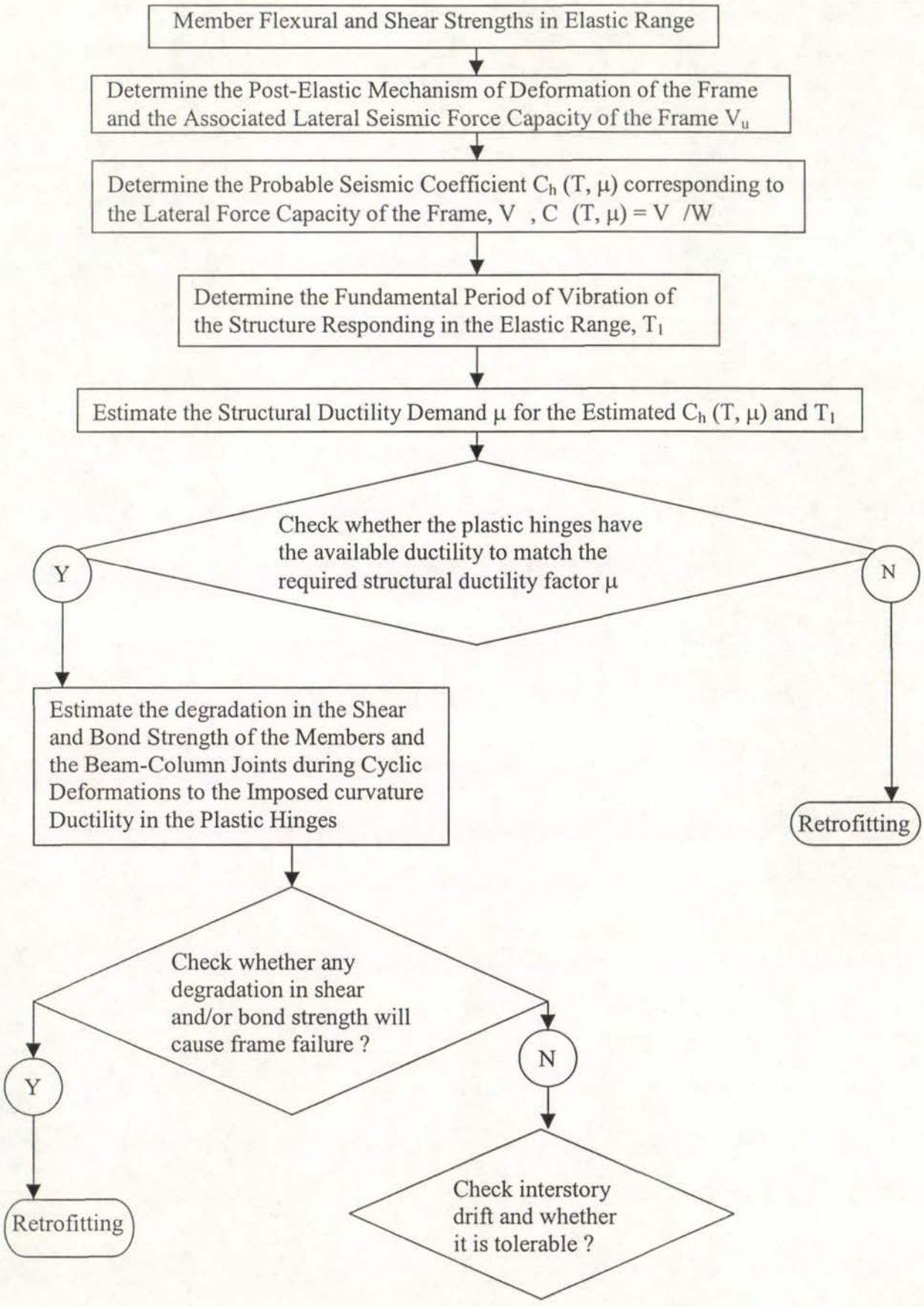

Fig. 2.7 Procedures of Force-Based Seismic Assessment Approach

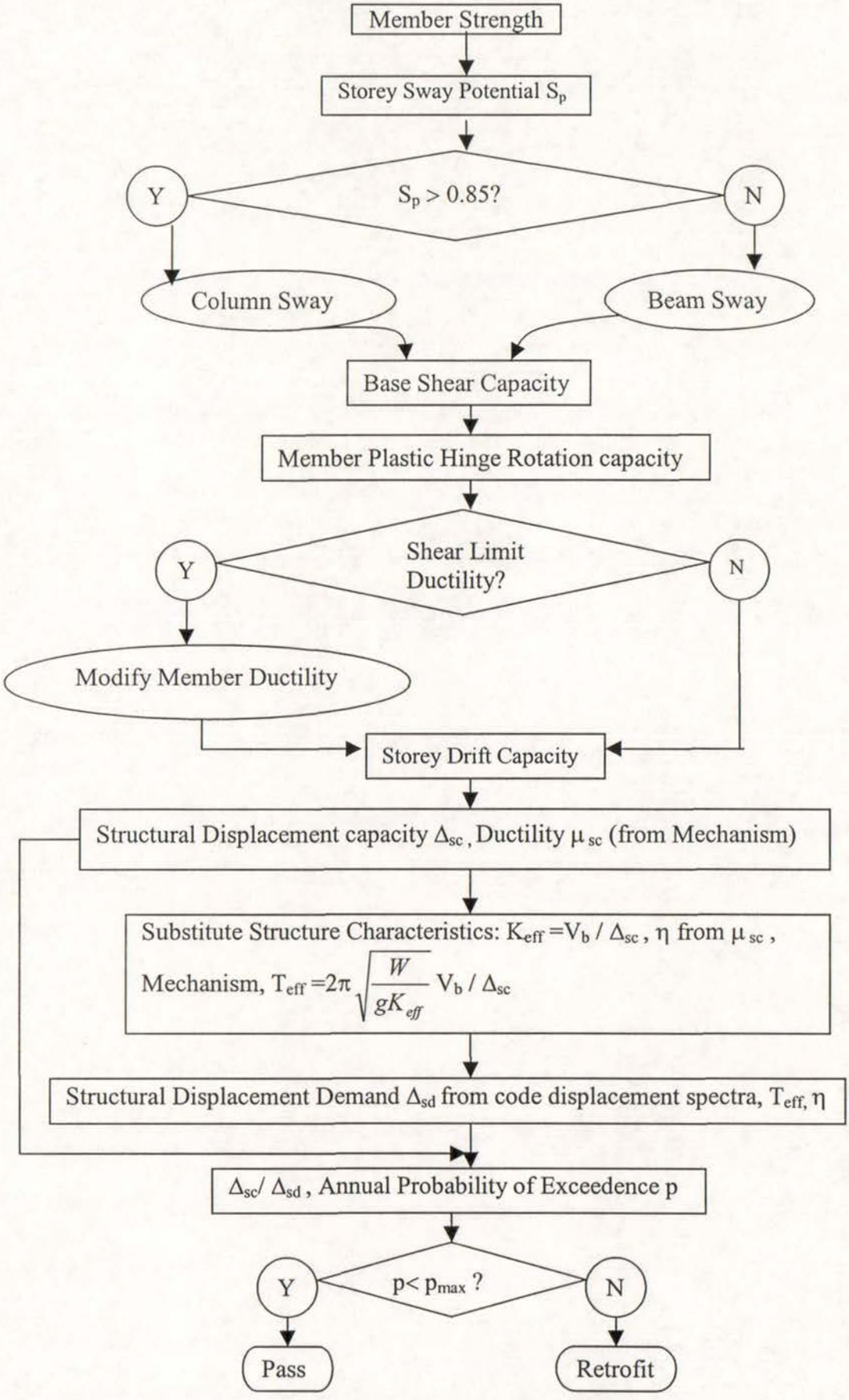

Fig.2.8 Procedures of Displacement-Based Seismic Assessment Approach

(2). The probability of exceedance for each limit state is determined by comparison with reference spectra representing code-specified seismicity, or a site-specific design spectrum.

2.4.4.2 Proposed Procedures

The seismic assessment procedures are summarised in Fig.2.7 and Fig. 2.8, for the force-based procedure and the displacement-based procedure, respectively, and they have been respectively described in detail by Park [P6] and Priestley [P21].

1. Seismic Assessment at the Serviceability Limit State

The structural response at the serviceability limit state is expected to be essentially elastic, hence elastic methods, such as modal analysis, are used to analyse the overall structural response at this state.

Once the best estimation of elastic flexural and shear strengths of beams and columns as well as the best estimation of elastic shear strengths in the beam-column joints are available, the serviceability limit state assessment can be carried out realistically. Here the elastic strengths are the strengths without considering strength degradation.

The quality of the seismic assessment results depends on the quality of the estimation of member strengths. Apart from the utilisation of realistic material strengths, proper methods to estimate member strengths should be used, and provisions in current design codes should not always be used for the purpose of seismic assessment because these provisions are only applicable to the design of new buildings and usually very conservative. A brief review of the determination of material strength can be seen in section 2.5.

2. Seismic Assessment at the Ultimate Limit State

As seen in Figs. 2.7, for the force-based assessment procedure, the system lateral load strength and the overall structural deformation capacity of the post-elastic collapse mechanism need to be found, and the combination of the system lateral load strength and the overall structural ductility capacity of the post-elastic collapse mechanism gives an equivalent elastic response force level, which, by comparison with the design elastic response spectrum, could be used to determine annual probability of exceedence corresponding to development of structural capacity.

Similar to the force-based assessment procedure, for the displacement-based assessment procedure, the system lateral load strength and the overall structural ductility capacity of the post-elastic collapse mechanism are also needed in order to construct the substitute structure, as seen in Fig. 2.8.

Hence, the fundamental aspect in seismic assessment of existing reinforced concrete structures using force-based and displacement-based assessment procedures is the determination of the post-elastic collapse mechanism of the system, including the identification of the post-elastic collapse mechanism of the system and the estimation of its associated lateral load strength and the structural ductility capacity (or displacement capacity).

2.4.4.3 Determination of the Critical Post-Elastic Collapse Mechanism

According to capacity design philosophy, the ductile behaviour of the critical post-elastic failure mechanism at the ultimate limit state is achieved by inelastic flexural deformations in well defined plastic hinge regions (mainly in the beams), and the relative strengths of undesirable failure modes should be high enough to preclude the occurrence of undesirable failure modes of inelastic deformation. A series of provisions regarding structural proportioning and reinforcing details are specified in current codes to achieve the desired structural ductile behaviour. However, for the existing reinforced concrete structures, the ductile structural response of the critical post-elastic collapse mechanism may be hampered by the occurrence of undesirable failure modes, as a result of lack of capacity design philosophy in now outdated seismic codes.

Capacity design based seismic assessment procedure suggests that the determination of the critical post-elastic collapse mechanism be determined by using a modified form of capacity design principle which allows some local element failure provided that the overall structural integrity is not jeopardised. This will involve the identification of the critical collapse mechanism, the determination of the available lateral load strength and the overall structural ductility capacity of the post-elastic collapse mechanism and the check to see whether the occurrence of the undesirable failure modes of the element is possible [P5, P6].

Park outlined in detail the methods for determining the post-elastic collapse mechanism of the system [P6 by Park in 1997], and it is reviewed below.

1. Identification of the Critical Post-Elastic Collapse Mechanism

Many older reinforced concrete frame buildings can be expected to have a mixed post-elastic mechanism, instead of simply a beam sidesway mechanism or a column sidesway mechanism (see Figure 2.9). The consequences of particular failures need to be assessed relative to each other. For example, column shear failure is very serious, since it is associated with the loss of gravity load capacity and could result in total collapse of the structure. Joint shear failure is less likely to result in catastrophic collapse. It must also be recognised that the shear strength of beams and columns in plastic hinge regions is dependent on the level of flexural ductility imposed. Hence a mechanism which initiates with flexural plastic hinges may degenerate into plastic hinges with shear failure as the ductility demand increases.

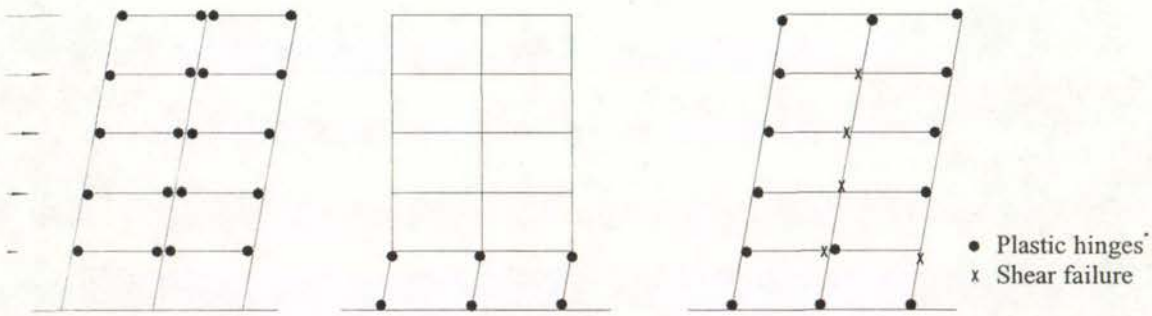

(a) Beam sidesway mechanism

(b) Column sidesway mechanism

(c) Mixed sideway mechanism with plastic hinges and shear failure

Fig. 2.9 Mechanisms of Post-Elastic Deformation of Seismically Loaded Moment Resisting Frames

To investigate whether the plastic hinges form in the beams or columns at a particular joint, the sum of the probable flexural strengths of the beams and the columns at the joint centroid can be compared, (see Fig. 2.10). The flexural strength ratio at the joint may be defined as:

$$S_r = \frac{M_{bl} + M_{br}}{M_{ca} + M_{cb}}$$

where M_{bl} and M_{br} = beam flexural strengths at the left and the right of the joint, respectively, at the joint centroid, and M_{ca} and M_{cb} =column flexural strengths above and below the joint, respectively, at the joint centroid.

When $S_r > 1$ plastic hinges in the columns can be expected.

To investigate whether a column sway mechanism (soft story) can be expected, a sway potential index S_i can be defined as the sum of all the S_r values for the beam-column joints at a floor level. Thus at a floor level,

$$S_i = \sum S_r$$

If the value of the flexural strength ratio S_r for the beam-column joints at the floors above and below a storey are all greater than 1.0, a column sidesway mechanism can be assumed to occur in that storey since plastic hinges can form at the top and bottom of all columns in that storey.

If the sway potential index S_i for the beam-column joints of the floors above and below a storey are both greater than 1.0, it is possible that a column sidesway mechanism will occur. However, the presence of some joints with a flexural strength ratio S_r<1.0 will prevent a column sidesway mechanism even if S_i>1.0.

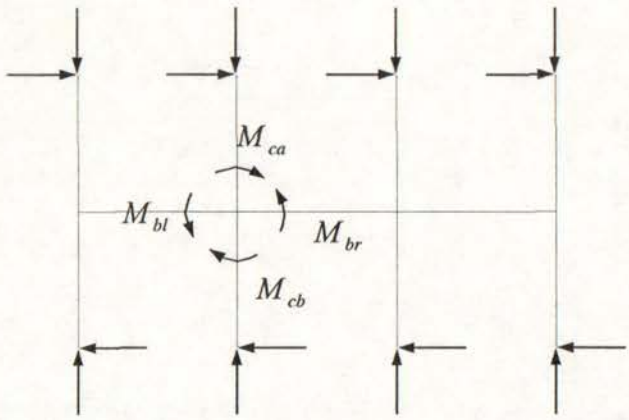

Fig.2.10 Bending Moments Acting at a Beam-Column Joint at a Floor Level

Due to the possible increase in column moments due to higher mode effects, it is suggested that column plastic hinges can be assumed to form if $S_r > 0.8$.

The probable lateral seismic load capacity of the critical post-elastic collapse mechanism of the frame in the general case can be found by assuming that the structural performance is dominated by flexure only. Whether the undesirable failure modes hamper the maintenance of the flexural strengths with the development of displacement will be checked later on.

Park suggested three possible methods for determining the lateral load strength of the corresponding mechanism, when the probable lateral seismic load capacity of the frame is only dependent on the flexural strengths of members.

- Method 1

Linear elastic structural analysis is used to determine the lateral seismic force corresponding to the development of the first plastic hinge. For this method, the equivalent static earthquake forces are increased from zero until the first plastic hinge forms. The lateral seismic force corresponding to the development of the first plastic hinge gives a lower bound to the probable lateral force capacity of the critical collapse mechanism, and this will be equal to or less than the actual lateral force capacity. In reality, moment redistribution in post-elastic range will permit higher lateral seismic forces to be resisted while further plastic hinges form until a mechanism develops.

- Method 2

If the mechanism of post-elastic deformation is obvious from the onset, the lateral seismic force capacity corresponding to the critical collapse mechanism can be calculated directly. This estimate gives an upper bound to the probable lateral force capacity of the frame and will be always equal to or greater than the actual lateral force capacity. The danger of calculating the lateral force capacity by the upper bound approach is that the lateral force capacity may be overestimated as a result. The mechanism giving the least lateral force capacity is the correct one and must be sought.

- Method 3

The most complete approach is to use nonlinear push-over structural analysis. That is, the lateral seismic forces acting on the frame are gradually increased until the mechanism forms. The behaviour of the frame is in the elastic range until the first

plastic hinge forms and then the post-elastic deformations at the plastic hinges need to be taken into account. The number of plastic hinges forming increases with increase in lateral force until a mechanism develops, giving the actual probable lateral force capacity.

2. Determination of the Ductility Capacity of the Critical Post-Elastic Collapse Mechanism

The available structural ductility can be estimated by taking into account the plastic hinge rotation capacity and /or section ductility according to the level of detailing.

Park suggested three methods for determining the available structural ductility [P6].

- Method 1:

A simplistic approach is to compare the detailing of the structure with that recommended by current codes for ductile structures and to assess the available ductility on that basis.

Typically for a structure where a beam sidesway mechanism is expected, when the transverse reinforcement detailing in the potential beam plastic hinge regions meet the current code requirement, an available displacement ductility factor of $\mu = 6$ may be assumed for the frame, but when the transverse reinforcement detailing in the potential beam plastic hinge regions are very sparse and poorly anchored, an available displacement ductility factor of $\mu = 2$ may be assumed for the frame. For the intermediate situation, interpolation method for determining the available displacement ductility factor is used.

For potential plastic hinge regions at the base of columns where a beam sidesway mechanism is shown to be likely, or for frames of one or two storeys in height, where a column sidesway mechanism is likely, if the transverse reinforcement detailing is satisfactory according to current design code, an available structural ductility factor of $\mu = 6$ may be assumed; and if the transverse reinforcement is not well anchored and has a big spacing, typically greater than 16 times the bar diameter, an available structural ductility of 2 may be estimated. For the frame structures of more than two storeys in height where the column sidesway mechanism is likely, an available μ of 1.5 can be assumed if the transverse reinforcing details are poor.

- Method 2

A more accurate method would be to first determine the available curvature ductility factors at the plastic hinge regions taking into account the amount of transverse reinforcement present, the available structural ductility may then be found from the mechanism by pushing the mechanism laterally until the critical available curvature ductility is reached.

This is an approximate approach since not all the plastic hinges in the mechanism form simultaneously because for one reason, the vertical profile of horizontal displacement of the frame will not be linear, for example, as a result of the effect of the higher modes of vibration. That is, the drift (lateral displacement of a storey divided by the storey hight) will not be the same for each storey.

- Method 3

The most complete approach for determining the available displacement ductility μ is to use a nonlinear structural push-over analysis in which lateral seismic forces on the frame are gradually increased until the available ultimate curvature is reached first at the critical plastic hinge.

This method is believed to be essential for frames in which mixed sidesway mechanisms form as shown in Fig.2.9 (c), since such frames can not be easily analysed by the simpler methods.

3. Check the Possibility of Occurrence of Undesirable Member Failure Modes

It needs to be realised that the determination of the lateral seismic load strength and the overall ductility capacity of the critical post-elastic collapse mechanism, described above, is based on the assumption that the flexural strengths of members dominated the seismic performance of the frame structures at the ultimate state. Whether or not the other non-ductile failure modes possibly dominate the post-elastic performance of the system needs to be identified. Cyclic loading tests frequently demonstrate that the final failures of the existing reinforced concrete members reinforced by deformed bars are likely to be dominated by shear failure due to the observed degradation in shear strength at plastic hinges and beam-column joints with the increase in the imposed ductility level. A mechanism which initiates with flexural plastic hinges may degenerate into plastic hinges with shear failure as the ductility demand increases.

Hence the strength degradation associated with other failure modes (such as, shear failure and bond/anchorage failure) with increase in the imposed ductility levels needs to be checked to make sure that the degradation of the non-desirable failure modes (for example, shear strength and bond strength) in the plastic hinges does not hamper the maintenance of the flexural strength.

2.4.4.4 Discussions

As revealed by outlining the development of seismic design codes in section 2.2.1, the structural design without incorporation of capacity design philosophy, as was the case before mid 1970s around the world, contributes greatly to the uncertainty of the structural post-elastic behaviour. Therefore, the key point in assessing the seismic performance of an existing reinforced concrete structure is to investigate the structural global behaviour, that is, the structural lateral load capacity and structural ductility of the critical post-elastic mechanism of the structure, rather than only local behaviour. This is especially true for an existing reinforced concrete building frame where the post-elastic critical mechanism is a mixed sidesway mechanism with the development of the beam hinges, columns and shear failures likely at different locations within the frames. In this case, a simple check-list assessment procedure, which compares the local member details of the as-built reinforced concrete structures with the requirements of current seismic codes, will rarely be successful. Furthermore, the evidence of tests and analysis as well as the observed earthquake damage also demonstrate that not all structures designed to now outdated codes will response poorly to severe earthquakes, even when according to current standards the detailing of reinforcement in some regions is substandard [P3].

Apparently capacity design based seismic assessment procedures are more realistic and more adequate, compared to check list procedures. Especially, if the decision to retrofit the structure has been made after structural assessment using a check list type of procedure, the prevention of problem shifting rather than problem solving resulting from one potential retrofit technique only can be fulfilled by using capacity design based seismic assessment procedures. This is apparently a prominent advantage of capacity design based seismic assessment procedures over the check-list type of procedures.

To investigate the structural global behaviour in the post-elastic range, the required information on local behaviour of individual members includes the members' strength and deformation capacity. On important aspect in the consideration of member local behaviour is to investigate the strength degradation of undesirable failure modes. For reinforced concrete members containing deformed bars, the major concern is the shear strength degradation of members and beam-column joints.

Obviously, the quality of the seismic assessment of existing reinforced concrete structures greatly depends on how realistic the estimation of the probable member strength and deformation capacity and the estimation of the strength degradation of undesirable failure modes are. Hence the assessment of member strength and deformation capacity by test and analysis becomes fundamental to achieve the best seismic assessment of structures.

2.4.5 Summary

Check list assessment procedures, such as, "Standard" in Japan, ATC method in USA and the rapid evaluation method in New Zealand, assess the seismic performance of existing reinforced concrete structures by referring to the earthquake damage of structures of similar structural type observed in the past earthquakes. Core element of check-list procedures is the statistical relationship between potential earthquake vulnerable factors and the earthquake damage in the past earthquakes. Check list procedures only take into account the local behaviour of the individual concrete elements, and inadequately representing the interactions between the actions of different members, which is the key advance of current design codes compared to the old design codes. Hence, the check-list seismic assessment procedures are basically based on working stress philosophy. However, the check-list seismic assessment procedures are easy to follow, and so can be used for City Earthquake Disaster Prevention and Preparation Programs.

In contrast, capacity design based assessment procedures, force-based and displacement- based procedures, aim at investigating the available strength and deformation capacity of the post-elastic failure mechanism of the system, and hence realistically assess the structural post-elastic response. The needed information for conducting seismic assessment using capacity design based seismic assessment procedures includes the initial strength of individual existing reinforced concrete

members and the strength degradation with the increase in the imposed displacement level. Typically, premature shear failure in members (beams and columns) and beam-column joints could occur when the deformed bars are used for longitudinal reinforcement, hence shear strength degradation with the increase in the imposed displacement level should be investigated in this case.

Current design code equations are considered not to be suitable for determining the shear strengths of existing reinforced concrete members, and the information on probable strength and strength degradation of existing reinforced concrete components should be obtained from cyclic tests on as-built reinforced concrete components.

2.5 METHODS FOR DETERMINING MEMBER STRENGTH AND DEFORMATION CAPACITY

The determination of the post-elastic collapse mechanism is based on a knowledge of member strength and deformation capacity, as seen from Figs. 2.7 and 2.8. The basis of realistic assessment should be to obtain a "best estimate" of member strength and deformation properties. Hence, apart from using realistic values of material strengths, proper methods rather than code design equations need to be used for determining member strength and deformation capacity.

For the design of each individual concrete member, capacity design philosophy requires that its relative strengths of the different failure modes preclude the occurrence of undesirable modes of inelastic deformation, such as may result from shear or anchorage failures. Hence, for existing reinforced concrete members, the study on member strength and deformation performance should identify the dominant failure mode, determine the probable flexural strengths of members and investigate whether the strength corresponding to the most critical non-ductile failure mode could hamper the development of the post-elastic deformation due to the possible strength degradation with the progress of post-elastic cyclic deformations.

When deformed longitudinal reinforcement is used, the shear performance of the as-built concrete members and beam-column joints was often observed to dominate the final failure [H1, Hakuto et al 1995]. This occurred due to the shear strength degradation with the increase in the imposed displacement level in post-elastic range. In this case, the degradation of shear strength with the increase in the imposed displacement level apparently needs to be investigated in order to find whether the degradation in shear strength can hamper the development of post-elastic deformation. Some laboratory testing has been carried out to study the shear strength degradation of as-built concrete components and beam-column joints reinforced by deformed bars in the post-elastic range. As a result, the methods for estimating the available shear strength and the shear strength degradation of as-built concrete members and beam-column joints have been tentatively developed.

Representatives of the current methods, for determining the probable flexural strength and the shear strength degradation of as-built concrete members and beam-column

joints when using deformed longitudinal bars, are the methods proposed respectively by Priestley et al [P5] and by Park [P6].

2.5.1 Material Strengths

To achieve the best estimate of member strength and performance properties, it is inappropriate to use nominal or specified material strengths and strength reduction factors. This has been addressed by many researchers [C6, P5, P6].

2.5.1.1 Reinforcement

Site sampling and testing in pre-1970s reinforced concrete structures frequently showed that the reinforcement used is likely to possess a characteristic yield strength significantly greater than the specified value. For instance, Chapman [C6] reported that the reinforcement in New Zealand construction built during the 1930 to 1970 period is likely to possess a characteristic yield strength 15 to 20% greater than the nominal value, which was 250 to 275 MPa at that time. Whenever possible, samples of steel from the structure should be tested to obtain a better estimation of the probable yield strength of the reinforcement. Otherwise, a value of $1.1\,f_y$ should be adopted as the probable reinforcement yield strength, where f_y is the nominal yield strength [P22].

A further consideration is whether the longitudinal reinforcement is from deformed or plain round bars. For instance, plain round bars were commonly used before the mid-1960s in New Zealand. The use of plain round longitudinal reinforcement would result in very different structural performance, compared with the case with deformed longitudinal reinforcement. This can be seen later from the test results of this research project.

2.5.1.2 Concrete

The actual concrete compressive strength of old reinforced concrete buildings is likely to considerably exceed the nominal value as a result of conservative mix design, age and the less finely ground cement particles. Results on the concrete of 30 year old bridges in California consistently showed compressive strengths approximately 1.5 times to twice the nominal strength [P22]. Concrete from the columns of the Thorndon overbridge in Wellington has a measured compressive strength about 30 years after construction of about 2.3 times the specified value of 27.5MPa [P6].

The increase in concrete strengths usually has not significant influence on member's flexural and shear capacity. For instance, an increase of 50% in concrete compressive strength could only result in about 5 to 10% increase in flexural and shear capacities of beams and columns. Therefore the utilisation of 1.5fc' for probable concrete strength is accurate enough in seismic assessment of existing reinforced concrete structures when there is a lack of information on the actual concrete compressive strength.

In addition, the quality of the concrete should be inspected since if compaction was poor a lower concrete compressive strength may need to be assumed.

2.5.2 Flexural Strengths of Beams and Columns

The probable flexural strengths of beams and columns were suggested by Priestley [P5] and Park [P6] to be calculated using the probable material strengths, standard theory for flexural strengths, and assuming a strength reduction factor of unity.

2.5.3 Shear Strength of Reinforced Concrete Columns

Priestley, based on extensive laboratory testing, proposed a method for estimating the probable shear strength of columns. Priestley recommended to use a shear strength reduction factor of 0.75 and he suggested that the probable shear strength of columns is the sum of components due to concrete contribution (V_c), transverse reinforcement (V_s) and axial load (V_n). Thus,

$$V_p = V_c + V_s + V_n \tag{1}$$

In which,

$$V_c = v_c \ 0.8 \ A_g = \mathrm{k}\sqrt{f_c'} \ 0.8 \ A_g \tag{2}$$

$$V_s = \frac{A_v f_{yt} d''}{s} (\cot 30°) \text{ for rectangular sections} \tag{3a}$$

$$V_s = \frac{\pi}{2} \frac{A_{sp} f_{yt} d''}{s} (\cot 30°) \text{ for circular sections} \tag{3b}$$

and

$$V_n = \mathrm{N}^* \tan \alpha \tag{4}$$

where:

k = 0.29 prior to shear strength degradation

v_c = nominal shear stress carried by the concrete mechanisms,

A_g = gross area of the column,

$f_c^{'}$ = probable concrete compressive cylinder strength,

A_v = total area of hoops and cross ties in the direction of the shear force at spacing s

A_{sp} = area of spiral or circular hoop bar,

f_{yt} = probable yield strength of the shear reinforcement,

$d^{"}$ = depth of the concrete core measured in the direction of the shear force for rectangular hoops and the diameter of the concrete core for spiral or circular hoops.

N^{*} = the axial load acting on the column

α = for a cantilever beam, the angle between the longitudinal axis of the column and the straight line between the centroid of the column section at the top and the centroid of the concrete compressive force of the column section at the base, and for a column in double curvature α is the angle between the longitudinal axis of the column and the straight line between the centroids of the concrete compressive forces of the column section at the top and bottom of the column.

Evidently, Priestley assumed that the critical diagonal tension crack is inclined at 30° to the longitudinal axis of the column in calculating the shear resisted by transverse reinforcement, see Equations 3a and 3b.

The degradation of shear strength of concrete members is caused due to the decrease in the contribution of concrete mechanism with the increase in the imposed flexural displacement level. The degradation of shear strength of columns proposed by Priestley [P5] is depicted in Fig. 2.11, in terms of the degradation of k.

Park [P6] suggested using a shear strength reduction factor of 0.85, rather than 0.75 as by Priestley. The general expression proposed by Park for estimating the probable shear strength of columns is exactly the same as equation (1) by Priestley. The determination of V_c and V_n are also by equations 2 and 4 respectively. However, Park suggested that V_s be given as follows:

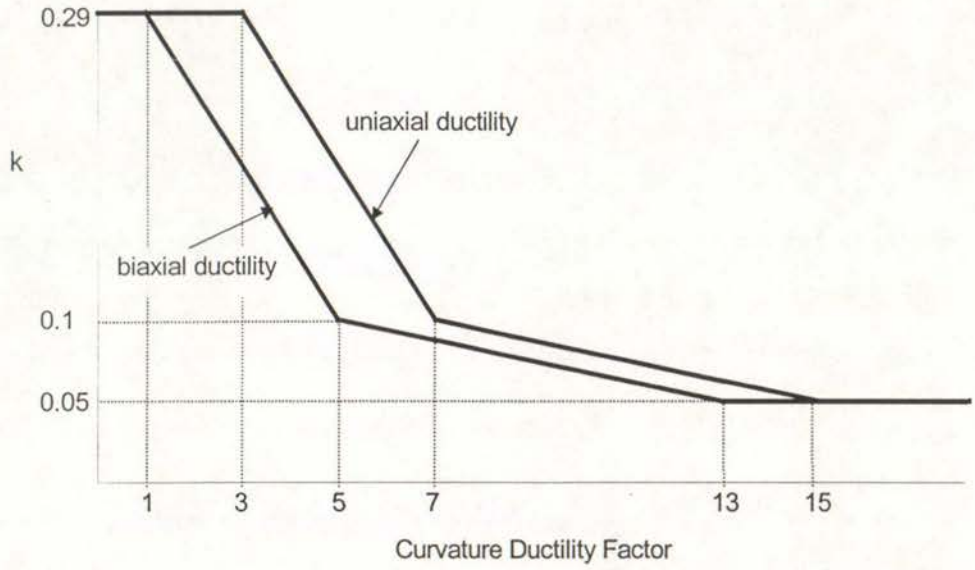

Fig.2.11 Degradation of Concrete Shear Strength with Ductility for Columns [P22]

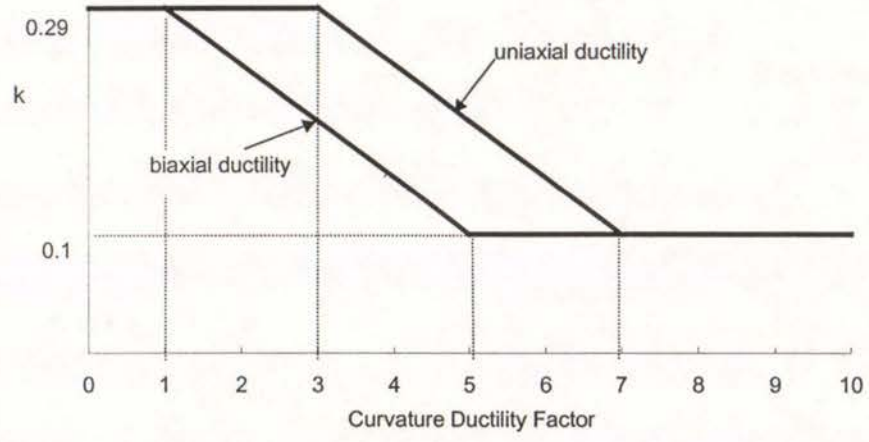

Fig.2.12 Degradation of Concrete Shear Strength with Ductility for Columns [P6]

$$V_s = \frac{A_v f_{yt}(d'' - c)}{s}(\cot 30°) \quad \text{for rectangular sections} \qquad (3a')$$

$$V_s = \frac{\pi}{2}\,\frac{A_{sp} f_{yt}(d'' - c)}{s}(\cot 30°) \quad \text{for circular sections} \qquad (3b')$$

where:

c = distance from neutral axis to the extreme compression fibre of the section

A_v, A_{sp}, f_{yt}, and d'' have the same meanings as for Equations 3a and 3b.

It is seen that the method proposed by Priestley and the method proposed by Park for estimating the probable shear strength of columns are basically the same, and the only difference is that Park uses $d^{"}$ - c, rather than $d^{"}$ as for the method proposed by Priestley [P5], in calculating the shear resisted by the shear reinforcement. Park[P6] points out that such a modification is based on the suggestion made by Kowalsky, which indicates only the portion of the transverse reinforcement on the tensile side of the neutral axis crossing the potential shear failure plane.

Proposed degradation of concrete shear strength with ductility for reinforced concrete columns by Park [P6] is depicted in Fig. 2.12.

In a word, Priestley and Park proposed basically the same method for estimating the shear strength of columns, except that they recommended using different shear strength reduction factors in estimating the column shear strength.

2.5.4 Shear Strength of Reinforced Concrete Beams

Priestley directly extended his model for estimating the shear strength of reinforced concrete columns to reinforced concrete beams [P22]. Priestley recommended that the probable shear strength of reinforced concrete beams with rectangular stirrups or hoops be given by:

$$V_p = \mathrm{k}\sqrt{f_c^{'}}\ 0.8\ A_g + \frac{A_v f_{yt}(d-d^{'})}{s}(\cot 30°) \qquad (5)$$

where:

$f_c^{'}$ = probable concrete compressive cylinder strength,

A_g = gross sectional area of beams,

A_v = area of transverse shear reinforcement at spacings,

f_{yt} = probable yield strength of the shear reinforcement,

d = effective depth of beam,

$d^{'}$ = thickness of the concrete cover,

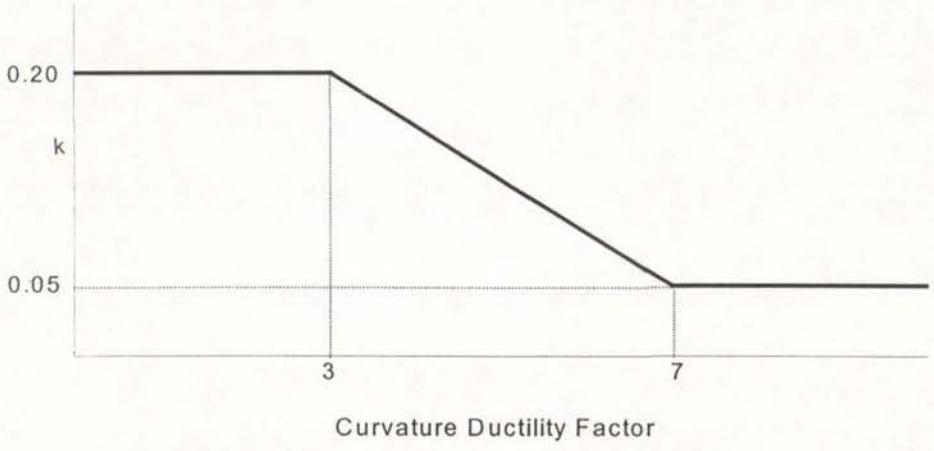

Fig.2.13 Degradation of Concrete Shear Strength with Ductility for Beams

The suggested degradation of beam shear strength by Priestley, expressed in terms of coefficient k, is described in Fig.2.13, and it is based on Hakuto's tests with deformed longitudinal bars.

Park [P6] used an approach similar to the New Zealand code equation [NZS3101:1995] for estimating beam shear strength. Park recommended that the probable shear strength of beams with rectangular stirrups or hoops be given by:

$$V_p = \mathrm{k}\sqrt{f_c'}\ b_w \mathrm{d} + \frac{A_v f_{yt} d}{s} \qquad (5')$$

where b_w is the width of beam, and the other parameters have the same meanings as in Eq.(5).

The suggested degradation model for beam concrete shear resisting mechanism by Park [P6] is the same as depicted in Fig.2.13 by Priestley.

Comparison of equations (5) and (5') shows that a major difference between the method proposed by Priestley and the method proposed by Park is the assumed inclination angles of the critical diagonal tension cracks. Priestley [P5] believes that there should not be much conceptual difference in the shear resisting mechanisms between a beam and a column with zero axial load, and that the critical diagonal tension cracks are inclined at 30° to the longitudinal axis of the beam, similar to that for the columns. However, Park [P6] assumes that the critical diagonal tension cracks are inclined at 45° to the longitudinal axis of the beam, as is in NZS3101: 1995.

As for columns, Priestley and Park suggested different shear strength reduction factors. The shear strength reduction factors were 0.75 and 0.85 respectively for the methods proposed by Priestley and Park.

2.5.5 Shear Capacity of Reinforced Concrete Beam-Column Joints

It is very common that there is no, or insignificant, transverse reinforcement in the beam-column joint cores in pre-1970s reinforced concrete frame structures. In this case, NZS3101: 1995 implies that the shear strength of the joint core is negligible. However Hakuto et al[Hakuto 1995] and Priestley [P22] pointed out that beam-column joints without any, or insignificant, transverse reinforcement in the joint cores, do have some shear strength, particularly if the joint core is uncracked or if plastic hinges undergoing cyclic deformations in the post-elastic range do not occur adjacent to the joint core.

Conceptually, the shear resisting mechanisms between interior and exterior beam-column joints are different. Hence the probable shear strength of the interior beam-column joints is expected to be different from that of the exterior beam-column joints.

2.5.5.1 Interior Beam-Column Joints

Having reviewed the vast body of test data, useful in this regard, assembled by Japanese, New Zealand and USA researchers, Priestley proposed tentative recommendations to estimate shear strength of interior beam-column joints.

Priestley [P5] outlined that the joint shear failure is due to either the principal tension stress or the principal compression stress in the joint concrete.

When the beam longitudinal reinforcement is light or high column axial forces exist, the critical parameter is the principal tension stress in the joint, rather than the shear stress level. In this case, Priestley recommended using the model as shown in Fig.2.14, which was developed by Hakuto, Park and Tanaka, based on tests on as-built beam-column joints with deformed longitudinal reinforcement. The degradation of joint shear strength is expressed in terms of k in Fig.2.14. Hakuto et al [H1] suggested that for beam-column joints without shear reinforcement the maximum probable horizontal joint shear force that can be resisted is:

$$V_{jh} = v_{ch}\, b_j \mathrm{h} = \mathrm{k}\sqrt{f_c'}\,\sqrt{1+\frac{N^*}{A_g k\sqrt{f_c'}}}\, b_j \mathrm{h} \qquad (6)$$

where v_{ch}=nominal horizontal joint shear stress carried by a diagonal compressive strut crossing the joint, b_j=effective width of the joint, h = depth of column, N^* is the axial load on columns, and other parameters have the same meanings as before.

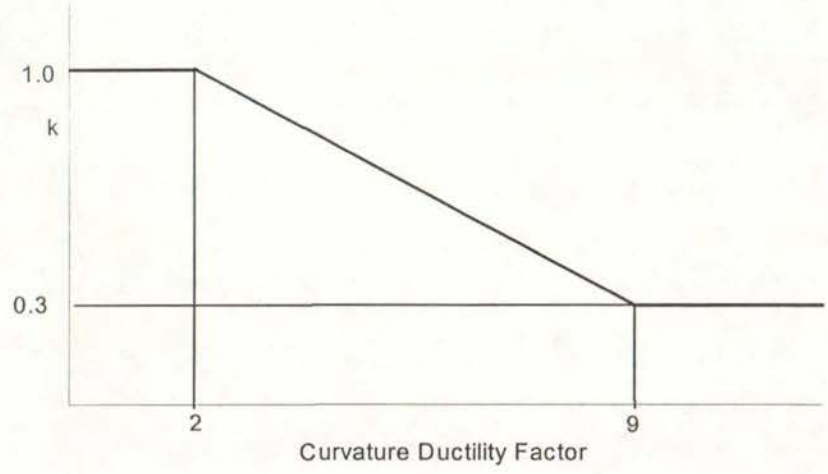

Fig. 2.14 Principal Tension Model of Degradation of Concrete Shear Resisting Mechanism of Interior Beam-Column Joints [Hakuto et al 1995]

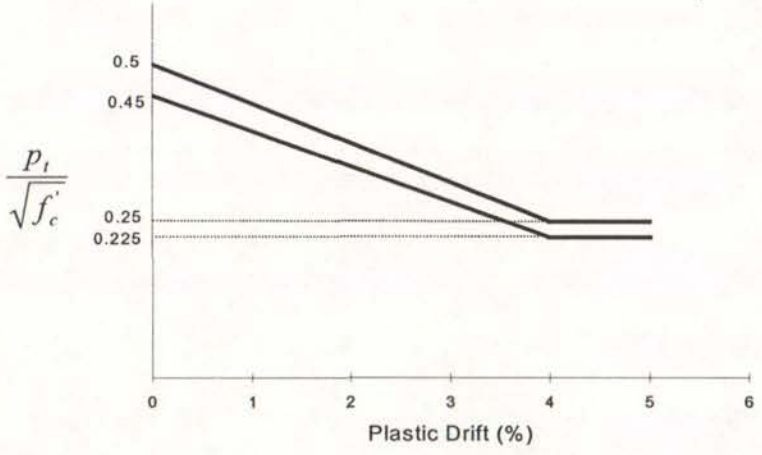

Fig.2.15 Principal Compression Model of Degradation of Concrete Shear Resisting Mechanism of Interior Beam-Column Joints [P22]

When the shear stress level is high in the joint, interior beam-column joints tend to fail in shear, regardless of the amount of joint shear reinforcement. In this case, the failure is as a result of the principal compression stress. The model proposed by Priestley for estimating the joint shear strength in this case is the principal compression model. The

postulated principal compression model is shown in Fig.2.15, which was deduced by setting the upper limit in association with the principal compression stress not greater than 0.5 concrete compression strength.

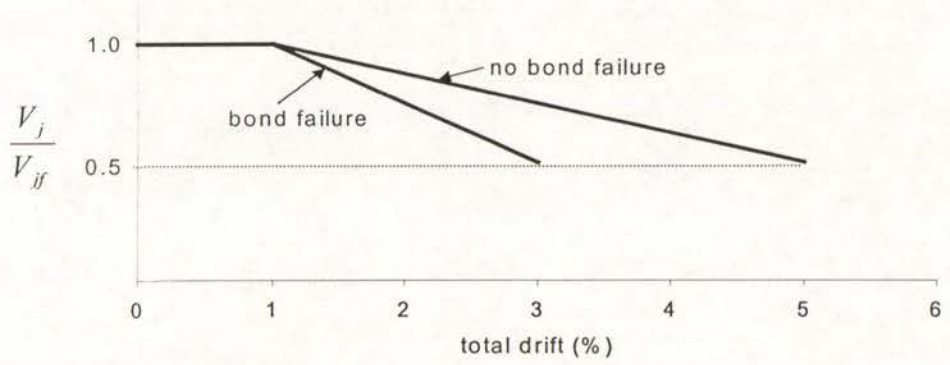

Fig.2.16 Possible Shear Strength Model of Interior Beam-Column Joints [P22]

However, Priestley did not give clear definition for principal tension failure and principal compression failure.

In addition, Priestley also postulated a simpler model as shown in Fig.2.16 in order to allow for the influence of bond performance on the joint shear strength degradation. The degradation is assumed to start at 1% drift, regardless of poor bond or adequate bond and regardless of the actual shear stress or principal stress level. However, this model has no support from test results.

Park also recommended using the model developed by Hakuto et al as shown in Fig. 2.14 for degradation of shear strength resisted by concrete mechanism of interior beam-column joints without joint horizontal shear reinforcement, but without clarifying the failure type of the joints. This model is clearly the principal tension model Priestley used.

Apparently, more testing needs to be conducted to identify different failure modes of the joints and develop reliable models for estimating the degradation of joint shear strength correspondingly.

2.5.5.2 Exterior Beam-Column Joints

Similar to interior beam-column joints, the maximum probable horizontal joint shear force that can be resisted by exterior beam-column joints without shear reinforcement is suggested to be calculated by equation 6.

The degradation of the horizontal joint shear strength, when expressed in terms of k, is proposed to be represented by Fig. 2.17 by Priestley, and it was based on the tests of unreinforced exterior and corner joints. The degradation of the horizontal joint shear force, when expressed in terms of k, is proposed by Park to be represented by Fig.2.18, and it was based mainly on test results of Hakuto et al.

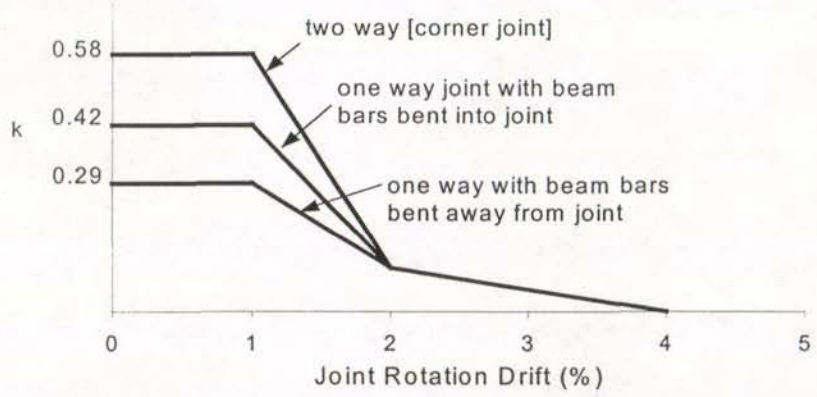

Fig. 2.17 Degradation of Joint Shear Force Resisted by Concrete Mechanism for Exterior Beam-Column Joints [Prietley P22]

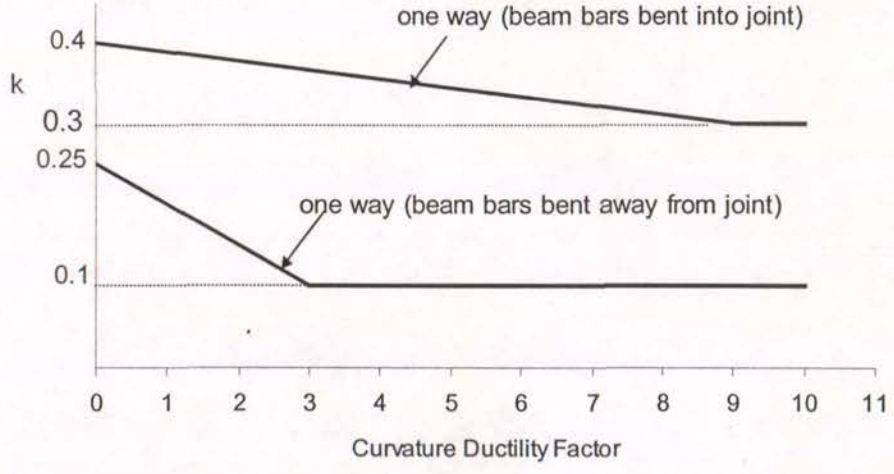

Fig. 2.18 Degradation of Joint Shear Force Resisted by Concrete Mechanism for Exterior Beam-Column Joints [Park, P6]

Both the model proposed by Priestley and the model proposed by Park assumed that the joint shear failure in exterior beam-column joints is as a result of large principal tension stress. A significant difference of the model proposed by Priestley, from the model proposed by Park is that Priestley prefers to use drift as an index of the post-elastic deformation.

It is noted that the models proposed by Priestley and Park are based on very limited test results. Evidently, more tests on as-built beam-column joints are needed in order to refine the models.

2.5.6 Flexural Deformation Capacity in Plastic Hinges

Assessment of the displacement ductility capacity of the structures needs to define the plastic rotation capacity of beams and columns. Rotational capacity of plastic hinges is given by

$$\theta_p = (\phi_u - \phi_y) l_p \qquad (7)$$

where:

ϕ_u and ϕ_y are respectively the ultimate and yield curvatures of the members, and l_p is the equivalent plastic hinge length.

Priestley [P22] and Park [P6] proposed exactly the same methods for determining l_p, ϕ_u and ϕ_y.

l_p is calculated by:

$$l_p = 0.08\mathrm{L} + 0.022\ f_y\ d_b \qquad (8)$$

where:

f_y is the yield strength of the longitudinal reinforcement,

d_b is the diameter of the longitudinal reinforcement

and L is the distance from the critical section to the point of contraflexure.

In calculating the ultimate curvatures of beams and columns, the ultimate concrete strain ε_{cu} for unconfined concrete is suggested to be 0.005, and that for confined concrete is given by:

$$\varepsilon_{cu} = 0.004 + 1.4\,\rho_s f_{yh} \varepsilon_{su} / f'_{cc} \qquad (9)$$

$$\rho_s = 1.5\ \frac{A_v}{b_c s} \qquad (10)$$

where:

A_v =total area of transverse reinforcement in a layer at spacing s

b_c = width of member core measured from centre to centre of the peripheral transverse reinforcement in the web

f_{yh} = the yield strength of transverse reinforcement

ε_{cu} = the strain of the transverse reinforcement at maximum stress

and $f_{cc}^{'}$ = the compression strength of the confined concrete

2.5.7 Summary

To realistically estimate member strength and deformation capacity, probable material strength rather than nominal material strength should be used. In the case of the lack of information on the actual material strength, 1.1 times the nominal steel yield strength and 1.5 times the nominal concrete compression strength should be used.

Unlike modern reinforced concrete structures designed to current codes, premature shear failure of members (beams and columns) and joints of existing reinforced concrete structures, when reinforced by deformed longitudinal reinforcement, is observed to degrade with the increase in the imposed flexural deformation. As a result, a mechanism which initiates with flexural plastic hinges may degenerate into plastic hinges with shear failure as the ductility demand increases. Consideration of degradation of shear strength is very critical in this case. Design code equations are considered to be not suitable in estimating the member strength and deformation capacity.

The current method for estimating member flexural strength is basically the same as code equation, except that probable material strength and a strength reduction factor of unity are used.

The current method for estimating the initial column shear strength and its degradation with the increase in the imposed flexural deformation is based on extensive test results, and one major difference from design code equation is that the influence of column axial load on the enhancement of column shear strength is taken as the horizontal component of the column compressive strut.

Meanwhile, the current method for estimating the initial beam shear strength and its degradation has not been adequately testified. There is no agreement for the assumed angles of the critical diagonal tension cracks to the longitudinal axis of the beam.

Estimation of shear strength of beam-column joints is still the most difficult task. Current models for predicting joint shear strength and deformation capacity propose to use different models for different failure modes, but only the principal tension models, which assume that the joint shear failure is due to large principal tension stress generated in the joint concrete, were established based on very limited test data. Apparently, the failure mechanism of beam-column joints is still unclear.

A major concern is that the current methods are based on the tests with deformed longitudinal reinforcement. When plain round longitudinal bars are used, reinforced concrete components may have different critical failure modes. The strength and deformation capacity of correspondent critical failure modes in this case needs to be investigated.

2.6 Retrofit of Existing Reinforced Concrete Structures

2.6.1 General

In most cases retrofit methods are associated with an increase in the strength and stiffness of regions of the structure. Possible retrofit measures need to be carefully assessed to ensure that the seismic characteristics of the structure will be improved. Seismic assessment procedures based on capacity design can be used in this regard provided the information on the strength and deformation capacity of retrofitted members is available.

Retrofit methods typically involve adding new structural components to the existing structure, such as movement restrainers, walls, steel bracing, and jacketing [A7, H1, P23, P24, P25, R1, R2, S9].

2.6.2 RETROFITTING OF COLUMNS

Columns are particularly vulnerable elements in buildings. Several methods for increasing the strength and/or ductility of existing columns have been developed, tested and used in the United States and New Zealand. These methods include jackets of new concrete containing longitudinal and transverse reinforcing [R2, S9], grouted site welded circular thin jackets [P23], site welded elliptical thin steel jackets filled

with concrete, grouted stiffened or built-up rectangular steel jackets, grouted composite fiberglass/epoxy jackets [P25], or prestressing steel wrapped under tension[P23]. Methods for calculating the required size of jackets are given elsewhere, for example reference P23.

The column retrofit can be designed so as not to increase the flexural strength, but to provide only additional transverse reinforcement for concrete confinement, restraint against buckling of existing longitudinal bars, shear resistance and restraint against bond failure of lap splices of longitudinal reinforcement. In such case the strengthening is not continued beyond the ends of the column, so that the flexural strength of the column ends is not increased. Alternatively, the strengthening can be continued beyond the ends of the column so that the flexural strength of the column ends is increased. This requires passing longitudinal reinforcement through the floors in the case of a building.

The most successful technique for providing additional transverse reinforcement, without additional longitudinal reinforcement, has been the use of thin steel jackets[P23]. For circular columns the thin jacket is constructed slightly oversize in two semi circular halves which are welded up vertical seams in situ. The jacket is terminated about 25 mm from the face of the beams or footing at the column ends. The gap between the steel jacket and the column is subsequently pressure filled with a cement-based grout which contains a small quantity of water reducing expansive additive. For rectangular columns an elliptical thin steel jacket is used to provide continuous confinement, with concrete placed between the jacket and the column. A rectangular thin steel jacket would not be so effective for confinement, due to the sides bowing out when dilation of the concrete occurs during a major earthquake, resulting in confinement applied mainly in the column corners.

The use of fiberglass/epoxy jackets for columns of buildings and bridges is becoming common in New Zealand. Typically the fiberglass sheets with epoxy are wrapped around the columns and are not grouted.

2.6.3 RETROFITTING OF BEAM-COLUMN JOINTS

Beam-column joint regions can be retrofitted by jacketing, using either external steel jacketing[A7] or jacketing with new reinforced concrete [P23]. This can be a very labour intensive and costly procedure, due to the drilling of holes through the existing

joint to pass new reinforcement through. One solution, which has been proposed as a result of tests on full scale beam-column joint assemblies is to enlarge the existing beam-column joints without placing new hoops [A7]. It has been found that no new hoops are required in the added jacket if the resulting nominal horizontal shear stress in the enlarged joint core is reduced to less than $0.3\sqrt{fc'}$ MPa [A7,H1].

Another solution, which has been adopted for beam-column joints, has been to remove the existing concrete joints and to replace the whole joint region with new reinforced concrete.

2.7 Conclusions

The possible design deficiencies in existing reinforced concrete structures designed to pre-1970s seismic design codes are as a result of two major failings in outdated seismic design codes. One is that the now outdated seismic codes did not have the design specifications associated with the member local ductility behaviour, the other is that the now outdated seismic codes did not have the design specifications associated with the structural global behaviour during the post-elastic loading cycles. As a consequence, the greatest uncertainty of the seismic performance of existing reinforced concrete structures is the post-elastic behaviour in a major earthquake.

There are currently two types of assessment procedures, check list type and capacity design based. Check list seismic assessment procedures emphasise the statistical study of the observed earthquake damage in past earthquakes and emphasise member local behaviour, but did not identify the critical post-elastic failure mechanism, failing in adequately assessing the structural post-elastic seismic performance, which is the core element needed to be investigated. Hence, check list assessment procedures could give irrational results. However, check list procedures are easy to follow, are suitable for statistical study of earthquake damage because of the procedures' nature. Therefore they can be used for City Earthquake Disaster Prevention and Preparation Programs.

Capacity design based seismic assessment procedures aim at investigating the post-elastic response of existing reinforced concrete structures, and thus can realistically assess the seismic performance of the structures.

When capacity design based seismic assessment procedures are used for the seismic assessment of an existing reinforced concrete structure, the required information is

member strength and deformation capacity, namely, member local behaviour. The fundamental aspects here are to determine the most critical failure mode of the member and to determine the strength degradation of identified critical failure mode with the increase in the imposed flexural deformation.

When deformed bars are used for longitudinal reinforcement, shear failure in members (beams and columns) and beam-column joints is observed to be very critical. The determination of degradation in shear strength of members and joints, in this case, is of particular importance. Several models for determining the shear strength degradation of members and beam-column joints are developed, but they are based on very limited test results. This is especially true for the models for reinforced concrete beams and beam-column joints designed to now outdated seismic codes. More testing is urgently needed to refine the current models.

Variety of seismic retrofit techniques have been developed, some retrofit techniques aim at improving the member strength and/or ductility capacity, and the others aim at improve the structural global behaviour during the post-elastic loading cycles. One needs to investigate the post-elastic performance of the upgraded structure during a major earthquake to make sure that the used retrofit technique did not shift the problem.

Finally, the steel type (deformed bars or plain round bars) can make a big difference in not only the critical failure mode of the members, but also in the member strength and deformation performance. Therefore, when plain round longitudinal bars are used, proper models for estimating strength and deformation capacity of reinforced concrete members need to be developed based on laboratory testing.

CHAPTER 3

REVIEW OF PREVIOUS RESEARCH PROJECTS RELEVANT TO THIS PROJECT AT UNIVERSITY OF CANTERBURY

The research program "Seismic Assessment and Retrofit of Existing Reinforced Concrete Structures" started in 1989 at the University of Canterbury sponsored by the Earthquake Commission of New Zealand. Four research projects have been conducted since then and the proposed project here is a continuation of the previous four research projects.

3.1 THE INVESTIGATED STRUCTURE

The subject structure of the previous four research projects was a seven-storey reinforced concrete frame structure constructed in Christchurch, New Zealand, in the 1950s, and it has been thoroughly investigated. The typical deficiencies identified of this reinforced concrete frame building are as follows [H1]:

(1). Columns with inadequate longitudinal reinforcement to ensure strong column-weak beam behaviour.

(2). Columns and beams with inadequate transverse reinforcement for concrete confinement and prevention of premature buckling of longitudinal compression bars, and/or inadequate transverse reinforcement for shear resistance.

(3). Small quantities of joint shear reinforcement or no joint shear reinforcement at all.

(4). Greater diameter of the beam longitudinal reinforcement passing through the joints than that required by NZS3101: 1995 [N1], hence significant loss of anchorage of reinforcement would occur in that region if ductile structural behaviour is required.

(5). Poor anchorage details of longitudinal beam bars in exterior columns.

(6). Longitudinal beam and column bars with lap splices in potential plastic hinge regions near beam-column joints.

3.2 ANALYSIS OF THE AS-BUILT STRUCTURE

Hakuto, Park, and Tanaka [H1] carried out a static analysis of the whole as-built building using the current code approach to estimate the lateral load capacity of the structure, and the shear and ductility demands of the members and beam-column joints; in addition they also conducted a non-linear dynamic analysis using the two-dimensional time-history non-linear frame analysis program "RUAUMOKO" of the whole building to investigate the drift demand of the structure, and the shear and ductility demands of the members and joints under the El Centro and the Bucharest earthquake records. The analysis of this reinforced concrete frame building indicated that the available lateral load strength of the complete structure approached the design seismic force assuming elastic response obtained from the current New Zealand standards. The inelastic failure mechanism of the frame was identified to be a mixture of flexural and shear failures in the beams and columns.

A critical aspect with respect to shear was found to be the behaviour of the beam-column joints with little or no shear reinforcement, as a result of the relatively large joint shear forces. The estimated maximum nominal joint shear stresses in the lower storey by the static analysis, calculated from the beam face moments and column shear forces acting on the joints, ranged from $1.2\sqrt{f_c'}$ MPa to $1.5\sqrt{f_c'}$ MPa for the interior beam-column joints, and ranged from $0.6\sqrt{f_c'}$ MPa to $1.0\sqrt{f_c'}$ MPa for exterior beam-column joints. These by far exceeded the joint shear stress level associated with the estimated joint shear strength reached at the stage of initial diagonal tension cracking of the joint core. Typically the maximum exterior joint shear capacity is $0.25\sqrt{f_c'}$ MPa for the case with the beam longitudinal reinforcing bars bent away from the joint core if estimated using the proposed procedures by Park [P6]. Hence, the seismic performance of the early reinforced concrete frames was likely to be governed by joint shear failure.

The estimated maximum axial column load level by the static analysis was 0.24 for the interior column and 0.3 for the exterior column, in the first storey respectively, when the roof horizontal displacement was 1% of the total height. The estimated maximum axial column load level by the dynamic analysis was 0.26 and 0.31 for the interior column and exterior column in the first storey respectively. The axial column load level was

expressed as $N^* / A_g f_c^{'}$. Evidently, axial column load was very significant in some cases, and neglecting its influence on the seismic behaviour of the beam-column joint units could give misleading results.

The maximum inter-storey drift angle found by the static analysis using the code approach was approximately 1.20%, and the maximum interstorey drift angle found by the dynamic analysis was 0.7% under El Centro record and 2.9% under Bucharest record.

3.3 THE FIRST STAGE OF THE RESEARCH SERIES - COLUMNS

The first stage of the experimental research series involved the simulated seismic loading tests on four near full-scale column replicas of the first storey of the subject building at the University of Canterbury [R1, R2]. The aim of this project was to investigate the seismic performance of as-built columns and the increase of strength, stiffness, and ductility which can be achieved by jacketing existing damaged or undamaged reinforced concrete columns with new reinforced concrete. The as-built columns, which were 350 mm square, were reinforced by plain round reinforcement and contained low quantities of transverse reinforcement. The column units represented the column region between the mid-heights of successive stories. Two columns units were tested as-built to study the seismic behaviour and damage during major earthquakes, and then repaired and strengthened by reinforced concrete jacketing and retested. The other two column units were strengthened by reinforced concrete jacketing before being damaged and then tested. The new longitudinal reinforcement in concrete jacket was placed through the floor slab. Two arrangements of transverse reinforcement in the jacket were devised to properly tie the longitudinal reinforcement. The as-built columns displayed low available ductility and significant degradation of strength during testing due to inadequate column transverse reinforcement and severe bar slip owing to the utilisation of plain round longitudinal bars. The jacketed columns behaved in a ductile manner with higher strength and much reduced strength degradation during testing. The retrofit of columns using reinforced concrete jackets was found to be successful but labour intensive.

3.4 THE SECOND STAGE OF THE RESEARCH SERIES –INTERIOR BEAM-COLUMN JOINT ASSEMBLIES

The second stage of this experimental research series involved the simulated seismic loading tests on three full-scale replicas of the interior beam-column joint region of the perimeter frame of the subject building in order to investigate the seismic performance of existing reinforced concrete structures and the effectiveness of reinforced concrete jacketing as a repair and strengthening measure [H1, H2].

The test units were identical to that part of the frame between the mid-span of the beams and the mid-height of the interior columns of the as-built reinforced concrete frame structure as described previously [H1]. The reinforcing details in the members and joints were as in the as-built structure, and hence did not meet the requirements of the current New Zealand concrete design code NZS 3101:1995. Deformed reinforcement was used for longitudinal reinforcement.

One of the interior beam-column joint replicas was tested as-built subjected to simulated seismic loading. The test confirmed that the performance of the as-built beam-column joint region would be poor in a major earthquake, mainly due to the lack of joint shear reinforcement and poor anchorage of longitudinal beam bars in the beam-column joint region. The damaged (tested) beam-column joint unit and the other two undamaged (not tested) beam-column joint units were then retrofitted by jacketing with new reinforced concrete to increase the strength and ductility of the existing frame. All retrofitted interior beam-column joint units were then tested subjected to simulated seismic loading and performed in a very satisfactory manner. It was found that the concrete jacketing technique could be used for extending the life of existing reinforced concrete structures and for the repair of damage arising from major earthquakes.

3.5 THE THIRD STAGE OF THE RESEARCH SERIES - INTERIOR AND EXTERIOR BEAM-COLUMN JOINT UNITS

The third stage of the research series involved the seismic load testing and analysis of four full-scale replicas of other beam-column joint regions of the 1950s building frame [H1, H3]. Deformed longitudinal reinforcing bars were used for longitudinal reinforcement again. Two of the subassemblies were further interior beam-column joint subassemblies which lacked joint shear reinforcement. These two specimens had different

column depth to beam bar diameter ratios and were tested mainly to investigate the effect of the bond conditions along the beam bars passing through the joint on the seismic behaviour of beam-column joints without joint shear reinforcement. Changing the beam bar diameter to column depth ratio from 1/25 to 1/18.75 was found not to have a significant effect on the seismic performance of joints without joint transverse reinforcement. The other two specimens were exterior beam-column joints with limited shear reinforcement and with different arrangements of beam bar hooks in the joint core. One exterior beam-column joint specimen had the beam bar hooks bent away from the joint core, as was common in many early frames; and the other exterior beam-column joint specimen had the beam bar hooks bent into the joint core, as is the current practice. Tests demonstrated that the seismic performance of the exterior beam-column joints with little shear reinforcement was significantly influenced by the directions in which the tails of the beam bars in the joint core were bent. It was found that the exterior beam-column joint subassemblies of early frames in which the tails of the beam bars were bent out of the joint core would behave unsatisfactorily during a major earthquake.

3.6 THE FOURTH STAGE OF THE RESEARCH SERIES - INTERIOR BEAM-COLUMN JOINT UNITS

Two additional full-scale replicas of interior beam-column joints in which the longitudinal beam bars were lap spliced in the plastic hinge regions of the beams were also tested by Wallace 1996 [W1]. One specimen contained plain round longitudinal bars and the other contained deformed longitudinal bars. Tests illustrated very limited ductility available from this poor detail during seismic loading, especially when plain round bars were used.

3.7 SUMMARY

Evidently, the research work in this research program conducted so far has been focused on the study of the possible seismic performance and retrofit methods of as-built reinforced concrete frame structures, with the emphasis on the use of deformed bar reinforcement. Actually, plain round bar reinforcement was used in New Zealand until about the mid 1960s when deformed bar reinforcement became widely available. The

reliability of using the obtained information in the past research stages for the existing reinforced concrete structures reinforced by plain round bars apparently needs to be re-examined. Actually, the observed evidence of severe bond slip for the tests on as-built columns conducted in the first stage already suggested the need for the investigation of the seismic performance of existing reinforced concrete structures with plain round longitudinal bars.

In addition, these previous beam-column joint tests were conducted with zero axial column load. The estimated maximum column axial load level by Hakuto et al was as high as 0.31, the influence of so high axial column load on the seismic behaviour of the actual structural performance is apparently significant, and needs to be allowed for.

CHAPTER 4

TEST UNITS AND THEORETICAL CONSIDERATIONS

4.1 INTRODUCTION

Review of the researches at the University of Canterbury into the seismic assessment and retrofit of pre-1970s reinforced concrete frame structures, conducted in chapter 3, indicates that the as-built beam-column joint subassemblies tested in the previous research projects used deformed longitudinal reinforcement and hence the resulting information on the member local behaviour from the previous beam-column joint tests is only applicable to the situations where deformed bars are used for longitudinal reinforcement. There is an urgent need for obtaining the information on the local behaviour of beam-column joint subassemblies, which are reinforced by plain round bars and designed to now outdated seismic design codes.

Hence experimental work carried out in this current research project investigated the failure mechanism, the available strength, stiffness and ductility capacity of as-built beam-column joint subassemblies when reinforced by plain round bars. The effective retrofit methods of as-built beam-column joint subassemblies reinforced by plain round bars are also testified where necessary. Emphasis is placed on the effect of the plain round longitudinal bars used on the seismic behaviour of as-built beam-column joint subassemblages, compared to the cases with deformed longitudinal reinforcement.

This chapter introduces the units tested in this test scheme of the current research project.

4.2 DETAILS OF TEST UNITS

4.2.1 General

The as-built beam-column joint subassemblies, reinforced by deformed bar reinforcement and representing the subject frame building constructed in 1950s in New Zealand, have been tested under simulated seismic loading by Hakuto et al at the university of canterbury [H1]. The beam-column joint test units in the current research project were designed to be identical to the test units conducted by Hakuto et al [H1], except that the plain round bars were used for the longitudinal reinforcement. Such a test unit design aimed at identifying the effect of the use of plain round longitudinal reinforcement by

comparing the observed test evidence in this project with the test evidence observed by Hakuto [H1].

Totally the current project involved six as-built full-scale beam-column joint test units and one retrofitted exterior beam-column joint unit. The six as-built test units include two interior beam-column joint units and four exterior beam-column joint units.

4.2.2 Details of the Interior Beam-Column Joint Units

Two identical one-way interior beam-column joint units were constructed, each full-scale in size, containing plain round longitudinal reinforcement and with reinforcement details typical of the 1950s construction in New Zealand. These two units were identical to Hakuto's Unit O1 except that Hakuto used deformed longitudinal bars, and were referred to as Unit 1 and Unit 2. The overall dimensions and reinforcing details of the two identical as-built interior beam-column joint units are shown in Fig. 4.1.

The beams were 500 mm in depth and 300 mm in width, and the columns were 300 mm in depth and 460 mm in width. The test units were identical to that part between the mid-span of the beams and the mid-height of the columns of a seven-storey existing reinforced concrete frame structure constructed in the 1950s in New Zealand, which has been described previously [H1].

The beams were unsymmetrically reinforced, contained four 24 mm diameter Grade 300 plain round bars in the top ($p = 0.013$) and two 24 mm diameter Grade 300 plain round bars in the bottom ($p' = 0.0068$). The beam transverse reinforcement was from 6 mm diameter Grade 300 plain round bars placed at 380mm centres, and the first stirrup was 300 mm from the column face. The columns were symmetrically reinforced, and contained three 24 mm diameter Grade 300 plain round bars on both sides ($p_t = 0.02$). The column transverse reinforcement was from 6 mm diameter Grade 300 plain round bars placed at 230 mm centres, and the first tie was 100 mm from the beam face. The beam-column joint cores contained no transverse reinforcement or intermediate column bars (at the mid-depth of the columns).

The concrete for Units 1 and 2 was normal weight. The units were cast in one stage in the horizontal plane. Table 4.1 lists details of concrete compressive cylinder strengths of Units 1 and 2 at the time of testing the units and the axial load ratios applied to the columns during testing. For both units, all R24 plain round longitudinal reinforcing bars were taken from the same steel batch. Similarly, all R6 transverse reinforcement was

taken from the same steel batch. Table 4.2 lists details of the reinforcement for Units 1 and 2.

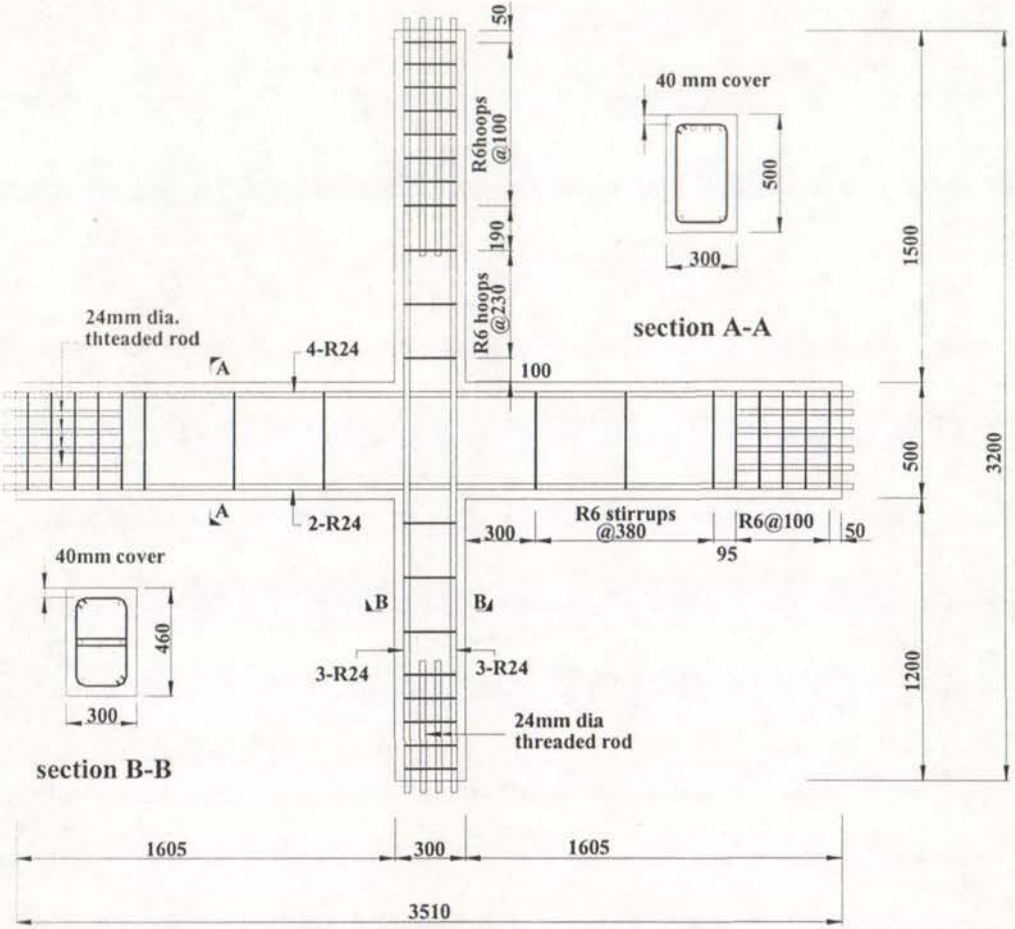

Fig.4.1 Reinforcement Details of the Two Interior Beam-Column Joint Specimens

Table 4.1 Compressive strengths of concrete at the time of testing the Units

Unit	f_c'(MPa)	$N^*/A_g f_c'$
Unit 1	44	0
Unit 2	49	0.12

Table 4.2 Details of Reinforcement in the Units

Part of Unit	Longitudinal Reinforcement						Transverse Reinforcement		
	d_b (mm)	f_y MPa	ε_y $x10^{-6}$	p %	p' %	p_t %	d_b (mm)	f_{yt} (MPa)	s (mm)
Beam	24	321	1560	1.36	0.68		6	318	380
Column	24	321	1560			1.97	6	318	230

4.2.3 Details of the Exterior Beam-Column Joint Units

Four one-way exterior beam-column joint units, which were identical to each other except for the anchorage of the beam longitudinal bars in the exterior columns, were constructed. Each unit contained plain round longitudinal reinforcement and had other reinforcement details typical of the 1950s construction in New Zealand.

The first two exterior beam-column joint units were identical to each other, and had beam bar hooks bent away from the joint core in exterior columns. The straight extension of the beam bars beyond the bends was four times the bar diameter, as was typical of pre-1970s construction in New Zealand. These two units are referred to as Units EJ1 and EJ3. Unit EJ1 and Unit EJ3 were identical to Hakuto's Unit O7 except that Hakuto used deformed longitudinal reinforcement. The overall dimensions and reinforcing details of the as-built test units EJ1 and EJ3 are shown in Fig.4.2 (a). The other two exterior beam-column joint units were also identical to each other, and had the beam bar hooks bent into the joint core in the exterior columns. The straight extension of the beam bars beyond the bends was twelve times the bar diameter, as is the current practice [N1]. These two units are referred to as Units EJ2 and EJ4. Unit EJ2 and Unit EJ4 were identical to Hakuto's Unit O6 except that Hakuto used deformed longitudinal reinforcement. The overall dimensions and reinforcing details of the as-built test units EJ2 and EJ4 are shown in Fig. 4.2 (b).

The beams of each exterior beam-column joint unit were 500 mm in depth and 300 mm in width and the columns were 460 mm square. The size of these units are identical to those of the perimeter planar frame of a seven-storey existing reinforced concrete frame structure constructed in the 1950s in New Zealand, which has been described previously [H1].

The beam was unsymmetrically reinforced, contained three 24 mm diameter Grade 300 plain round bars in the top ($p = 0.01$) and two 24 mm diameter Grade 300 plain round bars in the bottom ($p' = 0.0066$). The beam transverse reinforcement was from 6 mm diameter Grade 300 plain round bars placed at 380 mm centres. The columns were symmetrically reinforced, contained two 24 mm diameter Grade 300 plain round bars on both sides ($p_t = 0.0085$). The column transverse reinforcement was from 6 mm diameter Grade 300 plain round bars placed at 305 mm centres outside the joint region and at 250 mm centres within the joint region. The first column tie was 305 mm from the beam face.

The concrete was normal weight for all exterior beam-column joint units. The four units were cast in one stage in the horizontal plane. The R24 plain round longitudinal reinforcing bars of the four units were taken from the same steel batch. Similarly, all R6 transverse reinforcement of the four units was taken from the same steel batch. Table 4.3 lists details of concrete compressive cylinder strengths of Units EJ1, EJ2, EJ3 and EJ4 at the time of testing and the axial load ratios applied to the columns during testing. Table 4.4 lists details of the reinforcement for Units EJ1, EJ2, EJ3 and EJ4.

Table 4.3 Compressive strengths of concrete at the time of testing the Units

Unit	$f_c^{'}$ **(MPa)**	$N^* / A_g f_c^{'}$
Unit EJ1	33.7	0
Unit EJ2	29.2	0
Unit EJ3	34	0.25
Unit EJ4	36.5	0.23

Table 4.4 Details of Reinforcement in the Units of EJ1, EJ2, EJ3 and EJ4

Part of Unit	Longitudinal Reinforcement						Transverse Reinforcement		
	d_b (mm)	f_y MPa	ε_y x10^{-6}	p %	p' %	p_t %	d_b (mm)	f_{yt} (MPa)	s (mm)
Beam	24	321	1605	1.0	0.66		6	318	380
Column	24	321	1605			0.85	6	318	305

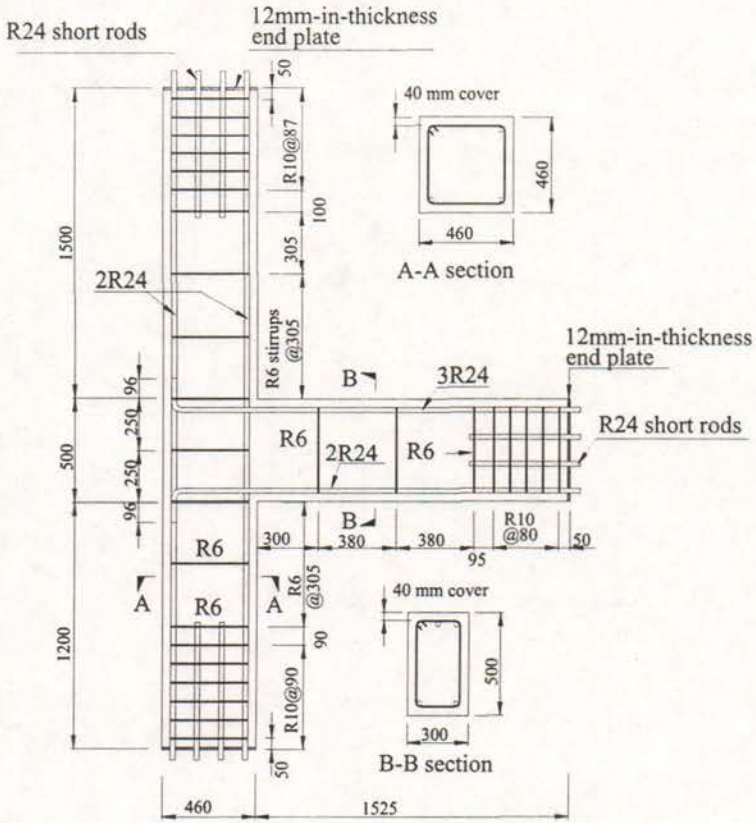

(a) Units EJ1 and EJ3 with Beam Bar Hooks Bent Away from Joint

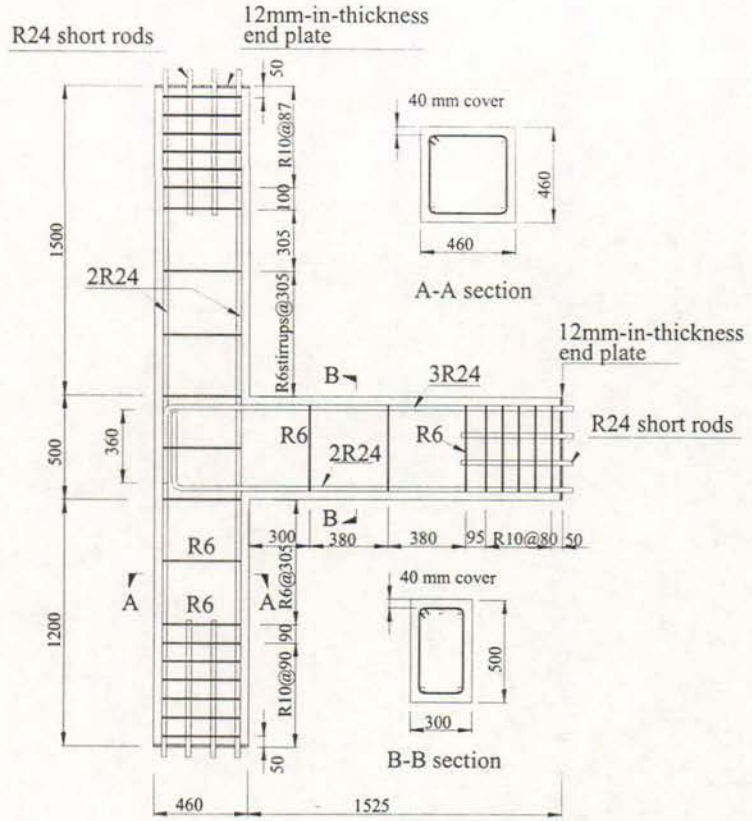

(b) Units EJ2 and EJ4 with Beam Bar Hooks Bent into Joint

Fig. 4.2 Overall Dimensions and Reinforcing Details of Exterior Beam-Column Joint Units

4.3 SEISMIC ASSESSMENT OF AS-BUILT TEST UNITS

The probable seismic performance of the as-built test units were assessed theoretically at first, and the assessment includes the identification of the critical failure mechanism, the calculation of the theoretical flexural strengths and curvature ductility capacity of the members, the estimation of the probable shear strength capacity of beams, columns and beam-column joints, and the investigation of the anchorage details of longitudinal reinforcement especially within the beam-column joints. The detailed theoretical assessment of the as-built interior and exterior beam-column joint units can be seen in Appendix A.

4.3.1 Interior Beam-Column Joint Test Units

4.3.1.1 Theoretical Flexural Strengths

Table 4.5 Theoretical Flexural Strengths and Curvature Properties of Members

		Flexural strengths (kN-m) ($\times 10^{-6}$)	Yield curvature ϕ_y (mm^{-1}) ($\times 10^{-5}$) +	Ultimate curvature ϕ_u (mm^{-1}) ($\times 10^{-5}$) +	Curvature ductility factor ϕ_u / ϕ_y +	$\frac{\sum M_{column}}{\sum M_{beam}}$
Unit 1	Beam negative	250	5.0	8.3	16	0.63
	Beam positive	129	4.4	10.3	23	
	Column *	108	8.6	10.6	12	
Unit 2	Beam negative	251	5.0	8.0	16	1.16
	Beam positive	129	4.4	10.8	25	
	Column **	198	10.7	6.4	6.0	

+ Calculated assuming no bond slip of longitudinal bars

* with zero axial column load present ** with axial column load present of $0.12 A_g f_c'$ (=800kN)

The flexural strengths of the beams and columns were calculated for the two interior beam-column joint units using the measured material strengths, assuming an extreme fibre concrete compressive strain of 0.003 and a rectangular compressive stress block as recommended by NZS3101: 1995 [N1] and a strength reduction factor ϕ of unity. The calculation was made on the basis of the assumption of perfect bond between steel and concrete. The curvatures at first yield and at ultimate for the beams and the columns were also calculated for both units assuming no bond slip of longitudinal bars using standard

theory [P1]. The ultimate curvature was calculated assuming that the ultimate compressive strain of the concrete was 0.004, which is a lower limit for the strain just before crushing and spalling of the compressed concrete. The theoretical flexural strengths, yield curvatures, ultimate curvatures and curvature ductility factors of the members are summarised in Table 4.5. From Table 4.5, it is evident that Unit 1 would develop plastic hinges in the columns and Unit 2 would develop plastic hinges in the beams during simulated seismic loading test. The storey shear at the theoretical flexural strengths of the critical members of the units was 80 kN for Unit 1 and 128 kN for Unit 2.

4.3.1.2 Investigation of Amount of Transverse Reinforcement

The investigation of the amount of transverse reinforcement in the members and the joints of existing reinforced concrete structures is of particular interest because out-dated seismic codes did not specify capacity design philosophy. The amount of transverse reinforcement according to NZS 3101: 1995 [N1] not only has to meet the requirement associated with the shear strength, but also has to meet the requirement associated with the confinement of the compressed concrete and prevention of the longitudinal bars from buckling.

In order to investigate the amount of transverse reinforcement associated with the shear strength, the imposed shear forces on the members and the joints during testing, which are associated with the above calculated theoretical flexural strengths of the units, are compared with the available shear strengths of the members and the joints in Table 4.6. The available shear strength of the plastic hinge regions were calculated using the methods of NZS3101: 1995 [N1] for structures designed for ductility, using the measured material strengths and assuming a strength reduction factor ϕ of unity. The shear strengths of the other regions were calculated using the non-seismic provisions of NZS3101: 1995. It is to be noted that NZS3101 does not give a method for calculating the shear strength of existing beam-column joints. The amount of transverse reinforcement needed to restrain the longitudinal bars against premature buckling in plastic hinge regions according to NZS 3101:1995 for structures designed for ductility are also compared with the actual quantities in Table 4.6. For the units, the column axial load ratios were low. Hence, the transverse reinforcement required to confine the compressed concrete of the columns was not as critical as that required for preventing the longitudinal bar buckling.

Table 4.6 Shear Forces Imposed and Shear Capacities of Beams, Columns, and Joints and Lateral Restraints of Longitudinal Bars

Parts of Units	Shear Requirement				Transverse Reinforcement for Lateral Restraint of Longitudinal Bars in Plastic Hinge Zones			
	Max. Imposed Shear Force (kN)		Shear Force Capacity (kN)		Required amount		Actual amount	
	Unit 1	Unit 2	Unit 1	Unit 2	Spacing (mm)	Area per set (mm^2)	Spacing (mm)	Area per set (mm^2)
beam	67	143	146 (204)	22 (70)	115	91	380	57
column	80	128	41 (134)	250 (358)	75	60	230	113
joint (H)	483	744	(268)	(550)	200	79	∞	0

Note: 1. (H) = horizontal direction

2. Maximum imposed shear forces and shear force capacities are calculated assuming that the plastic hinges formed in the columns of Unit 1 and in the beams of Unit 2; and the maximum imposed shear forces are calculated assuming that the Units reached their flexural strengths at the plastic hinges.
3. Shear force capacities shown without brackets are those calculated using the methods of NZS3101:1995 [N1] for ductile frames at the plastic hinges and for elastic behaviour elsewhere.
4. Shear force capacities shown with brackets are those calculated using the methods of Reference P6 assuming curvature ductility factor greater than 10 at the plastic hinges and elastic behaviour elsewhere. That is, the values of k used were:

   Unit 1 : For beams k = 0.2, columns k = 0.1 and joint k = 0.3
   Unit 2 : For beams k = 0.05, columns k = 0.29 and joint k = 0.3
5. The nominal shear stresses at the theoretical flexural strength of the columns of Unit 1 was $0.10\sqrt{f_c'}$ in the columns and $0.073\sqrt{f_c'}$ MPa in the beams;

   The nominal shear stresses at the theoretical flexural strength of the beams of Unit 2 was $0.15\sqrt{f_c'}$ in the columns and $0.15\sqrt{f_c'}$ MPa in the beams.
6. The nominal horizontal joint shear stresses at the theoretical flexural strength of the columns of Unit 1 was $0.5\sqrt{f_c'}$ MPa, and that at the theoretical flexural strength of the beams of Unit 2 was $0.8\sqrt{f_c'}$ MPa.

From Table 4.6, it is apparent that, for both units, both the spacing and the diameter of the beam and column transverse reinforcement in the plastic hinge regions met neither the requirement of NZS3101: 1995 [N1] for shear strength nor the requirements for the prevention of longitudinal bar buckling for structures designed for ductility.

Also shown in brackets are the shear force capacities of the beams, columns and beam-column joints calculated using the method recommended by Park [P6]. It is evident that the shear force capacities calculated using the methods proposed by Park are greater than those calculated using the methods of NZS3101: 1995 [N1]. For the two interior beam-column joint units, the shear force capacities calculated using the method recommended by Park [P6] were adequate except for the beams of Unit 2 and the beam-column joints of the units.

4.3.1.3 Anchorage Development of the Longitudinal Reinforcement

The development length of longitudinal reinforcing bars within the joint region is of concern as well, especially when plain round longitudinal reinforcement is used. The ratio of column depth to beam bar diameter, for both beam-interior column joint units, was $\frac{h_c}{d_b}$=12.5. According to NZS3101: 1995 [N1], the ratio of column depth to beam bar diameter when deformed longitudinal bars are used should not be less than 14.7 for Unit 1 assuming that plastic hinges form in the columns and 17.4 for Unit 2 assuming that plastic hinges form in the beams. The use of plain round longitudinal bars would require at least twice this needed development length, and on this approximate basis the ratio of column depth to beam bar diameter should not have been less than at least 30 for Unit 1 and 35 for Unit 2. Therefore, the available development length of the plain round beam bars was quite inadequate.

NZS3101: 1995 also has requirement for the development length of column longitudinal reinforcing bars within the joint region. The ratio of the beam depth to the column bar diameter for both interior beam-column joint units was 20.8. According to NZS3101: 1995, for ductile frames, the ratio of beam depth to column bar diameter, when deformed longitudinal bars are used, should not be less than 15.1 for Unit 1 assuming that plastic hinges form in the columns and 11.5 for Unit 2 assuming that plastic hinges form in the beams. As before, the use of plain round longitudinal bars would require at least twice this needed development length, and this means that the ratio of beam depth to column bar

diameter should not have been less than at least 30 for Unit 1 and 23 for Unit 2. Again, the available development length of the plain round column bars was inadequate.

Hence significant bond degradation, resulting in slip along the longitudinal bars, would be expected within the beam-column joint region of both units. Bond deterioration along the longitudinal reinforcement within the joint region may reduce the flexural strength and stiffness of the linear members and reduce ductility capacity of the whole building, but it may improve the shear strength of the joint core due to easier actuation of the joint concrete strut mechanism. The investigation into the joint performance is of particular importance because the beam-column joint cores of the as-built reinforced concrete structure were identified to be very critical in shear by the analysis of the whole structure.

4.3.1.4 Discussion of the Seismic Assessment

In a word, the conducted seismic assessment of the two as-built interior beam-column joint units identified three design deficiencies for Units 1 and 2.

(1). The amount of transverse reinforcement in the plastic hinge regions was not adequate for the prevention of the longitudinal bar buckling, according to current seismic code NZS3101: 1995.

(2). The shear force resisting capacities in beam-column joint cores of both units and in the beams of Unit 2 were inadequate.

(3). Significant bar slip within the beam-column joint regions along the longitudinal reinforcement would be expected. This was due to the combined effects of relatively small anchorage development lengths of the longitudinal reinforcement and the use of the plain round longitudinal bars.

However, it is to be noted that both the current seismic code NZS 3101: 1995 and the seismic assessment procedure proposed by Park [P6] are only applicable to the situations where the deformed longitudinal reinforcement was used, especially the procedure proposed by Park [P6], which was derived from limited experimental evidence obtained from beam-column joint assemblies reinforced by deformed longitudinal reinforcement. The predicted significant bar slip along the longitudinal reinforcement within the beam-column joint regions may improve the shear behaviour of the beam-column joint cores. This occurs due to the enhanced joint shear capacity resulting from the easier concrete

crack closing in the flexural compression side of the framing members. Also when plain round longitudinal reinforcement is used, the main shear resisting mechanism in linear reinforced concrete members becomes the robust concrete thrust, which is very different from the ones with deformed longitudinal bars, so the beams of Unit 2 may be not critical in shear.

As a result, the most critical design aspects of the units became big fixed-end rotations, due to severe bond degradation and slip along the longitudinal reinforcement within the joint core and/or inadequate transverse reinforcement required for preventing the longitudinal bar buckling and confining the compressed concrete, especially for preventing the longitudinal bar buckling in this case with relatively low level of column axial load.

4.3.2 Exterior Beam-Column Joint Test Units

4.3.2.1 Theoretical Flexural Strengths

As for the interior beam-column joint units, the flexural strengths curvatures at first yield and at ultimate of the beams and columns of the four exterior beam-column joint units were calculated assuming no bond degradation and using the measured material strengths, a rectangular compressive stress block as recommended by NZS3101: 1995 [N1] and a strength reduction factor ϕ of unity. Again the ultimate compression strain of the concrete was assumed to be 0.004 in calculating the ultimate curvature and 0.003 in calculating the flexural strengths of the members. The detailed investigation of the amount of transverse reinforcement in the members can be found in Appendix A. The theoretical flexural strengths, yield curvatures, ultimate curvatures and curvature ductility factors of the members are summarised in Table 4.7 for the four units. From Table 4.7, it is evident that all the four units would develop plastic hinges in the beams during simulated seismic load testing. The strengths of the test units in terms of storey shears at the theoretical flexural strength of the critical member, the beam, of Units EJ1, EJ2, EJ3 and EJ4 were about the same, being about 67 kN when governed by the beam negative flexural strength, and 45 kN when governed by the beam positive flexural strength. This was because the variation of concrete compressive strength has only small effect on the flexural strengths of members, as described by Brunsdon and Priestley in 1975 [B1], and the yield strength of the longitudinal reinforcement dominates the flexural strength of the members. The

longitudinal reinforcement steel used in Units EJ1, EJ2, EJ3 and EJ4 was from the same steel batch and was of the same steel property.

Table 4.7 Theoretical flexural strengths and curvature properties of members for exterior beam-Column Joints EJ1, EJ2, EJ3 and EJ4

Unit	Component of the Unit	Flexural strength of members (kN-m)	ϕ_y (mm^{-1}) $(\times 10^{-6})$	ϕ_u (mm^{-1}) $(\times 10^{-5})$	μ_ϕ $(=\frac{\phi_u}{\phi_y})$	$\frac{\sum M_{column}}{M_{beam}}$
EJ1	beam	129 (+) 190 (-)	4.5 (+) 4.9 (-)	9.9 (+) 8.6 (-)	22 (+) 18 (-)	2.07 (+)
	Column*	120	4.8	11.3	24	1.40 (-)
EJ2	beam	128 (+) 189 (-)	4.6 (+) 5.0 (-)	9.8 (+) 8.2 (-)	21 (+) 16 (-)	2.07 (+)
	column*	119	4.9	10.9	22	1.40 (-)
EJ3	beam	129 (+) 190 (-)	4.5 (+) 4.9 (-)	10 (+) 8.7 (-)	22 (+) 18 (-)	6.76 (+)
	column**	392	7.9	2.4	3	4.59 (-)
EJ4	Beam	129 (+) 190 (-)	4.5 (+) 4.9 (-)	10 (+) 8.7 (-)	22 (+) 18 (-)	6.90 (+)
	column***	400	7.7	2.5	3	4.68 (-)

\+ beam positive bending direction
\- beam negative bending direction
* with zero axial column load present
** with axial column load present of 0.25 $f_c^{'}A_g$
*** with axial column load present of 0.23 $f_c^{'}A_g$

4.3.2.2 Investigation of Amount of Transverse Reinforcement

Similar to the case for the interior beam-column joint units, the amount of transverse reinforcement in the members and the joints is also investigated for the four exterior beam-column joint units, and details can be seen in Appendix A.

The imposed shear forces on the members, which are associated with the above-calculated theoretical flexural strengths of the units, are compared with the available shear strengths of the members in Table 4.8. The available shear strengths of the members are calculated using the measured material strengths and assuming a strength reduction factor ϕ of unity.

Table 4.8 Shear, concrete confinement and anti-buckling

	Part of Units	Maximum Imposed Shear (kN)				Shear Force Capacity (kN)			
		EJ1	EJ2	EJ3	EJ4	EJ1	EJ2	EJ3	EJ4
Shear strength requirement	beams	113	113	113	113	22 (62)	22 (59)	22 (62)	22 (63)
	columns	67.5	67.2	67.5	67.5	156 (325)	147 (304)	255 (512)	257 (528)
	joint (H)	368	368	368	368	(141)	(361)	(505)	(933)
Concrete confinement and anti-buckling	Part of Units	Required Amount				Actual Amount			
		Spacing (mm)		Area (mm^2)		Spacing (mm)		Area (mm^2)	
	beam	115		68		380		56.6	
	columns	153		43		305		56.6	
	joint (H)	200		79		250		56.6	

1. H means horizontal joint shear.
2. The imposed horizontal shear force on the joint at the attainment of the theoretical strength of the units would result in a nominal horizontal joint shear stress $v_{jh} = V_{jh} / A_j$ of $0.05 f_c^{'}$ MPa, $0.06 f_c^{'}$ MPa, $0.05 f_c^{'}$ MPa and $0.05 f_c^{'}$ MPa, for Units EJ1, EJ2, EJ3 and EJ4, respectively. These v_{jh} values are also equivalent to $0.3\sqrt{f_c^{'}}$ MPa, $0.3\sqrt{f_c^{'}}$ MPa, $0.3\sqrt{f_c^{'}}$ MPa and $0.3\sqrt{f_c^{'}}$ MPa, for Units EJ1, EJ2, EJ3 and EJ4, respectively.
3. The maximum nominal shear stresses in the beams of all the Units at the negative flexural strengths of the beams were 0.82MPa, being $0.14\sqrt{f_c^{'}}$ MPa for EJ1, $0.15\sqrt{f_c^{'}}$ MPa for EJ2, $0.14\sqrt{f_c^{'}}$ MPa for EJ3 and $0.14\sqrt{f_c^{'}}$ MPa for EJ4.
4. The maximum nominal shear stresses in the columns were 0.35MPa, being $0.06\sqrt{f_c^{'}}$ MPa for Units EJ1, EJ2, EJ3 and EJ4.
6. The values with brackets are the estimated shear force capacities using the seismic assessment proposed in Reference P6, and the values without brackets are the estimated shear force capacities using current code method of NZS3101: 1995.

The available shear force strengths of the beams were calculated using the method of NZS3101: 1995 for structures designed for ductility because the beams of all the four tests were expected to form plastic hinges, and the available shear force strengths of the columns were calculated using the non-seismic provisions of NZS3101: 1995, since they

were not expected to develop plastic hinges. In addition, the available shear strengths of the members were also calculated using the seismic assessment procedures suggested by Park [P6], and the values are shown in brackets in Table 4.8. Table 4.8 shows that the shear force capacities of the members estimated using the method of current code NZS3101: 1995 are very conservative, compared to those estimated using the seismic assessment procedures proposed by Park [P6]. It is apparent from Table 4.8 that, for all the four exterior beam-column joint units, the available beam shear force strengths were quite inadequate according to both NZS3101 method and the seismic assessment procedure proposed by Park [P6]. The beam shear performance was hence expected to be very critical for all the four exterior beam-column joint tests.

The imposed shear forces on the joints during testing are calculated at the theoretical strengths of the units and are compared with the available joint shear strengths in Table 4.8 as well. The available shear strengths of the beam-column joints are estimated for the four exterior beam-column joint units only using the procedure proposed by Park [P6] because current code NZS3101 does not give a method for calculating the available shear force capacities of existing beam-column joints. Evidently, the available joint shear strengths estimated using the method proposed by Park [P6] are adequate except the joint shear capacity of Unit EJ1, which was tested with zero axial column load and had the beam longitudinal reinforcement bent away from the joint core.

Finally, the amount of transverse reinforcement needed for the confinement of the compressed concrete and for the prevention of the longitudinal bars from buckling by NZS3101: 1995 [N1] was also calculated and compared with the actual quantities in Table 4.8. The seismic assessment procedure proposed by Park [P6] gives no method for assessing the required amount of transverse reinforcement for preventing the longitudinal bar buckling and confining the compressed concrete. Table 4.8 illustrates that neither the spacing nor the cross sectional area of the beam and column transverse reinforcement met the requirement of NZS3101: 1995 for confinement of the compressed concrete and for the prevention of longitudinal bar buckling. In this case, significant bar buckling might take place, especially when high axial column load is present. For the tests, the axial column load was low, the column transverse reinforcement is more needed for anti-buckling than for confining the compressed concrete.

Another issue of concern could be the distance between the first set of ties in the column and that within the joint core for column bars not restrained against buckling by beam.

NZS3101: 1995 requires this distance not to be greater than 6 times the diameter of the column bar, namely, 124 mm. The actual distance was 305 mm, and this again indicates possible bar buckling of the outer column bars in the vicinity of the joint core.

4.3.2.3 Anchorage of Beam Longitudinal Reinforcement in Exterior Columns

The anchorage detail of the beam longitudinal bars in exterior column plays an important role in the transfer of the member forces across the joint core for exterior beam-column joint assemblies. NZS3101: 1995 requires the deformed beam longitudinal reinforcement to be bent into the joint core in exterior columns in order to engage the diagonal compression strut and hence to achieve the best force transmission path across the joint core, that is, corner to corner joint diagonal concrete compression strut. Apparently, the bending configuration of the beam longitudinal reinforcement in the exterior columns of Units EJ2 and EJ4 satisfied the current code requirement, but the used steel type did not satisfy the current code requirement. For Units EJ1 and EJ3, neither the used steel type of the longitudinal reinforcing bars nor the bending configuration of the beam longitudinal reinforcing bars in exterior columns met the requirements of the current seismic code NZS3101: 1995. As a result, two questions arise: one is how the member forces can be transferred across the joint cores of Units EJ1 and EJ3, and the other is how the use of the plain round bars affects the postulated joint shear force path for Unit EJ2 and Unit EJ4.

4.3.2.4 Discussion of the Seismic Assessment

In summary, the conducted seismic assessment of units EJ1, EJ2, EJ3 and EJ4 identified three critical issues.

(1). The beam transverse reinforcement was not adequate according to the requirement for shear resistance.

(2). The amount of transverse reinforcement in the beams and columns was inadequate for the prevention of buckling of the longitudinal reinforcement.

(3). The beam bar hook details of Unit EJ1 and Unit EJ3 did not provide the best force transfer across the joint cores and this is further aggravated by the use of the plain round longitudinal bars.

As stated in Section 4.3.1.4, severe bond degradation along the longitudinal reinforcement due to the use of plain bar reinforcement could cause the shear resisting mechanism in linear reinforced concrete members and the joint cores to be very different from the

postulated ones with the deformed bar reinforcement. The current seismic design and assessment procedures were established on the basis of the experimental data with deformed bars. Hence, the shear performance of the beam-column joint core of Unit EJ1 and the shear performance of the beam of the units may be not critical.

Regarding the effects of the beam bar hook details in the exterior columns and the use of the plain round longitudinal bars, the joint shear resisting mechanisms of the exterior beam-column joints are examined in detail in Section 4.4 in order to facilitate the understanding of the possibility of actuating an alternative joint force path when the beam bar hooks were bent away from the joint cores and also to facilitate the understanding of the effect of the use of plain round longitudinal bars.

4.4 SHEAR RESISTING MECHANISMS OF THE EXTERIOR BEAM-COLUMN JOINTS

4.4.1 Joint Shear Mechanisms of Exterior Beam-Column Joints EJ2 and EJ4

In designing exterior beam-column joints according to NZS3101: 1995[N1], the deformed beam longitudinal bars are required to be bent into the joint cores in exterior columns and adequate joint shear reinforcement needs to be provided. The postulated joint shear resisting mechanisms in this case by NZS3101: 1995 are a corner to corner joint concrete strut mechanism and one joint truss mechanism as shown in Fig. 4.3 (a) and 4.3(b).

As shown in Fig. 4.3, the resistance to the postulated joint concrete strut D induces lateral concrete tensile stresses around the beam bar hooks. This tendency is further exacerbated by the forces transmitted by the beam bar hooks to the outer layer of column longitudinal reinforcement, resulting in possible premature concrete failure due to tension cracking induced by the beam bar hooks. If this does occur, the beam bar hooks will open, similar to that of 90° stirrups after concrete cover spalling occurs, as suggested by the dotted line in Fig. 4.3 (c).

For well-designed exterior beam-column joint assemblies, deformed beam bar hooks are bent into the joint core and adequate joint horizontal hoop reinforcement is provided in the region of the beam bar hooks. Part of the beam tension force is transmitted to the joint core concrete by bond and resisted by the postulated joint truss mechanism shown in Fig. 4.3(b). Even if concrete tension cracking occurs along the beam bar hooks, adequate *joint horizontal shear reinforcement* can well restrain the opening action of the beam bar hooks, and an effective concrete strut mechanism can be activated within the joint core.

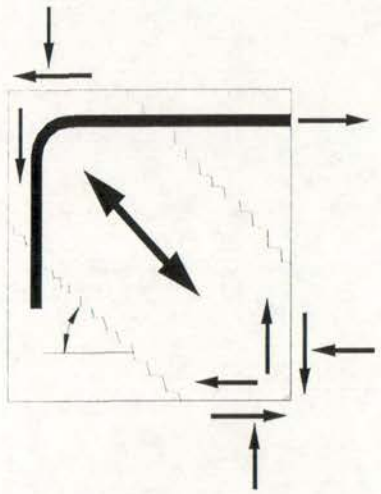

(a) Concrete Strut Mechanism

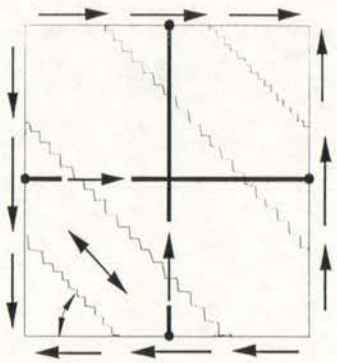

(b) Truss Mechanism

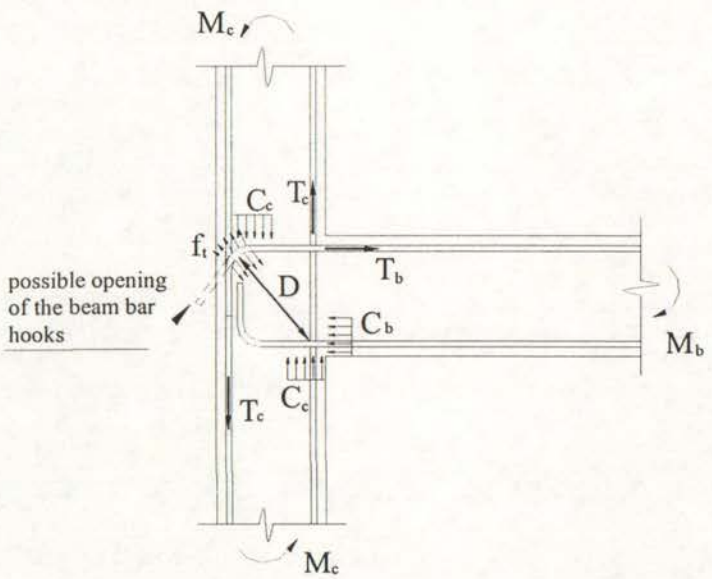

(c) Potential Straightening Action of the Beam Bar Hook

Fig.4.3 Shear Resisting Mechanism in Exterior Beam-Column Joints with the Beam Bar Hooks Bent into the Joint Core

The postulated joint concrete strut mechanism in Fig. 4.3(a) of exterior beam-column joint assemblies can only be actuated if the premature failure associated with the opening action of the beam bar hooks can be prevented.

For Units EJ2 or EJ4, typical design deficiencies were the use of plain bar reinforcement and very limited joint horizontal shear reinforcement present. Regarding the use of plain bar reinforcement, the resulting severe bond degradation and slip from the use of plain round bar reinforcement along the beam longitudinal bars within the joint core could increase the demand for transmitting the beam steel tension force at the bends of the beam longitudinal bars by the joint diagonal concrete strut, enhancing the possible premature concrete tension cracking failure initiated by the beam bar hooks and leading to increased demand for the joint horizontal shear reinforcement to prevent such a failure, compared to the case with deformed reinforcing bars. However the joint core of Units EJ2 or EJ4 contained only limited joint shear reinforcement and therefore premature failure associated with the opening action of the beam bar hooks could control the seismic performance of the system. As a consequence, the effectiveness of the joint concrete strut mechanism could diminish.

Evidently, the exterior beam-column joint assemblies reinforced by plain round longitudinal reinforcement and with the beam bar hooks bent into the joint cores, as was the case for Unit EJ2 or Unit EJ4, emphasise the need for joint horizontal shear reinforcement within the beam bar hooks.

4.4.2 An Alternative Joint Model for the Exterior Beam-Column Joints EJ1 and EJ3

As stated in section 4.3.2.2, for Units EJ1 or EJ3, neither the arrangement of the beam bar hooks in exterior column nor the plain round bars used satisfied the requirements of NZS3101: 1995. Apart from this, the amount of column transverse reinforcement was very inadequate according to NZS3101: 1995 requirements for anti-buckling, especially above and below the joint core.

When the beam longitudinal bars are bent out of the joint cores in exterior columns as for Units EJ1 or EJ3, the beam steel tensile force transfer within the bend has to be as illustrated in Fig. 4.4 (a). The resistance within the bend to the beam steel tension force could potentially cause the concrete tension cracking in the columns initiated by the beam bar hooks, and such concrete tension cracking could be further enhanced by column bar buckling above and below the joint core. If this does occur, the beam bar hooks will open

up as suggested in Fig. 4.4 (a). To restrain the opening of the beam bar hooks of Units EJ1 or EJ3 and to develop the concrete compressive struts, extensive *column transverse reinforcement immediately above and below the joint core* is required in the region of the beam bar hooks.

Due to the use of plain bar reinforcement for Units EJ1 and EJ3, severe bond degradation and bar slip would be expected along the longitudinal reinforcement. As a result, column bar buckling adjacent to the joint core along the outer layer of longitudinal column bars which are not restrained by the lateral beam would be enhanced. Also the beam steel tension forces at the column inner face would be mainly transmitted within the bend of the beam bars. Hence the possibility of the above described premature failure associated with the interaction of column bar buckling and the opening action of the beam bar hooks would increase, and the need for column transverse reinforcement above and below the joint core would further increase as well. However, the seismic performance of the whole system would be *irrespective of the amount of joint core shear reinforcement* in this case, contrary to Units EJ2 or EJ4.

For the exterior beam-column joint Units EJ1 or EJ3, column transverse reinforcement was sparse and the first set of column transverse reinforcement was far away from the beam faces. Column bar buckling, especially along the outer layer of the column longitudinal bars, above and below the joint core, would be unavoided. As a result, concrete cover spalling could take place in this region, enhancing the opening of the beam bar hooks and leading to the premature concrete cracking failure associated with the interaction of column bar buckling and the opening of the beam bar hooks.

Evidently, the alternative force path with the beam bar hooks bent out of the joint cores in exterior columns illustrated in Fig.4.4 (a) could be developed should sufficient column transverse reinforcement be provided adjacent to but outside of the joint core [P9]. Extensive column transverse reinforcement within the region of the beam bar hooks can not only control the above described premature concrete tension cracking failure, but also generate at the outer column face clamping forces which are necessary for the formation of the inclined concrete compression strut actions of D across the joint core and D_1 in the columns. In this case, the effective force path for transmitting the member forces across the joint core is a steeper concrete strut D running from one joint corner to the midway of the confined column zone, rather than corner to corner joint diagonal strut, as illustrated in Fig. 4.4.

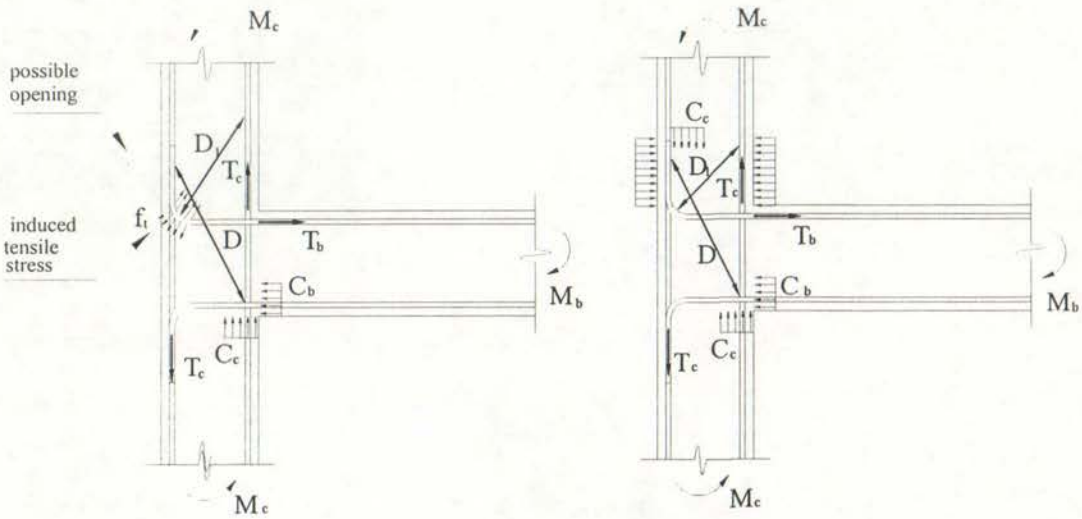

(a) An Alternative Force Path across the Joint Core

(b) Potential Straightening Action of the Beam Bar Hooks

Fig. 4.4 An Alternative Force Path across the Joint Cores of Units EJ1 and J3

4.5 RETROFIT SCHEME USED FOR UNIT REJ1

The postulation for achieving the alternative joint force path shown in Fig.4.4 was testified by conducting simulated seismic loading test on the retrofitted Unit REJ1, which was the damaged Unit EJ1.

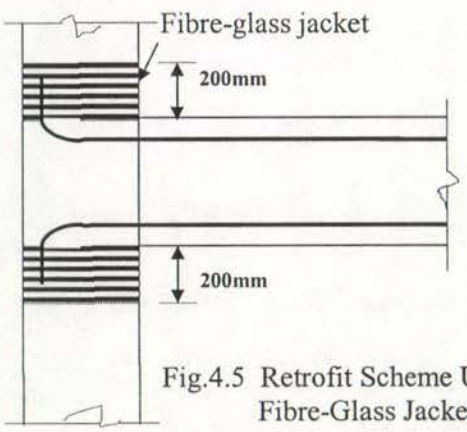

Fig.4.5 Retrofit Scheme Using Fibre-Glass Jacketing

Table 4.9 Properties of fibre glass

Ultimate tensile strength:	400MPa
Design tensile strength:	100MPa
Elastic Modulus:	20000MPa

A fibre-glass jacket of eight layers, which gave a cross sectional area per wrap of 508 mm^2, was used to wrap the column areas of 200 mm immediately above and below the joint core of the damaged Unit EJ1 (see Fig.4.5). The Unit then became Unit REJ1. The material properties of fibre-glass are shown in Table 4.9. Resin injection was used before the fibre-glass jacketing in order to enhance the damaged bond strength and to repair the cracked regions.

4.6 EFFECT OF AXIAL COLUMN LOAD

Should compressive axial load be present in the column, as for the tests on Units EJ3 and EJ4, the depths of column flexural compression zones will increase, leading to enhanced concrete strut capacity and also leading to enhanced force transmission of the beam steel tensile forces to the concrete by bond within the joint core. Due to enhanced force transmission from the beam tension steel to the concrete by bond, the portion of the beam steel tensile forces to be transmitted at the bend in the form of the resistance to D_1 reduces and the possibility of the premature failure caused by interaction of column bar buckling and the opening action of the beam bar hooks diminishes as well. At some stage when the axial column load is large enough, the concrete cracking initiated by the beam bar hooks may be totally avoided. In this case, retrofit using external passive confinement method in the column areas above and below the joint core will not make any difference in the seismic behaviour, compared with the seismic behaviour of the as-built units. However, the beneficial effect of column compressive axial load is not limitless. When the column axial load is large, the compressive strength of joint concrete compressive strut will govern the performance of the system.

CHAPTER 5

TESTS ON THE INTERIOR AND EXTERIOR BEAM-COLUMN JOINT UNITS

5.1 LOAD APPLICATION AND REACTION

Testing was carried out on the Structural Laboratory's Reinforced Concrete Strong Floor at the University of Canterbury. Each hold down point of the strong floor has a tensile capacity of 10 tonnes.

For the two identical interior beam-column joint units, Unit 1 was tested under simulated seismic loading with zero axial column load and Unit 2 was tested under simulated seismic loading with a constant axial column load of 800 kN, producing a column axial load ratio of 0.12 for Unit 2. The column axial load ratio is calculated by $N^*/f_c^{'}A_g$, where N^* is the axial column compressive load; $f_c^{'}$ is the measured concrete compressive cylinder strength; and A_g is the column gross cross-sectional area.

For the exterior beam-column joint units, as-built Units EJ1 and EJ3 as well as the retrofitted Unit REJ1 were tested under simulated seismic loading with zero axial column load, and as-built Units EJ2 and EJ4 were tested under simulated seismic loading with a constant compressive axial column load $N^*$of 1800kN, which produced a column axial load ratio of 0.25 and 0.23 respectively for Unit EJ3 and Unit EJ4, based on the measured concrete compressivecylinder strengths

Independent loading rigs were designed to accommodate the simulated seismic loading and the constant compressive axial load on the top of the columns, respectively.

Seismic loading was simulated by applying vertical forces at the beam ends while the column ends were prevented from displacing horizontally by holding columns in position using a horizontal strut to connect the top of column with the steel reaction frame (see Fig.5.1) in order to induce the desired moment reversed across the joint as

sketched in Fig. 5.2. The ends of the beams and columns were free to rotate, and the ends of the beams were also free to move axially. For the tests on interior beam-

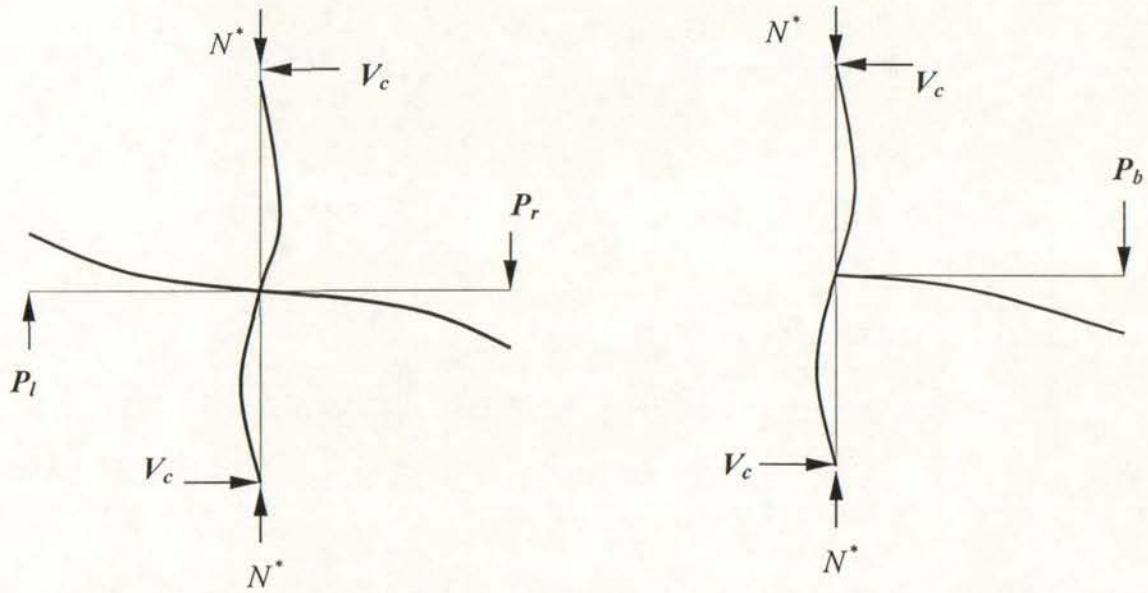

Fig. 5.1 Method of Loading Exterior Beam-Column Joints

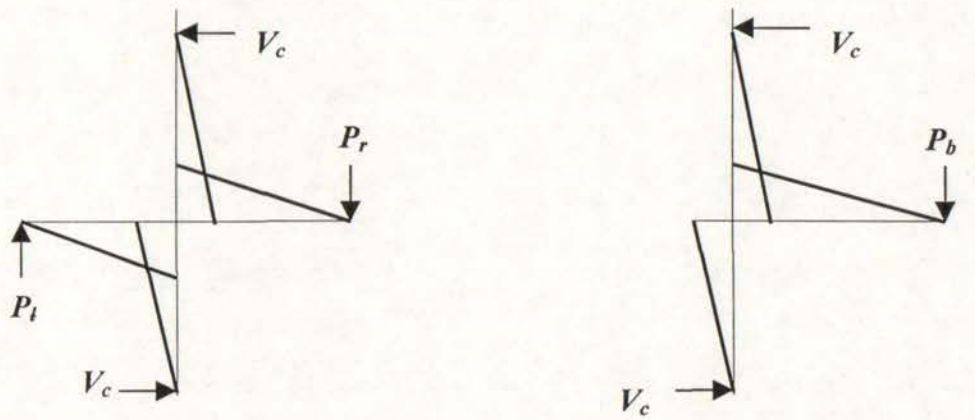

(a). Interior Beam-Column Joints (b) Exterior Beam-Column Joints

Fig. 5.2 Moment Reversed across the Joint Core during Earthquakes

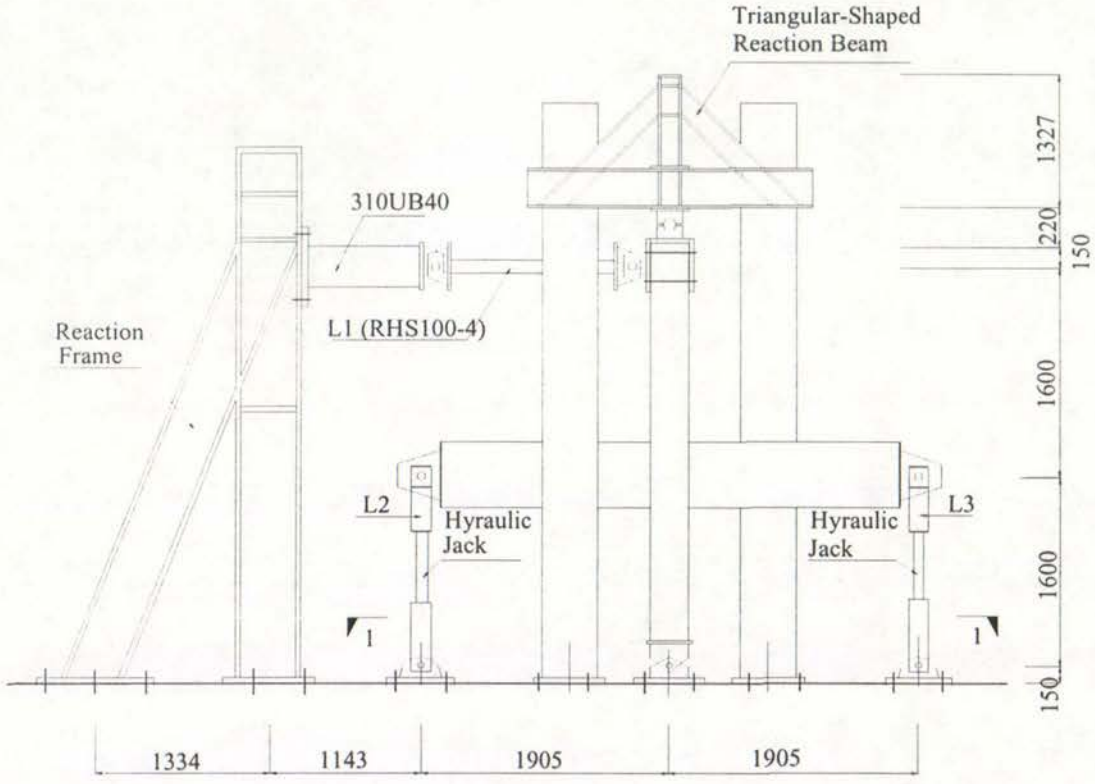

(a) Elevation

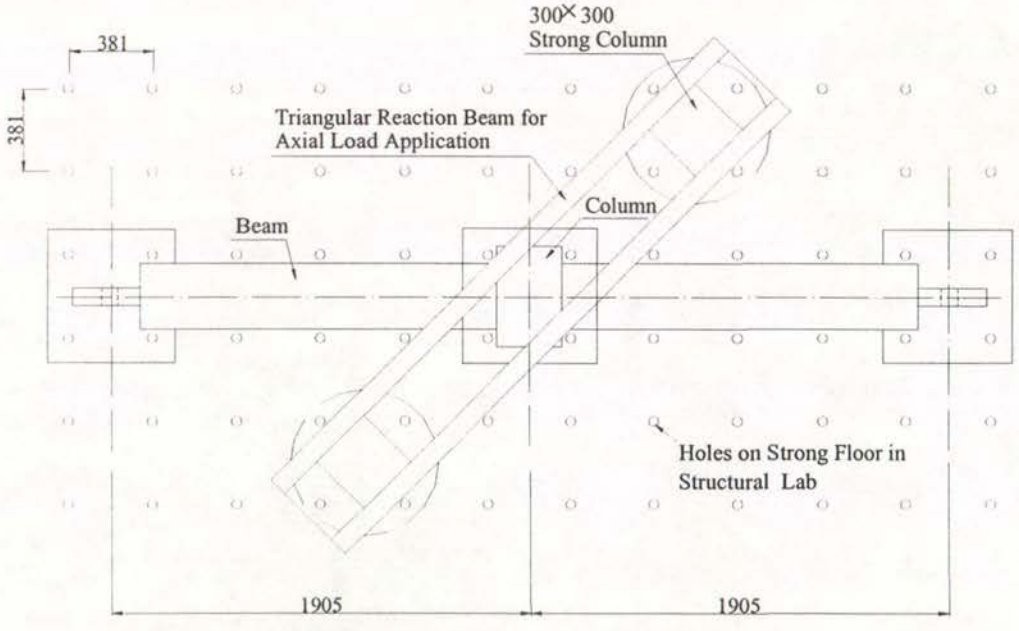

(b). Section 1-1 (Layout Plan)

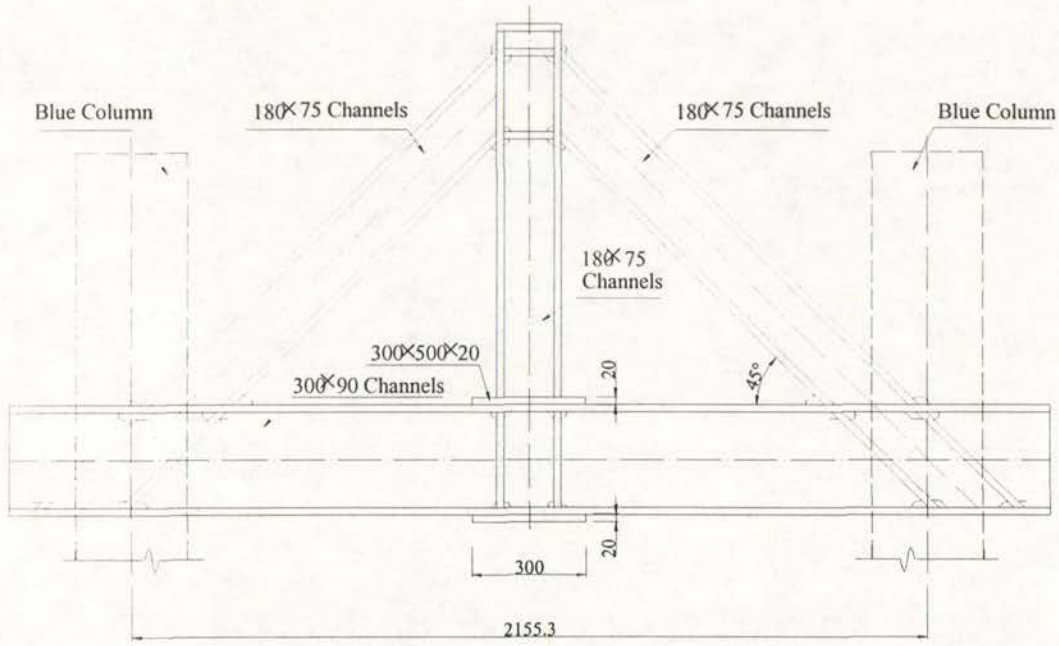

(c) Triangular-Shaped Reaction Beam

Fig.5.3 Overall Configuration of Loading Rigs for Testing Interior Beam-Column Joint Units

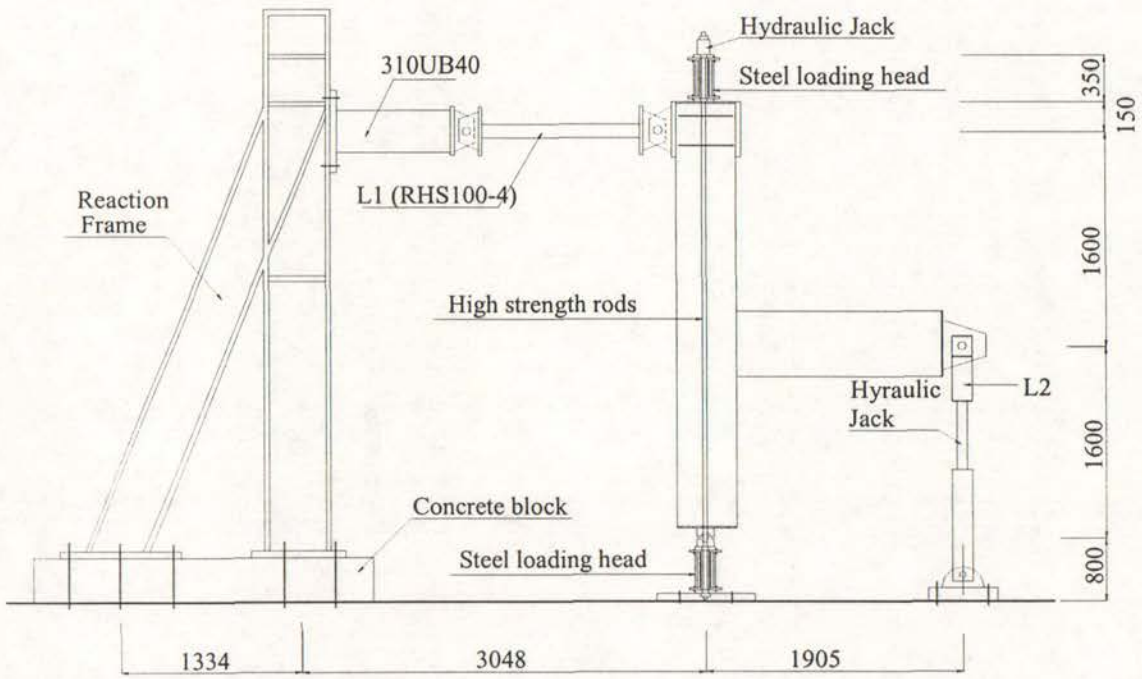

(a) Elevation

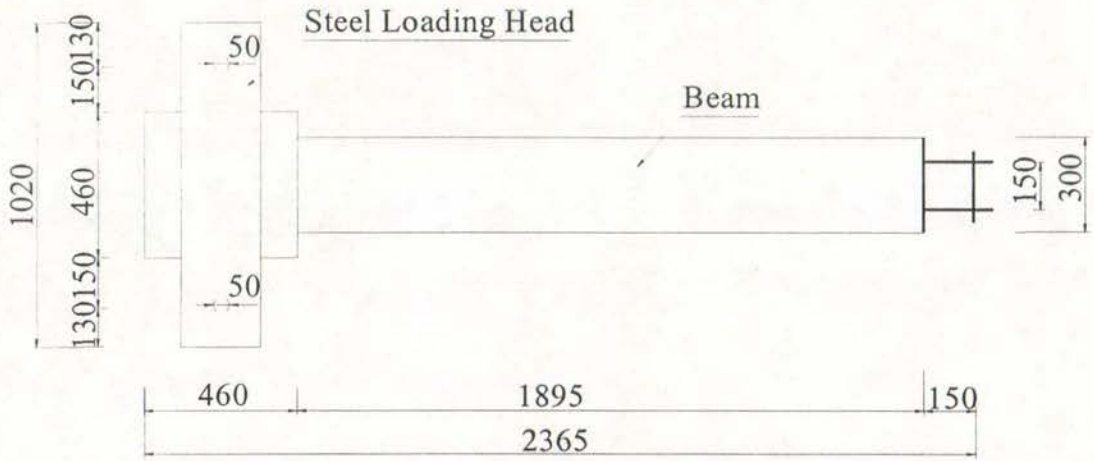

(b) Layout Plan

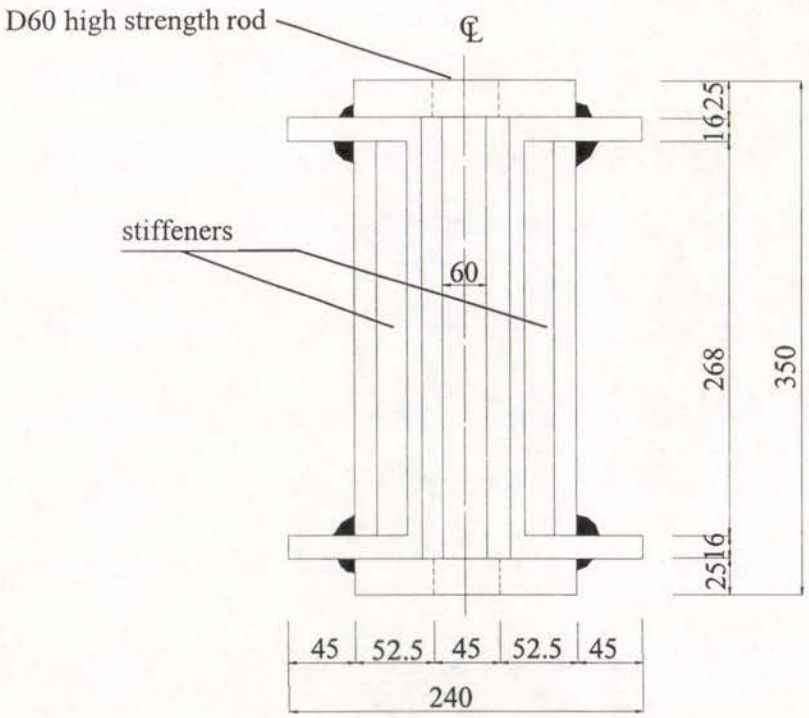

(c) Details of Steel Loading Heads (Steel Reaction Beams)

Fig. 5.4 Overall Configuration of Loading Rigs for Testing Exterior Beam-Column Joint Units EJ2, EJ2, EJ3 and EJ4

column joint units, two independent hydraulic jacks were used to apply vertical forces at two beam-ends. Vertical displacement of each beam end was maintained equal but opposite during displacement-controlled loading stages. For the tests on exterior beam-column joint units, one hydraulic jack was used to apply vertical force at the beam-end.

Apart from simulated seismic loading, a constant compressive axial load of 800 kN was applied to the column of Unit 2 by the axial loading rig which ran 45° to the lateral loading plane across the specimen and comprised of a triangular-shaped steel reaction beam and two strong steel reaction columns. Each of the two strong steel reaction columns in axial loading rig was connected with the reinforced concrete strong floor by four high strength bolts to transmit the induced reaction forces to the strong floor. Maximum tensile capacity of each bolt in the strong floor is 10 tonnes, and it meant that the maximum tensile axial load capacity of each steel reaction column was 400 kN and hence that the maximum possible compressive axial load applied to the columns of Unit 2 was 800 kN. The specified concrete compressive cylinder strength was 30 MPa for Unit 2, and this meant a column axial load ratio of 0.2 for test of Unit 2. However, the measured concrete compressive cylinder strength at the time of testing Unit 2 was 48.9 MPa, and it was 60% higher than the specified concrete compressive strength. Hence the axial column load of 800 kN gave only an column axial load ratio of 0.12 for Unit 2. The overall configuration of the loading rigs for testing interior beam-column joint units is shown in Fig. 5.3, where both the simulated seismic loading rig and the axial loading rig were employed. When Unit 1 was tested, axial loading rig was removed.

Similarly, a constant compressive axial load of 1800 kN was applied to the columns of Unit EJ3 and Unit EJ4 by a self-contained steel loading rig, which consisted of the top and bottom steel loading heads (reaction beams), hydraulic rams as well as two high strength tension rods. The measured concrete compressive cylinder strength at the time of testing was 34 MPa for Unit EJ3, and 36.5 MPa for Unit EJ4. Hence, the constant compressive axial column load of 1800 kN produced a column axial load ratio of 0.25 for test of Unit EJ3 and 0.23 for test of EJ4. The overall configuration of the loading rigs for testing exterior beam-column joint units is shown in Fig. 5.4,

where both the simulated seismic loading rig and the axial loading rig were employed. When Units EJ1 and EJ2 and REJ1 were tested, axial loading rig was removed.

To accommodate the column end rotations and maintain a vertical axial column load during testing, a rock seat was used for test of Unit 2 between the top of the column and the bottom surface of the triangular reaction beam. Similarly, a rock seat was used for tests of EJ3 and EJ4 between the bottom of the column and the top surface of the bottom steel reaction beam of the axial loading rig.

5.2 INSTRUMENTATION

5.2.1 Measurement to Determine the Hysteresis Loops

A property that needs to be appreciated in the evaluation of structural seismic performance is the force-displacement hysteretic response, and the force-displacement hysteretic response indicates the energy dissipation capacity of the structure by considering the shape of the hysteresis loops. In this study, the beam end loads (beam shears) and the correspondent beam end displacements were measured. The storey shear and the storey displacement could be found by considering the equilibrium criteria and the geometry of the unit on the basis of the measured beam end forces and displacements as described in the following. Hence the measurements of the beam end load(s) and the corresponding beam end displacement(s) enables the acquisition of the hysteretic responses of both the individual beam and the whole test units. For the sake of check, the storey (column) shear force was also directly measured during testing for both interior and exterior beam-column joint tests.

5.2.1.1 Force Measurement

For each interior beam-column joint unit, three load cells were used to measure loads. Load cell L1 was used to measure storey (column) shear force, and Load cells L2 and L3 were used to measure beam end loads, as shown in Fig.5.3 (a).

For each exterior beam-column joint unit, two load cells were used to measure loads. Load cell L1 was used to measure storey (column) shear force, and load cell L2 was used to measure the beam end load, as shown in Fig.5.4 (a).

Load cell L1, which was used to measure the storey shear force, was made in this laboratory by placing 8 strain gauges on the horizontal strut in such a way that a full bridge circuit was developed and the effects of flexure could be eliminated [H4]. Load cell L1 was calibrated in an Avery Universal Testing Machine.

The beam end load cells, L2 and L3, have built-in electrical circuits, giving a total resistance of 700 ohms. Each beam end load cell was connected in series with a hydraulic jack and had two outputs. One output of each beam end load cell was read directly using a strain indicator against which the load cell had been calibrated in an Avery Universal Testing Machine. Therefore it was possible to apply load during load-controlled stages by directly reading the load from the strain indicator. The other output of the beam end load cell was used to drive the Y-axis of the X-Y plotter. The X-axis of the X-Y plotter was driven by the signal from a linear potentiometer that measured the correspondent beam vertical displacement, see Section 5.2.1.2 below. Hence it was possible to obtain an instantaneous plot of beam end vertical force versus beam end lateral displacement for each beam.

5.2.1.2 Displacement Measurement

The displacement instrumentation for the interior and exterior beam-column joint tests is shown in Fig.5.5 and Fig.5.6 respectively. For all the tests on both interior and exterior beam-column joint units, two linear potentiometers of 300 mm travel were used to measure the vertical displacements at each beam end, and the linear potentiometer closer to the beam pin end was connected with the correspondent X-Y plotter to drive its X-axis. It was therefore possible for the X-Y plotter to give instantaneous plots of the beam-end lateral load versus beam-end displacement correspondingly. Meanwhile each linear potentiometer to drive the X-axis of X-Y plotter was also connected in parallel with a Digital Voltage Meter (DVM). Readings from the DVM manually gave immediately the value of the gross beam deflection,

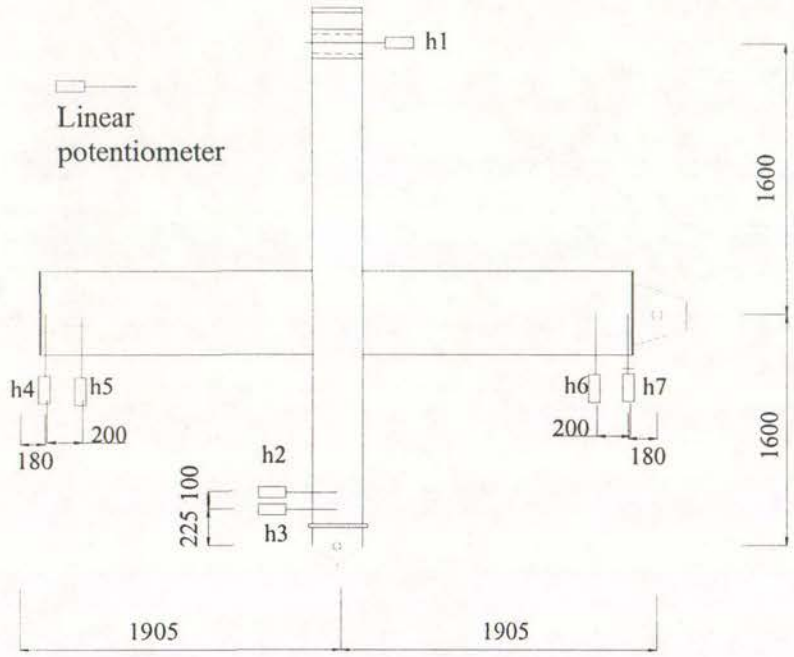

Fig.5.5 Displacement Measurement Method Using Linear Potentiometers for Interior Beam-Column Joint Unit 1 and Unit 2

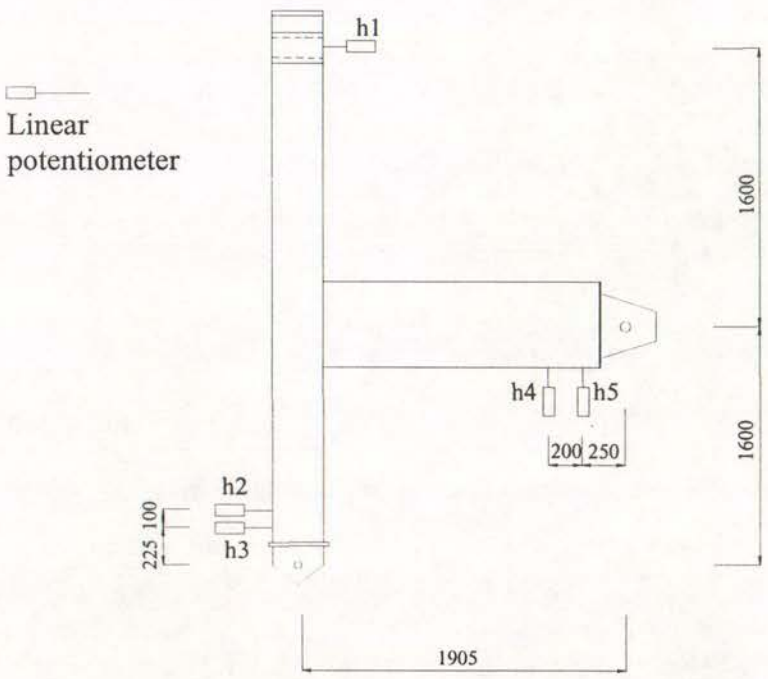

Fig.5.5 Displacement Measurement Method Using Linear Potentiometers for Exterior Beam-Column Joint Unit 1 and Unit 2

which was used to monitor the imposed beam end displacement in the displacement-controlled loading stages.

However, the recorded beam end load versus beam end displacement curves given by each of the X-Y plotters only served as a reference for monitoring the overall progress of the test unit, for the following reasons:

At first, the target positions for beam end displacement measurements are some distance away inward from the beam end pin positions, hence the measurements must be converted into beam end displacements at end pin positions by interpolating. Also, the measured beam deflections included the components due to the sidesway of the seismic loading rig. The real displacement should be relative to the line joining two column end-pins.

The horizontal movements of the beam-column joint assemblies referred as to be the sidesway of the seismic loading rig were detected by the linear potentiometers, h_1, h_2 and h_3 as shown in Fig.5.5 and Fig.5.6. The horizontal movement at the column top pin position was measured directly by potentiometer h_1, but the horizontal movement at the column bottom pin position was found by interpolating the measurements of potentiometers h_2 and h_3. With the horizontal movements at the column top and bottom pin positions known, the movement of the centre of column top pin position relative to the centre of column bottom pin position, δ_{cr}, could be reasonably estimated by:

$$\delta_{cr} = (h_1 + h_3) + (h_3 - h_2) \times 225/100 \qquad (5.1)$$

The equivalent storey drift, Δ_{co}, and the equivalent storey shear force, V_c, can be found by considering the geometrical and equilibrium relationships of the frame, as shown in Fig. 5.7. According to the imposed vertical displacements and lateral forces at the beam ends, the equivalent storey displacements and storey (column) shear force can be found as follows:

The equivalent storey displacement is as follows:

$$\Delta_{co} = \left[\frac{\Delta_{bl} - \Delta_{br}}{l_b} \right] l_c \quad . \quad \text{for interior beam-column joint tests} \qquad (5.2)$$

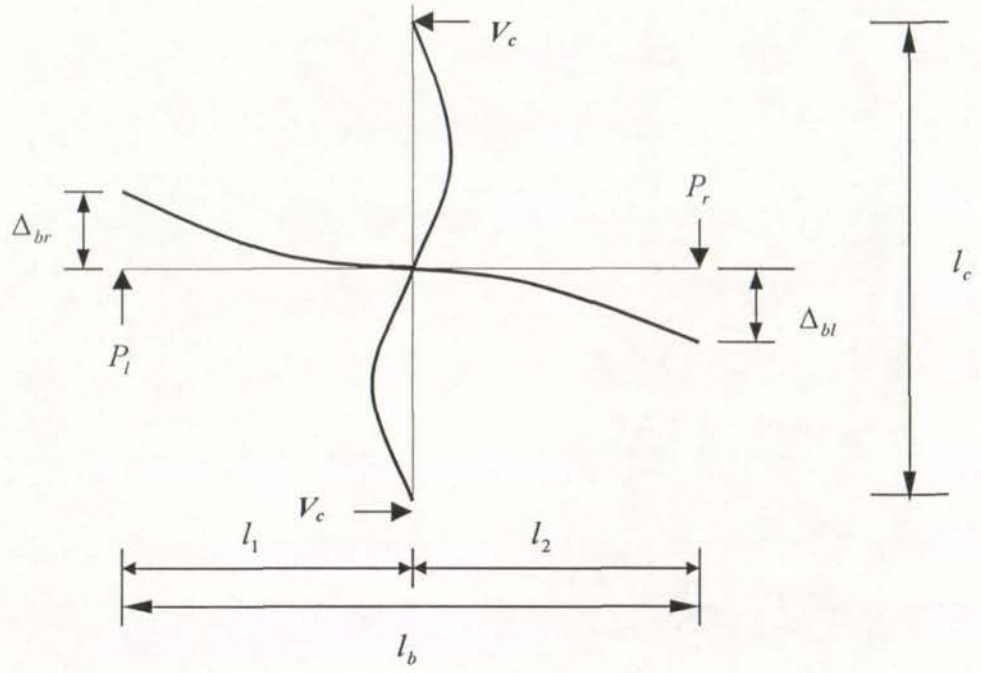

(a). Interior Beam-Column Joint Units

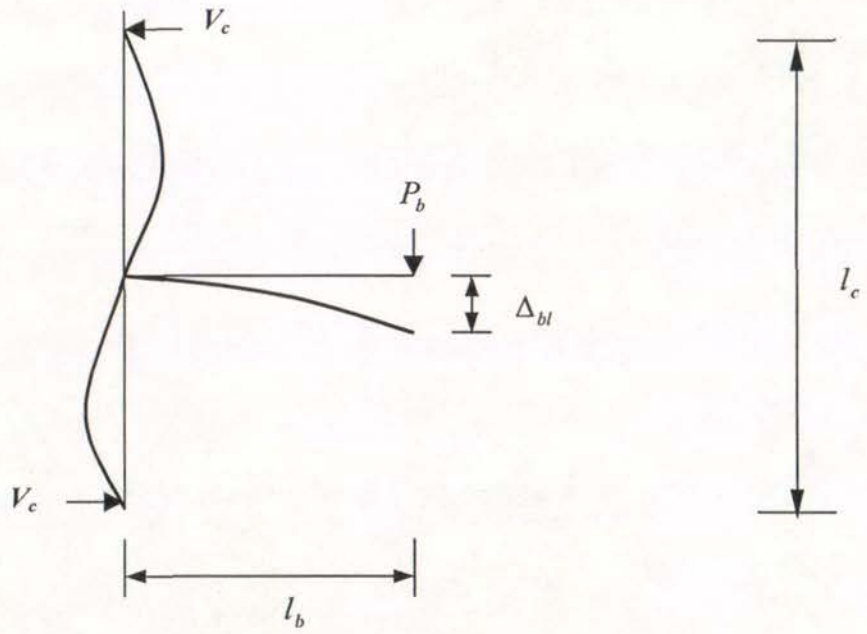

(b) Exterior Beam-Column Joint Units

Fig. 5.7 Determination of Equivalent Storey Shear and Storey Displacement

$$\Delta_{co} = \frac{\Delta_b}{l_b} \; l_c \qquad \text{for exterior beam-column joint tests} \quad (5.2)'$$

The equivalent storey (column) shear force is

$$V_c = \frac{P_l l_1 - P_r l_2}{l_c} \qquad \text{for interior beam-column joint tests} \quad (5.3)$$

$$V_c = \frac{P_b l_b}{l_c} \qquad \text{for exterior beam-column joint tests} \quad (5.3)'$$

where :

l_c = the storey height, which is 3200 mm for all test units

l_b = the beam span, being 3810 mm for the interior beam-column joint unit and 1905 mm for the exterior beam-column joint unit

Δ_{bl} and Δ_{br} = the imposed vertical displacements at the pin ends of the left beam and the right beam, respectively (negative downwards) for the interior beam-column joint units

Δ_b = the imposed vertical displacements at the beam pin end for the exterior beam-column joint units.

l_1 and l_2 = the loading spans of the left beam and the right beam, respectively, being 1905 mm for both interior beam-column joint units.

P_r and P_l = the lateral shears applied to the right beam and left beam, respectively (negative downwards), for interior beam-column joint units.

P_b = the lateral load applied to the beam end for exterior beam-column joint units.

Δ_{co} = the equivalent storey drift

V_c = the equivalent storey shear force

Upward acting forces and displacements, as shown in Fig.5.7, which is causing the hogging beam moments, are taken positive, while downward loads and displacements, which is causing sagging beam moments, are taken negative.

The equivalent storey drift % is then given by Δ_{co} /32 for both interior beam-column joint tests and exterior beam-column joint tests.

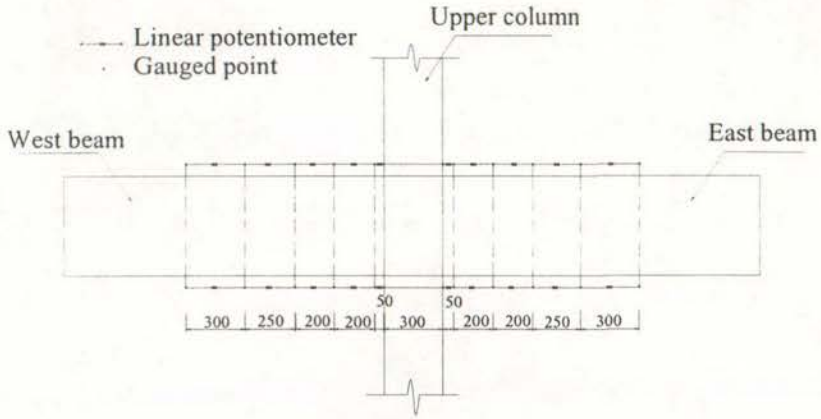

(a) Arrangement of Linear Potentiometers to Measure Beam Curvatures for Unit 1 & 2

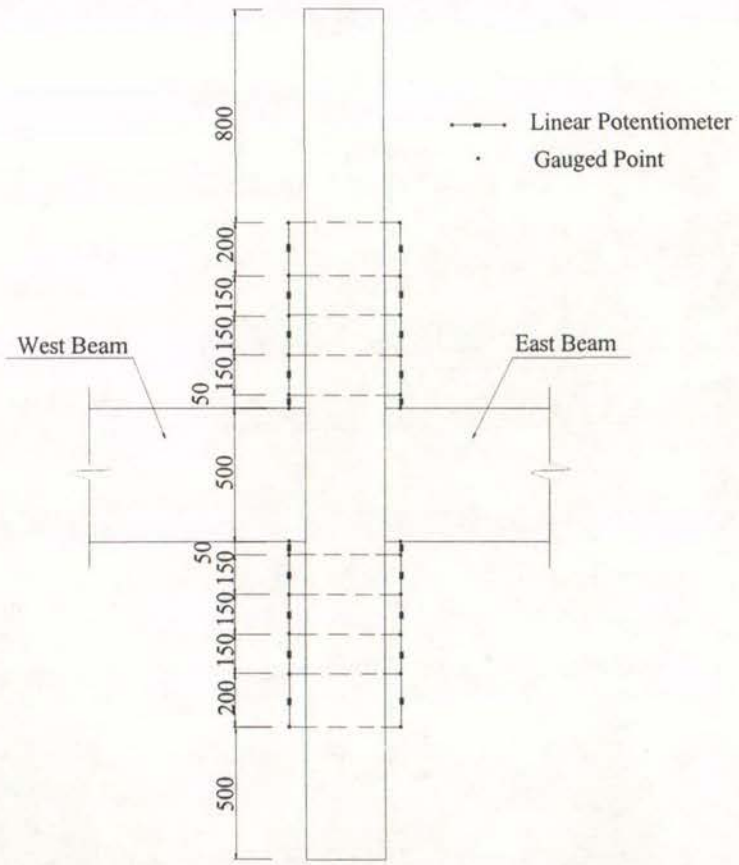

(b) Arrangement of Linear Potentiometers to Measure Column Curvatures for Units 1 and 2

Fig.5.8 Member Curvature Measurements for Interior Beam-Column Joint Units

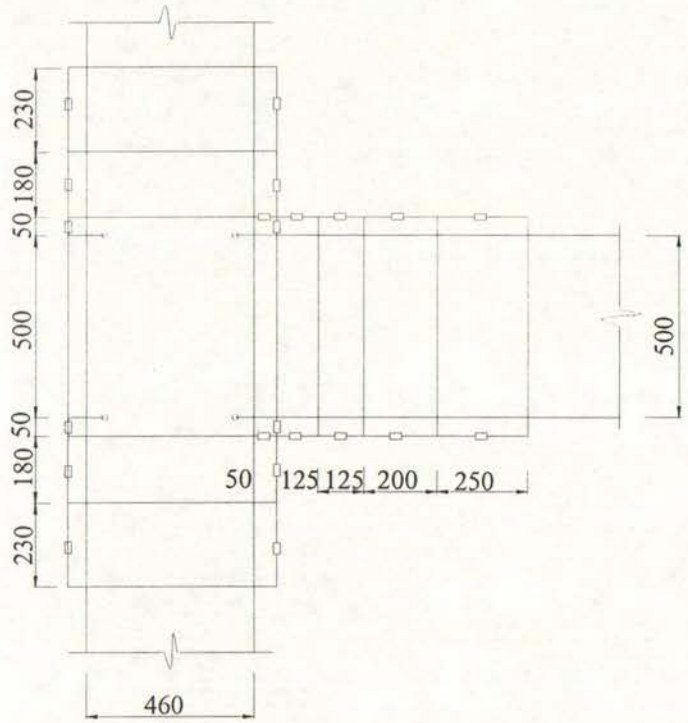

(a). for Test of EJ1

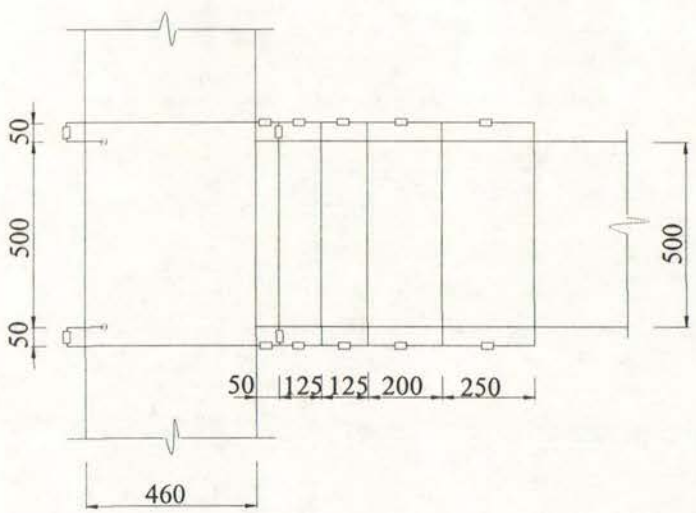

(b) for Tests of Unit EJ2, EJ3 and EJ4

Fig.5.9 Member Curvature Measurements for Exterior Beam-Column Joint Units

The real storey displacements should be obtained by deducting the components due to the deformations within the loading rig, δ_{cr}. This was necessary for plotting storey shear versus storey drift curves because considerable horizontal movement of the test unit was caused by the sidesway of the steel reaction frame.

5.2.2 Force Measurement to Determine the Axial Load on Column

For the interior beam-column joint Unit 2, a compressive axial load of $0.12 A_g f_c'$(= 800 kN) was applied to the column using a 100-tonne hydraulic jack and maintained constant during simulated seismic loading of that unit.

For the exterior beam-column joint Units EJ3 and EJ4, a compressive axial load of 1800 kN was applied to the column using two 100-tonne hydraulic jacks and maintained constant during simulated seismic loading of the units.

The maintenance of the constant column compressive axial load was monitored by a pressure gauge calibrated against a Universal Avery Testing Machine.

5.2.3 Measurement of Average Curvatures

A number of linear potentiometers of 30 mm or 50 mm travel were used to monitor member curvatures.

Each beam and each column employed several pairs of linear potentiometers in measuring the member curvatures within the gauged regions, and each pair of linear potentiometers were attached to the two ends of a steel rod embedded in the concrete. Fig. 5.8 (a) and Fig. 5.8(b) illustrate the arrangement of the curvature linear potentiometers for the beams and columns of the interior beam-column joint units, respectively. Fig.5.9 (a) and Fig.5.9 (b) illustrate the arrangement of the curvature linear potentiometers for test of Unit EJ1 and the other three exterior beam-column joint units, respectively. All steel rods were fixed into the mould using external steel brackets to hold them firm during concreting.

5.2.4 Measurement of Joint Shear Distortion and Joint Expansion

The average joint shear distortions and expansions were monitored by two diagonally placed linear potentiometers on the joint core as shown in Fig. 5.10.

The average joint shear distortion γ_j can be found by

$$\gamma_j = \gamma_1 + \gamma_2 = \frac{\delta_j - \delta_{j'}}{2l_j}(\tan\alpha_j + \frac{1}{\tan\alpha_j}) \qquad (5.4)$$

where δ_j and $\delta_{j'}$ are the changes in the lengths of the diagonals AB' and A'B respectively, l_j is the initial length of the diagonal in the joint core and α_j is the angle of the diagonal to the horizontal axis.

The joint core expansion index is defined as the average value of the length changes of the two diagonals, that is, $(\delta_j + \delta_{j'})/2$, because the joint expansion index so obtained is proportional to the increase in the volume of the joint core concrete. Evidently, the joint expansion index so obtained also can be used as an indicator of the joint core concrete failure.

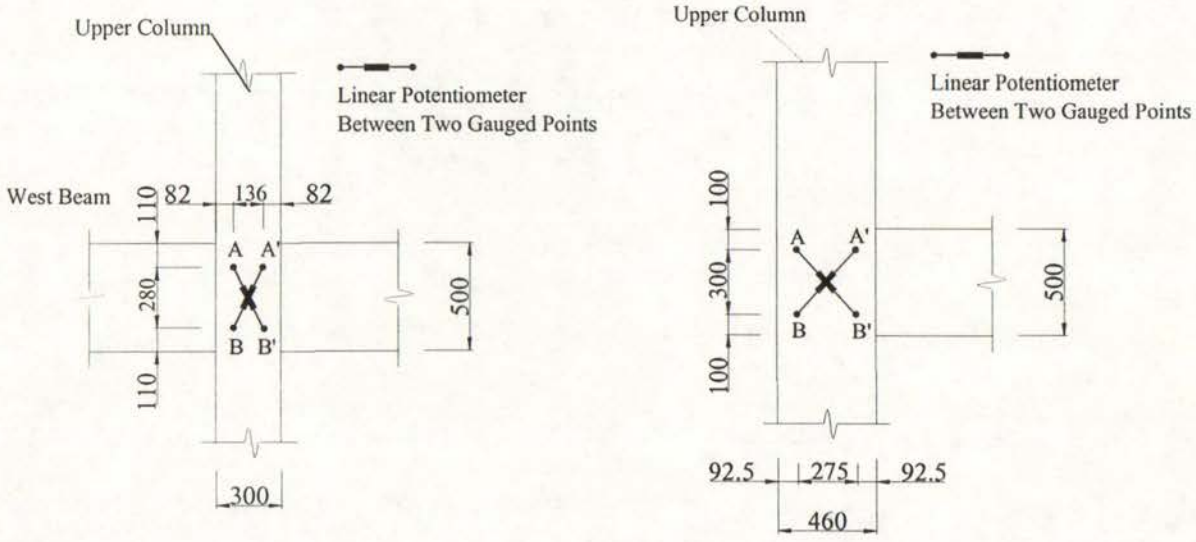

(a) Interior Beam-Column Joints (b) Exterior Beam-Column Joints

Fig.5.10 Estimation of Joint Shear Distortion

5.2.5 Measurement of Reinforcement Strains

Both electrical resistance strain gauges and linear potentiometers were used to measure reinforcement strains.

5.2.5.1 Measurements by Electrical Resistance Strain Gauges

The arrangement of electrical resistance strain gauges was exactly the same for the two interior beam-column joint units, and it is shown in Fig.5.11. Eighty-six Showa 120-ohm electrical resistance strain gauges (Type N11-FA-120-11) were used to monitor steel strain variations along the longitudinal and transverse reinforcement in the beams, columns and the joints of each unit.

The arrangement of electrical resistance strain gauges was also the same for the four exterior beam-column joint units, and it is shown in Fig.5.12. Fifty-three Showa 120-ohm electrical resistance strain gauges (Type N11-FA-120-11) were used for each Unit to monitor steel strain variation along the longitudinal and transverse reinforcement in the beams, columns and the joint.

The electrical resistance strain gauges were put on two opposite faces at the same location within the joint region because the steel strains in the joint core were to be carefully investigated, and the average values were taken as the real steel strains. Elsewhere only one gauge was placed at each location.

The distributions of electrical resistance strain gauges are summarised in Table 5.1 for the test units.

Table 5.1 Distribution of Electrical Resistance Strain Gauges for Unit 1 and Unit 2

Test Units	Components	No. of Strain gauges
Interior Beam-Column Joint Units 1 and 2	Beam longitudinal bars (R-24)	42
	Column longitudinal bars (R-24)	28
	Beam transverse steel (R-6)	4
	Column transverse steel (R-6)	12
	Total	86
Exterior Beam-Column Joint Units EJ1, EJ2 EJ3 and EJ4	Beam longitudinal bars (R-24)	22
	Column longitudinal bars (R-24)	24
	Beam transverse steel (R-6)	2
	Column transverse steel (R-6)	5
	Total	53

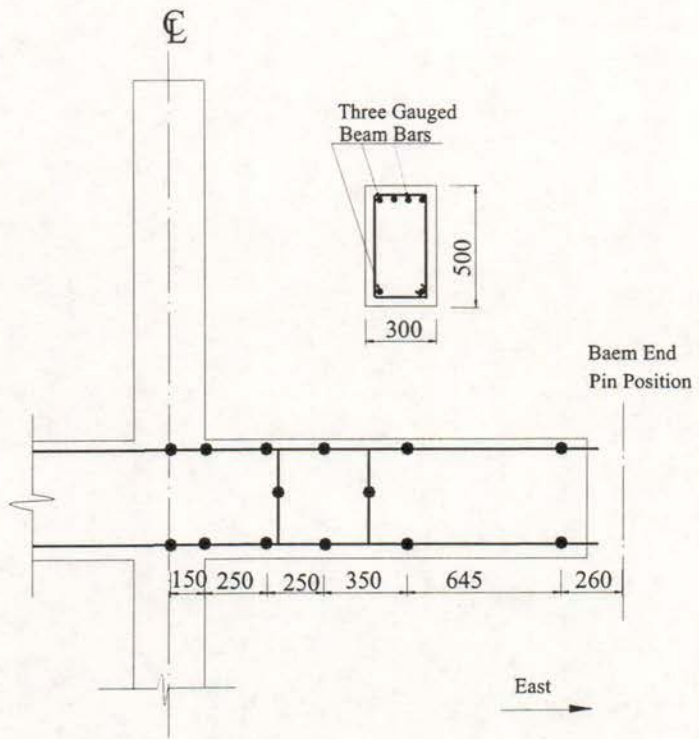

(a) Beam longitudinal and transverse reinforcement

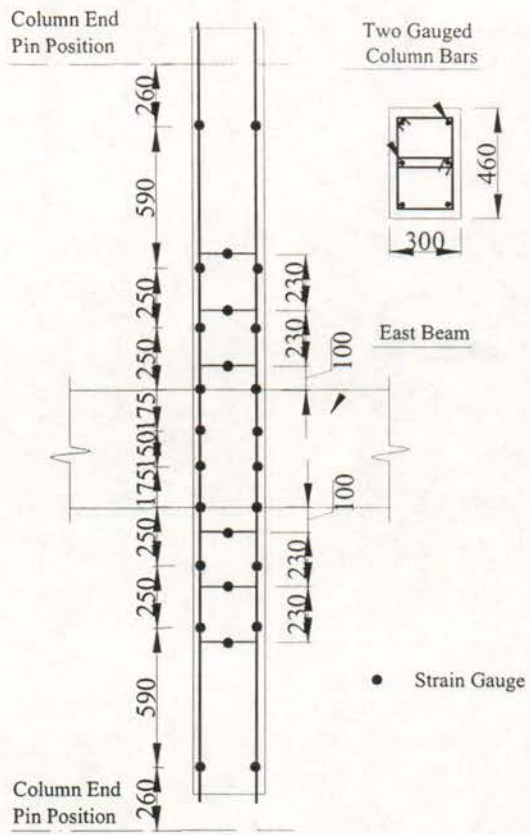

(b) Column longitudinal and transverse reinforcement

Fig.5.11 Arrangement of Electrical Strain Gauges for Interior Beam-Column Joint Units

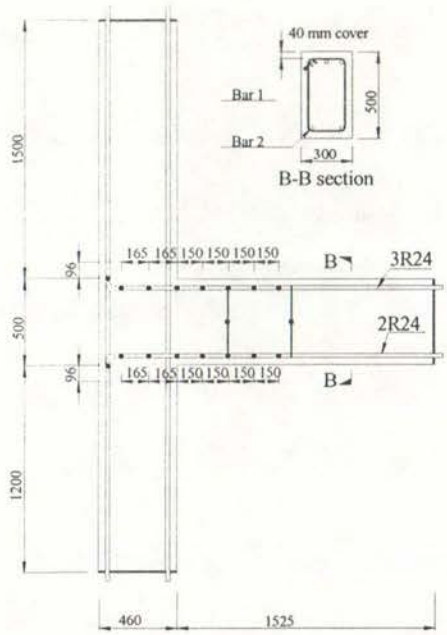

(a) Beam longitudinal and transverse reinforcement (Units EJ1 and EJ3)

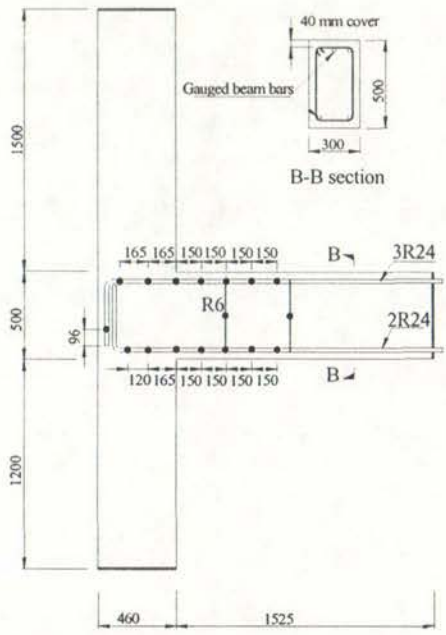

(b) Beam longitudinal and transverse reinforcement (Units EJ2 and EJ4)

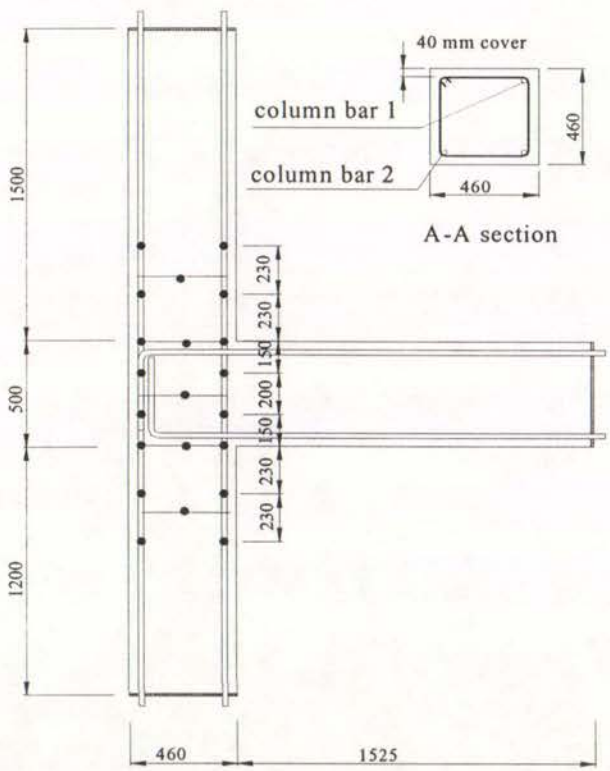

(d) Column longitudinal and transverse reinforcement

Fig.5.12 Arrangement of Electrical Resistance Strain Gauges for Exterior Beam-Column Joints with Beam Bar Hooks Bent into Joint

5.2.5.2 Linear Potentiometer Arrangement

One objective of using linear potentiometers to measure steel strains was to obtain the information on bar slip along the reinforcing bars within the joint core.

Each interior beam-column joint unit used thirty-six linear potentiometers to measure steel strain variations and bar slips within the joint core along the beam and column longitudinal reinforcing bars. Each exterior beam-column joint unit used fifteen linear potentiometers to measure steel strain variations and bar slips within the joint core along the beam and column longitudinal reinforcing bars.

The linear potentiometers for measuring steel strains were mounted to 10 mm steel rods welded to the beam and column main reinforcing bars. Therefore the measurements of the linear potentiometers represents the elongation of the reinforcing bars between the two gauged points. This method enabled the strain distribution in the reinforcing steel to be detected. With two static targets embedded in the joint core concrete, the bar slips within the joint region can be also detected. Fig.5.13 and Fig.5.14 show the positions of steel rods for mounting the linear potentiometers for the interior beam-column joint units and the exterior beam-column joint units, respectively.

5.2.6 Data Acquisition

each of the two interior beam-column joints Unit 1 and Unit 2 required 173 channels, for 3 load cells, 84 linear potentiometers and 86 electrical resistance strain gauges. Two data loggers, CEDACS of 64 channels and Metrabyte of 128 channels, were therefore employed for each test.

For the exterior beam-column joint Units EJ1, EJ2, EJ3 and EJ4, the required channel numbers for each test was less than 128 channels, and only Metrabyte of 128 channels was employed for each exterior beam-column joint test.

Because each bank of the data logger is of the same amplification factor, each bank of the data logger contained either electrical resistance strain gauges of the same gain or linear potentiometers.

Two different gains of 200 and 1000 (which are in fact the amplification factors) were set up for the electrical resistance strain gauges at critical locations and the electrical resistance strain gauges at the non-critical locations respectively, since very different steel strains were expected at the critical and non-critical locations. In other words, the gain for the electrical resistance strain gauges within the expected plastic hinge regions was set to be 200 since these gauges were expected to record large strains. In comparison, the gain for the electrical resistance strain gauges outside the expected plastic hinge regions was set to be 1000 because they were expected to record relatively low strains.

The linearity and repeatability of all linear potentiometers were checked after they were connected to the data loggers to make sure they would work properly during testing.

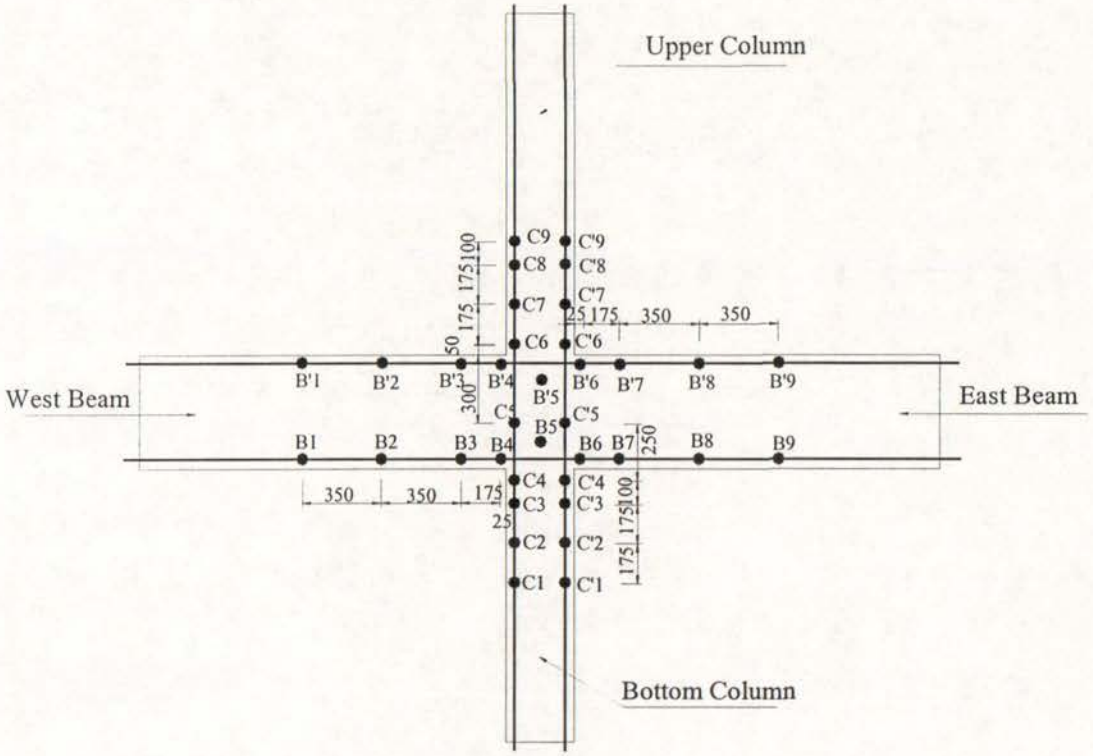

Fig.5.13 Positions of Steel Studs Welded on the Steel to Mount the Linear Potentiometers for Interior Beam-Column Joint Units

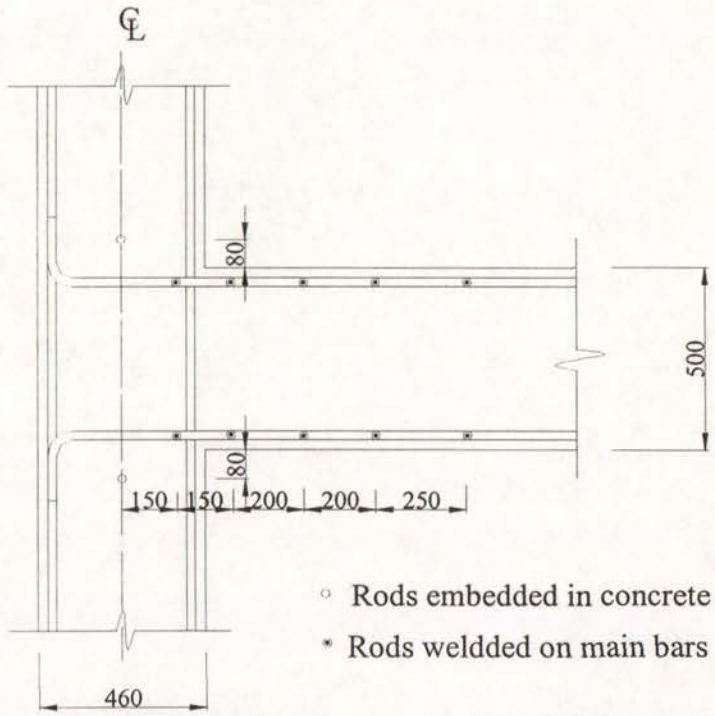

(a) Beam longitudinal reinforcement for Units EJ1 and EJ3

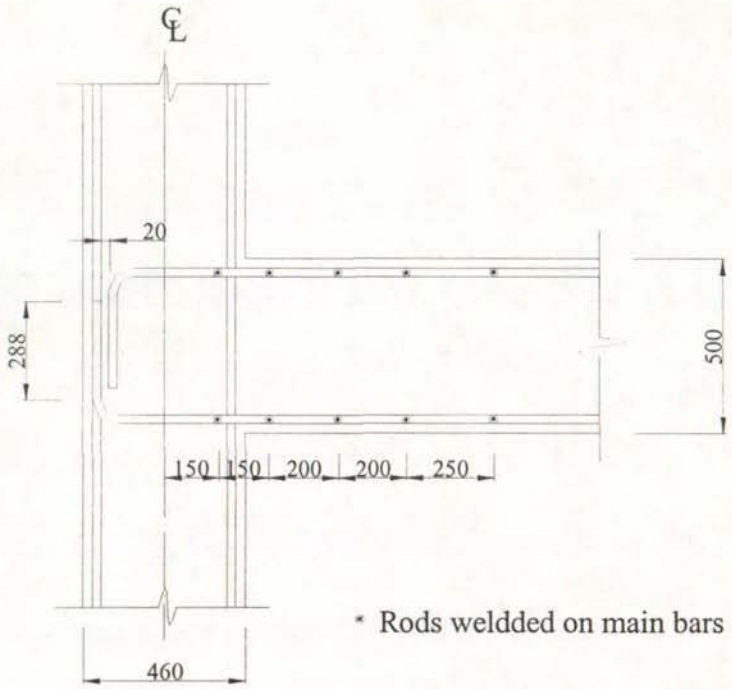

(a)

(b) Beam longitudinal reinforcement for Units EJ2 and EJ4

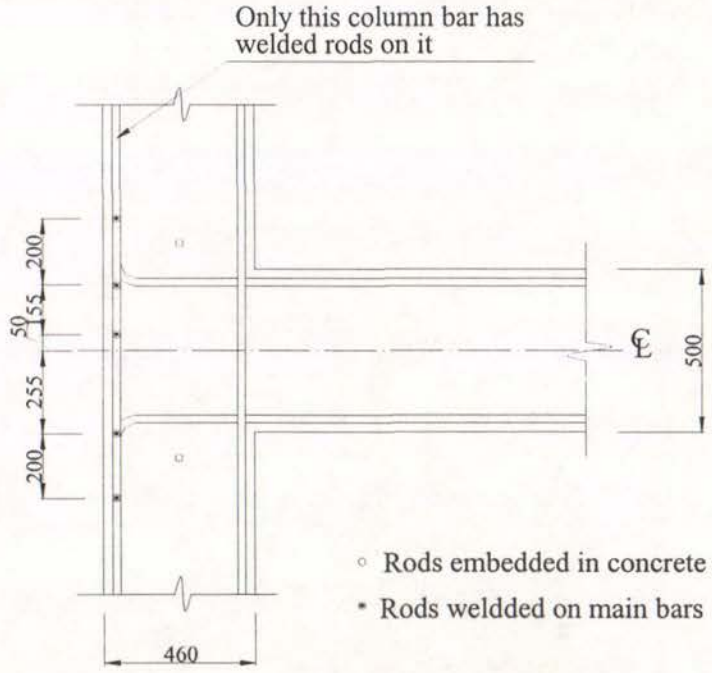

(c) Column longitudinal reinforcement of Units EJ1, EJ2, EJ3 and EJ4

Fig.5.14 Positions of Steel Studs Welded on the Steel to Mount the Linear Potentiometers for Exterior Beam-Column Joint Units

5.3 LOADING SEQUENCE

5.3.1 Cyclic Loading History

All the tests on the interior and exterior beam-column joint units followed the same quasi-static cyclic loading histories on the beam ends as depicted in Fig. 5.15 except that the compressive axial load of 800 kN was applied to the column for test on Unit 2 and the compressive axial load of 1800 kN was applied to the column for tests on Unit EJ3 and EJ4 in advance prior to cyclic loading. The first two loading cycles at the beam ends were load-controlled, including one cycle to 50% of the theoretical strength of the unit and one cycle to 75% of the theoretical strength of the unit. These two cycles in the elastic range were followed by a series of deflection-controlled inelastic cycles comprising two full cycles at displacement ductility factors of 1, 2 and 3. Each loading cycle included one half cycle clockwise loading and the other half anti-clockwise loading cycle. Clockwise loading for the interior beam-column joints meant downward loading at east (right) beam and upward loading at west (left) beam while clockwise loading for the exterior beam-column joints meant downward loading at the beam end.

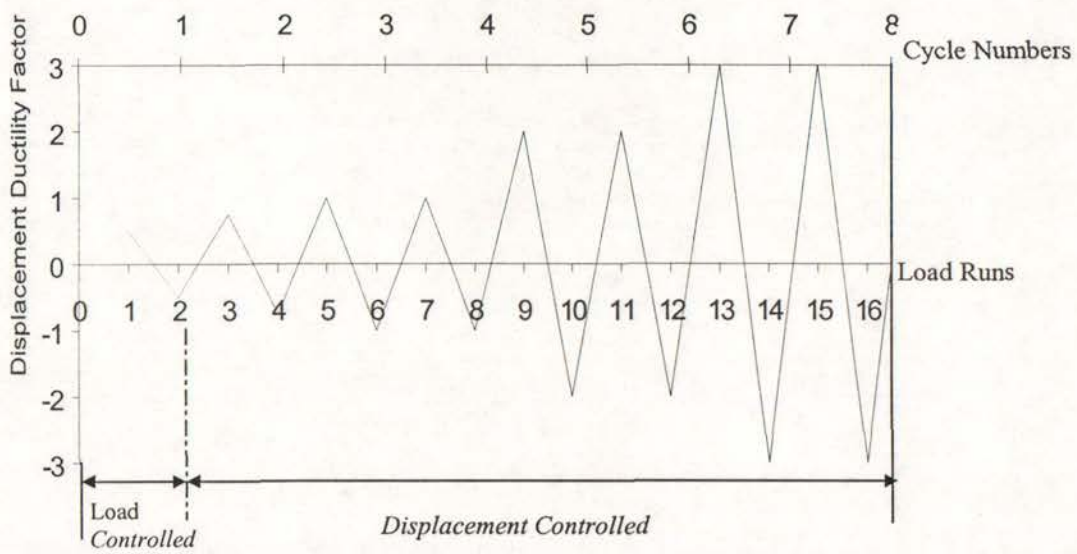

Fig. 5.15 Simulated Seismic Loading History

5.3.2 Determination of Yield Displacement and Initial Stiffness

It is widely accepted in New Zealand that the "first yield" displacement, $\Delta_{y,test}$, is found experimentally by extrapolating the measured stiffness at 75% of the theoretical strength linearly up to the theoretical strength of the unit. This method is graphically explained in Fig. 5.16, where V_i is the theoretical strength in terms of storey shear of the unit. The imposed displacement ductility factor μ_Δ, which was to be used in displacement-controlled loading stages, was then defined to be the imposed displacement divided by the measured yield displacement $\Delta_{y,test}$. The measured initial stiffness of the unit, K_e, was then found to be:

$$K_e = V_i / \Delta_{y,test} \qquad (5.5)$$

It is clear that, in situations when the measured displacement at first yield as defined above is much larger than the theoretically predicted first yield displacement, the attained storey drift is a more useful measure of deformation capacity of the subassemblage than the displacement ductility factor, since in that case high displacement ductility factors are associated with unrealistically high drifts. Alternatively, the imposed displacement ductility factor μ_Δ, which was to be used in displacement-controlled loading stages, should be defined to be the imposed displacement divided by the theoretical yield displacement $\Delta_{y,\,theoretical}$ in this case.

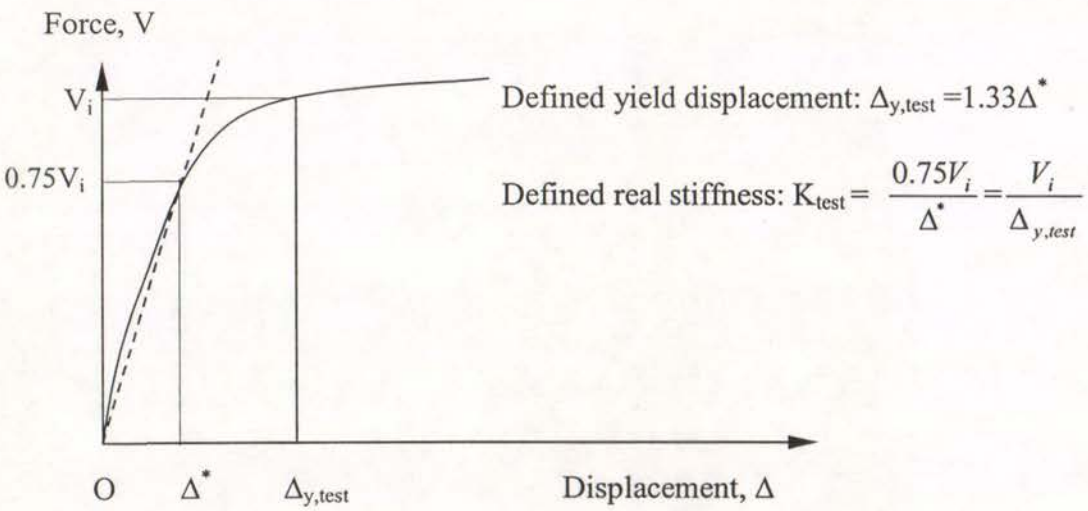

Fig.5.16 Experimental Determination of Displacement at First Yield

5.4 TEST PROCEDURE

Before any forces were applied to the test units, two complete sets of readings from all transducers were taken over 16 hours to check the stability of their readings.

After the specified compressive column axial load was applied to the test unit in advance, the cyclic vertical forces were applied to the beam-ends using hydraulic jacks. For the tests on interior beam-column joint units, the force application at the beam ends was coordinated manually to give equal rotations of the beams. The loading spans of the two beams were equal for the two interior beam-column joint units, hence equal beam rotations required equal amount of displacements applied at each beam end. In each load run, several force increments were taken before the target load or displacement was achieved so as to provide data for plotting continuous force-displacement curves.

After the maximum force or ductility level had been attained in each load run, unloading of the beams was carried out by two-step load control by removing 50% of the maximum force for that load run for the relevant beam.

At the peak of each load run, cracks on the front and the back faces were checked and the cracks on the front face were marked with felt-tip pens on the white painted surface. Photographs were taken usually at the peak of each load run, but also at other stages when it was felt necessary.

5.5 DISPLACEMENT COMPONENTS

5.5.1 General

As described in Section 5.1, seismic actions were simulated by applying vertical forces at the beam-end(s) of the test units while the equivalent storey (column) displacements and storey shears were calculated according to Eqs. 5.2 and 5.3. The storey (column) displacements were a combination of the elastic and inelastic deformations of the beams, the columns and the joint core. Namely,

$$\Delta_c = \Delta_{c,b} + \Delta_{c,c} + \Delta_{c,j} \qquad (5.6)$$

Where: Δ_c = the total storey displacement,

$\Delta_{c,b}$ = beam displacement component;

$\Delta_{c,c}$ = column displacement component;

$\Delta_{c,j}$ = joint displacement component.

Different displacement components can be estimated according to the measured member curvatures and the joint shear distortion, as stated in the following sections.

5.5.2 Deformations of the Beams

For the sake of the illustration of beam displacement estimation, the east beam in Fig. 5.8(a) is reproduced in Fig. 5.17.

The sign convention is defined as follows:

Beam positive curvatures and positive rotation angles were induced by beam positive bending moment, that is, beam positive curvatures and positive rotation angles corresponded to the bottom fibre in tension and the top fibre in compression. Similarly beam negative curvatures and rotation angles were induced by beam negative bending moment and corresponded to the top fibre in tension and the bottom fibre in compression.

The rotation over the region s_i is:

$$\theta_{b,i} = ({}_t\delta_i - {}_b\delta_i) / h_i \qquad (5.7)$$

The average curvature over the region s_i is

$$\phi_{b,i} = \theta_{b,i} / s_i \qquad (5.8)$$

where: h_i and s_i are shown in Fig. 5.17, ${}_t\delta_i$ and ${}_b\delta_i$ are the measurements of the top and bottom curvature linear potentiometers over the region i, and the measured compressive displacements by curvature linear potentiometers were taken as positive.

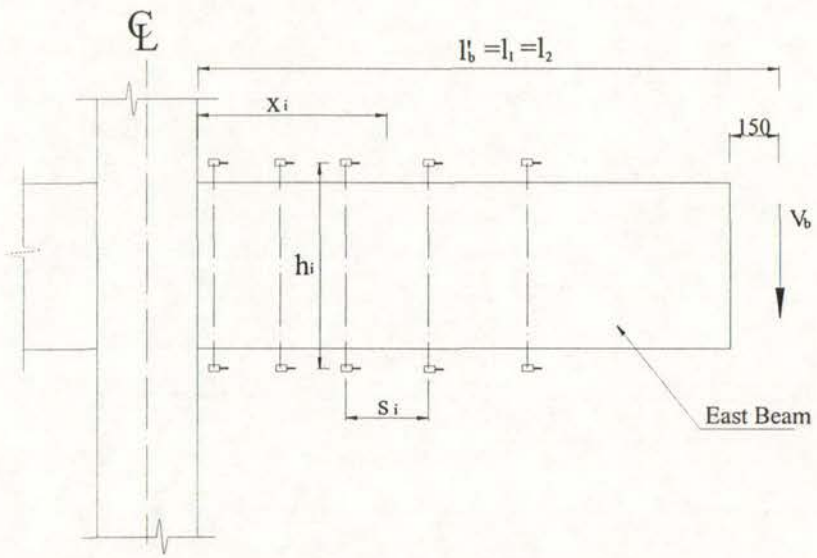

Fig.5.17 Estimation of Beam Deformation

The east beam end displacement ${}_E\delta_{bf}$ due to its flexural deformation only then can be found as follows:

$${}_E\delta_{bf} = \sum_i \theta_{b,i} (l_2 - x_i) \qquad (5.9)$$

where: l_2 is the distance from column face to the centre of the beam end pin (=1755mm), and x_i is the distance from column face to the centre of the region i.

The west beam end displacement ${}_W\delta_{bf}$ due to its flexural deformation only could be obtained in the same way, namely,

$${}_W\delta_{bf} = \sum_i \theta_{b,i} (l_1 - x_i) \qquad (5.9')$$

No instrumentation had been set up to measure the beam shear deformations because the beams were not expected to fail in shear owing to the use of plain round bars. This was later on verified by the test observations. Therefore, it was reasonable to neglect the shear deformations in beams.

The equivalent storey displacement (column displacement), $\Delta_{c,b}$, resulting from beam deformations, ${}_E\delta_{bf}$ and ${}_W\delta_{bf}$, is calculated as follows:

$\Delta_{c,b} = l_c / l_b \ ({}_W\delta_{bf} - {}_E\delta_{bf})$ for interior beam-column joint units (5.10)

$\Delta_{c,b} = - \delta_{bf} \ l_c / l_b$ for exterior beam-column joint units (5-10)'

where: l_c is the storey height, namely, vertical distance between the column end pins (3200mm) and l_b is the beam span or horizontal distance between the beam end pins (=3810mm for interior beam-column joint units, and = 1905 mm for exterior beam-column joint units).

In reality, the consequence of large beam deformations will complicate the structural force transfer path. Typically the increase in beam lengths will result in expansion of bay lengths of the frame structures, actuating the restraints against the beam deformations from columns. As a result, compressive axial beam load develops, then the beam flexural capacities are enhanced. This finally causes the adverse effect on the desired ratio of column moment capacities to beam moment capacities at the same joint.

5.5.3 Deformations of the Columns

The upper column of Fig. 5.8 (b) was reproduced in Fig.5.18.

Similar to the convention definition made previously for the beams, it was defined that positive column curvatures and positive column rotations were associated with the column left fibre in tension and the column right fibre in compression, and the measured compressive displacements by linear curvature potentiometers were taken as positive.

Therefore, the average rotation over the column region R_j could be as follows:

$\theta_{c,j} = ({}_r\delta_j - {}_l\delta_j) / d_j$ (4.11)

and the average curvature over this region R_j is

$$\phi_{c,j} = \theta_{c,j} / r_j \qquad (4.12)$$

where: ${}_l\delta_j$ and ${}_r\delta_j$ are the measurements of the left and right column curvature linear potentiometers over the region j, and d_j and r_j are as seen in Fig. 5.18.

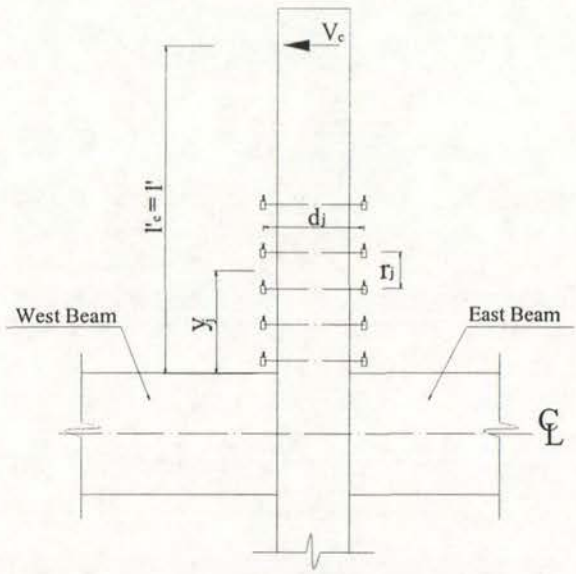

Fig.5.18 Estimation of Column Deformation

The flexural deformation of the upper column, ${}_U\delta_{cf}$, then can be derived as follows:

$${}_U\delta_{cf} = \sum_j \theta_{c,j}(l' - y_j) \qquad (5.13)$$

where: d_j, r_j, y_j and l' are shown in Fig. 5.18.

Like beams, column shear deformations were thought to be insignificant and were hence neglected. The observed test evidence during the testing also supported this assumption.

Similar schedules were used to find the deformations of the bottom column, ${}_B\delta_{cf}$.

The equivalent storey displacement, $\Delta_{c,c}$, resulting from the column deformations, ${}_U\delta_{cf}$ and ${}_B\delta_{cf}$, is calculated as follows:

$$\Delta_{c,c} = ({}_{U}\delta_{cf} - {}_{B}\delta_{cf})\,(l_c'/l_c) \qquad (5.14)$$

where: l_c' =1350mm, and l_c =3200mm

Unlike beams, the increases in lengths of columns due to the elastic and inelastic column deformations will consequently increase the column P-Δ effects, threatening the stability of the whole structure.

5.5.4 Deformations Due to Joint Shear Distortion

The equivalent storey displacement due to joint shear distortion, $\Delta_{c,j}$, can be obtained in the following way:

$$\Delta_{c,j} = \gamma_j \;(l_c - h_b - l_c \times h_c / l_b) \qquad (5.15)$$

where: γ_j is the joint shear distortion defined in Section 5.2.4, l_c is the storey height (=3200mm), l_b is the beam span (=3810mm), h_b is the depth of beam and h_c is the overall depth of the column.

5.5.5 Beam Fixed-End Rotation

The fixed-end rotation of the members adjacent to the joint is caused by the tensile strain or slip of the longitudinal bars anchored in the joint core. For these beam-column joint test units, significant bar slip would be anticipated due to the use of the plain round bars for longitudinal reinforcement and/or insufficient anchorage lengths within the joint core. Hence beam fixed-end rotations could be quite large.

In this test series, the fixed-end rotations of the beams were estimated by a pair of linear potentiometers located next to the column faces, fixed-end interfaces. From Fig. 5.17, the beam fixed-end rotation $\theta_{b,fe}$ can be derived by:

$$\theta_{b,fe} = ({}_{t}\delta_1 - {}_{b}\delta_1) / h_1 \qquad (5.16)$$

where: ${}_{b}\delta_1$ and ${}_{t}\delta_1$ are the bottom and the top displacement measured at the fixed-end interfaces and h_1 is the vertical distance between the linear potentiometers at the fixed-end interface.

The deformation due to beam fixed-end rotation, ${}_b\delta_{fe}$, can be obtained as:

$${}_b\delta_{fe} = \theta_{b,fe}\, l_b' \qquad (5.17)$$

where: $\theta_{b,fe}$ is the beam fixed-end rotation defined above and l_b' is the distance from the column face to the centre of the beam end pin.

The equivalent storey displacement due to fixed-end rotation of the beam, $\Delta_{b,fe}$, can be obtained as:

$$\Delta_{b,fe} = -{}_b\delta_{fe}\; l_c / l_b \qquad (5.18)$$

where: $\Delta_{b,fe}$ is the equivalent horizontal storey displacement due to beam fixed-end rotation, l_c is the storey height (=3200mm), and l_b is the beam span (=3810mm for interior beam-column joint units, and =1905 mm for the exterior beam-column joint units).

Although the linear potentiometers were placed as close as possible to the column faces, the fixed-end rotation so obtained includes some rotation due to elongation of the longitudinal bars over that region.

5.5.6 Column Fixed-End Rotation

Similar to beam fixed-end rotations, column fixed-end rotations were also monitored during testing because big column fixed-end rotations were anticipated.

In this test series, the component of equivalent storey displacement due to column fixed-end rotations were monitored by a pair of linear potentiometers located next to the beam faces, see Fig.5.18, the fixed-end rotation $\theta_{c,fe}$ can be derived by:

$$\theta_{c,fe} = ({}_r\delta_1 - {}_l\delta_1) / d_1 \qquad (5.19)$$

where: ${}_l\delta_1$ and ${}_r\delta_1$ are the measurements of the left and right column curvature linear potentiometers at the fixed-end interfaces;

d_1 is the distance between the two linear potentiometers.

The component of storey displacement due to column fixed-end rotations, $\Delta_{c,fe}$, is

$$\Delta_{c,fe} = \theta_{c,fe}\ l_c^{'} \qquad (5.20)$$

where: $l_c^{'}$ is the distance from the beam face to the centre of the column end pin;

and $\Delta_{c,fe}$ is the storey displacement due to column fixed-end rotation.

CHAPTER 6

TEST RESULTS OF INTERIOR BEAM-COLUMN JOINTS

6.1 TEST OF UNIT 1

6.1.1 Introduction

This test program involved two as-built full-scale interior beam-column joint units, Unit 1 and Unit 2. Unit 1, which was tested under simulated seismic loading with zero axial column load, was characterised by an expected weak column-strong beam mechanism, the use of plain round longitudinal and transverse reinforcement, low quantities of transverse reinforcement in the beams and the columns, no shear reinforcement in the joint core at all, and large diameter of the longitudinal bars passing through the joint core, as was typical of 1950s construction in New Zealand. Test on Unit 1 was identical to Hakuto's test on Unit O1 except the use of plain round reinforcing bars. Such a test design aimed at investigating the seismic performance of existing reinforced concrete moment resisting frame structures and the possible effect of steel type used on the seismic performance of existing reinforced concrete moment resisting frame structures.

According to the theoretical considerations conducted in Chapter 4, the emphasis is placed on the investigations into the effects of bond degradation and bar slip along the longitudinal bars and column bar buckling, and into the shear performance of the beams, columns and the joint core when plain round longitudinal bars are used.

6.1.2 Cracking and Damage

Fig. 6.1 shows the final appearance of Unit 1 at the end of testing. As illustrated by photograph in Fig. 6.1, the two columns of Unit 1 had major cracking at the final stage and the damage to Unit 1 was mainly limited to the columns. Evidently, a weak column - strong beam failure mechanism formed during testing as predicted theoretically in Table 4.5.

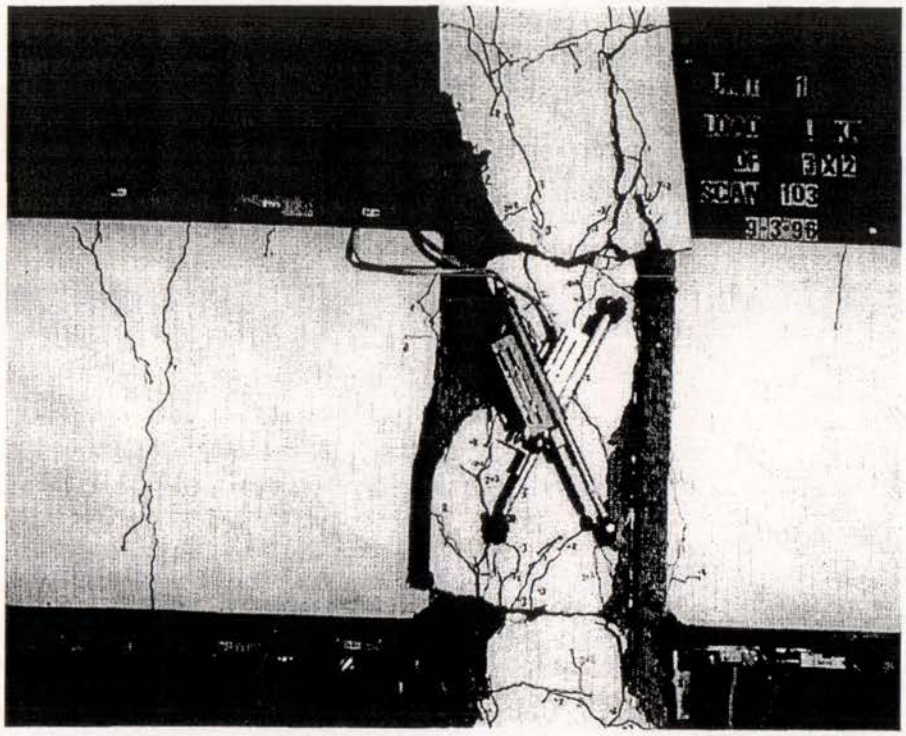

Fig. 6.1 Final Appearance of As-Built Interior Beam-Column Joint Unit 1

The damage to the columns tended to mainly concentrate in column horizontal flexural cracks above and below the joint panel although some damage was also observed in the form of vertical cracks running along both layers of the column longitudinal bars across the joint core. The damage concentration in two major column horizontal cracks above and below the joint core for Unit 1 occurred as a result of rapidly increased column fixed-end rotations, which were associated with significant bond degradation and slip of the column longitudinal bars within the joint core. The damage in the form of column vertical cracks along the column longitudinal bars across the joint core occurred as a consequence of column bar buckling resulting from bar slip and inadequate lateral restraint against column bar buckling.

The damage observed to the beams was by way of beam vertical flexural cracks adjacent to the joint panel, but it was not so pronounced as that for the columns, indicating that bond degradation and slip along the beam main bars within the joint core were not so critical as that for the columns.

The joint panel performed satisfactorily during testing although the theoretical consideration showed that the joint shear performance would be very critical due to

lack of joint horizontal shear reinforcement. Joint diagonal tension cracks did not develop with the increase in the imposed displacement level during testing, and the condition of the joint panel remained excellent till the completion of the testing, demonstrating that the joint shear failure did not govern the final failure.

No beam and column shear cracks were observed throughout the whole test history although the theoretical analysis identified insufficient column shear capacity, indicating that the use of plain round bars as was the case for Unit 1 led to an reduced demand for member transverse reinforcement in resisting shear. This is because bond degradation resulting from the use of plain round reinforcing bars changed the shear resisting mechanism in linear members into a thrust mechanism rather than a truss mechanism as was the case with deformed bars. The actuation of a thrust mechanism, unlike a truss mechanism, does not need the participation of transverse reinforcement in resisting shear. This was also reported by Maffei, J. 1997 [M1, M2].

Therefore, the bond degradation and bar buckling of the plain round longitudinal bars, especially in the columns, were believed to initiate the final failure of Unit 1. The member transverse reinforcement was more needed for preventing longitudinal bar buckling than for providing shear capacity when plain round bars are used for longitudinal reinforcement.

Whereas in the case of Hakuto's test of Unit O1 the final failure was due to the joint shear failure and severe bond degradation along the column and beam longitudinal bars within the joint core, the final failure of Unit 1 was attributed to more severe bond degradation along the column longitudinal reinforcement within the joint region and column bar buckling. The appearance of the joint of Unit 1 at the final stage was of much better integrity than Hakuto's Unit O1. Hakuto's Unit O1 was identical to Unit 1 except that Hakuto's Unit O1 used deformed reinforcing bars. Evidently, the use of plain round reinforcing bars as was the case of Unit 1 increased the need of column transverse reinforcement for anti-buckling but led to greatly improved joint shear performance due to the enhancement of the joint concrete strut mechanism in this case.

6.1.3 Hysteretic Response

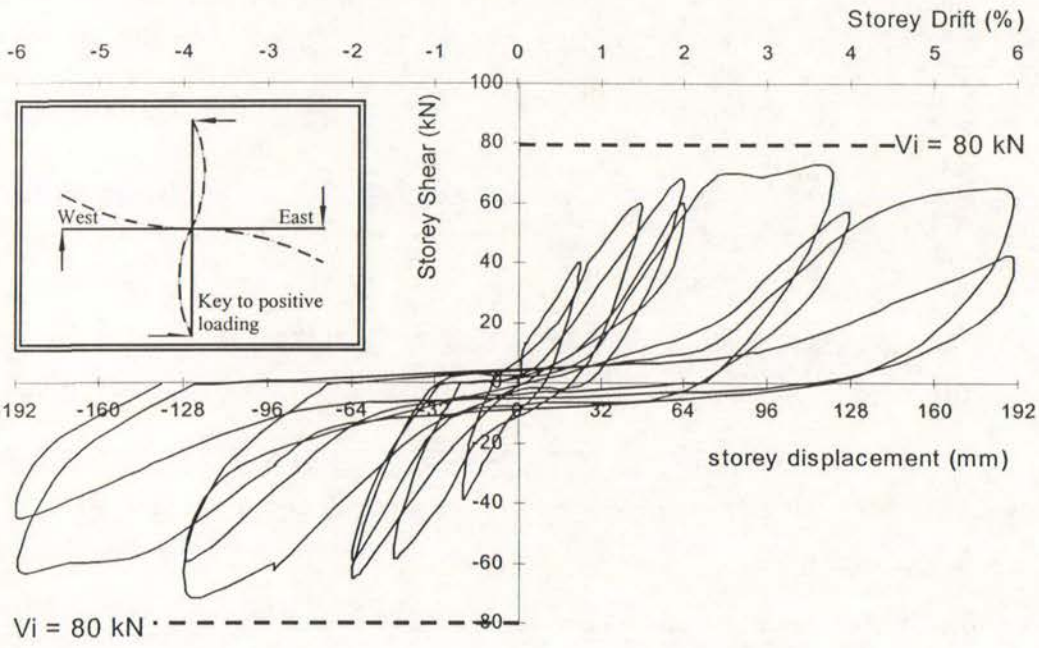

Fig.6.2 Storey shear versus storey displacement hysteresis loops of Unit 1

Fig.6.2 shows the storey (horizontal) shear force versus storey (horizontal) displacement hysteretic response measured for Unit 1. Also shown is the ideal theoretical storey shear strength of the unit, V_i, which was governed by the theoretical column flexural strengths calculated using the New Zealand code approach [N1] but using the measured material strengths and assuming a strength reduction factor of unity as previously described. Figs. 6.3 and 6.4 show the vertical deflections at the beam-ends plotted against the corresponding beam shears for Unit 1. These plots confirm the poor seismic behaviour of the unit as a whole.

The first yield displacement obtained for the test of Unit 1 using the method described in section 5.3.2 was 57 mm. This was equivalent to a storey drift of 1.8% and nearly three times the predicted first yield displacement of 20mm using conventional theory. The predicted first yield displacement did not include the effect of the fixed-end rotations due to bar slip within the joint and in the members. Also of interest is that the first yield displacement obtained for the test of Unit 1 was 1.5 times the value obtained in a previous test on an otherwise identical beam-column joint assembly

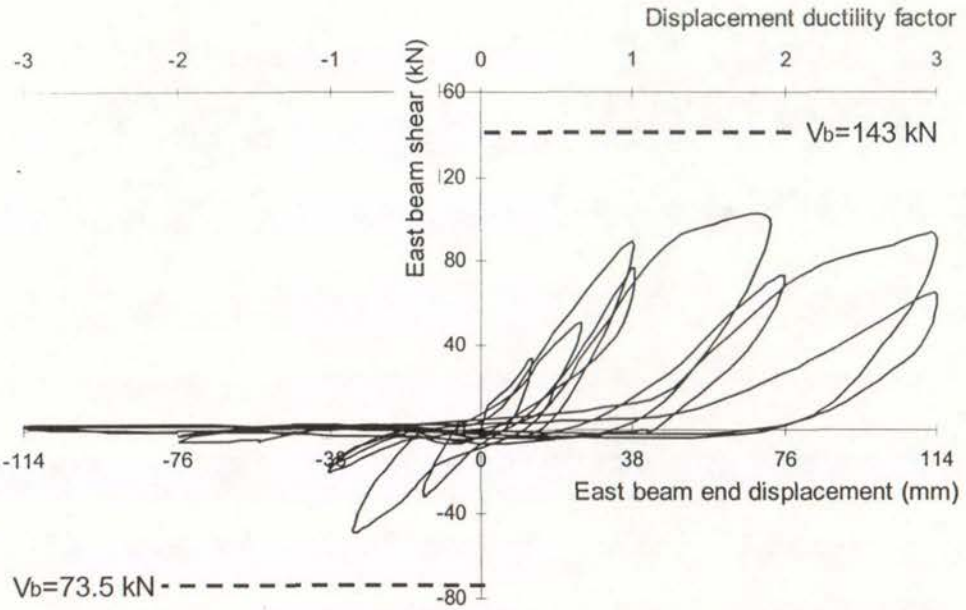

Fig.6.3 Hysteresis Loops of East Beam of Unit 1

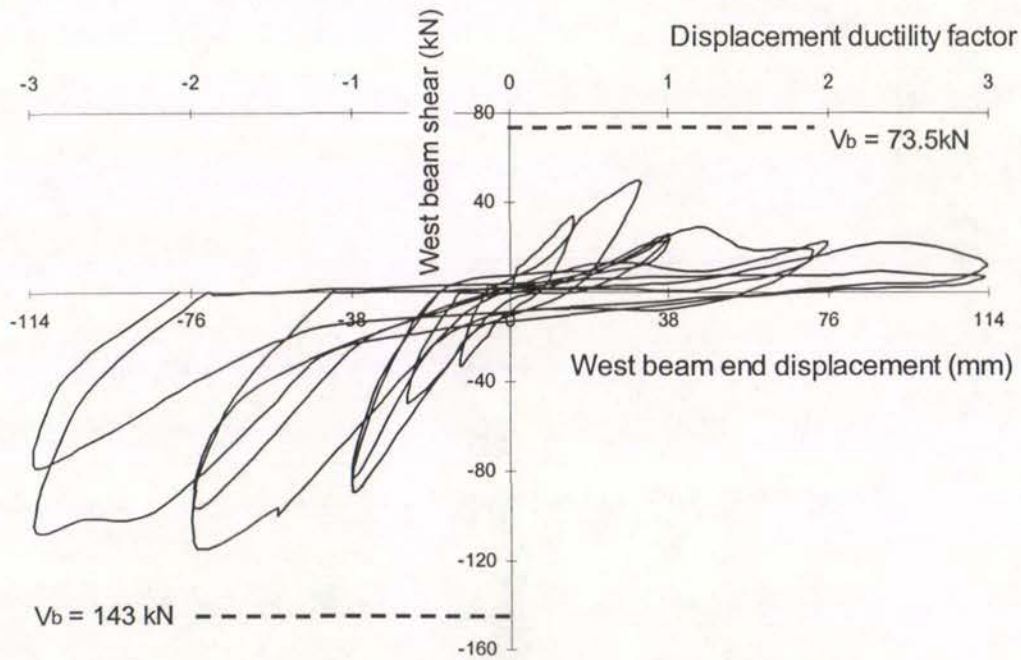

Fig.6.4 Hysteresis Loops of West Beam of Unit 1

but reinforced by deformed bars in which the storey drift was 1.2% at the measured first yield displacement [H1]. Hence, when existing reinforced concrete structures use plain round bars for longitudinal reinforcement, the available stiffness of the structures would be much smaller than the predicted value due to severe bond degradation along the longitudinal bars within and adjacent to the joint cores. As a result, the type of structure tested would become extremely flexible. On this basis the displacement ductility factor calculated using the measured first yield displacement becomes meaningless. In this case, the displacement ductility should be calculated using the theoretically predicted first yield displacement. Alternatively, storey drift can be a much better index of the displacement of existing beam-column joint subassemblages. The use of the storey drift index for the imposed displacement level is also supported by the evidence that different beam-column joint test units achieved their maximum strengths at a similar drift level of 2% [A6, B3].

Significant pinching of the loops is evident in Figs. 6.2, 6.3 and 6.4, indicating very poor energy dissipating capacity of Unit 1. The pinching started at the early loading stages and became more and more pronounced with the imposed displacement levels. The softness of the test unit at the beginning of each loading run occurred at the stage before the commencement of the concrete contribution to the flexural compression. The softness was due to the major open flexural cracks adjacent to the joint core in the compression zones of the columns and beams caused by tension in the previous loading run. These wide flexural cracks adjacent to the joint core occurred due to the significant bond degradation and bar slip of the longitudinal reinforcement within the joint region and at the adjacent ends of the members. After the two faces of the major cracks closed together, shear and compression could be transferred along and across these cracks and the stiffness increased rapidly again.

Fig. 6.2 shows that, unlike well-designed beam-column joint units where the theoretical strength or even the overstrength can be attained, the maximum storey shear strength measured for Unit 1, which was attained in the first loading run at a storey drift of almost 4%, was about 10% less than the theoretical storey shear strength of Unit 1 of 80 kN. In comparison, the theoretical storey shear strength of Hakuto's Unit O1 was reached during testing. The low attainment of the storey shear

strength for Unit 1 was due to severe bond degradation and slip of the longitudinal reinforcing bars, especially in the columns, which caused the plane section theory to overestimate the actual flexural strengths of the members at the plastic hinges, similar to the findings reported by Lees and Burgoyne [L2] and by Hakuto, Park and Tanaka [H5].

Figure 6.2 also shows that Unit 1 demonstrated a significant reduction in strength with increase in the imposed displacements after the maximum strength was attained. Apart from this, the second loading cycle had very significant strength degradation compared with the first cycle at the same displacement level. This was due to the progressive bond slip and buckling of the longitudinal column bars under cyclic loading.

It was also noticed from the hysteresis loops of each individual beam measured for Unit 1 in Figs. 6.3 and 6.4 that the attained strength of each beam at a certain displacement level for two loading directions was not proportional to their theoretical flexural strengths. Typically, for Unit 1, the beam which was experiencing downward displacement balanced higher percentage of the column bending moments imposed on the same joint while the beam which was experiencing upward displacement balanced lower percentage of the imposed column bending moments. This occurred due to much more severe bond degradation along the bottom beam bars than that along the top beam bars resulting from the initial higher bond stresses in the bottom beam bars during load-controlled elastic loading stages. Hence it is concluded that the more severe the bond degradation along the longitudinal bars, the less the attained strength in terms of the percentage of the corresponding theoretical flexural strength. The effect of bond degradation on the attainment of member flexural strengths apparently needs to be taken into account in modeling the member hysteretic response.

In summary, Unit 1 reached storey shears that were approximately 15% and 10% less than the theoretical storey shear strengths at storey drifts of approximately 2% and 4%, respectively, accompanied by a great deal of softening with cyclic loading and pinching of the hysteresis loops. Bond degradation and bar slip along the longitudinal bars played the major rule in the attainment of the member flexural strength.

6.1.4 Column Behaviour

6.1.4.1 Column Curvature Distributions

Figs 6.5 and 6.6 illustrate the measured average column curvature profiles by linear potentiometers for Unit 1, where the average column curvatures are calculated using the method described in Section 5.5.3, the positive column curvatures mean the column left side in tension and the column right side in compression, and the negative column curvatures mean the column left side in compression and the column right side in tension as defined in Section 5.5.3. In Fig.6.5 and Fig.6.6, + represents clockwise loading, 0.5 and 0.7 represent the loading cycle of 0.5 V_i and 0.75V_i. The theoretical column curvatures at first yield are the same for both loading directions and are also shown in some of these figures.

From Fig. 6.5, it is seen that the column curvatures measured over the fixed-end regions, which were defined to be the regions of 50 mm from the beam faces, were much larger than those over the other regions. This occurred due to severe bond degradation along the column main bars within the joint region and the ends of the adjacent members. Apparently taking into account only the column fixed-end rotations in calculating the column flexural deformation will give adequate results.

To facilitate the understanding of the member flexural deformation characteristics under the circumstance of severe bond degradation along the longitudinal reinforcement, the column curvatures over other regions are still investigated in the following (see Fig.6.6), where the column curvatures over the fixed-end regions are eliminated for the sake of explicit illustration.

Figs. 6.5 and 6.6 show that measured column curvatures increased with the increase in the imposed lateral load as theoretically predicted. However, big discrepancies exist for Unit 1 in the magnitudes of the measured column curvatures and the theoretical ones where the theoretical curvatures are predicted based on the measured member shear force and plane section assumption. For instance, the generated column curvatures over some regions in the loading to clockwise 0.5V_i exceeded significantly the theoretical column curvatures at first yield in Fig. 6.6 while the imposed bending moments over those regions at this specific stage were much smaller than the theoretical column moment capacity at first yield. The discrepancy was especially pronounced over the column fixed-end regions due to more significant bond

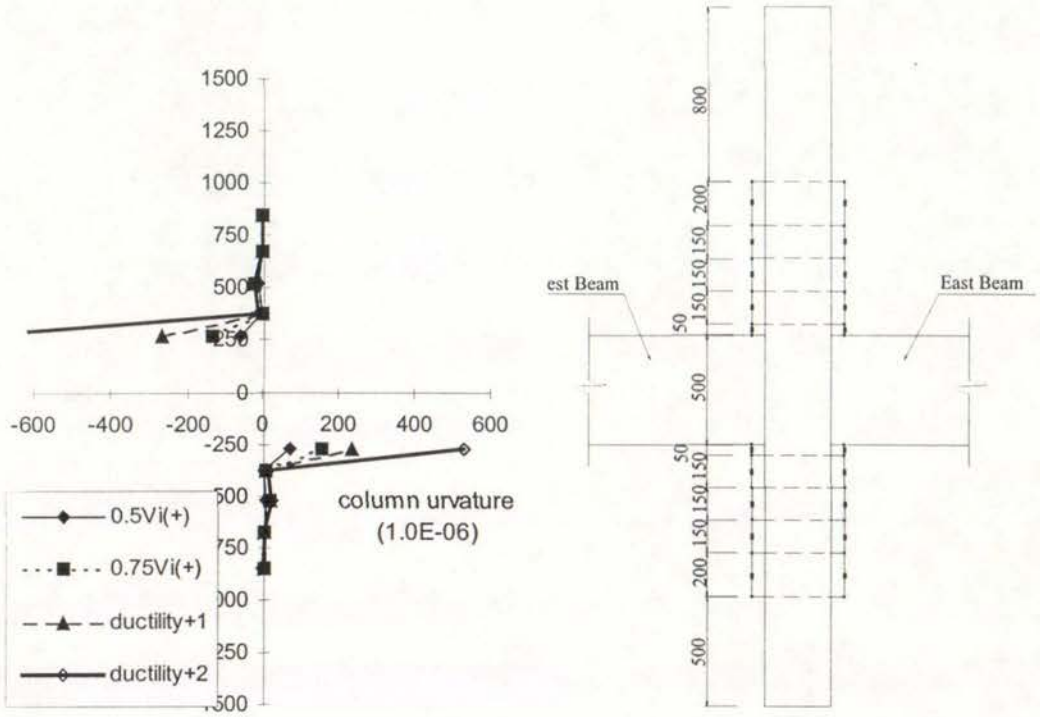

Fig. 6.5 Column Curvature Profile Measured at Clockwise Loading Peaks for Unit 1

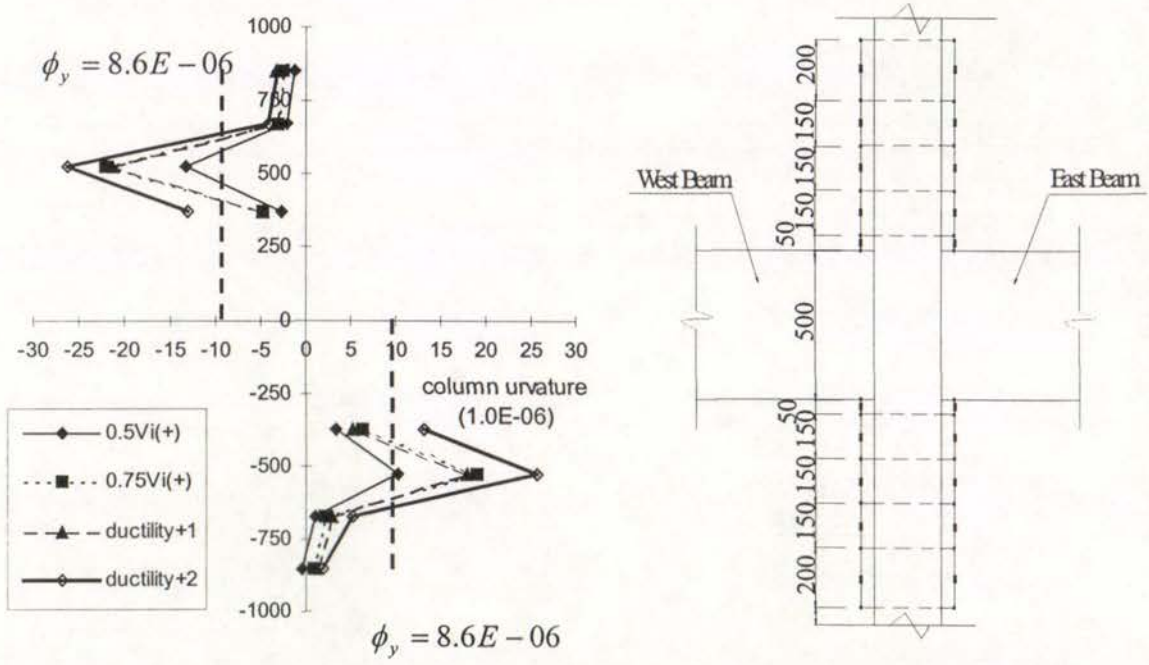

(a) Column curvature at clockwise loading peaks

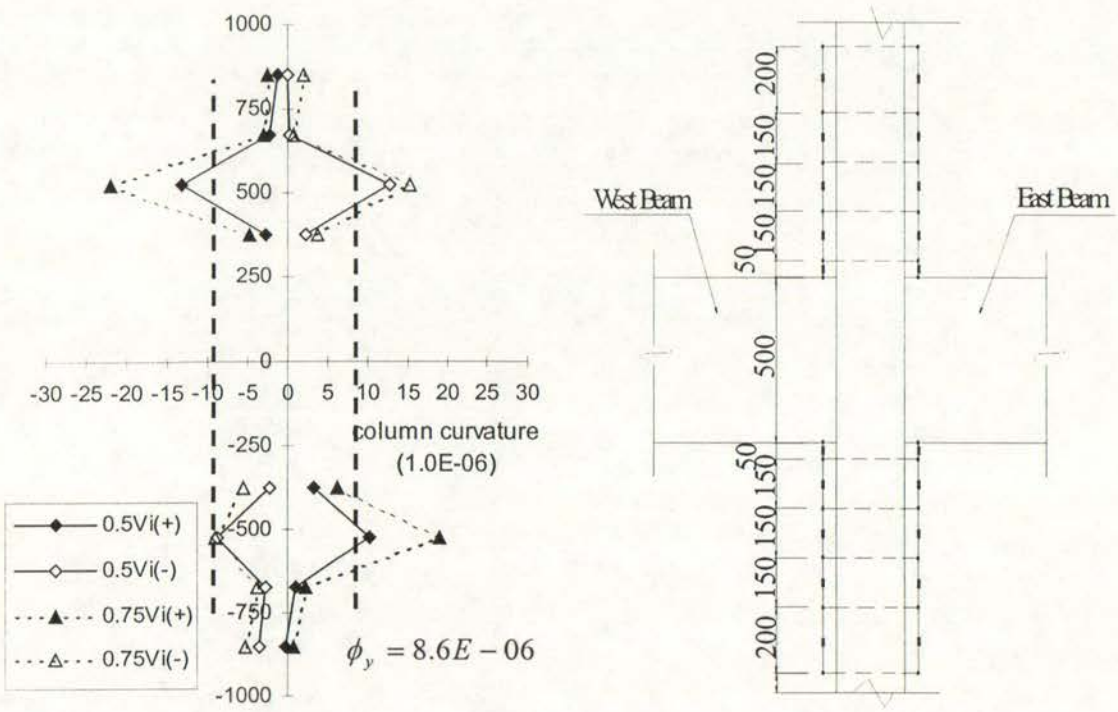

(b) Column curvature for the first two loading cycles

Fig.6.6 Column Curvature Profile of Unit 1 without Fixed-End Regions Included

degradation along the column longitudinal bars within fixed-end regions. The measured column curvature over the fixed-end regions in Fig.6.5 reached up to about 150 times the theoretical prediction using standard theory and plane section assumption.

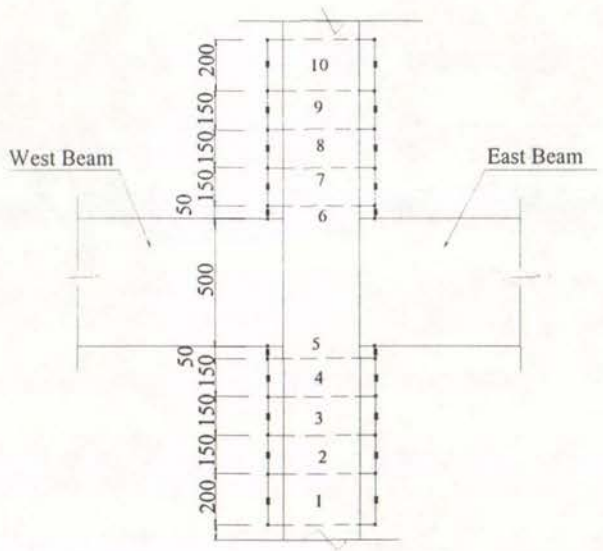

Fig.6.7 Numbering of Gauged Regions to Measure Column Curvature

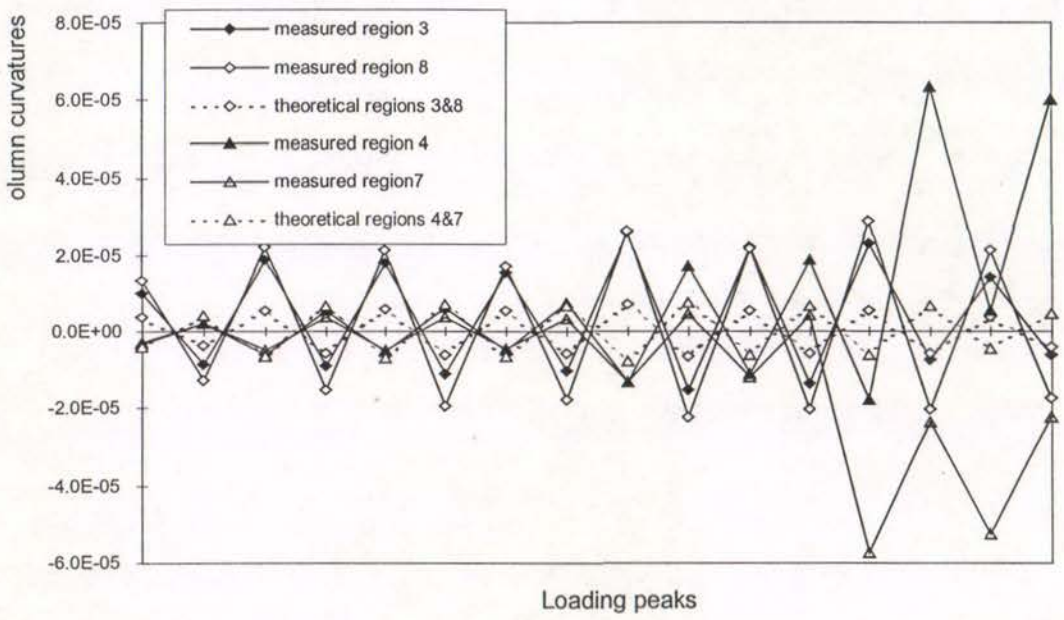

Fig. 6.8 Discrepancies between Measured Column Curvatures and Theoretical Ones

Fig. 6.8 shows the discrepancies at the specified loading stages for regions 3, 4, 7 and 8, using the region definition in Fig.6.7. From Fig.6.8, it is seen that the measured column curvatures were generally larger than the theoretical predictions, and the discrepancies increased with the loading due to the progress of the bond degradation.

The cause of the above-described discrepancies could be well explained by looking at the used curvature measurement method as described in Section 5.2.3. It is to be realised that the measurements of the linear potentiometers in measuring the column curvatures include the concrete deformations and the widths of cracks within the gauged regions. Severe bond degradation would lead to wider concrete cracks as a result of the sustained large steel strain; hence the induced column curvatures would be generally larger than the theoretical predictions as seen in Fig.6.8.

In addition, the bond degradation also caused very uneven distributions of the measured column curvatures as a consequence of the flexural deformation concentration in fewer but wider cracks in the case of bond degradation. Theoretically, the induced column curvatures at a specified loading stage will increase along the member longitudinal axis from the free-end to the fixed-end due to the corresponding increases in the imposed column bending moments when perfect bond condition is assumed as was the case with deformed bars [H1]. The average column curvature distributions measured for Unit 1 significantly disagreed with the above-stated relationship between the measured curvature distributions and the imposed bending moment distributions, and this was the case even in the loading cycle to 50% of the theoretical strength of the unit. Typically, the column curvatures measured over the regions 4 and/or 7 for Unit 1 were consistently smaller than those over the regions 3 and/or 8 before the attainment of the maximum strength of the test unit at displacement ductility factor of 2 while the imposed bending moments over the regions 4 and/or 7 were generally larger than those over the regions 3 and/or 8 at a specified loading stage. Again, this test evidence could be explained by looking at the measurement method for column curvatures. The column curvatures measured over the regions having flexural cracks involved would be much larger than those over the regions having no flexural cracks. For Unit 1, the bond degradation of the column main bars over regions 4 and/or 7 must have been more severe than that over regions 3 and/or 8 due to higher bond stresses. Better bond condition over regions 3 and/or 8

would mean more flexural cracks due to higher force transmitted from the steel to the concrete within these regions compared to the regions 4 and/or 7. Hence the measurements of the linear potentiometers and the resulted curvatures over the regions 3 and/or 8 were much larger compared with those over the regions 4 and/or 7.

Therefore, severe bond deterioration along the column main bars not only caused the measured curvatures to be generally larger than the theoretical curvatures, but also caused the measured column curvature variation to be not in agreement with the imposed bending moment. This again demonstrated that plane section assumption was badly violated due to severe bond degradation along the longitudinal reinforcement.

The unpredictable characteristics of column curvatures, together with the fact that the majority of the column flexural deformation was from the fixed-end regions, means that the detailed investigation into the column curvature properties is meaningless under the circumstance of severe bond degradation along the longitudinal reinforcement.

6.1.4.2 Column Longitudinal Reinforcement Strains

As stated in Chapter 5, the column longitudinal reinforcement strains were monitored by both the electrical resistance strain gauges and the linear potentiometers.

1. Measurements by Electrical Resistance Strain Gauges:

The electrical resistance strain gauges behaved abnormally after the completion of displacement ductility factor of 1, so only the readings before the displacement ductility of 1 were studied here. It has to be pointed out that the electrical resistance strain gauge readings should be carefully explained in the case of severe bond degradation between the longitudinal steel and the concrete. Figs. 6.9, 6.10, 6.11 and 6.12 show the measured strains along the column longitudinal reinforcement by electrical resistance strain gauges for column bars 1 and 2 of Unit 1.

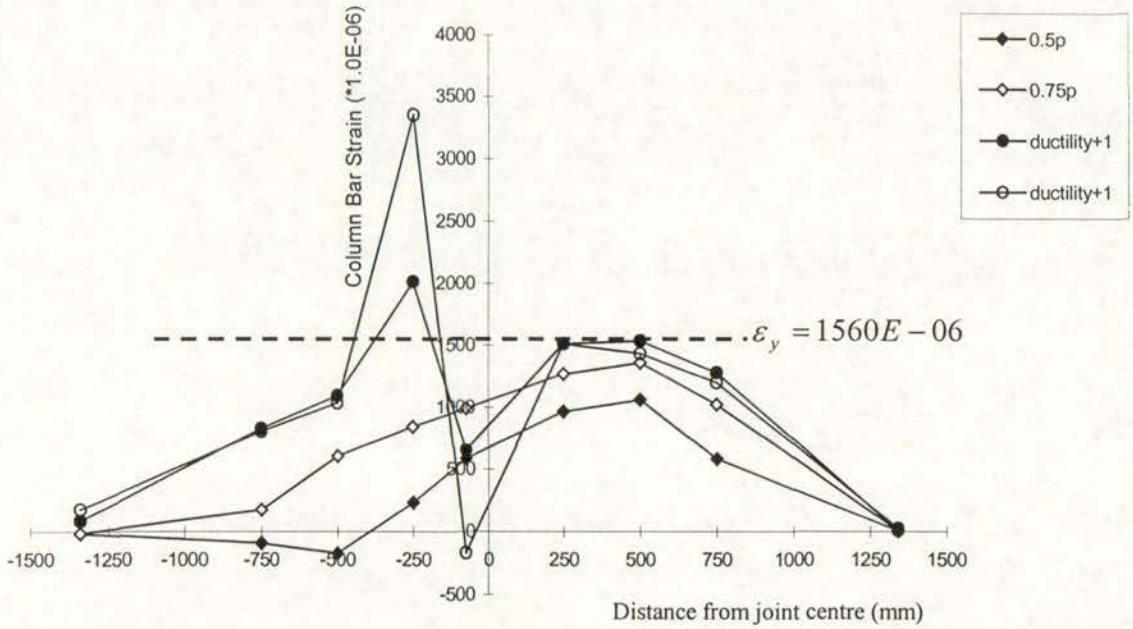

Fig.6.9 Strain Profile of Column Bar 1 of Unit 1

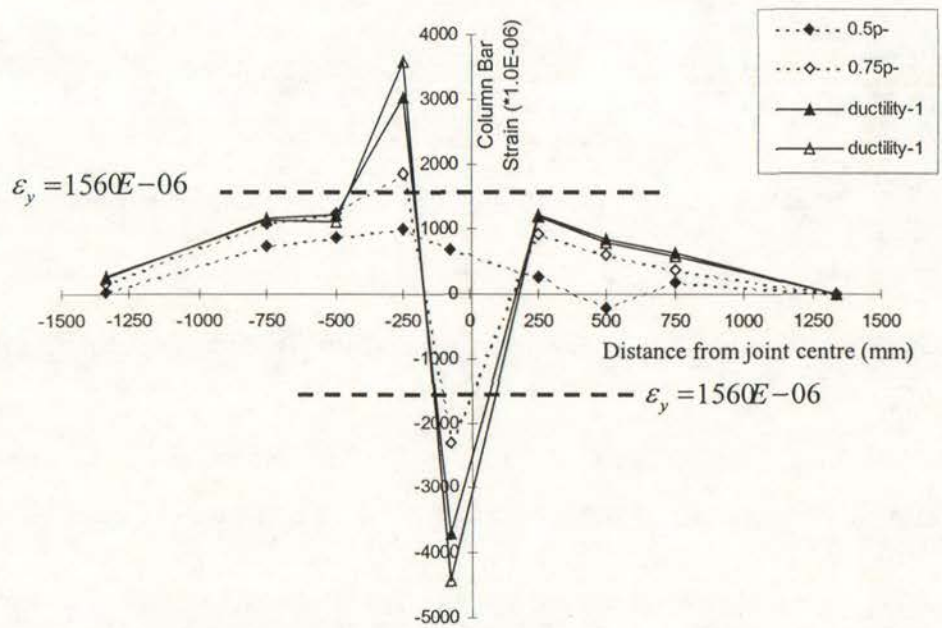

Fig. 6.10 Strain Profile of Column Bar 1 of Unit 1

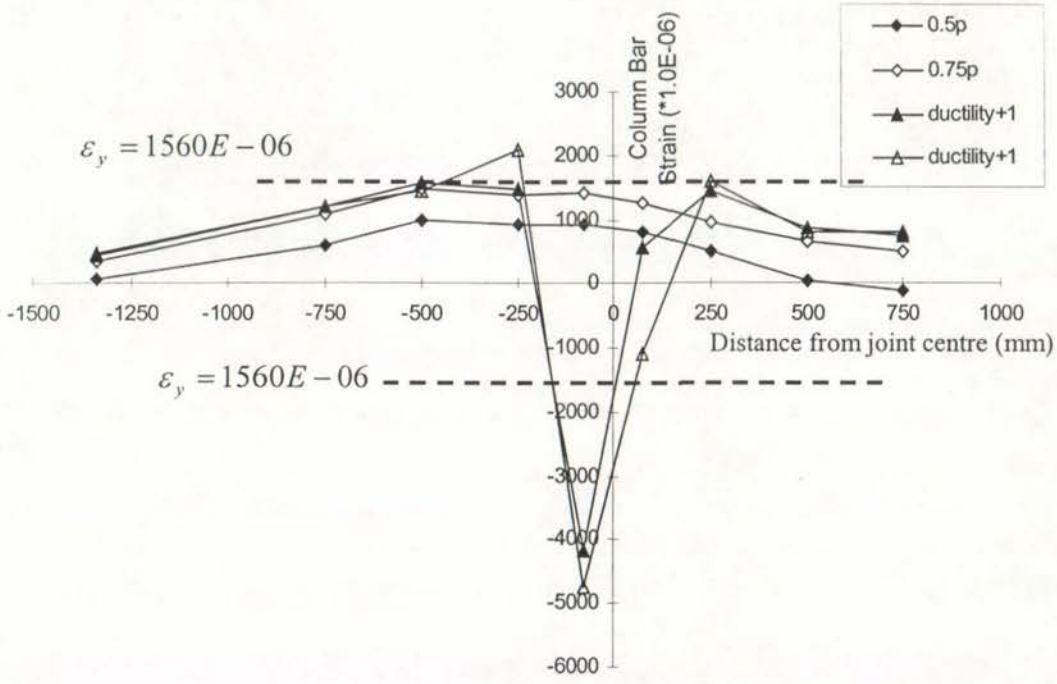

Fig.6.11 Strain Profile of Column Bar 2 of Unit 1

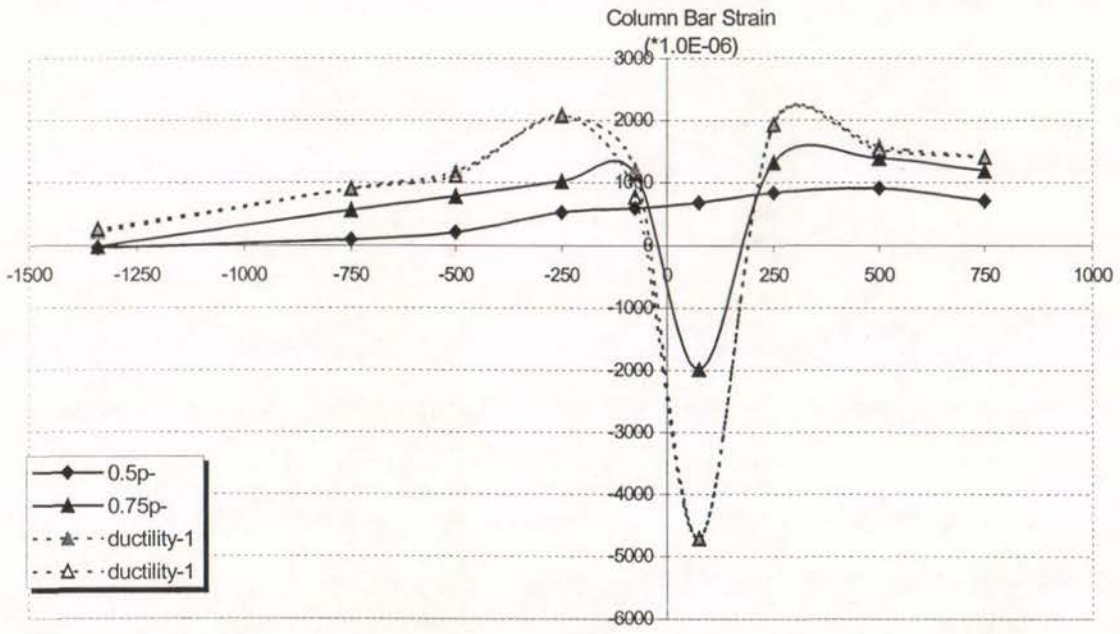

Fig.6.12 Strain Profile of Column Bar 2 of Unit 1

Figs. 6.9 to 6.12 show that the measured column reinforcing steel strains outside the joint region increased gradually as the test progressed due to the corresponding increase in the imposed bending moment, and the column longitudinal steel strain distribution along the column longitudinal axis agreed with the imposed bending moments. Evidently, as far as the linear members are concerned, the column longitudinal steel strain variation displayed a better correlation with the imposed column bending moment, compared to the column curvature properties. However the column longitudinal reinforcing steel strain profiles within the joint region displayed abnormal behaviour as the test progressed, and were characterised by the following features within the joint region:

- Severe bond degradation along column longitudinal reinforcing bars within the joint.

Figs. 6.9 to 6.12 demonstrate that severe bond degradation took place along the column longitudinal reinforcing bars within the joint region even at very early loading stages. As early as the loading stage of $0.5V_i$, the column longitudinal reinforcement had been in tension throughout the whole joint region due to inadequate bond strength within the joint region.

Compared to the test on an identical interior beam-column joint unit which used deformed bars [H1] where the column bars of the test unit were anchored at the opposite beam face (equal to 500 mm) at the loading stage of $0.5V_i$, the column bars of Unit 1 were observed to be anchored at a distance of about 1100mm from the considered beam face in the opposite column at the loading stage of $0.5V_i$, indicating that plain round bars require much longer anchorage length than that associated with the deformed bars. Severe bond degradation along the plain round longitudinal bars within the joint core caused very big column fixed-end rotations, greatly contributing to the enlarged first yield displacement.

- Discrepancies between the measured steel strains and the predicted steel strains

Figs 6.9 to 6.12 show that big discrepancies exist between the measured steel strains and the predicted steel strains along both flexural tensile bars and flexural compressive bars. The discrepancies for the flexural compression bars were obvious, and the column main bars at flexural compression side were actually in tension at beam face as a result of severe bond degradation and bar slip along the reinforcing

bars within the joint core. The measured column flexural tension steel strains were generally larger than the theoretical ones. For example, the measured column flexural tension steel strains at beam faces reached yield at the displacement ductility of 1 while the imposed bending moment on this section was only about 80% of column theoretical yield strength at the time. This once again illustrates that plane section assumption made in conventional flexural theory was violated due to severe bond degradation along the longitudinal reinforcement. Consequently, plane section assumption would underestimate the flexural tensile steel strains, as revealed by the measured column curvatures.

However, it is to be realised that the maximum steel stress could not exceed steel yield strength, therefore the above evidence means that severe bond degradation due to the use of plain round reinforcing bars would cause the available strengths to be lower than the theoretical flexural strengths as was seen in the test of Unit 1. This is very important in assessing the available strength of existing reinforced concrete structures.

The above-described discrepancies will affect the estimation of the joint shear inputs because the joint vertical shear force input is estimated using plane section assumption on the basis of the column shear force and the estimated column flexural steel tension forces at beam faces. Bond degradation along the reinforcing bars within the joint core would cause the flexural compression steel force to be in tension actually, greatly reducing the joint shear input, but the larger measured steel strains caused by bond degradation would cause the joint shear input to increase. Evidently, the estimation of the actual joint shear inputs should take these two factors into account.

- Occurrence of column bar buckling

Figs. 6.9 to 6.12 also show the evidence of column bar buckling within the joint region after the loading cycle of $0.75V_i$. It was observed that the column reinforcing bars 1 and 2 were in tension throughout the whole joint region up to the loading to $0.75V_i$ except Fig. 6.10, but turned to be in significant compression in the lower part of the joint region after the completion of the loading to $0.75\ V_i$ irrespective of the loading directions. Apparently, the remaining bond strength within the joint region after the loading to $0.75\ V_i$ was not high enough to convert the column steel tension forces at beam face into such big compression forces, and it was local column bar

buckling that caused the column bars to be in significantly compression on the face having the gauges on.

Hence it is concluded that, although the test of Unit 1 was conducted with zero axial column load, column bar buckling did occur at the later loading stages of the test of Unit 1 due to inadequate amount of column transverse reinforcement, as predicted in Chapter 4 "Theoretical Consideration".

2. Column Bar Slip Measured by Linear Potentiometers

Column bar slips within the joint core were found according to the measurements of linear potentiometers mounted on the steel rods welded on the column main bars, and this estimation is valid only if the joint core concrete deformation is negligible. The instrumentation for estimating column bar slips is shown in Fig.5.13. The slips of the column bars at points c5 and c5' relative to the static point embedded in the concrete were estimated at firstly, the slips at points c6, c4, c6' and c4' can be found by adding the measured deformations at these points relative to the points c5 or c5' then. This is graphically demonstrated in Fig. 6.13.

Fig. 6.14 shows the column bar slips within the joint region estimated for Unit 1. The maximum slips measured of column bars within the joint core for Unit 1 were as much as 10 mm. This means that the use of plain round reinforcing bars led to very significant column bar slips within the joint core, then very big member fixed-end rotations.

Evidently a proper method for calculating the first yield displacement should take into account the estimation of fixed-end rotations.

6.1.4.3 Column Transverse Reinforcement Strains

The measured column transverse reinforcement strains were all well below the steel yield strain. This was because the use of plain round reinforcing bars as was the case of Unit 1 actuated mainly arch action in resisting shear as described previously, and the transverse reinforcement does not engage in resisting shear in this case. Therefore the members reinforced by plain round bars are not shear critical compared with the case with deformed bars.

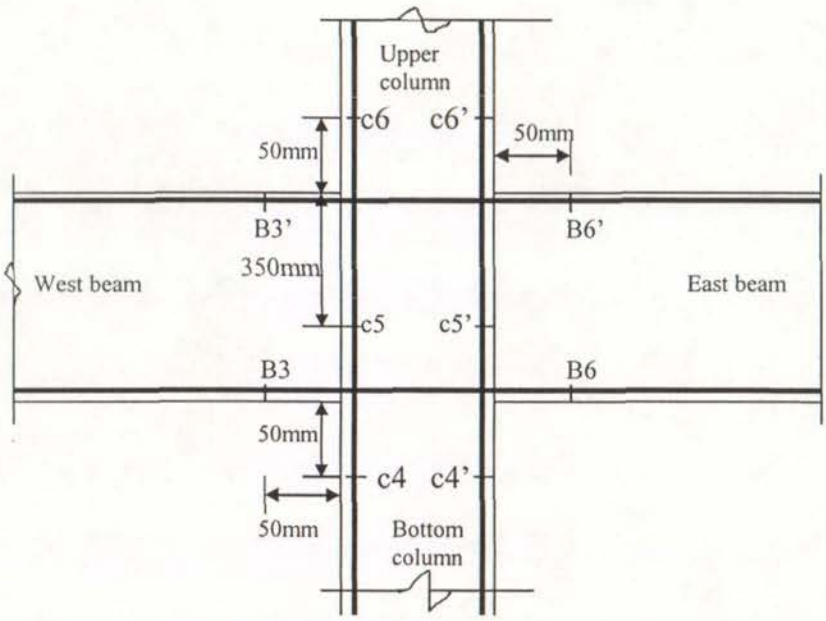

Fig. 6.13. Linear Potentiometers to Measure Column and Beam Bar Slip for Unit 1

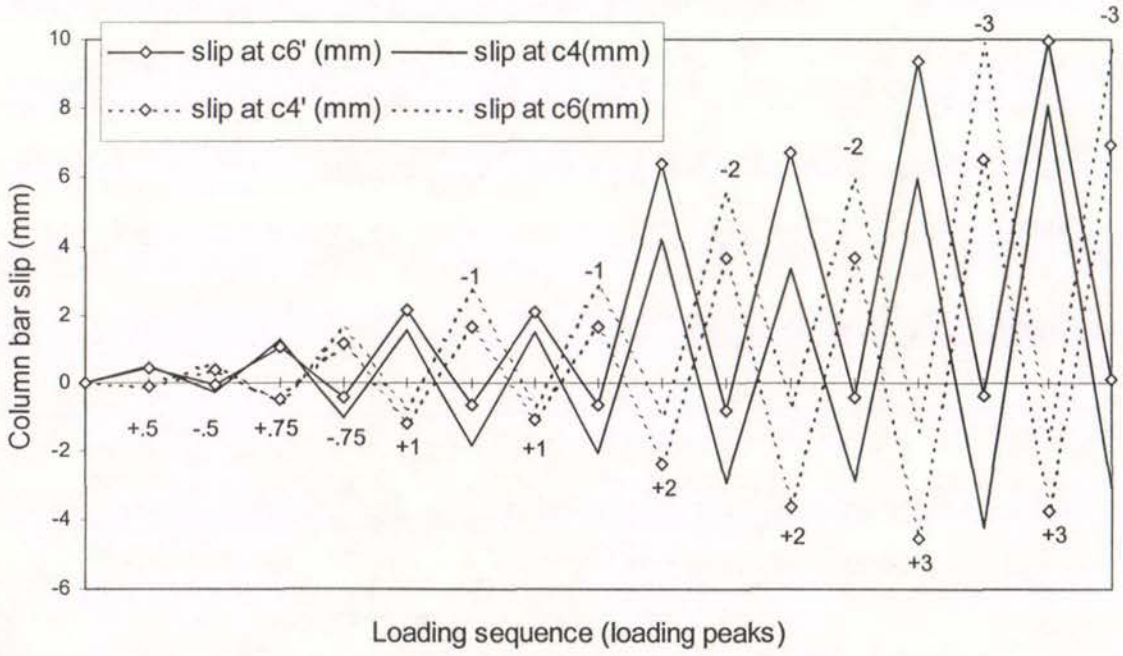

Fig. 6.14. Column Bar Slip Measured by Linear Potentiometers (mm)

6.1.5 BEAM BEHAVIOUR

6.1.5.1 Beam Curvature Distribution

Figs. 6.15, 6.16, 6.17 and 6.18 show the measured beam curvature profiles monitored using the methods described in Section 5.5.2 where the positive and negative beam curvatures were defined to be induced by positive and negative beam bending moments, respectively, and the theoretical negative and positive beam curvatures at first yield are also shown. During testing, the beams of Unit 1 were theoretically expected to be in elastic range.

Similar to the columns, the measured curvatures over the beam fixed-end regions shown in Fig. 6.15 were much larger due to significant bond deterioration of the beam bars within the joint region, in comparison with those over the other beam regions. Thus the beam fixed-end rotations were also the major sources of the beam deformation as was the case for the columns.

Significant discrepancies exist between the measured beam curvatures and the theoretical predictions as revealed by the measured column curvature distributions for this test. Typically, the measured beam curvature distribution (variation) along the beam lengths shown in Figs.6.17 and 6.18 did not follow the imposed bending moment distribution (variation) due to severe bond degradation along the beam longitudinal reinforcing bars.

Apparently heavily concentration of the member flexural deformation on the fixed end regions and relatively random member curvature distributions become two typical characteristics of the concrete members reinforced by plain round bars. The investigation into the member curvature profile in this case hence is less important, and the investigation of the member fixed-end rotations resulting from the bond degradation along the longitudinal reinforcement within and adjacent to the joint core will be of much more significance.

In addition, Figs. 6.15, 6.16, 6.17 and 6.18 show that whereas the column curvatures for Unit 1 increased gradually with the loading progress, the measured beam curvatures for Unit 1 gradually decreased with the loading progress, indicating that the beam failure did not initiate the final failure of the unit.

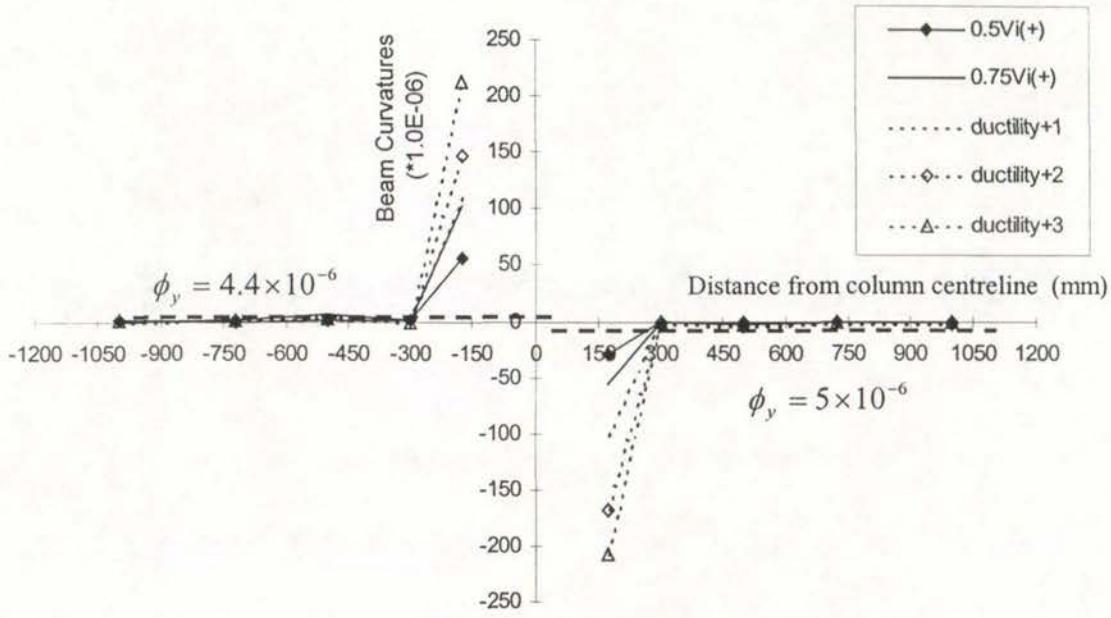

Fig. 6.15 Beam Curvature Profile of Unit 1 with Fixed-End Regions Included

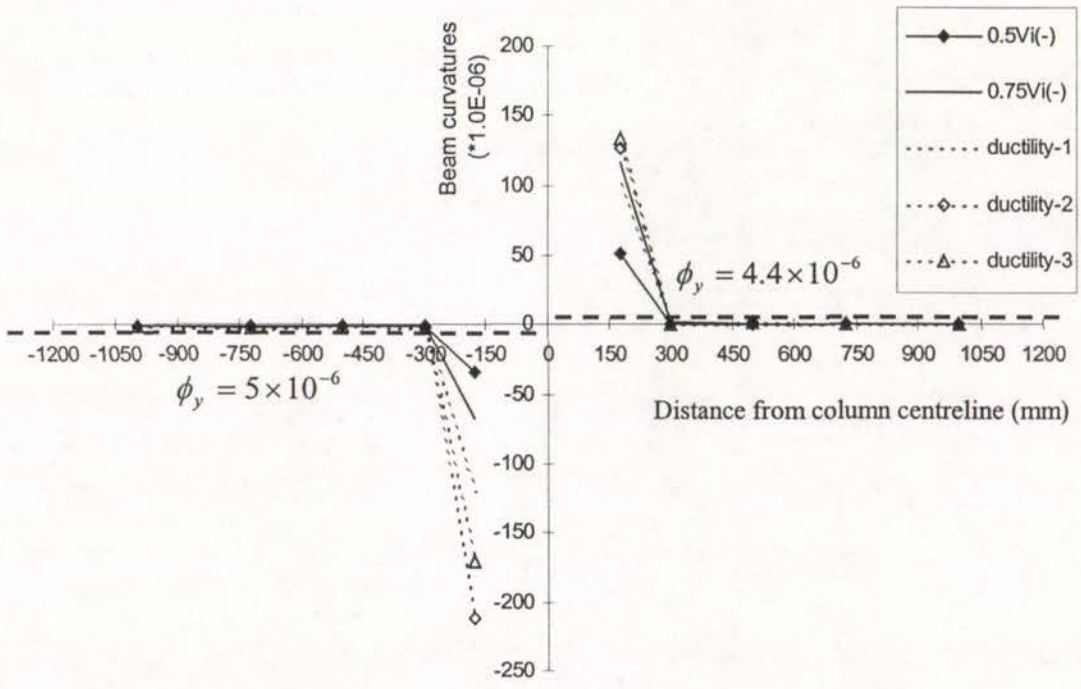

Fig.6.16 Beam Curvature Profile of Unit 1 with Fixed-End Regions Included

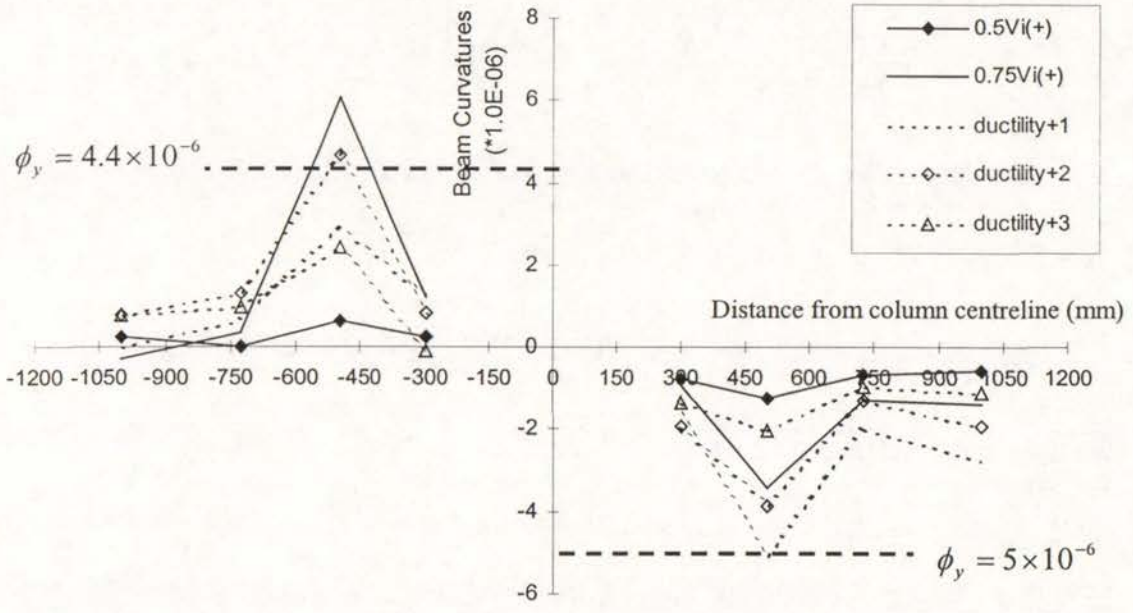

Fig. 6.17 Beam Curvature Profile of Unit 1 with Fixed-End Regions Excluded

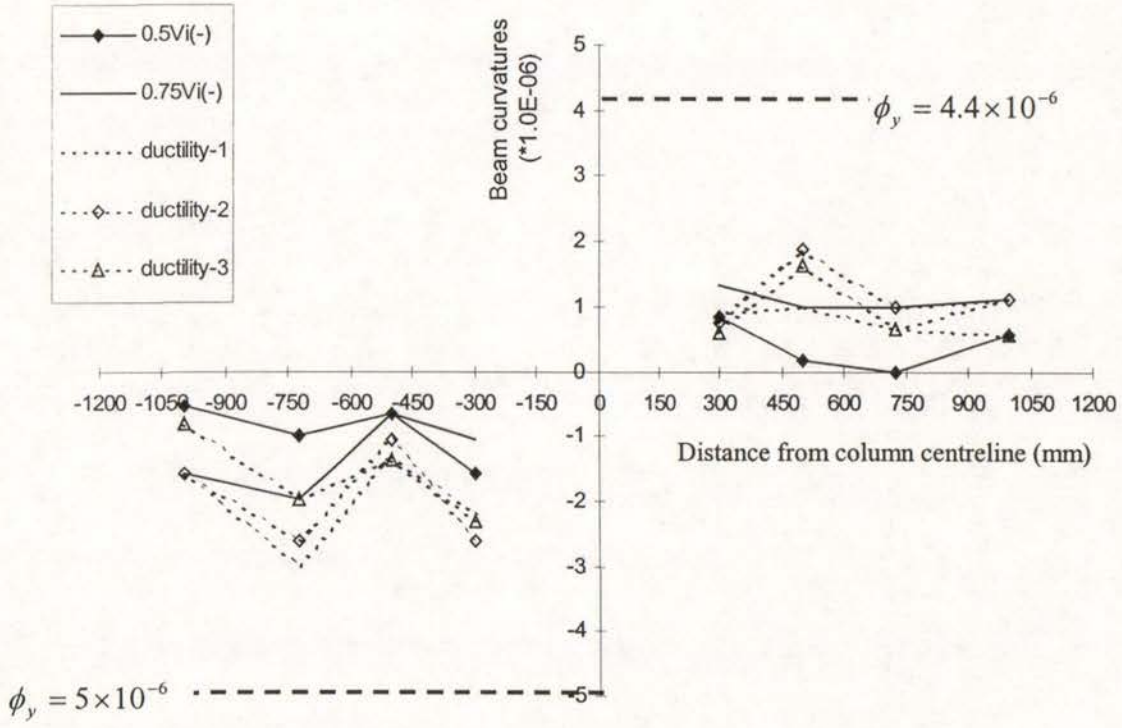

Fig.6.18 Beam Curvature Profile of Unit 1 with Fixed-End Regions Excluded

6.1.5.2 Beam Longitudinal Reinforcement Strains

The beam longitudinal reinforcement strains were monitored for Unit 1 by electrical resistance strain gauges as described in Section 5.2.5.1.

Figs. 6.19, 6.20, 6.22, 6.23 and 6.24 show the beam longitudinal steel strain profiles measured by electrical resistance strain gauges. Generally the recorded steel strains along the beam longitudinal bars had the similar features to the column longitudinal bars.

1. Better agreement between the measured beam steel strains and the imposed bending moments was seen, compared to the beam curvature properties. The measured beam flexural steel strains, although generally larger than the theoretical values predicted assuming plane section theory as was the case for the column bars, varied linearly from the column face toward the beam pin end as was the case for the imposed beam bending moment. For instance, the measured beam flexural tension steel strain at the column face was 0.00145 at the peak of the first clockwise displacement ductility 1 and this was 1.4 times the theoretical strain which was predicted using plane section theory and the measured west beam lateral load at this specific stage. The amplification of the measured beam flexural steel strains was not caused by tension shift because of no observed shear cracks in the beams and columns, and it was due to the violation of plane section assumption by severe bond degradation along the flexural reinforcing bars. Severe bond degradation along the flexural reinforcing bars caused the longitudinal bars in the flexural compressive side not to be able to carry so large compressive force as predicted, leading to larger concrete compressive force, larger concrete compressive depth and then smaller lever arm, compared to the theoretical values.

2. Even at very early loading stage of $0.5V_i$, the beam flexural compression bars were actually in tension in the region adjacent to and within the joint region due to severe bond degradation along the beam longitudinal bars. This is seen from Fig. 6.19 to Fig.6.24.

3. The measured beam steel strains were generally lower within the joint core than those at the column faces, indicating that the beam flexural steel did not engage in

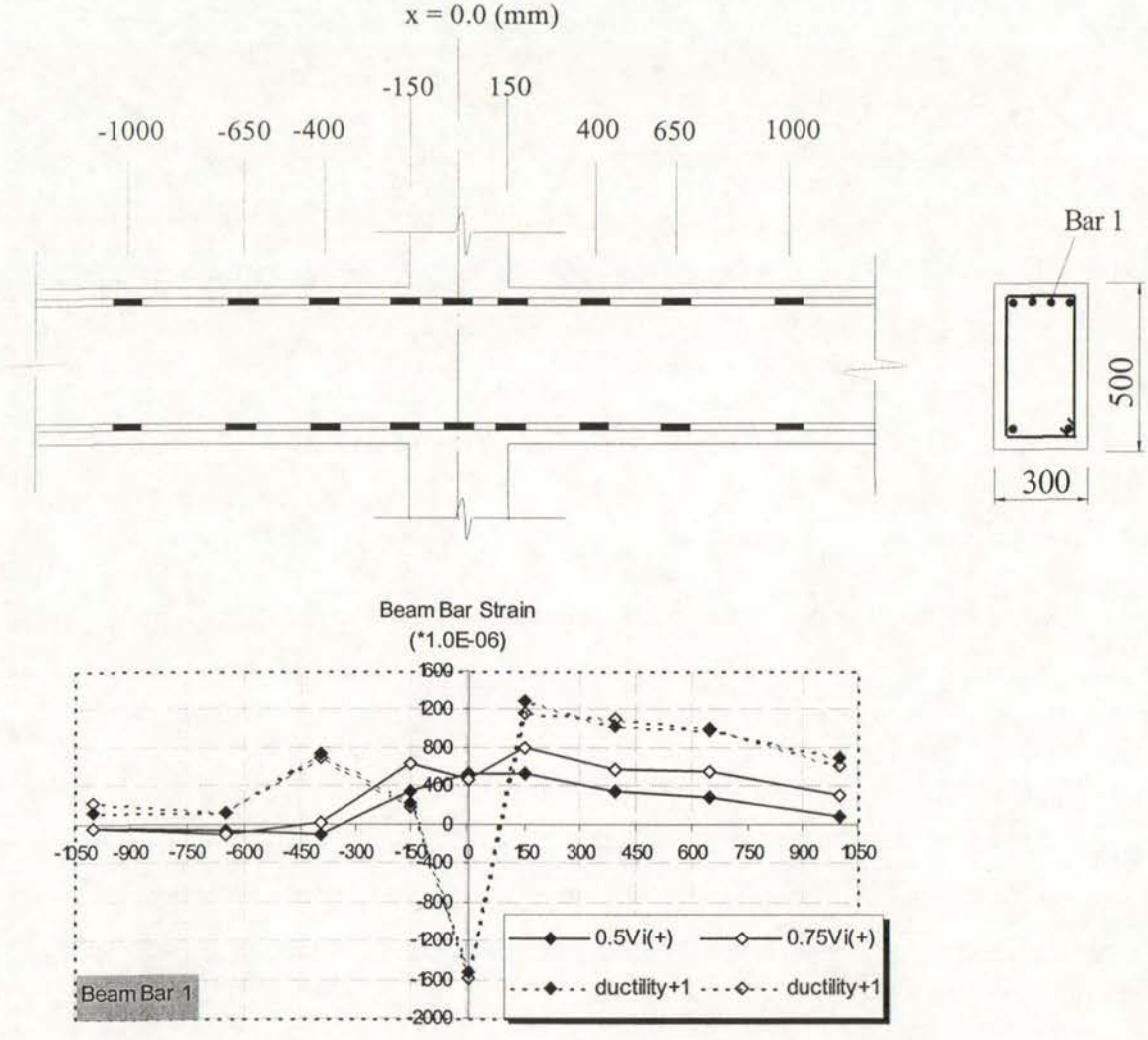

Fig. 6.19 Strain Profile of Beam Bar 1 by Electrical Resistance Strain Gauges

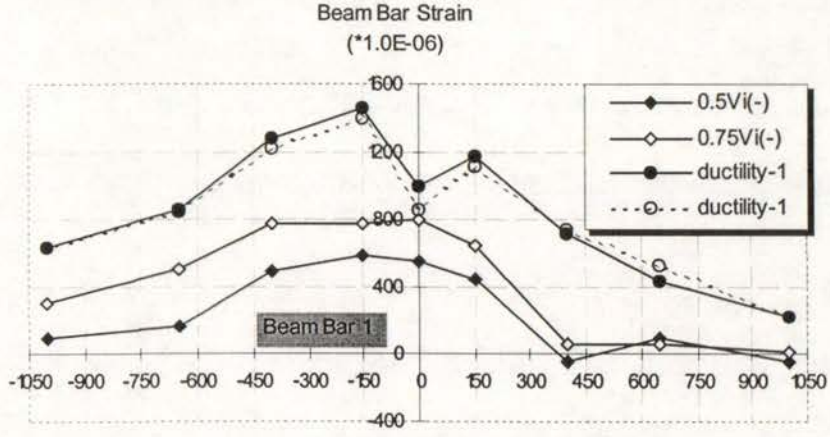

Fig. 6.20 Strain Profile of Beam Bar 1 by Electrical Resistance Strain Gauges

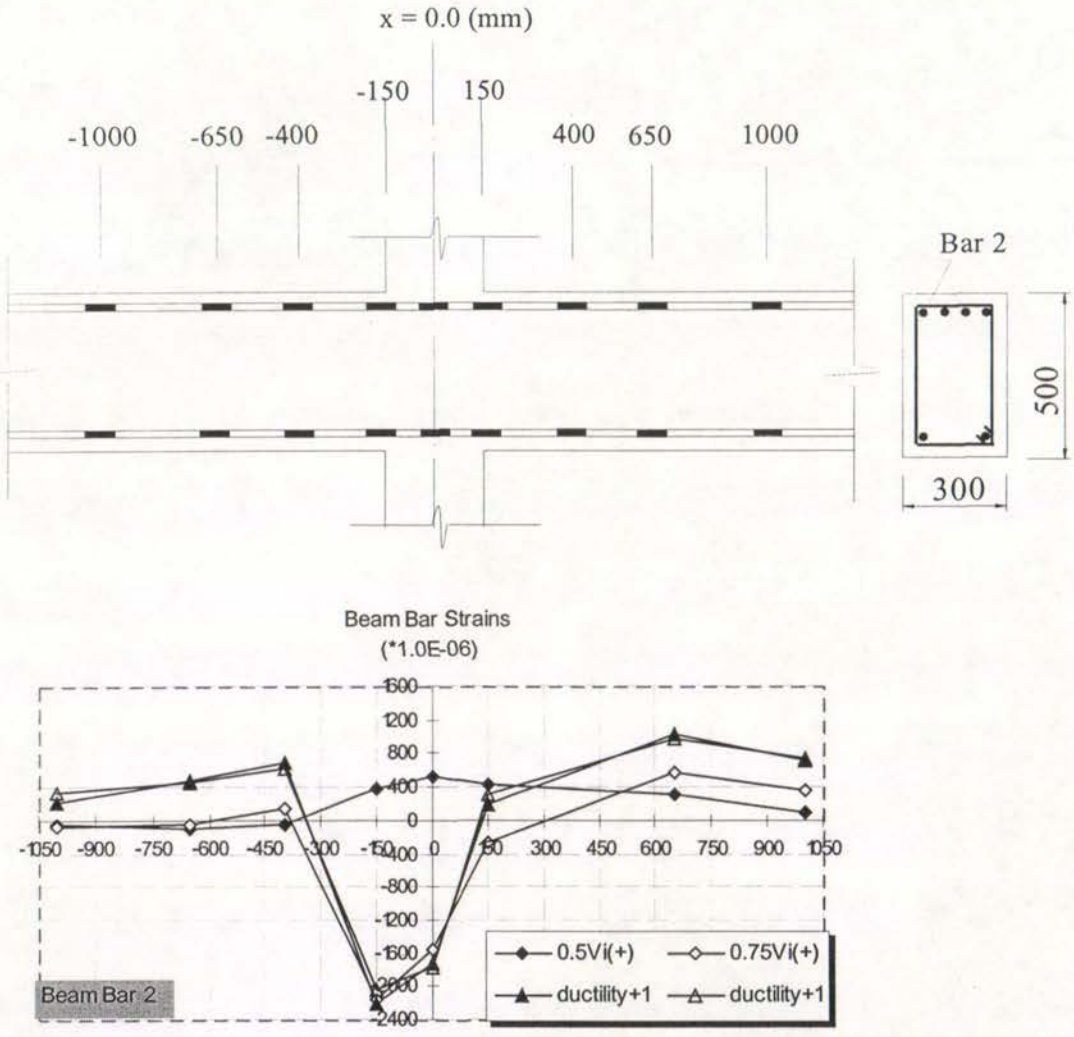

Fig. 6.21 Strain profile of Beam Bar 2 by Electrical Resistance Strain Gauges

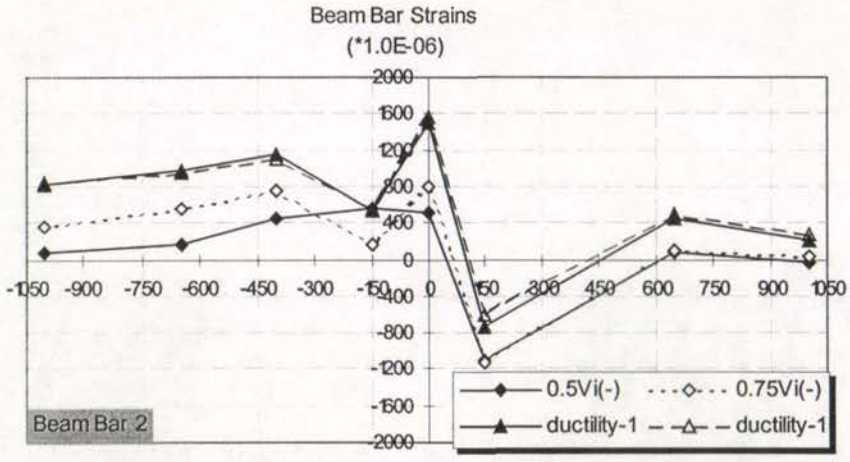

Fig.6.22 Strain Profiles of Beam Bar 2 by Electrical Resistance Strain Gauges

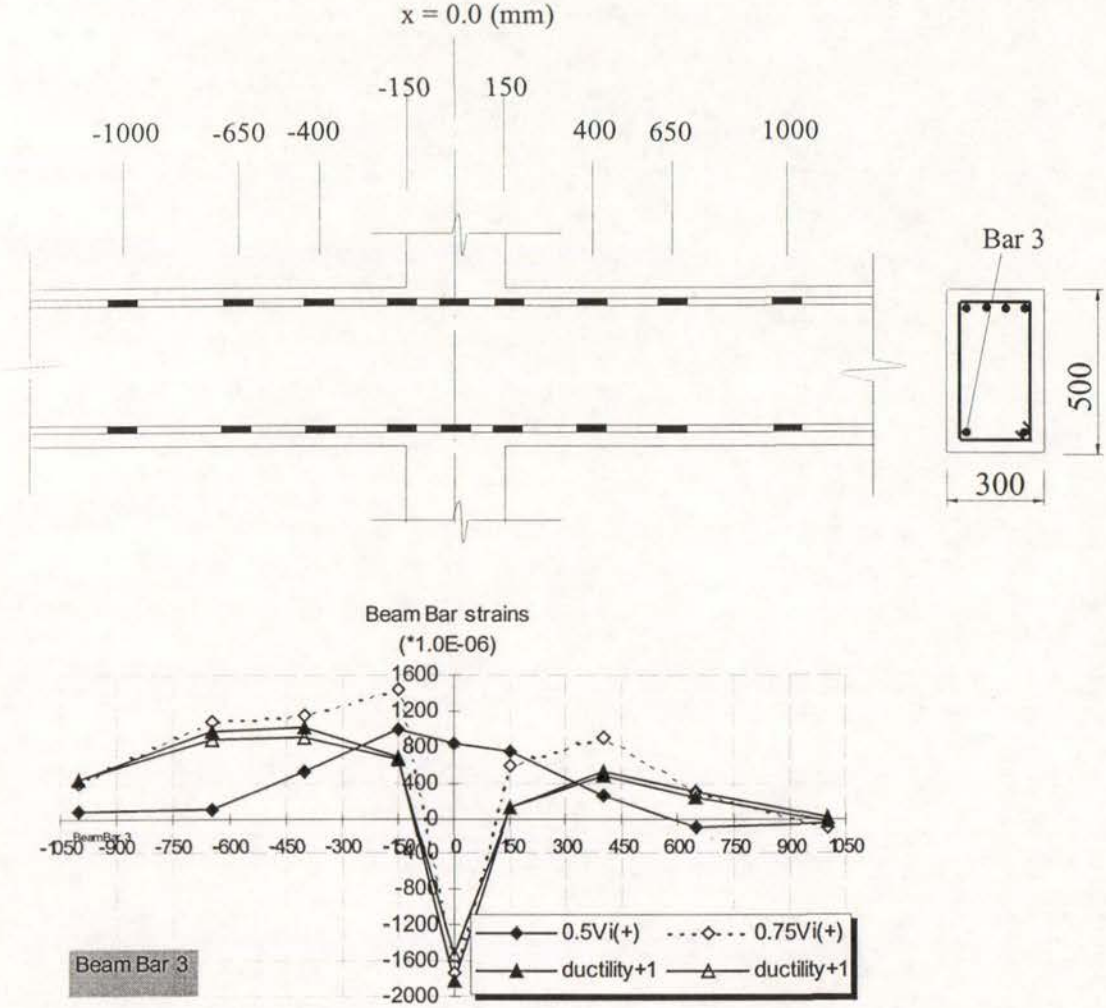

Fig.6.23 Strain Profiles of Beam Bar 3 by Electrical Resistance Strain Gauges

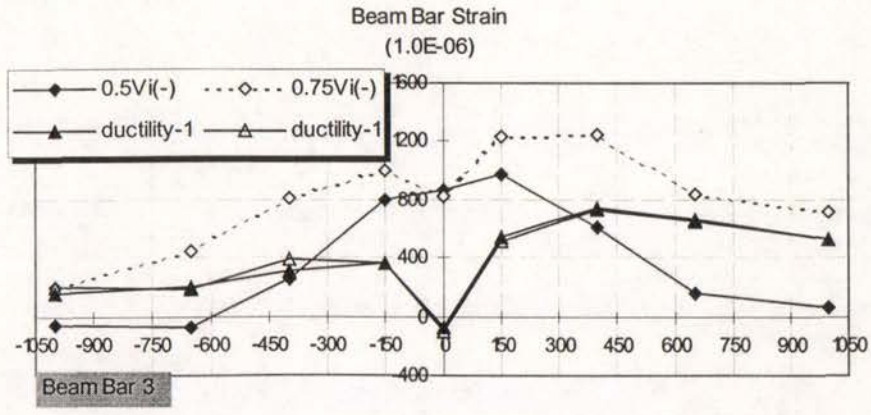

Fig.6.24. Strain Profile of Beam Bar 3 by Electrical Resistance Strain Gauges

joint shear resisting mechanism. This evidence is different from the test observation of Hakuto's Unit O1, hence the joint shear mechanism associated with plain round bars was different from that associated with deformed bars.

The beam flexural steel forces at column faces are directly incorporated into the calculation of the joint shear force demand, and bond degradation along the beam longitudinal reinforcement is more severe adjacent to the joint core. Quantitative determination of the amplification of the beam flexural steel forces at column faces due to bond degradation evidently becomes a major issue of concern in order to give a good estimation of the joint shear force input. This will be discussed elsewhere.

6.1.6 JOINT BEHAVIOUR

Fig. 6.25 illustrates the joint shear distortion γ_j and expansion $\frac{1}{2}(\delta_j + \delta_{j'})$ estimated using the method as described in Section 5.2.4.

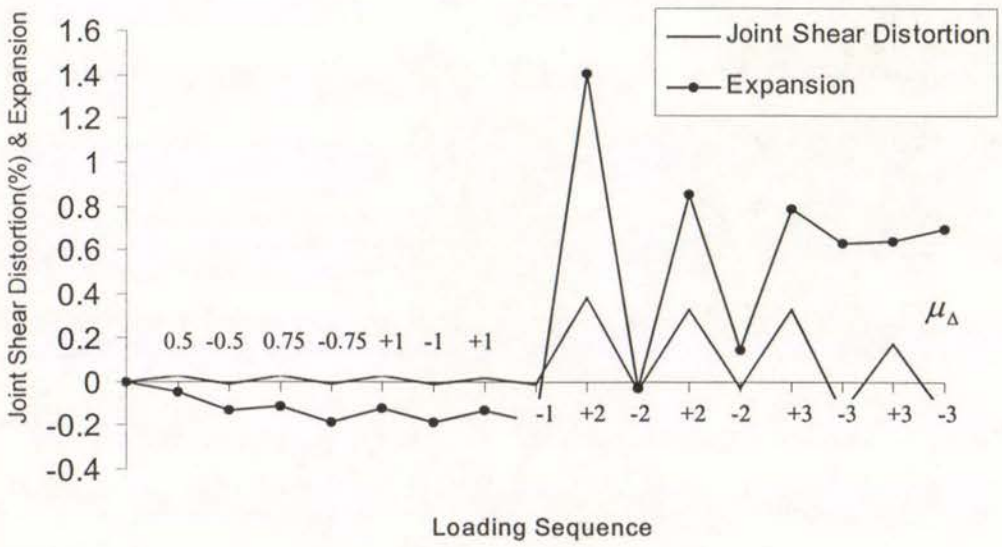

Fig. 6.25 Joint Shear Distortion and Expansion of Unit 1

The joint diagonal tension cracks initiated at the first clockwise ductility of 2, and this was also the stage of the attainment of the maximum strength of Unit 1. The estimated maximum nominal horizontal joint shear stress based on plane section theory was 3.2MPa, or $0.5\sqrt{f_c'}$ MPa for Unit 1, and this was also the nominal horizontal joint

shear stress at developing the joint diagonal tension cracking. A common approach to assess the shear capacities of beam-column joints without shear reinforcement at the stage of diagonal tension cracking of the joint cores is to use Mohr's circle for stress and assume the diagonal tension strength of concrete of $0.3\sqrt{f_c'}$ MPa. This gives that the joint shear strength at developing the joint diagonal tension cracking, in terms of the nominal horizontal joint shear stress, is $0.3\sqrt{f_c'}$ MPa in the case without axial column load. Evidently, the joint shear capacity measured for Unit 1 at diagonal tension cracking of the joint core was much larger than the theoretically estimated joint shear strength, indicating that the estimation of the joint shear strength using the above stated method could not give adequate prediction of joint performance in seismic assessment of similar existing reinforced concrete structures.

The development of joint diagonal tension cracks caused rapid increases in the joint shear distortion and expansion in Fig.6.25, as was expected. This was because joint diagonal elongation and expansion are mainly controlled by the joint shear reinforcement after joint tension cracking but the joint core of Unit 1 had no shear reinforcement. However, subsequent loading cycles caused gradual decreases in the measured joint shear distortion and expansion as seen in Fig. 6.25, indicating that the joint shear performance did not govern the seismic performance of the test unit.

Comparison of the joint behaviour of Unit 1 and Hakuto's Unit O1, which was identical to Unit 1 except the use of deformed reinforcing bars, could lead to the identification of the influence of steel type on the joint performance. Whereas in the case of Hakuto's Unit O1, the final failure was attributed to the joint shear failure, the joint performance observed of Unit 1 was excellent until the test completion. The attained maximum nominal horizontal joint shear stresses were $0.5\sqrt{f_c'}$ MPa or $0.075 f_c'$ MPa, for Unit 1, and $0.61\sqrt{f_c'}$ MPa or $0.095 f_c'$ MPa for Unit O1, and the induced maximum joint shear distortions were 0.37% for Unit 1 and 0.77% for Unit O1. Much improved joint shear performance of Unit 1 compared to Hakuto's Unit O1 was due to much enhanced joint concrete strut for Unit 1 resulting from severe bond degradation along the beam main bars.

Bearing in mind that bond degradation caused the actual steel stresses to be larger than the theoretical predictions, it could be concluded that the actual joint shear input may be larger than the theoretical predictions employed in the estimation of the nominal horizontal joint shear stress for Unit 1. Hence the attained maximum nominal horizontal joint shear stress or the attained nominal horizontal joint shear stress at developing joint diagonal tension cracking of Unit 1 may be actually larger than $0.5\sqrt{f_c'}$ MPa or $0.075 f_c'$ MPa. Hence it is concluded that the use of plain round longitudinal reinforcement actually enhanced the joint concrete strut mechanism, leading to much improved joint shear performance. This is evident because both Unit 1 and Unit O1 had not joint shear reinforcement at all.

6.1.7 Displacement Components

Fig. 6.26 illustrates the measured displacement components for the test of Unit 1 at the peaks of the loading cycles, in terms of percentages of the storey displacement. The estimations of displacement components were defined in Section 5.5.

Figure 6.26 shows that the major sources of the storey drift were the column fixed-end rotations. The contributions of the column fixed-end rotations to storey drift increased as the loading progressed, and reached up to about 81% of the storey drift at the final loading stages. In comparison, contributions of column flexural deformations outside column fixed-end regions to storey drift were very small, only about 8% of the total storey drift at final loading stages. This once again demonstrates that the use of plain round longitudinal bars caused the member flexural deformation to concentrate in the major cracks adjacent to the joint core. In comparison, the contribution of the column fixed-end rotations and column flexure to the total storey displacement measured for Hakuto's Unit O1 were about 25% and 30% respectively. Evidently, the use of plain round longitudinal reinforcement resulted in significant concentration of member flexural deformation on the member fixed-end regions.

The contribution of the beam deformation to the storey drift was small and fairly constant, and was about 10% throughout the whole loading history. In contrast, the

beam displacement contribution measured for Hakuto's Unit O1 was about 22%, and it was also fairly constant.

The contribution of the joint deformation to the total storey drift reached its maximum value of about 7% of the total storey displacement at the stage of displacement ductility of 2 where the maximum storey force strength of the test unit was achieved, and it decreased at the later loading stages, indicating that the joint condition did not deteriorate with the loading progress. In comparison, the displacement component of joint deformation measured for Hakuto's Unit O1 kept increasing as the loading progressed, and the maximum contribution of the joint deformation accounted for 31% of the total storey drift. This illustrated that bond deterioration along the longitudinal bars within and adjacent to the joint core of Unit 1 greatly enhanced the joint shear behaviour.

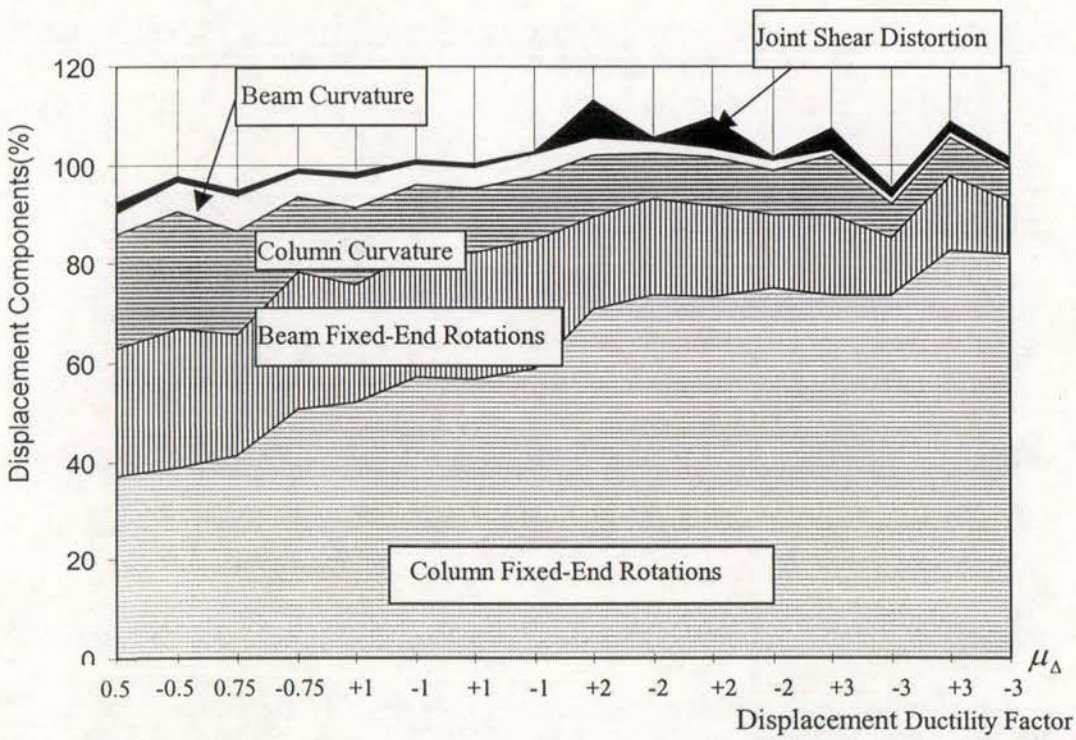

Fig. 6.26 Displacement Components of Unit 1

Evidently, the use of plain round longitudinal reinforcement enhanced the displacement contribution of fixed-end rotations from the flexurally weaker members. Obviously, a method, which could properly take the fixed-end rotations into account

in estimating the stiffness of the frame structures reinforced by plain round bars, is urgently needed.

6.1.8 Summary

Simulated seismic load test on an as-built full-scale one-way interior beam-column joint unit, referred to be Unit 1, was conducted with zero axial column load. For this test unit, the beams were flexurally stronger than the columns. The longitudinal and transverse reinforcement was from plain round bars, the beams and the columns had small amount of transverse reinforcement, the joint core had no shear reinforcement at all, and the diameter of the longitudinal bars passing through the joint core was larger than permitted in NZS3101: 1995, as was typical of pre-1970s construction in New Zealand. The test showed that the performance of similar existing reinforced concrete structures designed to outdated seismic codes would be very poor in terms of the available stiffness, strength and ductility in a major earthquake.

The available structural initial stiffness was only about 35% of the theoretical prediction at first yield. A proper method for estimating the structural stiffness, which can take the fixed-end rotations into account, is badly needed when plain round longitudinal reinforcement is used.

The maximum available strength of Unit 1, which was attained at a storey drift of 4%, was about 10% less than the theoretical prediction. Severe bond degradation along the longitudinal reinforcement resulting from the use of plain round longitudinal reinforcement caused plane section theory to overestimate the flexural strength, but underestimated the longitudinal steel strains and the member curvature values.

Severe bond degradation and bar slip, especially along the column longitudinal bars, due to the use of plain round bars and the insufficient anchorage length of the longitudinal reinforcement within the joint region, were identified as initiating the final structural failure.

The overall seismic performance was totally dominated by the flexural behaviour. Bond degradation and bar slip due to the use of plain round bars actuated a compressive strut shear resisting mechanism in linear reinforced concrete members rather than truss mechanism as was the case with the deformed bars. Consequently,

conventional theory underestimates the member shear capacity in this case, and the transverse reinforcement requirements for preventing the bars from buckling and for confining the compressed concrete rather than that for resisting shear is more critical when the plain round reinforcing bars are used.

Compared to Hakuto's as-built interior beam-column joint Unit O1, the test on Unit 1 illustrated that the severe bond degradation and bar slip associated with the use of plain round bars, although resulting in lower structural stiffness and a lower strength attainment as a percentage of the theoretical strength, greatly enhanced joint shear capacity associated with the joint concrete diagonal strut, and shifting the problem area from the joint core as was the case for Hakuto's Unit O1 to concern of the much reduced stiffness.

6.2 TEST OF UNIT 2

6.2.1 Introduction

As-built full-scale interior beam-column joint Unit 2 was identical to Unit 1 and it was tested under simulated seismic loading with the existence of a compressive axial column load of $0.12 A_g f_c^{'}$ in order to investigate the influence of the compressive axial load on the seismic behaviour.

According to the theoretical considerations conducted in Chapter 4, Unit 2 was characterised by an expected marginal weak beam-strong column mechanism (the beam and column flexural strengths were almost identical, see Table 4.5), the use of plain round longitudinal and transverse reinforcement, inadequate quantities of transverse reinforcement in the beams and the columns for anti-buckling and shear resistance, no shear reinforcement in the joint core at all, and large diameter of the longitudinal bars passing through the joint core. Hence the emphasis of the test result analysis of Unit 2 is mainly placed on the investigations into the effects of column bar buckling and bond degradation and bar slip along the longitudinal bars. Column bar buckling was anticipated to be more significant for Unit 2 than that for Unit 1, because of the existence of compressive axial column load for test of Unit 2. Shear performance of the beams, columns and the joint core still needs to be investigated.

6.2.2 Cracking and Damage

The appearance of Unit 2 at the end of testing is shown in Fig. 6.27.

Whereas in the case of Unit 1 the damage concentrated mainly in the columns and the column displacement component contributed as much as 90% of the total storey deflection at the final loading stage, the damage caused to Unit 2 spread throughout the whole test unit in the vicinity of the joint core. The measured column displacement component was 57% of the total storey deflection while the joint and beam displacement components contributed about equally to the rest of the total storey deflection at the final testing stage of Unit 2.

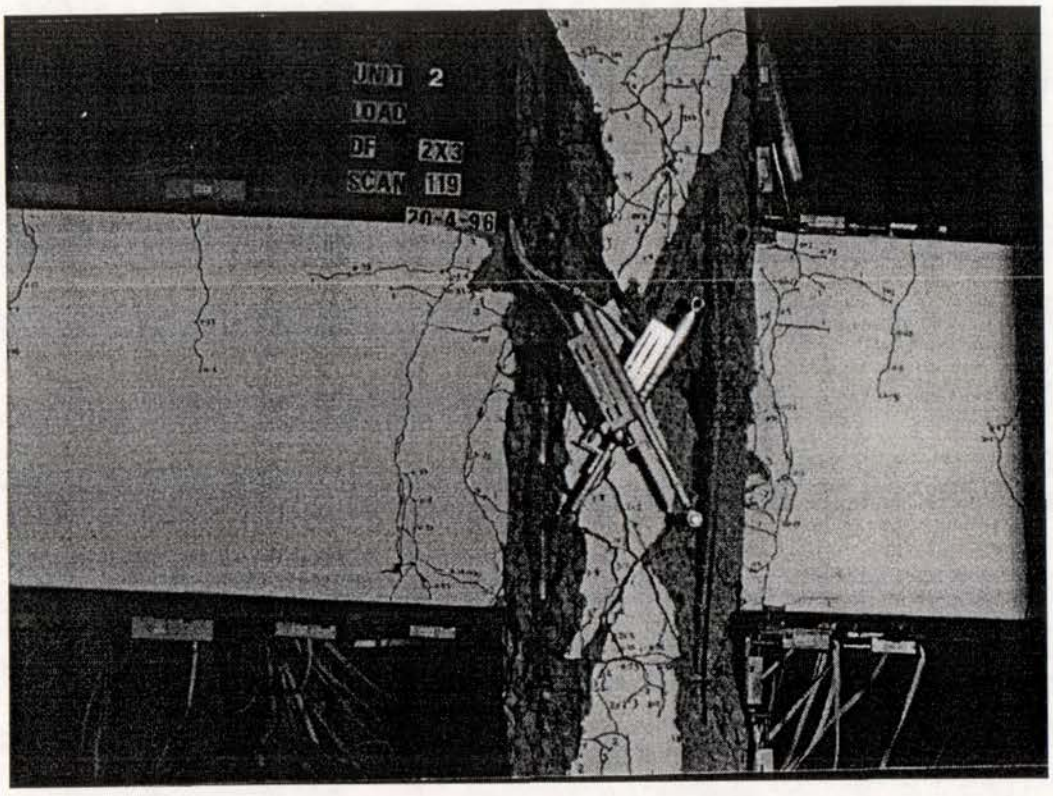

Fig.6.27 Final Appearance of Unit 2

The damage to the columns of Unit 2 concentrated in the areas adjacent to the joint core as a result of concrete spalling caused by severe buckling of the column longitudinal bars which was associated with significant bar slip and the existence of the compressive axial column load. The damage to the columns progressed with the loading progress, indicating that the column failure triggered the final failure of the unit. The damage to the beams concentrated in the wide beam flexural cracks adjacent to the joint core, and it did not progress during later loading stages, indicating that beam failure did not trigger the final failure of this theoretically marginal weak beam-strong column system. The damage in the joint core was by way of extensive diagonal tension cracks. The compressive axial load on the columns enhanced the transmission of longitudinal beam bar forces to the joint region through bond, leading to more concrete diagonal cracks in the joint core. In addition, the enhanced column bar buckling adjacent to the joint core due to the compressive axial load on the columns led to extensive concrete spalling adjacent to and within the joint core, weakening the joint force strength and increasing the joint deformation. As a consequence, the contribution of the joint core deformation to the total storey drift was much bigger, compared with the test of Unit 1. In this case, the joint concrete diagonal strut of Unit

2 was not so robust as that of Unit 1, due to larger transverse tensile strains imposed. The damage to the joint core of Unit 2 progressed as the test progressed, so the joint shear failure also attributed the final failure of the unit.

As was the case in the test of Unit 1, no diagonal tension cracks were observed in the beams and columns of Unit 2 throughout the test, indicating that transverse reinforcement in the members reinforced by plain round bars was more needed for preventing bar buckling than for providing shear strength.

In a word, column bar buckling led to the final failure of Unit 2. Column bar buckling, which was more significant for Unit 2 than for Unit 1 due to the compressive axial load in the columns of Unit 2, not only facilitated the failure of the columns but also facilitated the damage to the joint core, leading to premature failure in the vicinity of the joint core of Unit 2.

6.2.3 Hysteretic Response

Fig. 6.28 shows the storey (horizontal) shear force versus storey (horizontal) displacement hysteresis loops for Unit 2. The measured hysteresis loops for each individual beam, in terms of beam shear and vertical displacement at beam end, are shown in Figs. 6.29 and 6.30 respectively. The measured hysteresis loops for Unit 2 in Figs. 6.28 to 6.30 confirm that the existence of the compressive axial column load could not improve the general performance of the test unit.

The measured first yield displacement for Unit 2 was equivalent to a storey drift of 2%, and this was comparable with that for Unit 1. Hence, the existence of the compressive axial column load in Unit 2 did not improve the structural stiffness behaviour even for this initial weak column-strong beam unit, and this disagreed with the observations with deformed bars made by Beres, White and Gergely in 1992 [B3, B4]. The compressive axial column load for Unit 2 did improve severe slip of longitudinal beam and column bars through the joint, reducing the contributions of beam and column deformations to the total storey deflection. At the same time, the compressive axial column load enhanced the column bar buckling in the vicinity of the joint panel and enhanced the beam steel force transfer by bond within the joint region, resulting in more joint diagonal tension cracks and thus a greater contribution of joint deformation to the total storey drift.

Significant pinching is observed in Figs.6.28 to 6.30. This occurred due to bar slip along the longitudinal reinforcement, premature column bar buckling and extensive joint diagonal tension cracking.

As shown in Figure 6.28, the maximum strength reached by Unit 2, which occurred in the first loading cycle at a storey drift of 2%, was 23% less than the theoretical strength of 128 kN for the unit. This can be compared with the test of Unit 1 where the achieved maximum strength at a storey drift of 2% was 15% less than the theoretical prediction. The lower percentage of the available force strength reached by Unit 2 was because the failure trigger, column bar buckling, was more severe for Unit 2 due to the presence of compressive axial column load and to the small amount of column transverse reinforcement.

The strength degradation after the maximum strength was attained, demonstrated by test of Unit 2 in Fig.6.28, was more significant, compared with that of Unit 1 in Fig. 6.2. This was again because the column bar buckling was accelerated by the existence of the compressive axial column load.

Compared with the test of Unit 1, pinching observed for test of Unit 2 in Figures 6.28 to 6.30 was more significant, the presence of the compressive column axial load caused earlier attainment of the maximum force strength of the unit, but more rapid strength degradation as reported in 1992 by Beres, White and Gergely [20, 21]. The above-described effect of compressive column axial load evidently should be taken into account in modelling the hysteresis responses of interior beam-column joint subassemblies when column transverse reinforcement is inadequate.

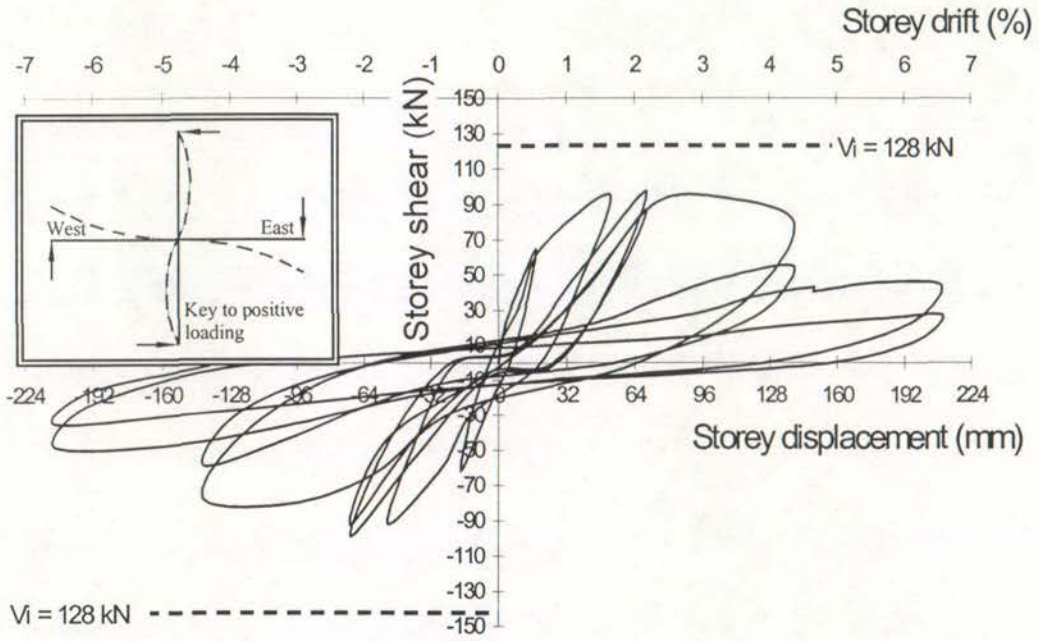

Fig. 6.28 Storey Shear versus Storey Displacement Hysteresis Loops of Unit 2

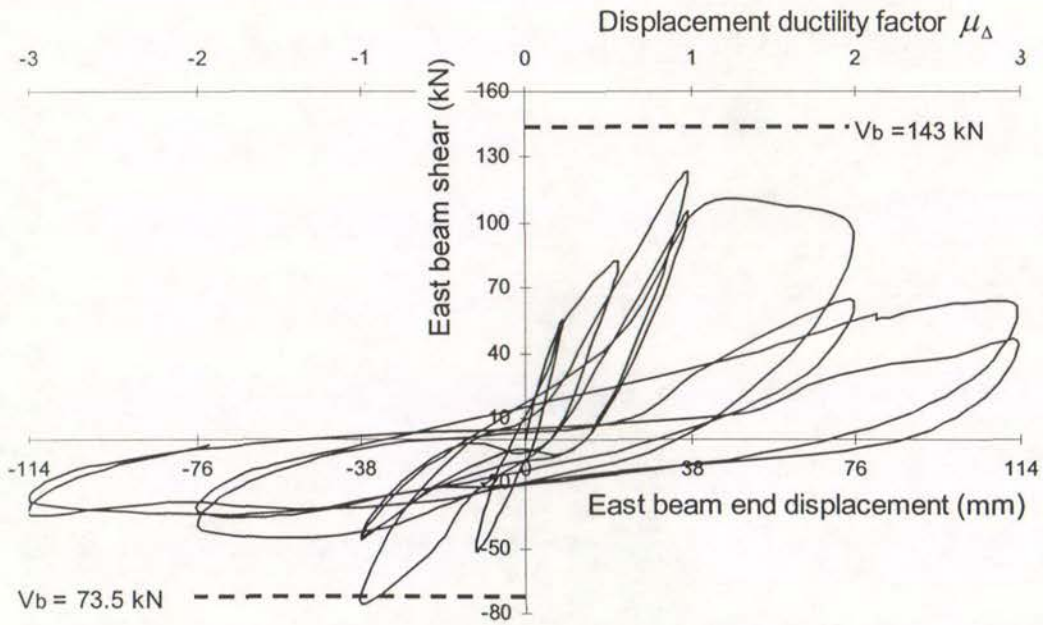

Fig.6.29 Hysteresis Loops of East Beam of Unit 2

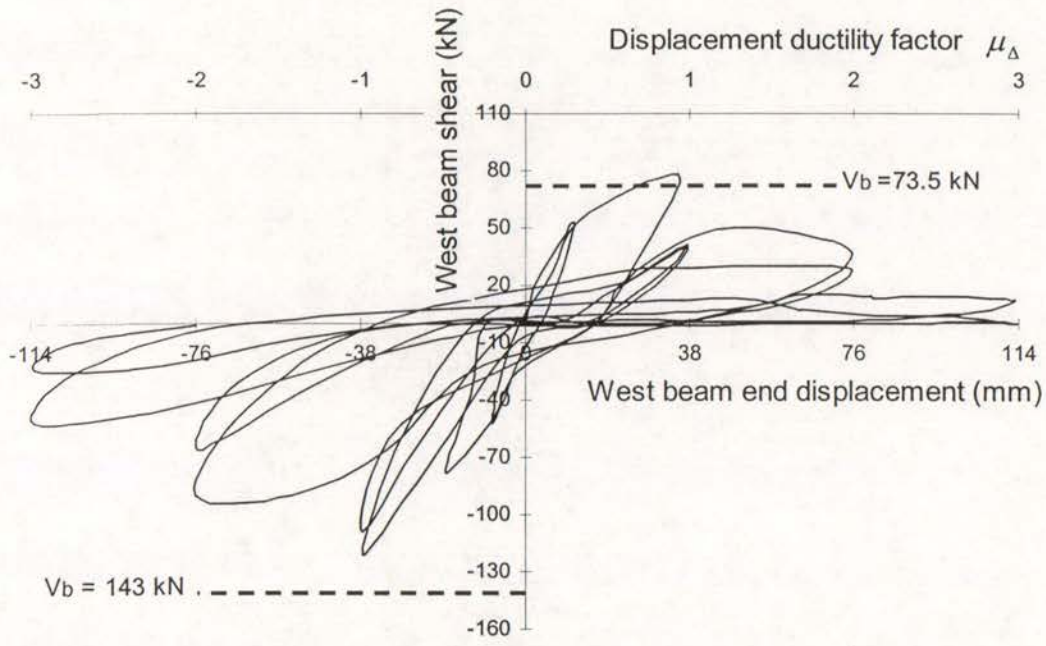

Fig. 6.30 Hysteresis Loops of West Beam of Unit 2

6.2.4 Column Behaviour

6.2.4.1 Column Curvature Distribution

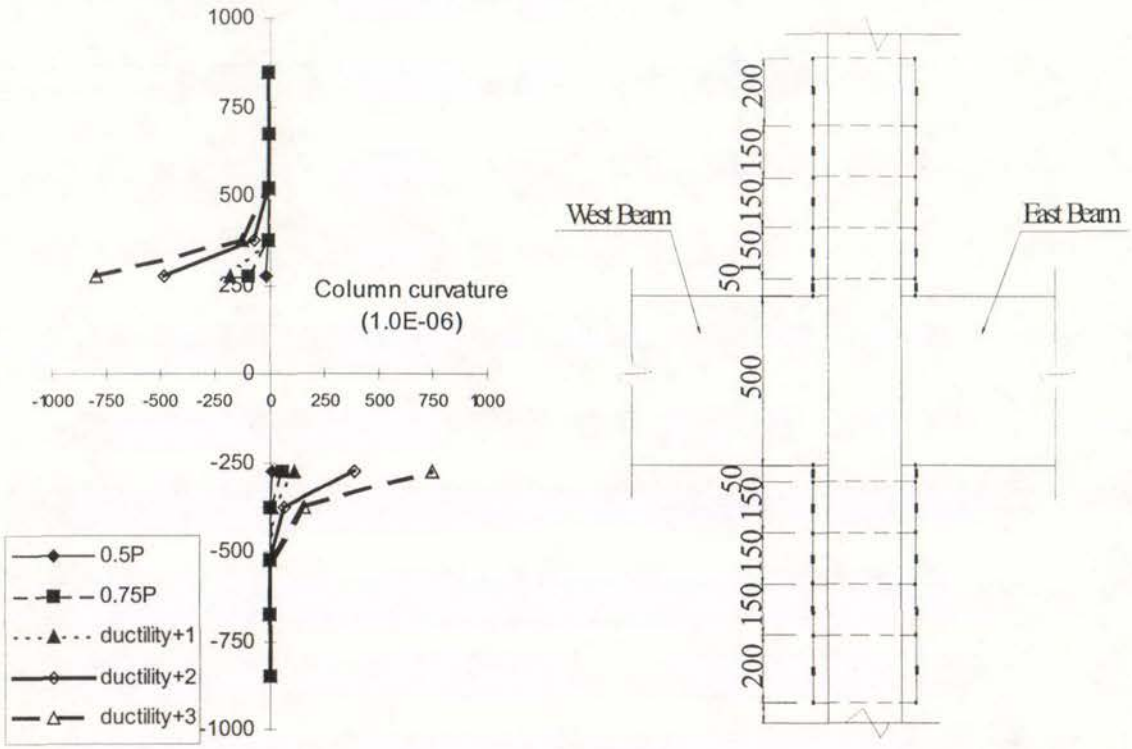

Fig. 6.31 Column Curvatures Measured of Unit 2 with Fixed-End Zones Included

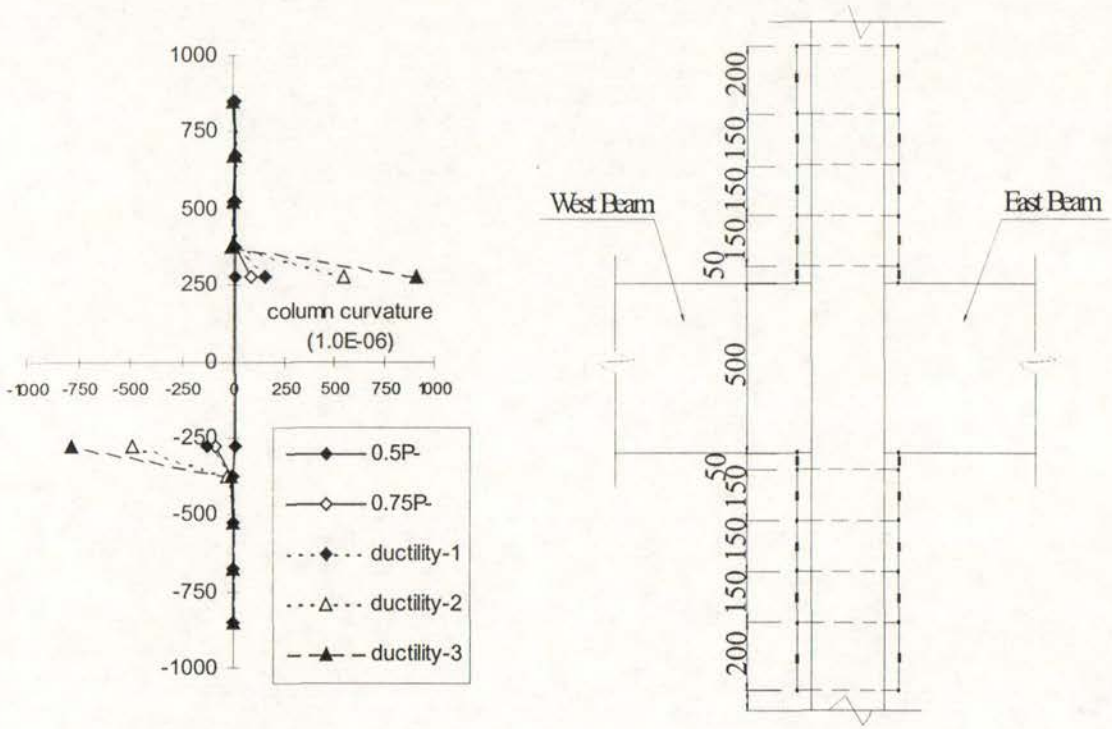

Fig.6.32 Column Curvatures Measured of Unit 2 with Fixed-End Zones Included

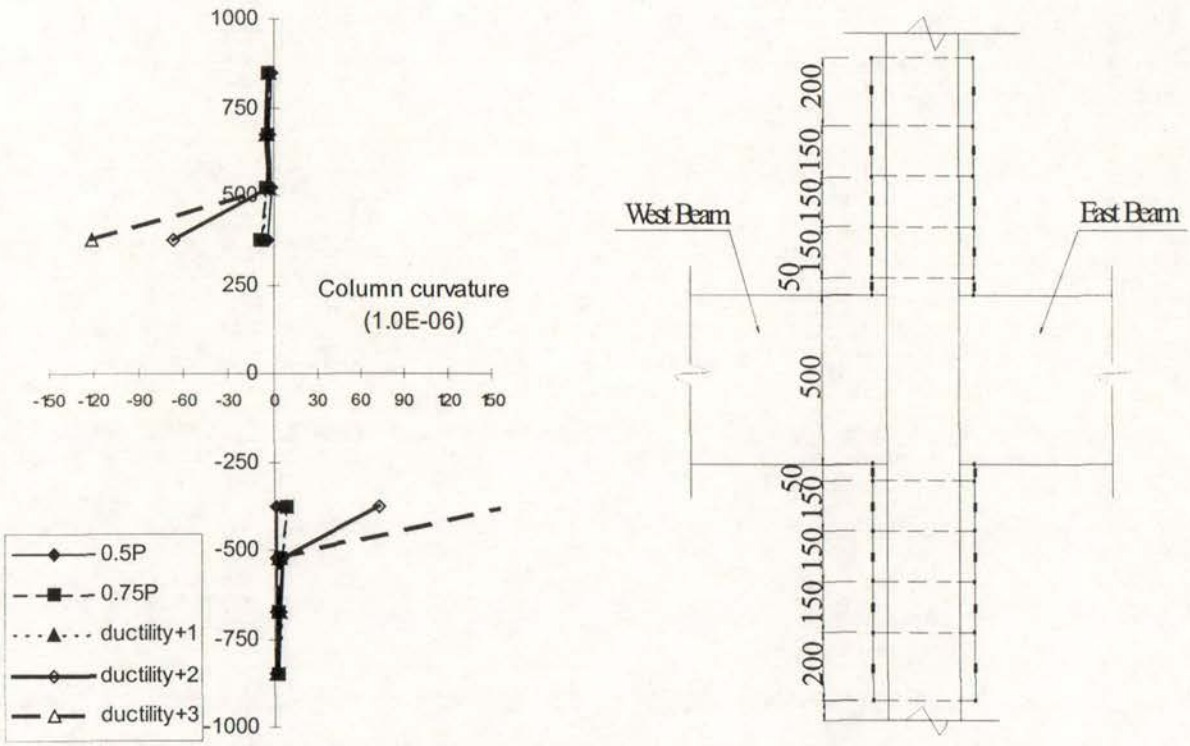

Fig.6.33 Column Curvatures Measured of Unit 2 with Fixed-End Zones Excluded

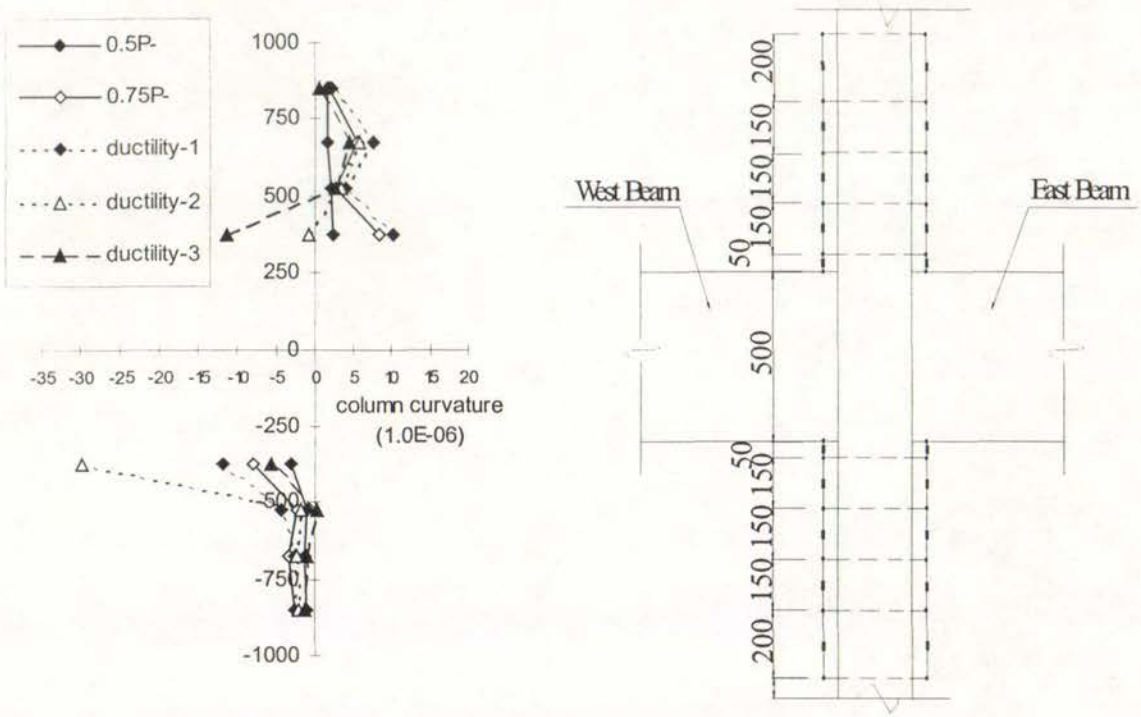

Fig.6.34 Column Curvatures Measured of Unit 2 with Fixed-End Zones

Figs. 6.31 to 6.34 illustrate the measured column curvature distributions using linear potentiometers for Unit 2, where the sign conventions were the same as for Unit 1. The theoretical column curvatures at first yield after taking the effect of axial column load into account are also shown in these figures.

Comparison of the column curvature profiles of Unit 1 and Unit 2 leads to the following finding:

For Unit 1, the column deformation concentrated in the fixed-end regions due to severe bond degradation along the column longitudinal bars within the joint region and at the adjacent ends of the members. For Unit 2, the concentration of the column deformation spread to a larger area including the column fixed-end regions and the column areas adjacent to the fixed-end regions. This occurred because the concentration of the flexural deformation on fixed-end regions was due to severe bond degradation along the column longitudinal bars within the joint region, and this was the case for Units 1 and 2 while severe column bar buckling, which occurred in Unit 2 due to the compressive axial column load, caused concrete spalling and caused the

column damage to spread to a larger area. This can be clearly seen by comparing Fig.6.1 with Fig.6.27.

The discrepancies between the measured column curvatures and the theoretical column curvatures calculated using plane section theory. Typically, the imposed column bending moments never approached the theoretical column moment capacity at first yield at any section, but the measured column curvatures in the column regions next to the fixed-end regions exceeded the theoretical column yield curvature of 8.7E-06 a great deal. Fig.6.35 compares the discrepancies over the regions 3 and 4 between the measured column curvature magnitudes and the theoretical curvature values for Units 1 and 2, where the region definition is seen in Fig.6.7. Fig.6.35(b) illustrates that the measured column curvatures for Unit 2 were generally larger than the corresponding theoretical ones estimated on the basis of the measured column shear forces and plane section theory as was the case for Unit 1. But correlations between the measured column curvatures and the theoretical predictions prior to displacement ductility factor of 2 were apparently better for Unit 2 than that for Unit 1. This occurred as a result of the improved bond condition along the column bars of Unit 2 due to the compressive axial column load, in comparison with the case of Unit 1. The observed poor correlations between the measured column curvatures and the theoretical ones after displacement ductility factor of 1 of Unit 2 in Fig.6.35(a) were due to the enhanced column bar buckling by the compression axial column load for Unit 2, in comparison with Unit 1.

As a consequence of the enhanced column bar buckling for test of Unit 2, column flexural deformation increased significantly at later loading stages and the column damage spread to a larger area. Hence the columns would shorten, and the support from the columns to the floor could be totally lost. In a word, the compressive axial column load actually could enhance the column damage, and increase the required retrofit area in columns.

6.2.4.2 Column Longitudinal Reinforcement Strains

Figs.6.36, 6.37, 6.38, and 6.39 show the column longitudinal reinforcement strains monitored by the electrical resistance strain gauges for Unit 2.

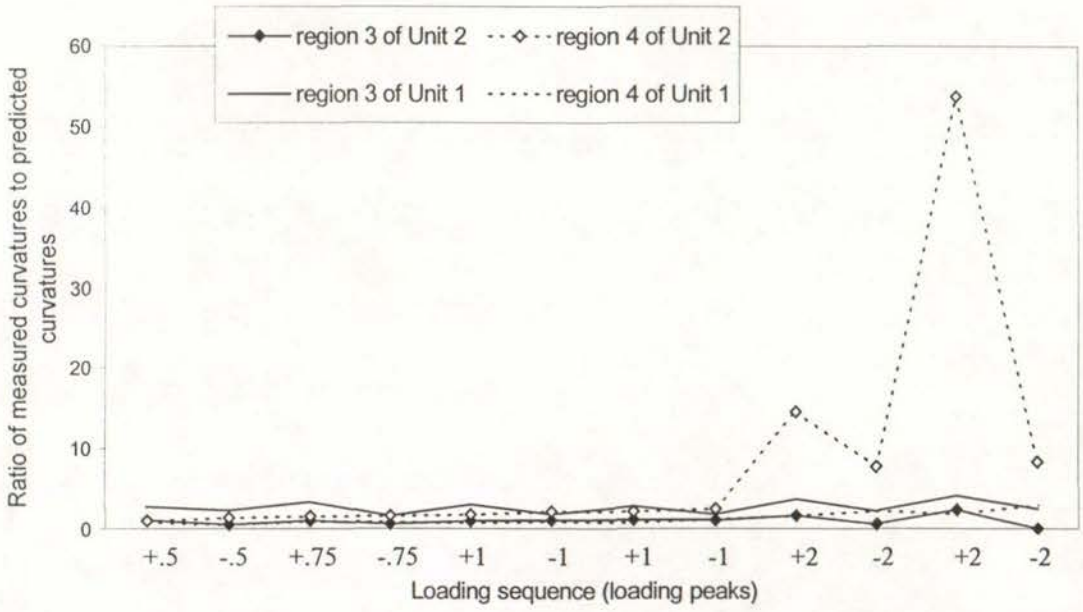

(a) Ratios of measured column curvatures to theoretical values using plane section theory

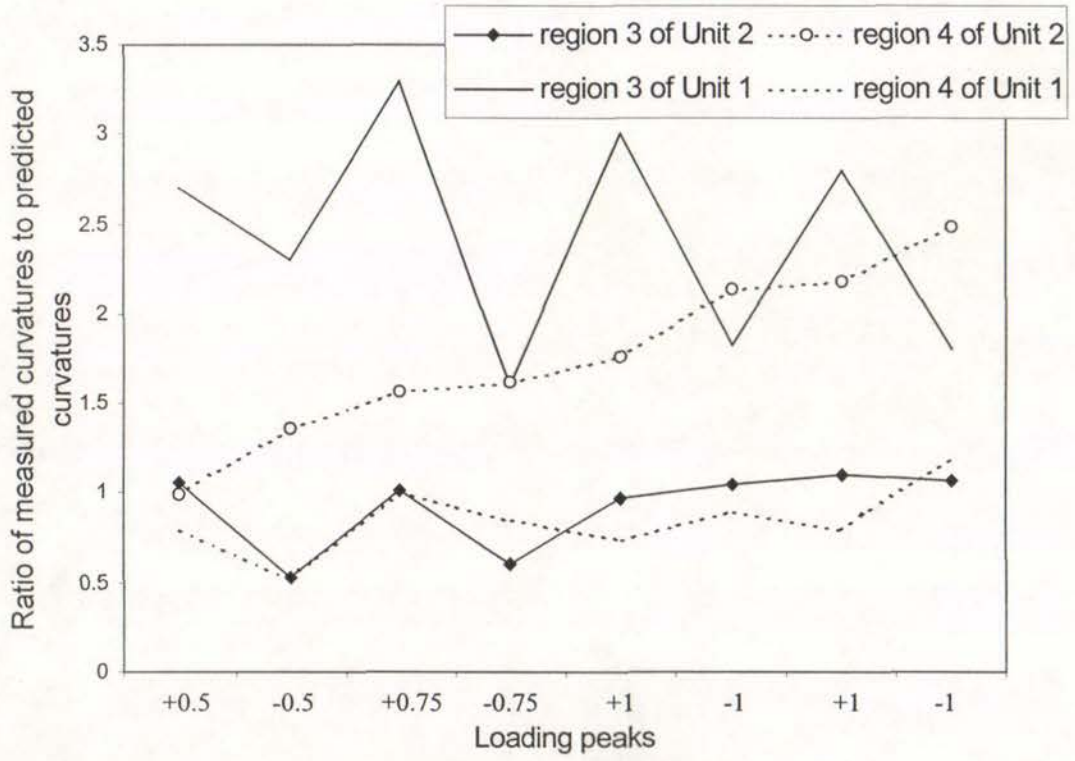

(b) Ratios of measured column curvatures to theoretical values using plane section theory

Fig. 6.35 Discrepancies of Column Curvatures for Units 1 and 2

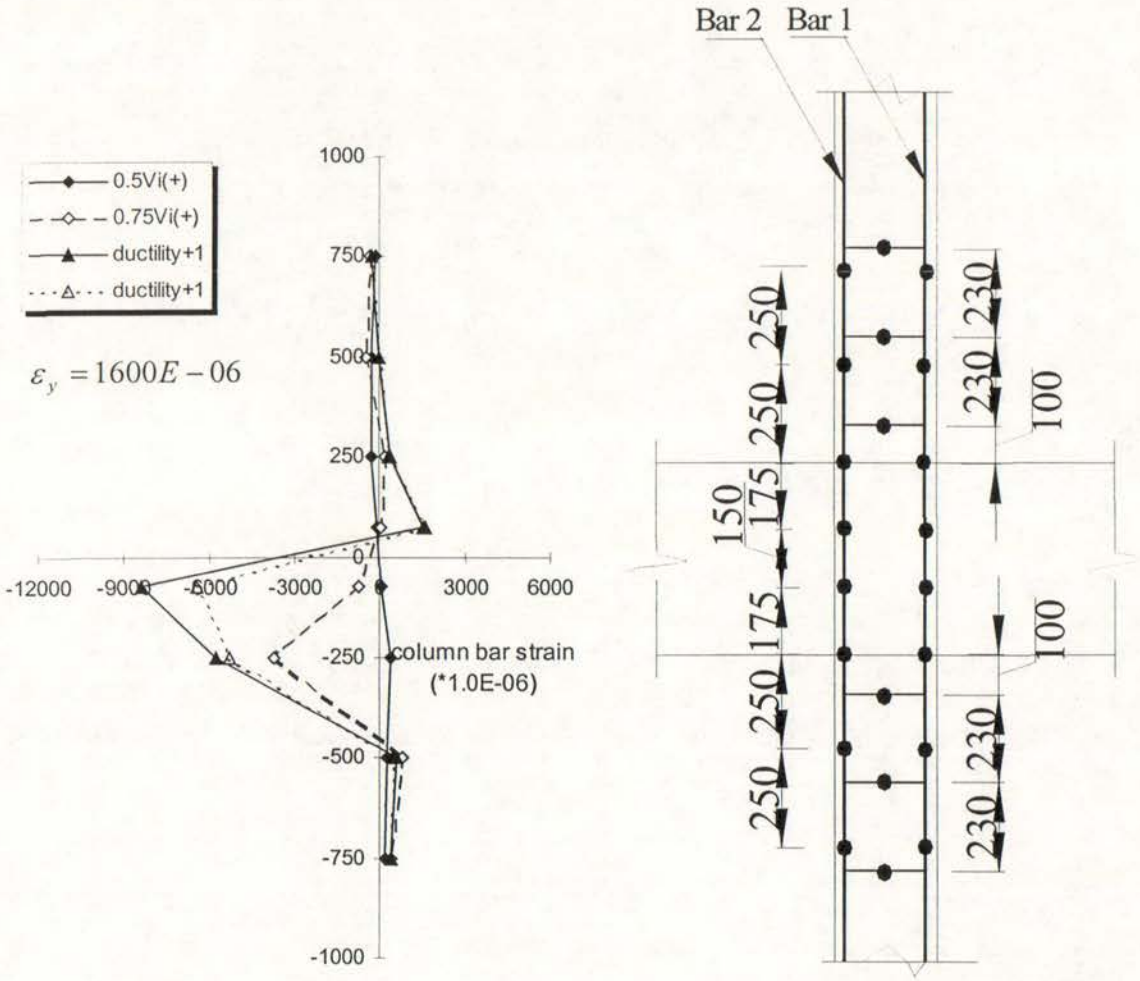

Fig. 6.36 Strain Profiles of Column Bar 1 of Unit 2

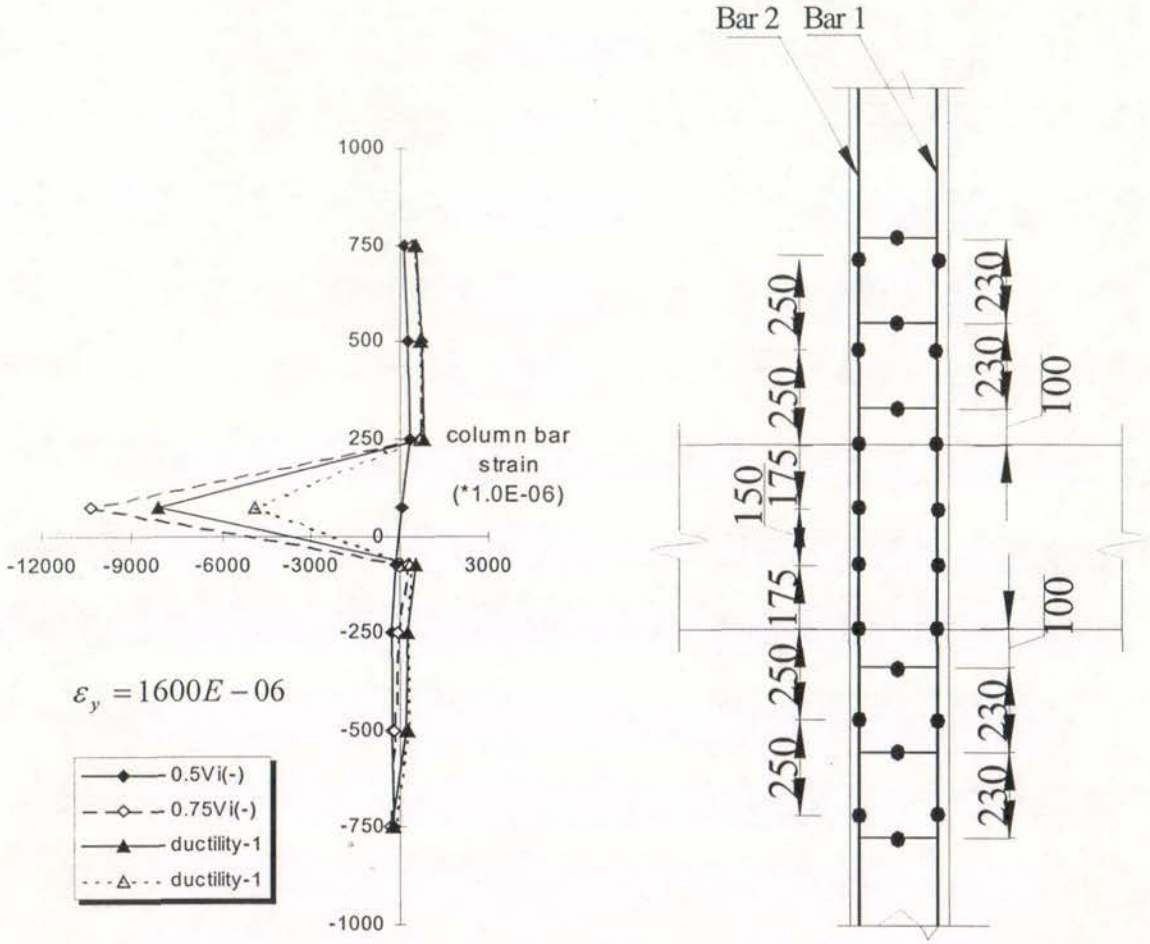

Fig. 6.37 Strain Profiles of Column Bar 1 of Unit 2

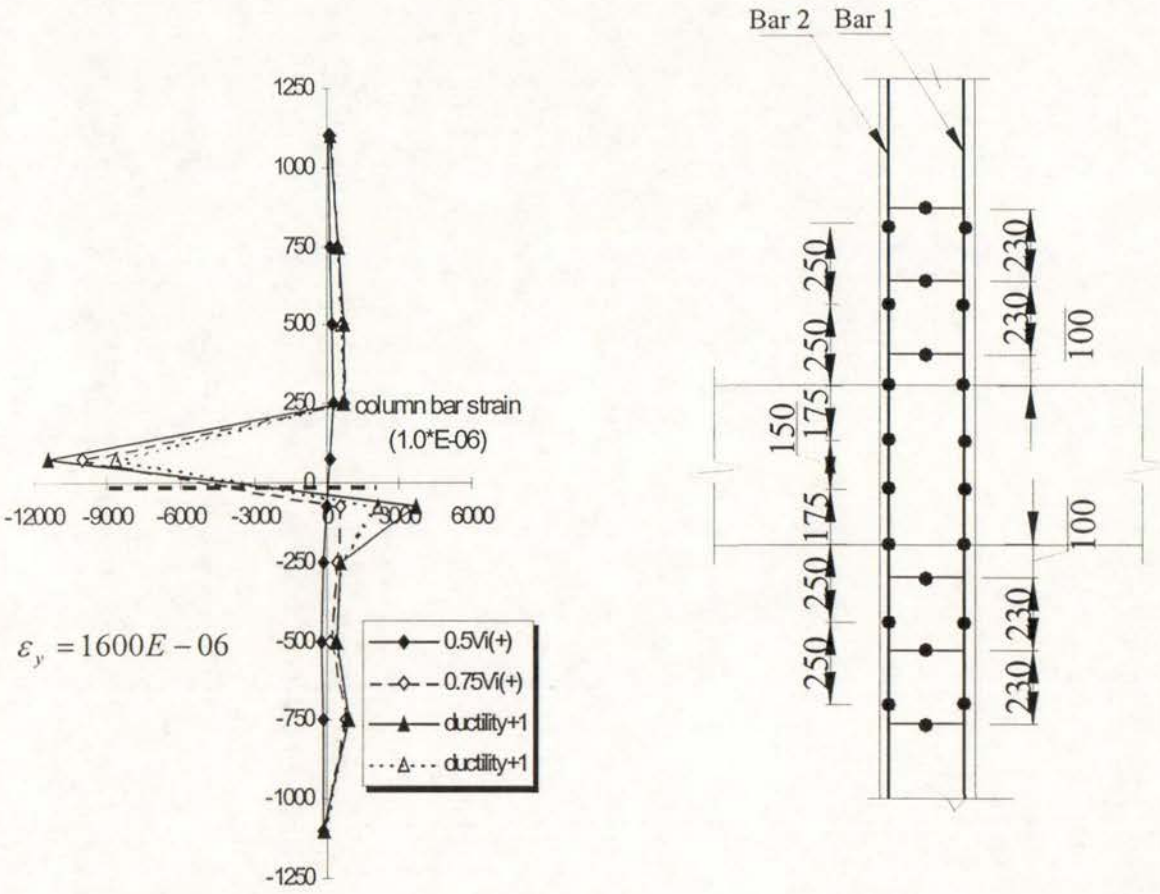

Fig. 6.38 Strain Profiles of Column Bar 2 of Unit 2

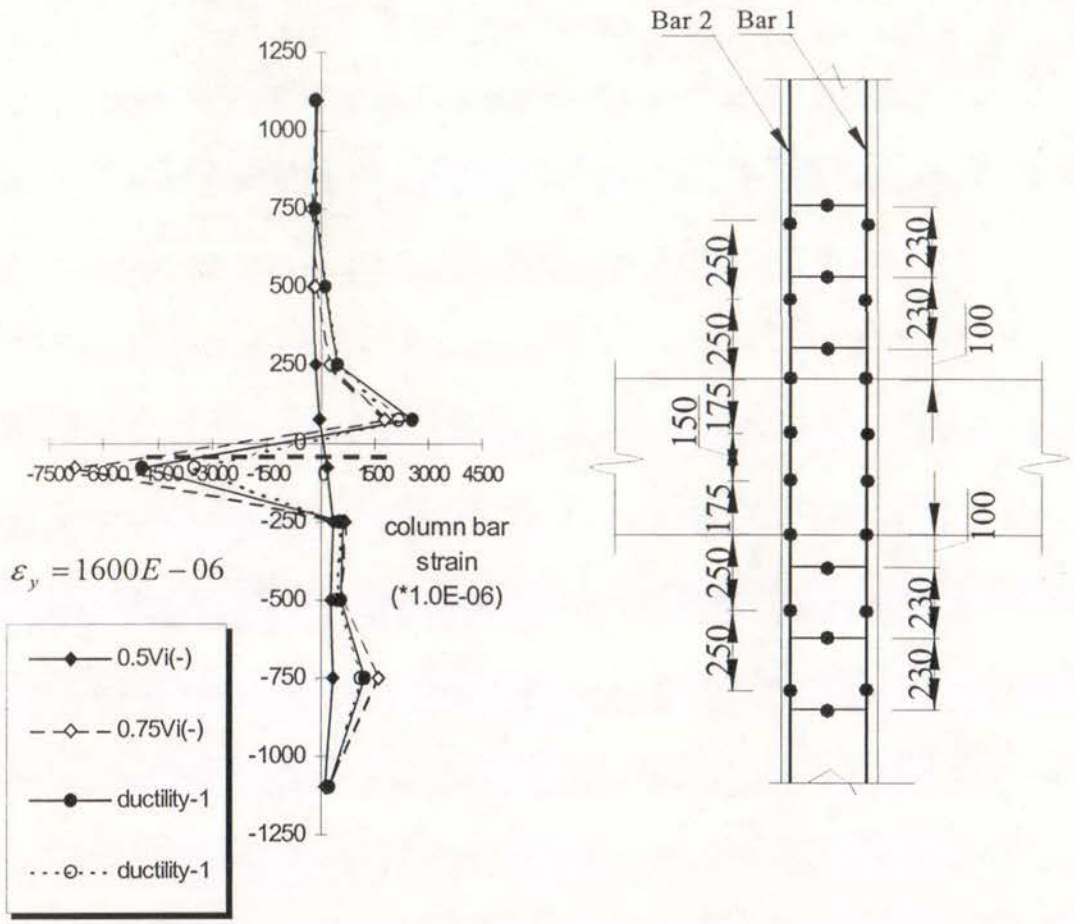

Fig. 6.39 Strain Profiles of Column Bar 2 of Unit 2

In comparison with the column longitudinal reinforcement strain profiles measured for Unit 1, the column longitudinal reinforcement strain profiles measured for Unit 2 show much more severe bar buckling along the column flexural tension bars of Unit 2 as described in Section 6.2.2 "cracking and damage". Column bar buckling occurred in Unit 2 caused the measured steel strains along the column flexural "tension" steel to be well beyond steel yield strain in compression in Figures 6.36, 6.37, 6.38 and 6.39. Significant bond degradation under tension action caused the column bars to be less confined laterally at the side of the joint core subjected to column flexural tension action, and the flexural compression steel forces applied to these bars at the other side of the joint core forced these bars to buckle.

Compared with the test of Unit 1, the influence of column bar buckling on the column bar strains occurred earlier and spread to a bigger area due to the enhancement of column bar buckling by the column compressive axial load. Typically, the changes of column steel strains from tension to compression at flexural tension side due to bar buckling for test of Unit 2 occurred after the completion of loading cycle of $0.5V_i$ instead of being after the completion of loading cycle of $0.75V_i$ for Unit 1, indicating that more severe column bar buckling occurred for Unit 2. The areas of influences of column bar buckling on the column bar strains for Unit 2 spread to the joint region and the column areas adjacent to the joint core, (see Fig. 6.36).

6.2.5 Beam Behaviour

6.2.5.1 Beam Curvatures

Figs.6.40 and 6.41 show the measured beam curvature distributions for Unit 2. Again, big beam curvatures were measured over fixed-end regions, so fixed-end regions were eliminated here for the sake of illustration. The theoretical beam curvatures at first yield, which were different for positive and negative directions, are also shown in Fig.6.40 and Fig.6.41.

In general, the beam curvature profiles measured for Unit 2 had similar trends to that of Unit 1. As was observed for Unit 1, the measured beam curvatures for Unit 2 were generally larger than the theoretical predictions by plane section theory. The beams of Unit 2 would be elastic throughout the whole test theoretically, hence the beam curvatures should be below the beam theoretical curvatures at first yield if plane section assumption was true. However the measured beam curvatures over some regions for Unit 2 were higher than the theoretical curvatures at first yield. Evidently severe bond degradation along the flexural bars and bar buckling caused the plane section assumption to underestimate the member curvatures.

The measured beam curvatures decreased gradually with the imposed displacement levels after the attainment of the maximum beam curvatures at displacement ductility factor of 1, indicating that beam failure did not govern the final failure of Unit 2.

6.2.5.2 Beam Longitudinal Reinforcement Strain

Figs 6.42 and 6.43 show the measured beam longitudinal steel strains along beam bars 1 and 2 of Unit 2 by electrical resistance strain gauges.

Similar to the test observations of Unit 1, the measured beam longitudinal steel strains outside the joint region increased consistently with the loading progress up to displacement ductility of 1, but they were much larger than the theoretical predictions on the basis of plane section theory. This was again because bond degradation had caused plane section theory to be badly violated in the regions adjacent to the joint core. It should be realised that bar slip resulting from severe bond degradation along the longitudinal reinforcement could have caused electrical resistance strain gauges to give unreliable readings.

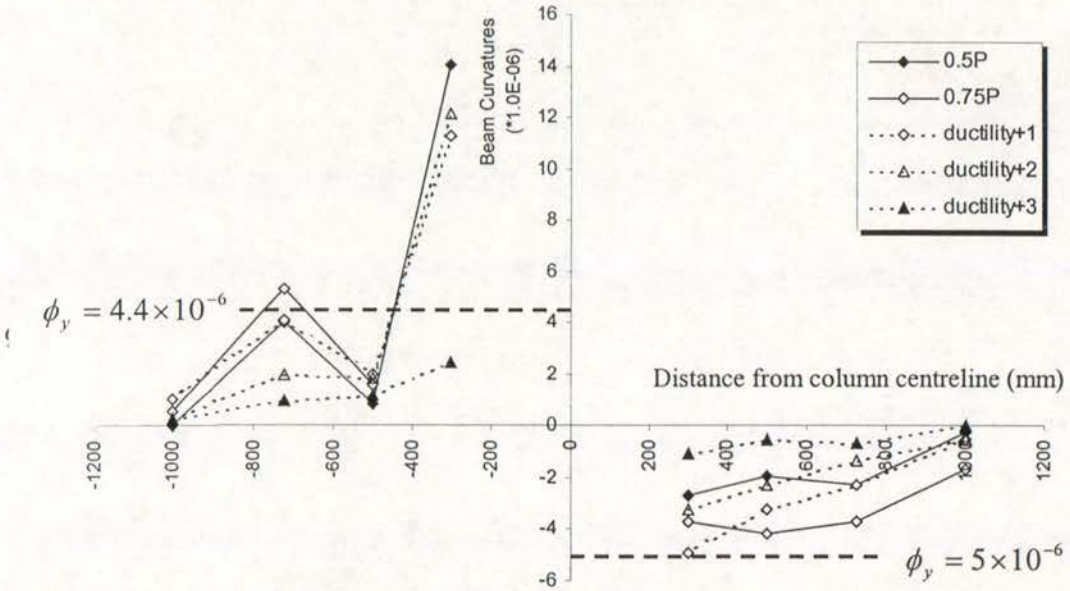

Fig. 6.40 Beam Curvature Profile of Unit 2 with Fixed-End Zones Eliminated

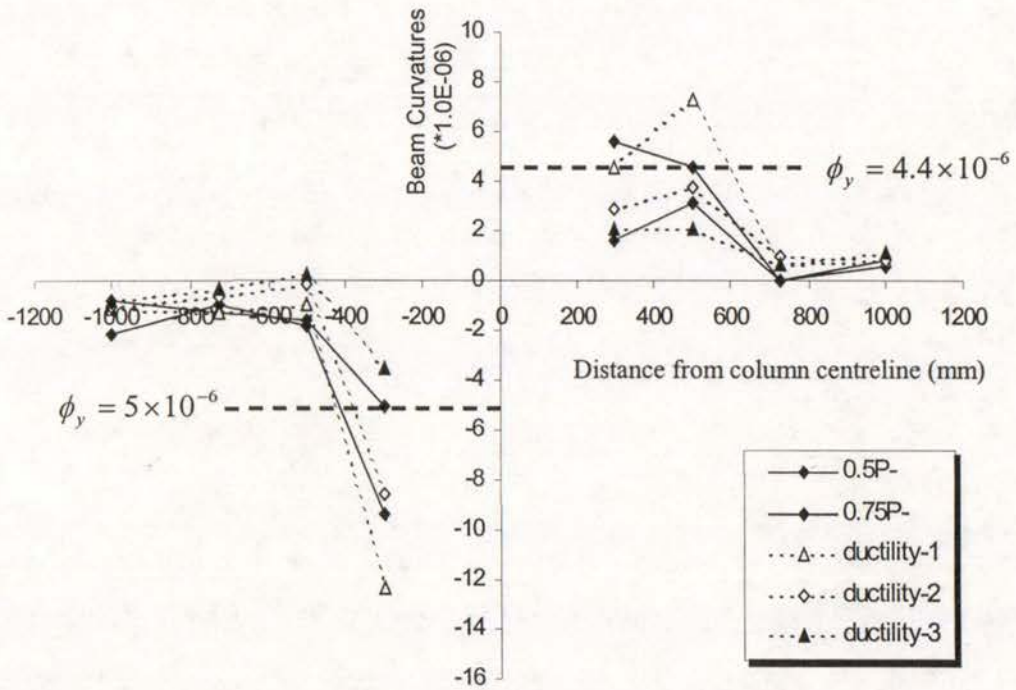

Fig. 6.41 Beam Curvature Profile of Unit 2 with Fixed-End Zones Eliminated

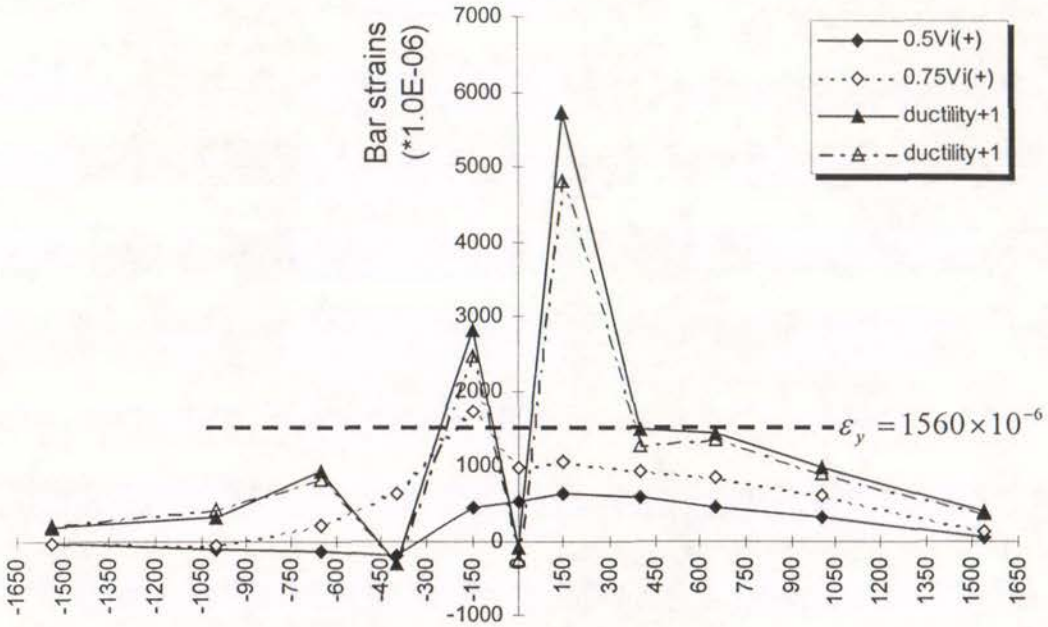

Fig.6.42 Strain Profile of Beam Bar 1 of Unit 2

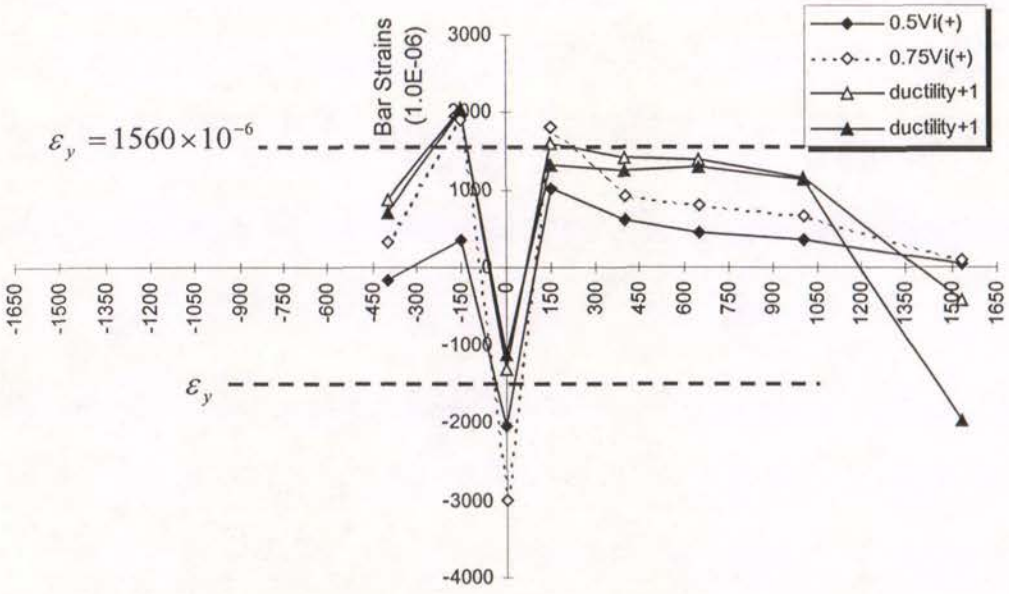

Fig.6.43 Strain Profile of Beam Bar 2 of Unit 2

6.2.6 JOINT BEHAVIOUR

Fig. 6.44 and Fig.6.45 show the measured joint shear distortion and the storey shear versus the joint displacement component hysteresis loops measured for Unit 2.

On the basis of plane section assumption and the measured beam lateral loads, the estimated nominal horizontal joint shear stress at joint diagonal tension cracking was $0.5\sqrt{f_c'}$MPa, or $0.076f_c'$MPa for Unit 1, and it was $0.63\sqrt{f_c'}$ MPa or $0.09f_c'$ MPa for Unit 2. Apparently, the joint shear capacity at developing joint diagonal cracking, in terms of nominal horizontal joint shear stress, was enhanced as a result of the existence of compressive column axial load. Quantitatively the estimated joint shear capacity enhancement resulting from the compressive axial load of $0.12A_gf_c'$at developing joint diagonal cracking reached as high as 26% in terms of the joint horizontal nominal shear stress after eliminating the influence of concrete compressive strength. One approach to estimate the influence of compressive axial column load on the joint shear capacity is to use the equation $\sqrt{1+\frac{N^*}{0.3A_g\sqrt{f_c'}}}$, and this gave the joint shear capacity enhancement of 13.7% for Unit 2. So the actual enhancement of the joint shear capacity at joint diagonal tension cracking due to the compressive axial column load of Unit 2, which was estimated based on the test observations, was higher than the theoretical prediction. Caution needs to be taken in explaining the above statement because the plane section assumption could give misleading results in the case of severe bond degradation and slip along the longitudinal reinforcement.

Unlike the test evidence of Unit 1 where the joint diagonal tension cracks did not develop with the increase in the imposed displacement level, joint diagonal tension cracking, which initiated at the clockwise loading to $0.75V_i$, progressed with the loading for Unit 2, the joint shear distortion and the joint displacement component continued to increase after the maximum strength of the unit was reached at the displacement ductility of 1 as shown in Figs.6.44 and 6.45, indicating that joint shear failure did contribute to the final failure of Unit 2. Quantitatively, Fig. 6.46 compares the joint shear distortions measured for Unit 1 and Unit 2. Clearly the joint shear

distortions estimated for Unit 2 were much larger than those for Unit 1. More severe joint shear failure of Unit 2 than that of Unit 1 was because the force transfer from the steel to the surrounding concrete within the joint region by bond was enhanced for Unit 2 by the compressive axial column load. In addition, more significant concrete spalling resulting from column bar buckling occurred in Unit 2 also contributed to the more severe joint shear failure of Unit 2.

The maximum joint displacement component was 7% of the total storey drift for Unit 1, but about 40 % of the total storey drift for Unit 2, illustrating much more severe joint shear failure for Unit 2 compared to Unit 1. Hence unlike Unit 1 where the integrity of the joint core was good till the end of the test, the joint shear failure of Unit 2 did contribute to the final failure.

The maximum nominal horizontal joint shear stress of Unit 2, which was reached at the first clockwise displacement ductility of 1, was $0.65\sqrt{f_c'}$ MPa or $0.09f_c'$ MPa.

Comparison of the observed joint behaviour of Units 1 and 2 came to the following conclusion:

In the seismic assessment of existing reinforced concrete structures designed to pre-1970s seismic codes, the estimation of the beneficial effect of compressive column axial load on the joint shear capacity using the code approach could be very conservative prior to joint diagonal tension cracking. After joint diagonal tension cracking, the significant increase in the joint displacement component due to the enhancement of force transmission from steel to the concrete within the joint region and the adverse effect of column bar buckling caused by the compressive column axial load could result in rapid increase in the joint displacement component.

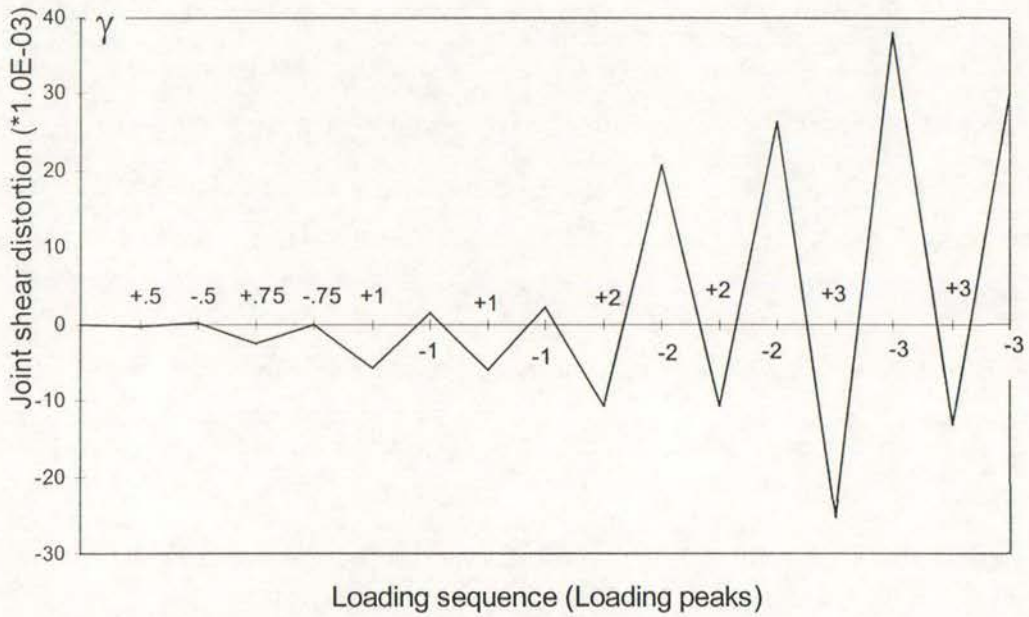

Fig. 6.44 Joint Shear Distortion of Unit 2

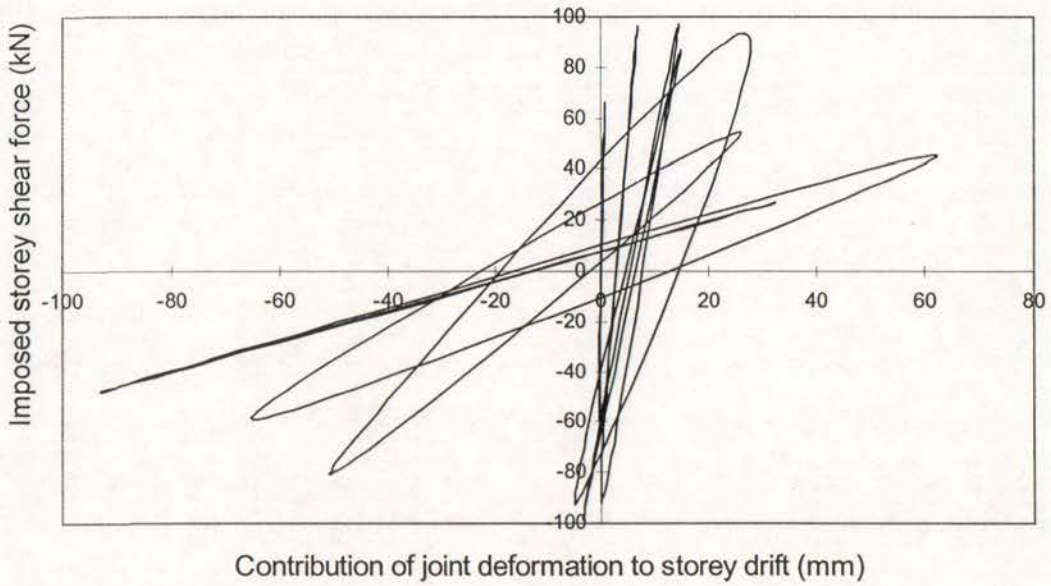

(a) Storey shear versus joint displacement component for Unit 2

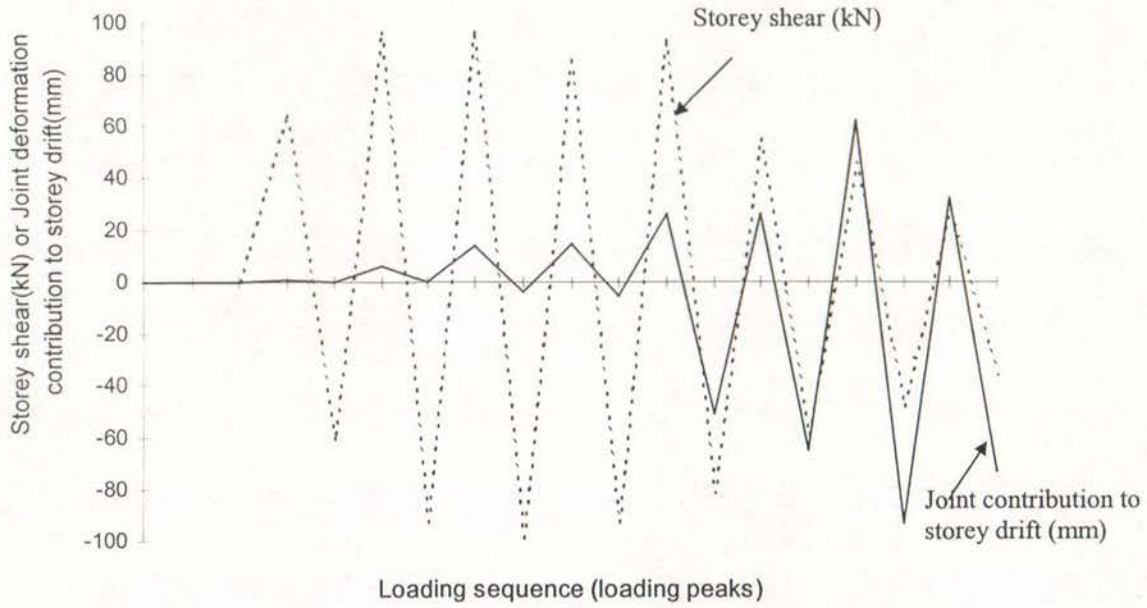

(b) Storey Shear and Joint Displacement Component with the Loading for Unit 2

Fig.6.45 Measured Storey Shear and Joint Displacement Component Loops of Unit 2

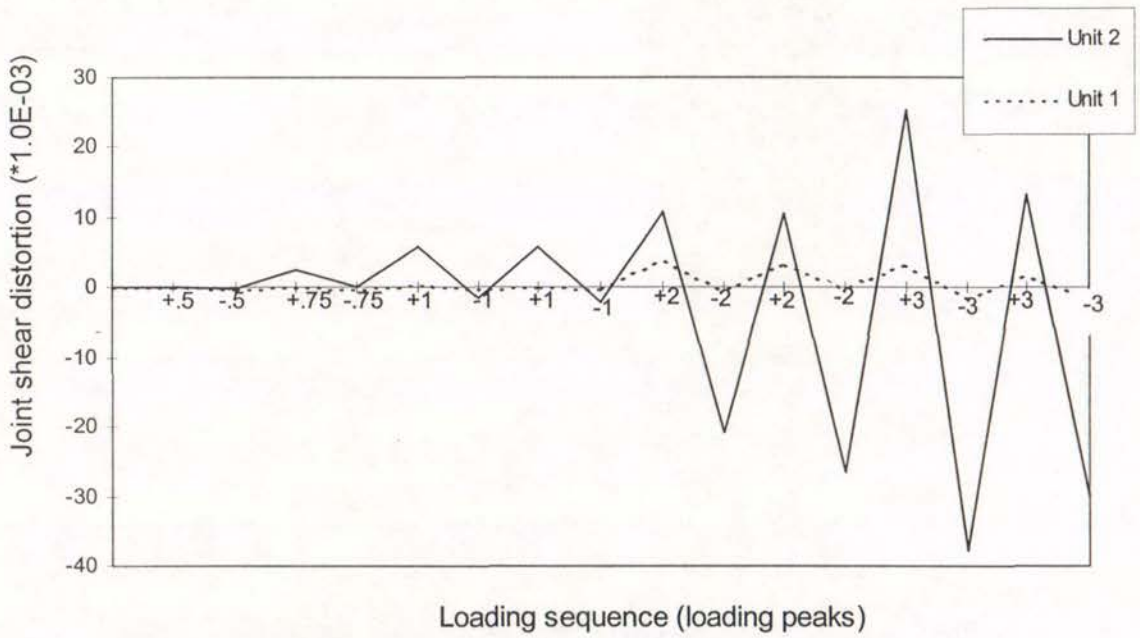

Figure 6.46 Comparison of Joint Shear Distortions of Unit 1 and Unit 2

6.2.7 Displacement Components

Fig. 6.48 illustrates the measured displacement components for Unit 2 at the peaks of the loading cycles, expressed as percentages of the storey displacements. Various displacement components were estimated as defined in Chapter 5.

It is apparent in Fig.6.47 that the column and joint displacement components, especially the component of column fixed-end rotation, progressed with the loading progress, and the final failure of Unit 2 was clearly triggered mainly by the column bar buckling.

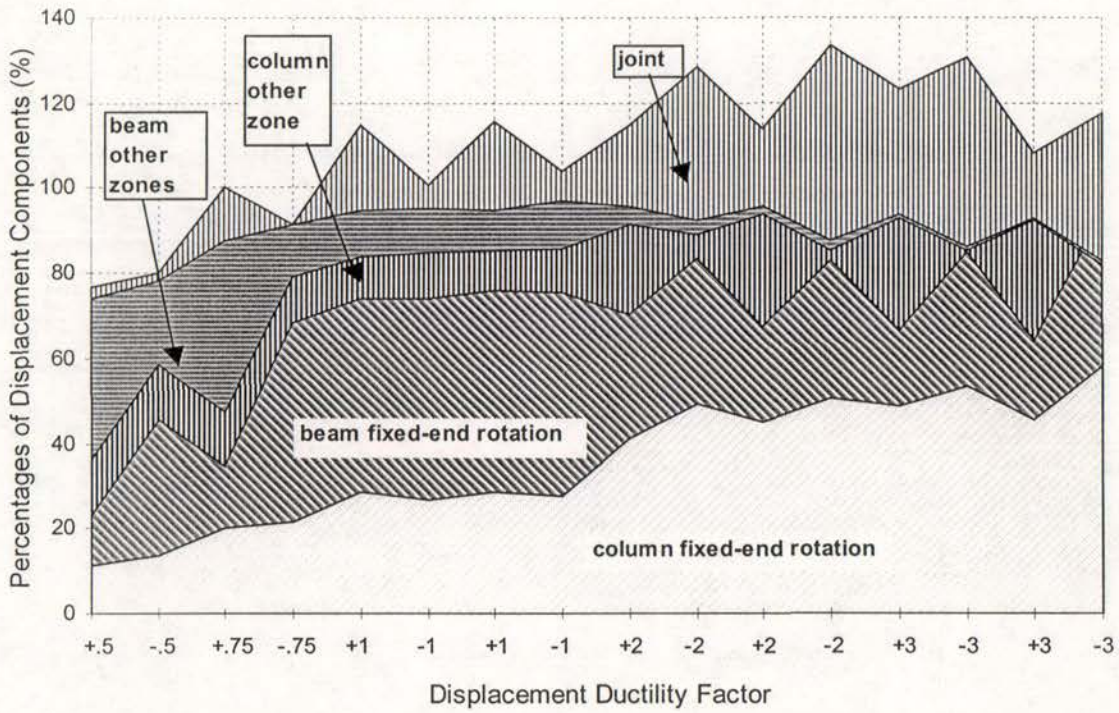

Fig. 6.47 Estimated displacement components for Unit 2

6.2.8 Summary

Simulated seismic load test was conducted on an as-built full-scale interior beam-column joint unit, referred to be Unit 2, with the existence of the compressive axial column load of $0.12 A_g f_c^{'}$ in order to investigate the influence of the compressive axial load on the seismic behaviour. Unit 2 was identical to the previous test Unit 1, the only difference between the test of Unit 1 and the test of Unit 2 was that Unit 1

was tested under simulated seismic loading with zero column axial load while Unit 2 was tested under simulated seismic loading with the compressive column axial load of $0.12\,A_g f_c^{'}$, which meant that the test of Unit 2 was expected to develop beam plastic hinges. Test of Unit 2 demonstrated that general seismic performance of existing reinforced concrete structures could not be improved by the compressive column axial load, when reinforced by plain round bars and contained very small amount of transverse reinforcement.

The maximum storey shear strength attained by Unit 2, which was reached at a storey drift of 2% was 77% of the theoretical storey shear strength of the unit. The measured stiffness for Unit 2 was comparable with that for Unit 1, and it was about 30% of the theoretical stiffness at first yield. Low attainment of the available storey shear strength and stiffness observed for Unit 2 was due to enhanced column bar buckling resulting from the existence of the compressive axial column load for Unit 2. Column bar buckling enhanced by the compressive axial column load triggered the final failure of the test of Unit 2.

Similar to test of Unit 1, test of Unit 2 demonstrated that transverse reinforcement in reinforced concrete linear members, especially in the columns, was more needed for preventing bar buckling and for confining the compressed concrete than that for providing shear strength when plain round longitudinal reinforcement is used.

Comparative study of test results of Units 1 and 2 illustrated that compressive axial column load did not improve the structural stiffness behaviour for Unit 2 and caused the attained load strength by Unit 2 to be reduced if expressed as the percentage of the theoretical load strength due to the enhanced column bar buckling resulting from the compressive axial column load. Whereas the attained strength of Unit 1 was 10% less than the theoretical strength of the unit, the storey shear strength reached by Unit 2 was 23% less than the theoretical storey shear strength of the unit. In addition, compressive axial column load for Unit 2, although enhanced the joint shear capacity at joint diagonal tension cracking, caused extensive concrete spalling adjacent to the joint core resulting from enhanced column bar buckling, leading to more severe joint damage and larger damage areas adjacent to the joint core.

6.3 CONCLUSION

1. The simulated seismic load tests on two identical full–scale one-way interior beam-column joint units, Unit 1 and Unit 2, which were reinforced by plain round longitudinal reinforcement and were representative of reinforced concrete frame structures constructed in New Zealand in the 1950s, showed that similar existing reinforced concrete structures designed to outdated seismic codes would show low available stiffness and strength in a major earthquake.

   Units 1 and 2 were tested with axial compressive column load of zero and $0.12A_g f_c'$, respectively. The measured stiffness of the Units was very low, being about 30% of the theoretical stiffness at first yield. This theoretical stiffness at first yield did not include the effect of bond slip along the longitudinal reinforcement within the joint and in the members. Also, the storey shear strengths reached by Units 1 and 2 at a storey drift of 2% were 85% and 77%, respectively, of the theoretical force strengths based on the flexural strength of the members. Column bar buckling was found to be the cause of the eventual failure of both tests.

   Severe bond degradation along the longitudinal reinforcement associated with the use of plain round bars caused plane section theory to overestimate the member flexural strengths, but underestimate the member curvatures and the longitudinal reinforcement strains.

2. The compressive axial column load caused the attained strength of Unit 2, expressed as the percentage of the theoretical strength, to be reduced. It was found that the compressive axial column load enhanced the joint shear failure and the column bar buckling when the column transverse reinforcement is inadequate, and it did not improve the structural stiffness behaviour.

3. Comparative study of the test results of Unit 1, in which the axial column load was zero, with the results of test on an identical beam-column joint unit reinforced by deformed longitudinal reinforcement led to the following conclusions:

(a). When plain round longitudinal reinforcement is used, the shear performance of members and the joints is greatly improved, but the available structural stiffness and force strength in terms of percentages of the theoretical strength are significantly lower, in comparison with the case with deformed longitudinal reinforcement. Hence the critical concern became structural stiffness and strength performance in this case.

(b). Severe bar slip resulting from the utilisation of plain round longitudinal reinforcement can greatly enhance the joint shear force capacity associated with the joint concrete diagonal strut action.

(c). Therefore, the information on structural behaviour obtained from tests with deformed longitudinal reinforcement could be misleading, when used for estimating the probable seismic performance of existing reinforced concrete structures reinforced by plain round longitudinal reinforcement and containing small amount of transverse reinforcement in members.

4. The flexible performance of the Units in the elastic range (approximately 2% storey drift at first yield) suggests that the interaction of such frames with masonry infills should not be ignored. Many frame buildings designed to pre-1970s seismic codes have masonry infills which are not separated from the frames.

5. The flexible performance of the Units also suggests that P-Δ effects of similar existing reinforced concrete frame buildings should be allowed for.

6. Tests of the two as-built interior beam-column joint Units showed that the column longitudinal reinforcement in similar as-built reinforced concrete structures was not adequate to prevent the formation of weak column-strong beam failure mechanism, and allowance for the contribution of reinforced concrete slabs could further enhance such a tendency.

CHAPTER 7

TEST RESULTS OF EXTERIOR BEAM-COLUMN JOINTS

7.1 GENERAL

Four full-scale one-way exterior beam-column joint units, named as EJ1, EJ2, EJ3 and EJ4, were constructed into two groups of two units each. The four units had identical overall dimensions and reinforcing details except the different arrangements of the beam bar hooks in the joint core. The longitudinal and transverse reinforcement was from Grade 300 plain round steel, the joint cores contained very limited shear reinforcement, and the columns and the beams contained small amount of transverse reinforcement, as was the case for pre-1970s construction in New Zealand.

For each two identical test units of each group, one unit was tested under simulated seismic loading with zero axial column load, and the other unit was tested under simulated seismic loading with the existence of a constant compressive axial column load of 1800 kN. The as-built exterior beam-column joint Unit EJ1 with the beam bar hooks bent away from the joint core was retrofitted by wrapping the column parts above and below the joint core using fibre-glass jacket after testing as-built with zero axial column load, in order to testify the alternative force path as described in Chapter 4. The retrofitted unit, named as REJ1, was tested under simulated seismic loading with zero axial column load again.

Seismic assessment of the test units conducted in Chapter 4 using New Zealand Code approach and the capacity design based seismic assessment procedure shows that beam and column transverse reinforcement was inadequate for all the tests, according to the requirement for preventing the longitudinal reinforcement from buckling and confining the compressed concrete, and/or the requirement for providing the shear force strengths. The use of plain round longitudinal reinforcement and inadequate anchorage configuration of the beam bar hooks when bent away from the joint cores made it very critical to transfer the member forces across the joint core. Examination of exterior beam-column joint shear mechanisms conducted in theoretical

consideration of Chapter 4 identified that different beam bar hook details could actuate different joint force transfer paths and therefore emphasise the need for column transverse reinforcement at different locations. Concrete tension cracking failure initiated by the opening of the beam bar hooks could occur prior to the actuation of postulated joint force paths due to insufficient column transverse reinforcement within beam bar hook ranges and the utilisation of plain round longitudinal reinforcement. Seismic assessment also showed that the shear force capacities of the beam-column joint cores were adequate except for the test of EJ1, which had the beam bar hooks bent away from the joint core and was tested with zero axial column load.

It is noted that New Zealand code approach and the capacity design based seismic assessment procedure are established on the basis of experimental results with deformed longitudinal reinforcement. Experimental evidence observed for the two as-built interior beam-column joint units reinforced by plain round longitudinal reinforcement conducted in this project revealed that reinforced concrete linear members (beams and columns) with small amount of transverse reinforcement can eliminate shear failure if plain round longitudinal reinforcement is used. Reinforced concrete linear members designed according to similar design philosophy, that is, to similar codes, must be of similar behaviour, irrespective of interior or exterior beam-column joint assemblies. Therefore for these exterior beam-column joint tests, beam and column behaviour would be more likely to be dominated by flexure, rather than by shear, and the focus of investigating the possible seismic performance of the exterior beam-column joint test units is on the member force transfer across the joint core. The joint performance is investigated with emphases on the observed joint shear performance, the column transverse reinforcement strains at different locations, and the failure trigger, which determines the force capacity of the weakest link. Of course the effects of different beam bar hooks and compressive axial column load are also investigated in a comparative study way.

As revealed by the tests on two as-built interior beam-column joint tests conducted in this project, there are big discrepancies between the measured member curvatures and theoretical values for members reinforced by plain round longitudinal reinforcement

due to the violation of the plane section assumption, and the flexural deformation of such linear members tended to concentrate on the fixed-end regions. Evidently, detailed investigation of member curvature properties along the member is not of much significance, and the study of member fixed-end rotation became necessary.

7.2 TEST OF UNIT EJ1

7.2.1 Introduction

As-built full-scale exterior beam-column joint unit EJ1 had the beam bar hooks bent away from the joint core. The ratio of the column moment capacity to the beam moment capacity relative to the joint centre-line was 2.1 and 1.4 respectively when determined by the beam negative moment capacity and positive moment capacity. The theoretical storey shear strength of Unit EJ1 for clockwise loading, which was determined by the beam negative bending moment capacity was 67 kN, and the theoretical storey shear strength of the unit for anti-clockwise loading, which was determined by the beam positive moment capacity, was 45 kN. Unit EJ1 was tested under simulated seismic loading with zero axial column load. This test aimed at investigating the seismic performance of exterior beam-column joint components when reinforced by plain round longitudinal bars and containing reinforcing details typical of pre-1970 existing reinforced concrete moment resisting frame structures in New Zealand.

7.2.2 Crack Development and Damage

The crack development and the final appearance of Unit EJ1 are illustrated in Fig. 7.1.

Concrete tension cracking, orientated by the anchorage configuration of the top beam bars, initiated above the joint core in the upper column as early as at the peak load attainment of clockwise $0.5V_i$ (loading run 1). This occurred due to the interaction of the column bar buckling and the opening action of the beam bar hooks in tension as described in Fig 4.4(a). The development of flexural cracks in the beam and columns at this specific stage was also observed although the beam and columns were still in the elastic range. In loading run 3 which attempted to achieve clockwise $0.75\ V_i$, the existing crack directed by the anchorage configuration of the top beam bars rapidly

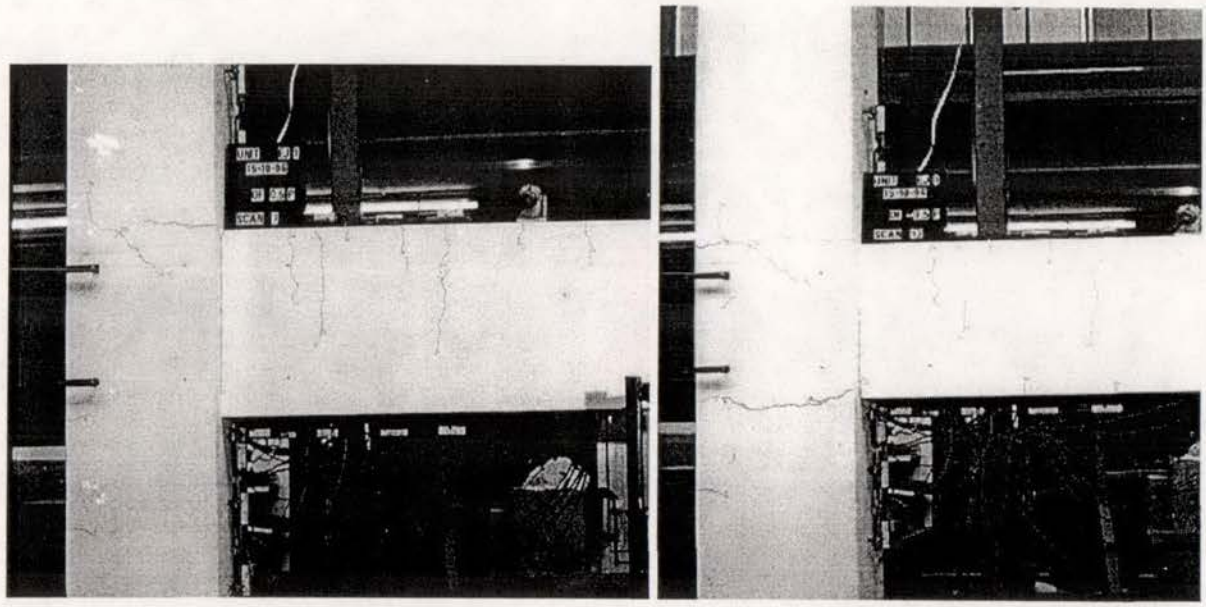

(a). Loading at Clockwise $0.5V_i$ (b). Loading at Anti-Clockwise $0.5V_i$

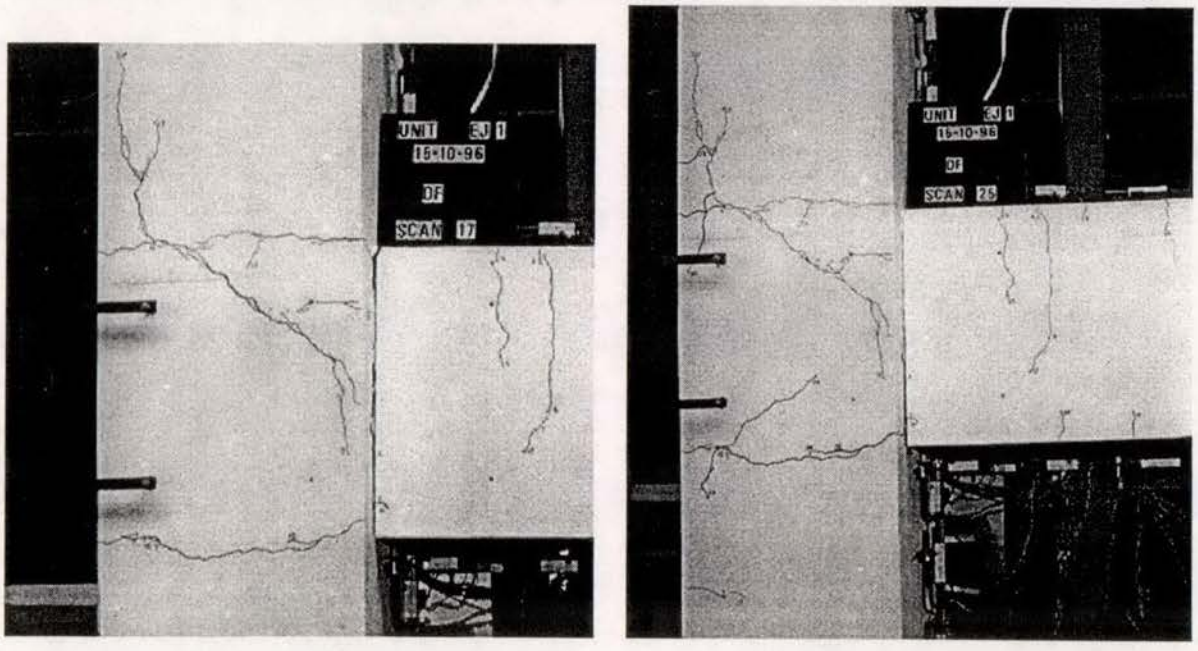

(c). Loading to Attain Clockwise $0.75V_i$ (d). Final Appearance

Fig.7.1 Crack Development and Final Appearance of EJ1 with Failure Initiated by Concrete Tension Cracking Orientated by Beam Bar Hooks

extended into the upper column as well as into the joint core although the attained storey shear strength remained nearly unchanged after it reached only $0.55V_i$. This was due to the failure in actuating the alternative joint shear model as a consequence of insufficient column transverse reinforcement adjacent to the joint core. In comparison,

the observed development of the existing flexural cracks was less apparent in loading run 3. Reversed anti-clockwise loading led to crack development similar to that with clockwise loading. In loading run 4 which attempted to achieve anti-clockwise $0.75V_i$, concrete tension cracking orientated by the bending configuration of the bottom beam bars initiated below the joint core in the column at the drift angle of 1% (see Fig.7.1(d) and it rapidly developed into the bottom column in the vertical direction and into the joint core in the diagonal direction, although the observed increase in the attained storey shear strength was not significant after 60% of the theoretical storey shear strength in the anti-clockwise loading direction.

The testing of as-built Unit EJ1 was terminated after the completion of two loading cycles, and the peak loading of $0.75V_i$ was not attained in both directions. It was believed that subsequent loading could only cause further development of the cracks orientated by the anchorage configuration of the beam bar hooks without achieving any higher strength.

In general, the observed flexural cracks in the columns were much less pronounced than those in the beam, indicating the formation of a weak beam-strong column failure mechanism as theoretically predicted. The flexural cracks in the beam were sparsely spaced with one major flexural crack adjacent to the joint core as a result of severe bond degradation and slip along the beam longitudinal reinforcing bars within and adjacent to the joint core. No beam and column shear cracks were observed for Unit EJ1, similar to that observed for linear members of Units 1 and 2. The joint core of Unit EJ1 was observed to be of good integrity throughout the whole test, although the theoretical seismic assessment identified that the shear capacity of beam-column joint core of Unit EJ1 was 62% less than that required at developing the theoretical strength of the unit (see *Table 4.8*). The seismic performance of individual members was therefore dominated by flexural failure, instead of shear failure. This demonstrated that both the current code method and the current seismic assessment procedure of Reference P6 could not give good prediction of the available shear strength for as-built linear members and as-built exterior beam-column joints should plain round longitudinal reinforcing bars be used, as revealed by other tests on concrete components reinforced by plain round bars [L1, M1, M2].

The influence of the used steel type on the overall seismic performance of exterior beam-column joint components is identified by comparing the observed test evidence of Unit EJ1 and Hakuto's Unit O7. Hakuto's Unit O7 was identical to Unit EJ1 except that Hakuto's Unit O7 used deformed longitudinal reinforcing bars, and both Unit EJ1 and Unit O7 were tested under simulated seismic loading with zero axial column load. For Hakuto's test on Unit O7, the final failure was due to the joint shear failure and the development of the joint diagonal tension cracks occurred earlier than the development of the crack orientated by the beam bar hook in the column. In comparison, the joint core of the as-built Unit EJ1 was of good integrity at the final stage, the development of joint diagonal tension cracks for Unit EJ1 occurred after the development of the crack orientated by the beam bar hook in the column. The final failure of Unit EJ1 was attributed to concrete tension cracking failure along the beam bar hooks in tension, which was due to the interaction between the column bar buckling and the opening action of the tensile beam bar hooks.

In a word, the use of plain round reinforcing bars enhanced the shear force capacities of the beam and beam-column joint, and the shear performance enhancement of the beam and beam-column joint reached a point where their seismic performance is governed by flexure, rather than by shear. However, the use of plain round reinforcing bars enhanced column bar buckling, facilitating concrete tension cracking failure associated with the opening action of the beam bar hooks and leading to increased need for column transverse reinforcement within the beam bar hook range, compared to the case with deformed bars. Evidently, the member force transfer across the joint core is evidently of more concerns if plain round bars are used for longitudinal reinforcing bars.

7.2.3 Load-versus-Displacement Response Measured for Unit EJ1

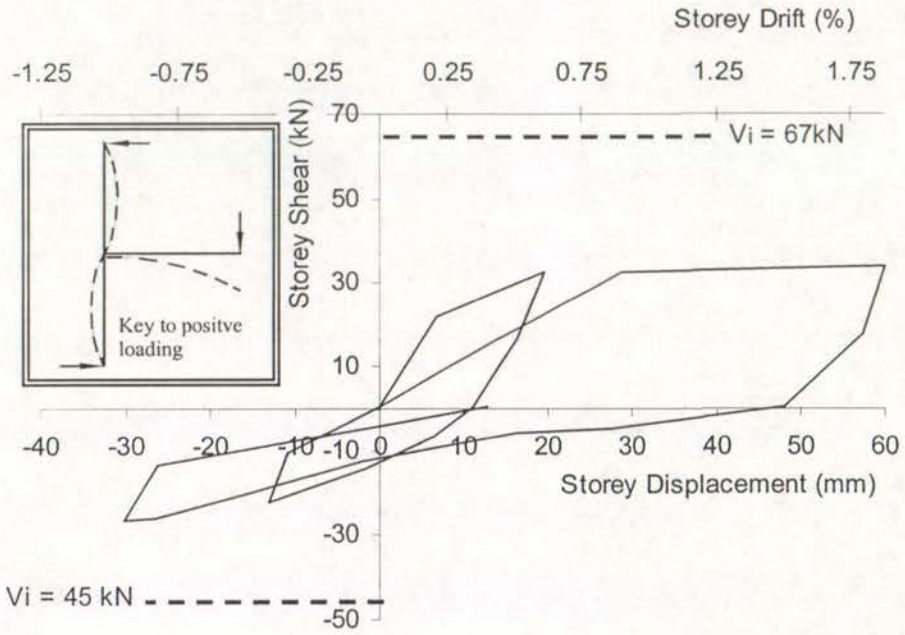

Fig.7.2 Storey Shear versus Storey Displacement Hysteretic Loops of Unit EJ1

Fig.7.2 shows the storey (horizontal) shear force versus storey (horizontal) displacement and storey drift hysteresis loops for the as-built unit EJ1. Also shown in Fig. 7.2 is the theoretical storey shear strength V_i of the unit at the attainment of the theoretical flexural strength of the unit, calculated using the New Zealand code approach but using the measured material strengths and assuming a strength reduction factor of unity as previously described. The plots in Fig. 7.2 confirm very poor general seismic behaviour of the as-built unit EJ1.

The first yield displacement could not be obtained using the adopted method specified in Section 5.3.2 due to failure to attain the peak of $0.75V_i$. The stiffness measured at the loading cycle of $0.5V_i$ was 1.7 kN/mm, and this was only 33% of the theoretically predicted initial stiffness of 5.1 kN/mm. Significant stiffness degradation observed in the loading cycle of $0.75V_i$ indicated that the measured initial stiffness would be lower than 1.7 kN/mm should the loading peak of $0.75V_i$ be attained. Significant disparity between the measured stiffness and the theoretically predicted stiffness was partially because the theoretical prediction of the initial structural stiffness did not take the

effect of member fixed-end rotations into account. The observed structural stiffness property of Unit EJ1 also can be contrasted with the measured initial stiffness of Unit O7 tested by Hakuto et al [H1] which was otherwise identical but reinforced by deformed bars. The measured initial stiffness for Unit O7 at 75% of the theoretical storey horizontal load strength of the test unit was 3.4 kN/mm on average, being 2 times the measured stiffness for Unit EJ1 at $0.5V_i$. The use of plain round longitudinal reinforcement led to a more than 50% reduction in the initial stiffness, compared to the available stiffness with deformed longitudinal reinforcement. Compared to the test evidence of as-built interior beam-column joint Unit 1 reinforced by plain round bars where the initial stiffness observed was about 67% of that observed for Hakuto's Test of Unit O1 which was otherwise identical to Unit 1 but reinforced by deformed bars. Hence the adverse effect resulting from the use of plain round longitudinal reinforcement on the structural stiffness property is more significant for as-built exterior beam-column joint components than for as-built interior beam-column joint assemblies. This occurred because of both the consequence of severe bond degradation along the beam longitudinal bars and the consequence of concrete tension cracking orientated by the beam bar hook configuration, which contributed to large beam fixed-end rotation. This once again demonstrated that the type of structure tested would become very flexible when plain round bars are used for longitudinal reinforcement.

Fig. 7.2 shows that unlike well-designed exterior beam-column joint units where the theoretical strength or even the over-strength can be achieved [P13], the maximum storey shear strengths measured for the as-built unit EJ1 in the clockwise loading direction and anticlockwise loading direction were respectively only 55% and 60% of the theoretical force strength of the unit, and they were attained at a storey drift of 2 % and 1% respectively. The low load capacity was attributed to failing to control the concrete tension cracking along the beam bar hook due to insufficient column transverse reinforcement above and below the joint core within the beam bar hook range. Comparison with the simulated seismic loading test on Hakuto's Unit O7 could lead to the identification of steel type with the seismic behaviour. The available strength of Unit EJ1 was only 70% of the available strength of Unit O7 after

eliminating the influences of material strengths. The lower load capacity of Unit EJ1 compared to Hakuto's Unit O7 was due to severe bond degradation along the column and beam longitudinal bars of Unit EJ1. Severe bond degradation along the column longitudinal bars enhanced premature column bar buckling, and severe bond degradation along the beam longitudinal bars of Unit EJ1 increased the need for the joint concrete strut mechanism and increased the induced concrete lateral tensile stress around the beam bar bend. As a result, the capacity in association with premature concrete tension cracking orientated by the beam bar hooks, which triggered the final failure of Unit EJ1, became very low.

Such low available load force strength and stiffness of the test unit EJ1 mean that investigation of other structural properties, such as, strength degradation and energy dissipating capacity, would be not meaningful.

7.2.4 Measured Steel Strains and Member Curvatures

The measured beam and column longitudinal reinforcement strains as well as the measured beam and column curvatures were below the corresponding yield values within the linear members except in the fixed-end regions.

The measured beam fixed-end rotation was large and it contributed as high as 90% of the total beam flexural deformation. Similarly, the column fixed-end rotation also was the major contribution of the column deformation and it contributed about 93% of the measured total column deformation. At the final loading stage, the measured beam fixed-end rotation was about 9.7 times the total beam rotation theoretically predicted according to conventional method and using the measured beam transverse shear. In comparison, the measured column fixed-end rotation at final loading stage was about 13 times the total column rotation theoretically predicted using conventional method and the measured storey shear force.

Apparently, for linear concrete members reinforced by plain round bars, the fixed-end rotation was the major source of the member deformation and the magnitude of the member fixed-end rotation, which increases as the loading progresses due to progressive bond degradation along the longitudinal bars within the joint and adjacent

to the members, can be as high as 10 to 15 times the theoretically predicted total member deformation.

7.2.5 Joint Behaviour

7.2.5.1 Joint Shear Stress

The estimated maximum nominal horizontal joint shear stress for clockwise loading direction, based on the measured force strength and plane section theory, was 1.0 MPa, or $0.17\sqrt{f_c'}$ MPa. In comparison, the estimated maximum nominal horizontal joint shear stress for anti-clockwise loading direction was lower, being 0.72 MPa, or $0.12\sqrt{f_c'}$ MPa. For both clockwise and anti-clockwise loading directions, the attainment of the maximum nominal horizontal joint shear stresses coincided with the extension diagonally into the joint core of the cracks orientated by the hook configuration of the tensile beam bars in the columns.

A common approach to assess the shear force strengths of beam-column joints at the stage of diagonal tension cracking of the joint cores is to use Mohr's circle for stress and assume the diagonal tension strength of concrete of $0.3\sqrt{f_c'}$ MPa. This gives that joint horizontal shear strength at the stage of joint diagonal tension cracking, in terms of the nominal horizontal joint shear stress, to $0.3\sqrt{f_c'}$ MPa when axial column load is zero as was for test on EJ1. Evidently, the maximum joint shear input of Unit EJ1 of $0.17\sqrt{f_c'}$ MPa was well below the joint shear capacity at diagonal tension cracking of $0.3\sqrt{f_c'}$ MPa, hence the above described crack extension diagonally into the joint core certainly was not attributed to the inadequate joint shear capacity, but it was attributed to the induced lateral concrete tension stress around the hook due to resistance to the beam steel force, as described before. Apparently, when plain round longitudinal reinforcement is used and the beam bar hooks are bent away from the joint core, premature concrete tension cracking failure caused by column bar buckling and the opening action of the tensile beam bars was very critical, compared to the concern of inadequate shear force capacity of the joint core without or with very limited joint shear reinforcement.

Comparison of the joint behaviour of Unit EJ1 and Hakuto's Unit O7, which was identical to Unit EJ1 except the use of deformed reinforcing bars, could lead to the identification of the influence of steel type on the joint performance. The joint performance observed of Unit EJ1 was much better than that of Hakuto's O7 in terms of the final appearance, as seen in Fig.7.1. Whereas in the case of Unit O7 the nominal horizontal joint shear stress at which the crack running along the beam bar hooks initiated was about $0.23\sqrt{f_c'}$ MPa for the clockwise loading cycle and $0.21\sqrt{f_c'}$ MPa for the anti-clockwise loading cycle respectively, the estimated nominal horizontal joint shear stress at which the crack running along the beam bar hook initiated for Unit EJ1 was $0.17\sqrt{f_c'}$ MPa and $0.12\sqrt{f_c'}$ MPa for clockwise and anti-clockwise loading directions respectively, where f_c' is the measured concrete compressive strength. This illustrated that the use of plain round bars for longitudinal reinforcement facilitated the column bar buckling, and increased the need to transmit the beam steel tension force at the bend, compared to the case with deformed bars. As a consequence, the failure associated with the concrete tension cracking orientated by beam bar hooks in tension was facilitated, which triggered the final failure of the test Unit EJ1.

7.2.5.2 Joint Shear Distortion

Fig. 7.3 illustrates the joint shear distortion and expansion estimated for Unit EJ1 using the method as described in Section 5.2.4.

The induced maximum joint shear distortion was 0.52% for Unit EJ1, and it occurred at the achievement of the maximum storey shear strength when the existing crack was observed to extend into the joint core. The maximum joint shear distortion measured for Unit EJ1 was only about 15% of the maximum joint shear distortion measured for Unit O7 by Hakuto et al, which was about 3.5% for both loading directions. Much better joint integrity observed for Unit EJ1 was attributed to more severe bond degradation and bar slip along the beam bars within the joint core of Unit EJ1, compared to the test on Unit O7.

Fig.7.4 shows the storey shear force versus joint diagonal elongation measured for test on Unit EJ1. Evidently, the joint shear deformation was mainly a consequence of

concrete tension cracking along the beam bar hooks and the concrete compressive strains along the supposed diagonal concrete strut was very small.

7.2.5.3 Joint Shear Reinforcement Strains

The measured steel strains in the column transverse reinforcement during the test on Unit EJ1 by electrical resistance strain gauges were generally well below the steel yield strain. However, the measured strain of the column transverse reinforcement CT-4 at the top beam face was well beyond the steel yield strain, as shown in Fig.7.5. For Unit EJ1, severe bond degradation along the beam longitudinal bars occurred owing to the use of plain round longitudinal reinforcement, and hence the beam tension steel force was mainly transferred within the bend. Due to the beam bar hooks bent away from the joint core, the member force transfer across the joint core for Unit EJ1 would follow the alternative force path as suggested by Fig. 4.4(a). The actuation of this alternative force path required the column transverse reinforcement within the beam bar hook range to be significantly strained in tension. Because there was only one set of column stirrup within the beam bar hook range, the measured strain for CT-4 was very large.

7.2.6 Displacement Components

Fig. 7.6 shows the measured displacement components for Unit EJ1. The beam and column displacement components accounted for about 70% and 40% respectively of the measured total storey displacement while the joint displacement component was less than 20%. It should be appreciated that concrete tension cracking orientated by the beam bar hook only contributed to the beam displacement component. Severe bond degradation and slip along the beam bars within the joint core not only enhanced the beam fixed-end rotations but also enhanced the concrete tension cracking orientated by the beam bar hook. Hence the utilisation of plain round

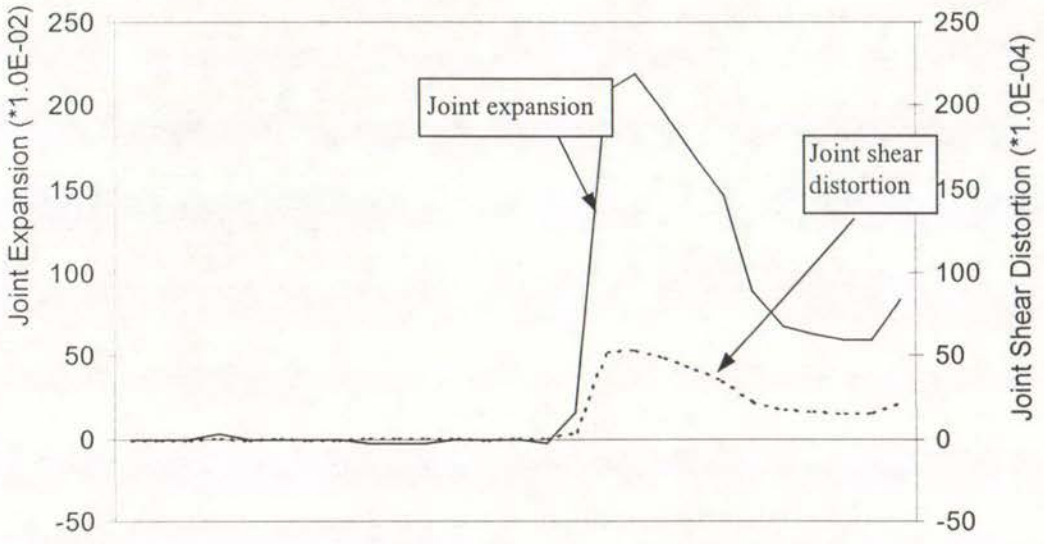

Fig.7.3 Joint Shear Distortion and Expansion Measured for Unit EJ1

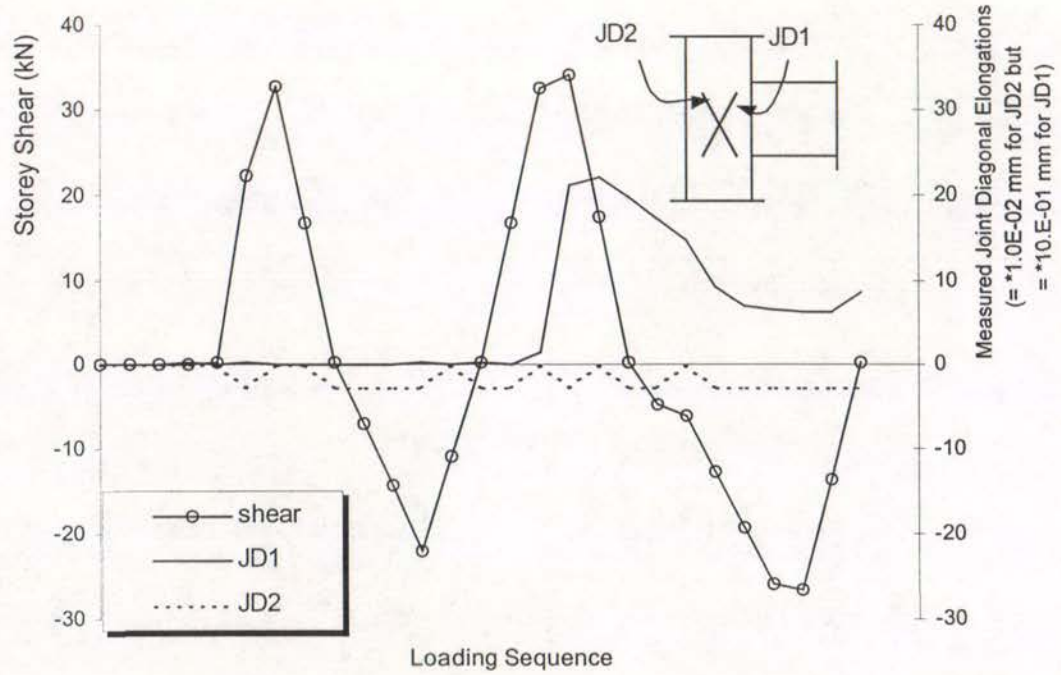

Fig.7.4 Storey Shear and Measured Elongation of Joint Diagonals for Unit EJ1

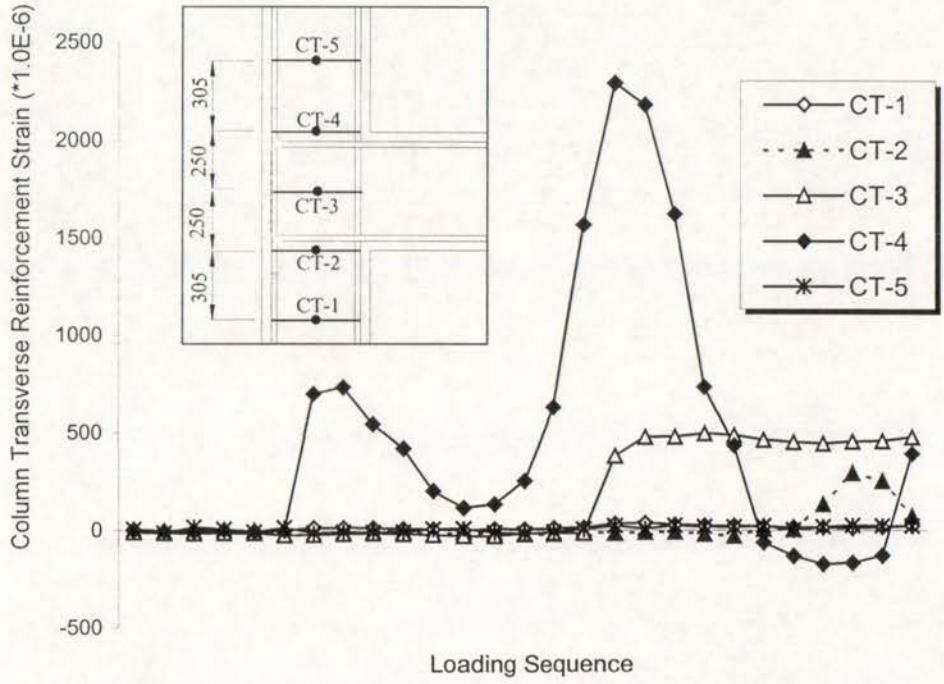

Fig.7.5 Measured Column Transverse Reinforcement Strains at Different Locations

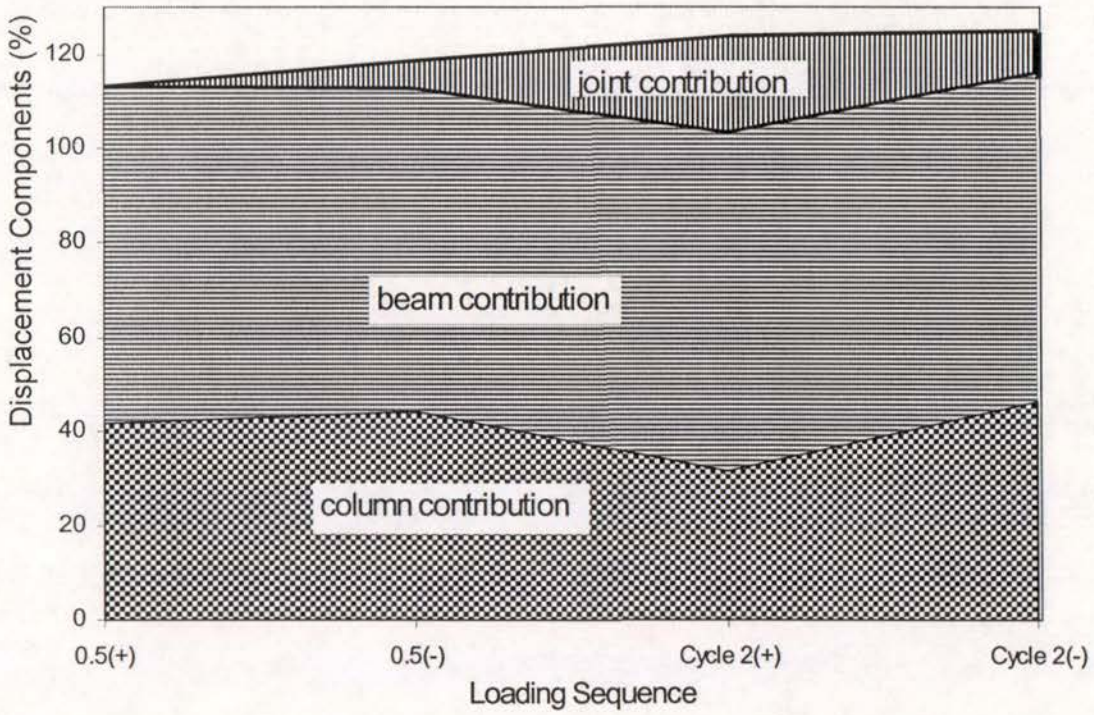

Fig. 7.6 Displacement components measured for Test of Unit EJ1

reinforcing bars as was the case of Unit EJ1 enhances the beam displacement contribution significantly, but reduces greatly the joint displacement component.

7.2.7 Summary

An as-built full-scale exterior beam-column joint unit EJ1 was tested under simulated seismic loading without axial column load. The design deficiencies of test unit EJ1 were (1). The beam longitudinal reinforcing bars were bent away from the joint core in the exterior column. (2). The longitudinal reinforcement was from plain round bars. (3). The joint core contained very limited shear reinforcement. (4). The beam and columns had small amount of transverse reinforcement, and the first set of transverse reinforcement was not close enough to the beam and column interface, according to current code requirement.

1. The test showed that the seismic performance of similar existing reinforced concrete structures with plain round longitudinal reinforcement designed to outdated seismic codes would generally be very poor in a major earthquake. The attained stiffness and the force strength would be very low, especially the stiffness.

2. The attained stiffness by Unit EJ1 was very low. The initial stiffness measured at the loading cycle of $0.5V_i$ was 1.7 kN/mm, and this was only 33% of the theoretically predicted structural stiffness and 50% of the measured initial stiffness for an otherwise identical test of Hakuto's Unit O7 but reinforced by deformed bars. The adverse effect of the utilisation of plain round longitudinal reinforcement on the structural stiffness property is more severe for as-built exterior beam-column joint assemblies, compared to that for as-built interior beam-column joint assemblies. It was concluded that the tested structure would be very flexible if plain round longitudinal reinforcement is used.

3. The available force strength of Unit EJ1 was also very low and it was only about 55% of the theoretical strength of the unit. The strength development of Unit EJ1 was governed by premature concrete tension cracking along the beam bar hooks, which occurred prior to the joint concrete diagonal tension cracking. Severe bond degradation between the longitudinal reinforcement and the surrounding concrete enhanced column bar buckling and enhanced the opening action of the beam bar

hooks. Consequently, premature concrete tension cracking failure along the beam bar hooks, rather than the shear failure in the beam and/or the joint, triggered the final failure of the unit.

4. For the existing reinforced concrete exterior beam-column joint components with the beam bar hooks bent away from the joint core in the exterior columns, the column hoops adjacent to the joint core, rather than the ones in the joint, are highly stressed.

5. For the existing reinforced concrete beams and column with plain round longitudinal reinforcement, the seismic performance was governed by flexure, rather than by shear. In this case, member's theoretical flexural strength could not be attained, member fixed-end rotation was much larger than the theoretical prediction and it was the major source of member flexural deformation.

6. Comparison with the simulated seismic loading test on an otherwise identical Unit O7 but reinforced by deformed bars showed that the use of plain round bars for the longitudinal reinforcement of as-built exterior beam-column joint assemblies not only caused the available shear force strength to reduce by about 30% after eliminating the effect of material strengths, but also caused the available stiffness of Unit EJ1 to reduce by about 50%. This occurred because the utilisation of plain round longitudinal reinforcement for Unit EJ1 greatly enhanced column bar buckling and the opening action of the beam bars in tension. Interaction between the column bar buckling and the opening action of the beam bars in tension then enhanced the propogation of concrete tension cracking orientated by the beam bar hooks, initiated the final failure of the test on Unit EJ1. However, the use of plain round longitudinal reinforcement for Unit EJ1 led to much improved joint shear performance due to severe bond degradation along the beam longitudinal reinforcement within the joint core. As a consequence, the problem area of as-built exterior beam-column joint unit was shifted from the joint shear failure for Unit O7 to concrete tension cracking orientated by the beam tensile steel hooks.

7.3 TEST OF RETROFITTED EXTERIOR BEAM-COLUMN JOINT REJ1

7.3.1 Introduction

As-built Unit EJ1 was retrofitted by wrapping the column areas adjacent to the joint core using fibre-glass jacketing after tested as-built under simulated seismic loading with zero axial column load, and then became Unit REJ1. Unit REJ1 was tested under simulated seismic loading with zero axial column load in order to testify the actuation of the postulated alternative joint shear model in Section 4.4.2.

7.3.2 Crack Development and Damage

The crack development and the appearance of Unit REJ1 at the completion of testing are shown in Fig. 7.7.

The existing beam and column flexural cracks, which were repaired by injecting epoxy resin before jacketing the damaged as-built Unit EJ1 using fibre-glass, started to open again as early as in the loading cycle to $0.5V_i$, especially the beam flexural crack at the inner column face. Apart from this, a vertical crack along the outer layer of the column main bars was observed within the joint core in the later loading stages. This was associated with the reopening of the existing cracks orientated by the beam bar hook and the column bar buckling within the joint core. However, the development of this vertical crack within the joint core was not so apparent as that of the major beam flexural crack at the column face.

Similar to the test observation for Unit EJ1, no diagonal concrete tension cracks were observed in the beam and columns of Unit REJ1. Hence the performance of individual linear members was dominated by flexural deformation. There were no new joint diagonal tension cracks developed within the joint core of REJ1. It is noted that thetheoretical seismic assessment conducted in Section 4.3 "SEISMIC ASSESSMENT OF AS-BUILT TEST UNITS" showed that the provided horizontal joint shear force capacity was only 38 % of the imposed horizontal joint shear force at developing the beam negative theoretical flexural strength and the attained storey shear strength by test of REJ1 was 75% of the theoretical storey shear strength for both loading directions. Furthermore the theoretical seismic assessment conducted in Section 4.3 showed that the available shear force capacity of the beam of Unit EJ1 was only 20% and 55% of the imposed shear at developing the theoretical strength of the unit by

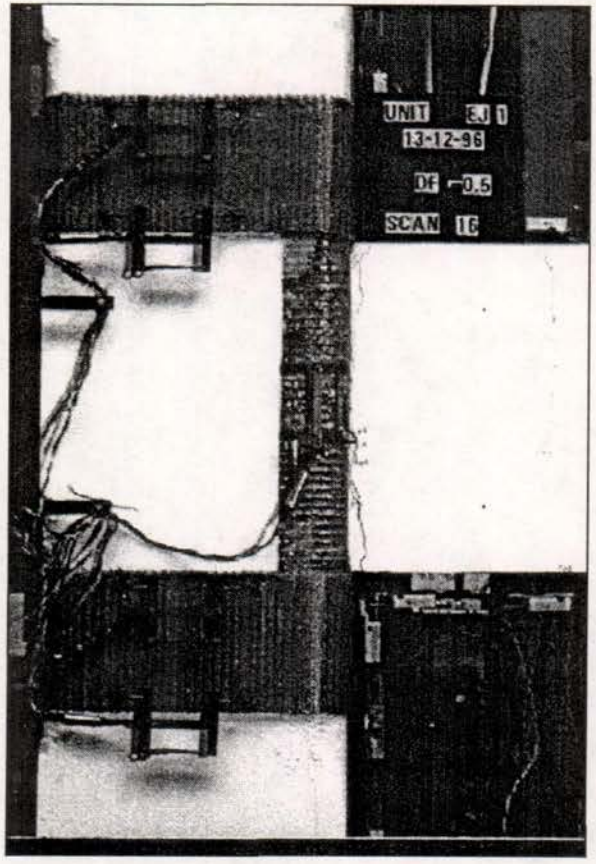

(a) Loading at 0.5Vi

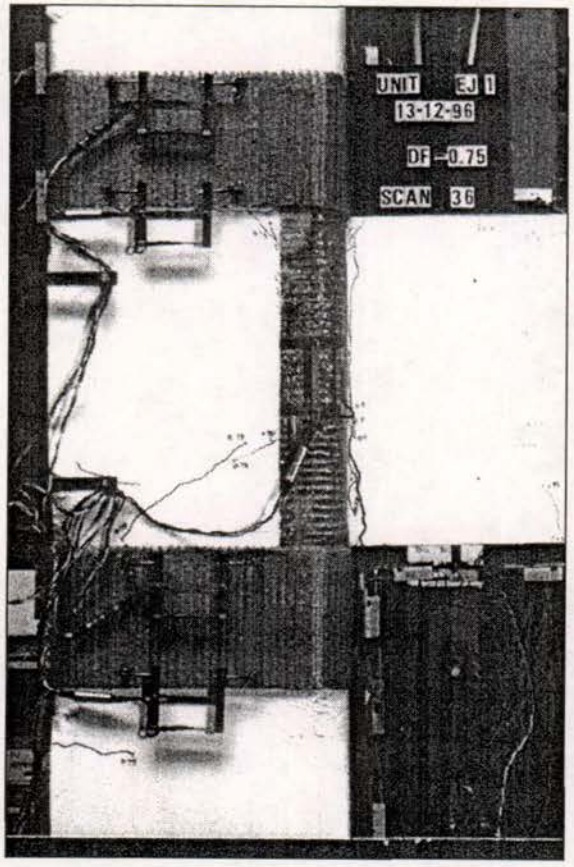

(b) Loading at 0.75Vi

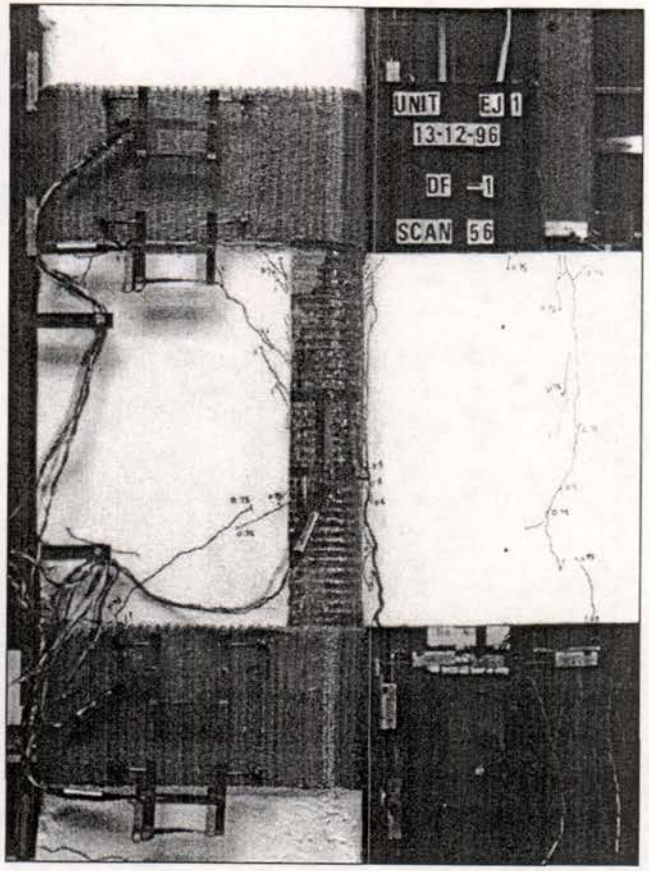

(c) End of Ductility 1

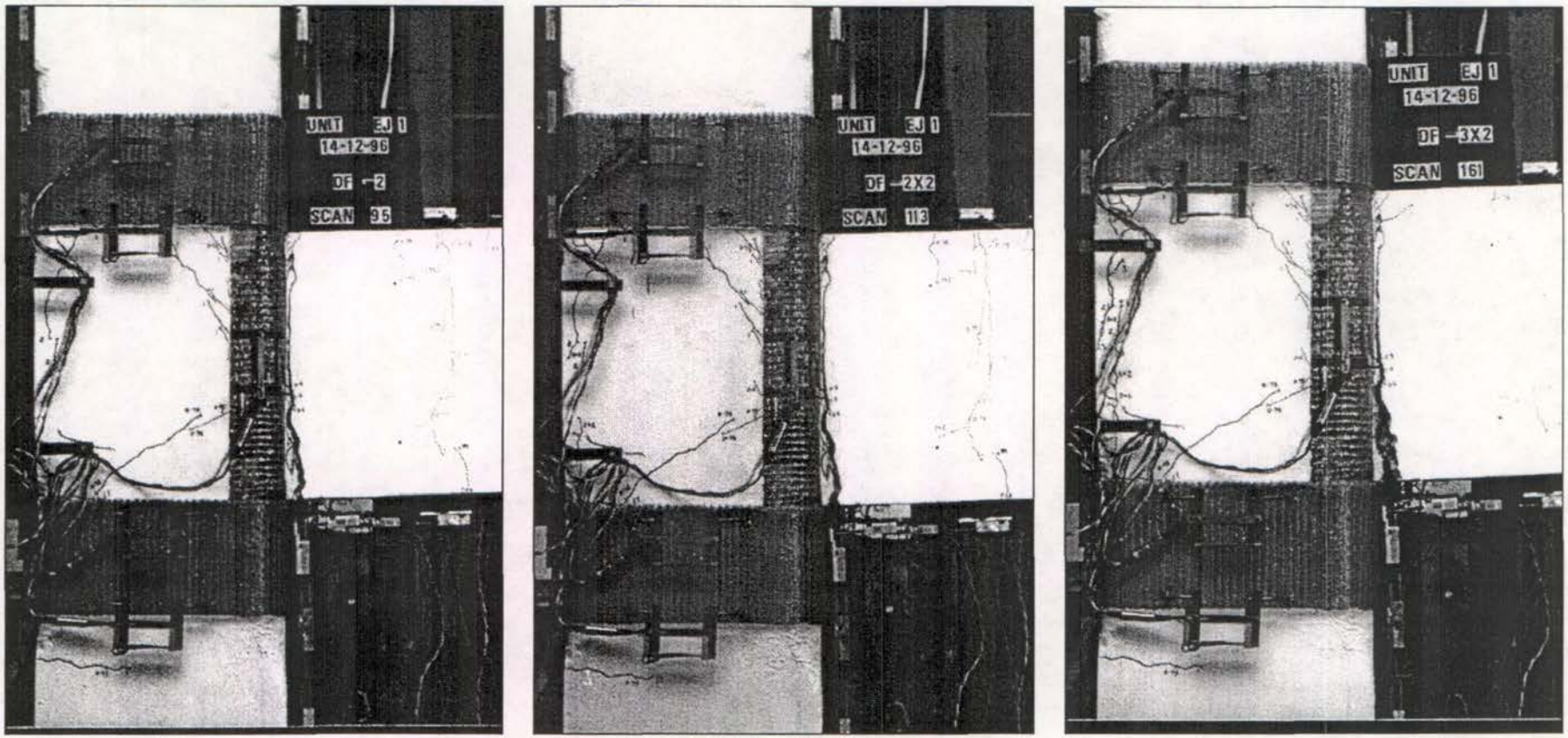

(d) End of Loadng at First Dcutility 2 (e) End of Loading at Ductility 3 (f) Final Look

Fig.7.7 Crack Development and Final Appearance of Unit REJ1

code approach and the approach suggested in reference P6 respectively. Hence both the current code method and the current seismic assessment method proposed in Reference P6 could not give good prediction of the shear force capacity in linear concrete members and beam-column joints if plain round bars are used for longitudinal reinforcement.

Hence, the seismic performance of the test of REJ1 was totally governed by beam flexural behaviour. Beam flexural deformation concentrated on the major flexural crack at column face due to severe bond degradation and slip along the beam main bars within and adjacent to the joint core of Unit REJ1 and beam fixed-end rotation became the major source of the beam flexural deformation.

Whereas in the case of the test on as-built unit EJ1 concrete tension cracking orientated by the beam bar hook configuration governed the strength attainment and triggered the final failure, test of Unit REJ1 evidently demonstrated that fibre-glass jacketing in the column areas adjacent to the joint core for Unit REJ1 controlled such premature concrete tension cracking and actuated the alternative force path postulated in Section 4.4.2. Consequently, the seismic performance of Unit REJ1 was governed by the flexural performance of the beam for this weak beam-strong column system.

7.3.3 Load-versus-Displacement Response Measured for Unit REJ1

Fig.7.8 shows the storey shear force versus storey displacement and storey drift hysteresis loops measured for the retrofitted as-built exterior beam-column joint unit REJ1. The theoretical storey shear strength of Unit REJ1, V_i, which was the same as that of the as-built unit EJ1, is also shown in Fig.7.8 for both loading directions. Compared to the hysteresis properties measured for Unit EJ1 in Fig.7.2, the hysteresis loops measured during the test of Unit REJ1 in Fig.7.8 demonstrated that wrapping the column parts above and below the joint core using fibre-glass greatly improved the seismic behaviour of as-built exterior beam-column joint assembly which had plain round beam longitudinal bar hooks bent away from the joint core in the exterior columns.

Big increase in the measured stiffness was observed for the test on Unit REJ1, compared to the test on Unit EJ1. The stiffness measured at clockwise $0.5V_i$ for the test on Unit REJ1 was 4.26 kN/mm, and this was 2.37 times the measured initial

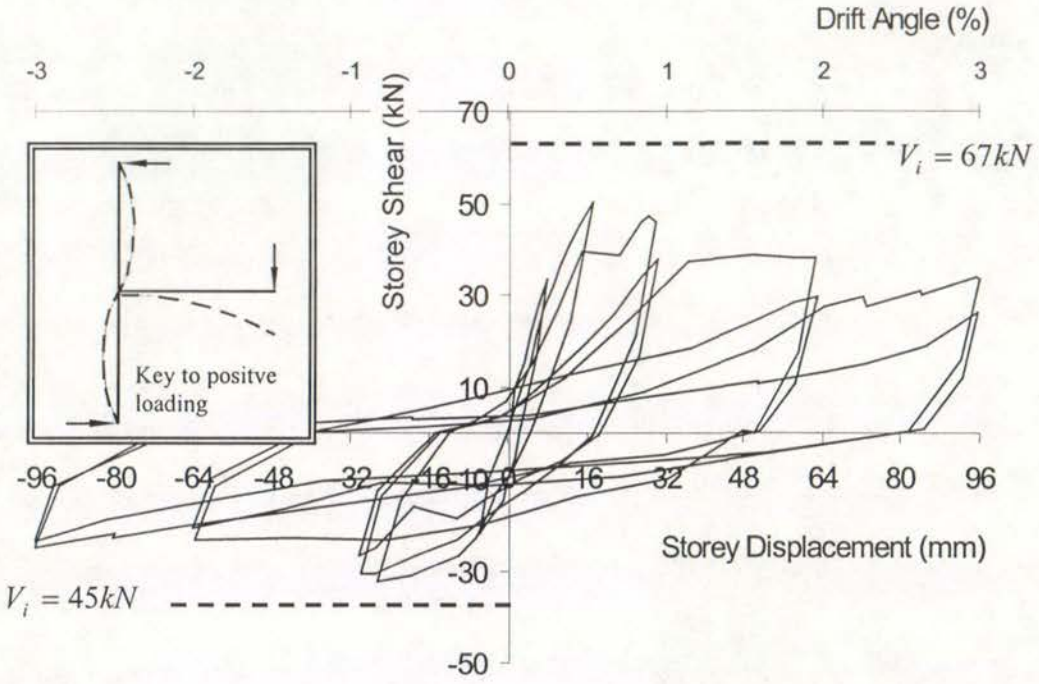

Fig.7.8 Storey Shear Versus Storey Displacement Hysteresis Responses of REJ1

stiffness of 1.7 kN/mm for the as-built unit EJ1 at loading cycle of 0.5 V_i. This occurred because the development of concrete tension cracking orientated by the beam longitudinal bar hooks in exterior columns was controlled by the lateral confinement provided by fibre-glass jacketing. The average initial stiffness measured for Unit REJ1 at the loading cycle to 0.75 V_i was 2.1kN/mm, and this was about 40% of the theoretical prediction of the initial stiffness. Obviously the available stiffness of the retrofitted as-built exterior beam-column joint Unit REJ1 was still very low. The low stiffness property was the case because of the following reasons: Firstly, the clamping actions in column areas adjacent to the joint core, which was necessary for actuating the alternative force path, was at the expense of large crack opening when passive jacketing, such as fibre-glass jacketing as was the case as for REJ1. Secondly, Beam flexural behaviour dominated the final seismic performance of the unit. Severe bond deterioration along the beam longitudinal bars within and adjacent to the joint core must have led to a very low beam flexural stiffness.

Also observed was a big increase in the measured force strength for Unit REJ1, in comparison with as-built Unit EJ1. The maximum storey shear strengths attained by Unit REJ1 in the loading cycle to 0.75 V_i for both clockwise and anti-clockwise loading directions were about 25% less than the corresponding theoretical storey shear strengths of the unit, and they were more than 15% higher than those attained by the as-built Unit EJ1. However, the attained storey shear strength by Unit REJ1 was still low and the seismic performance of the unit was dominated by the beam flexural behaviour for this weak beam-strong column system. This was attributed to the bar slip along the beam longitudinal bars, which caused the plane section assumption to overestimate the member's theoretical flexural strength, as revealed by the simulated seismic loading tests on as-built interior beam-column joints reinforced by plain round bars [L1].

Significant pinching is observed in the loops of Fig.7.8, and the pinching was observed to progress with the imposed displacement level. The softness of the test unit at the beginning of each load run occurred due to the major beam flexural crack at the inner column face, which formed as a consequence of severe bond degradation and slip along the longitudinal beam reinforcement within and adjacent to the joint core.

In summary, the retrofitted Unit REJ1 demonstrated much better seismic performance. The attained initial stiffness, although only about 40% of the theoretical value based on the plane section assumption, was more than 2 times the measured initial stiffness for the as-built unit EJ1. The attained storey shear strengths occurred at storey drifts of approximately 0.86%, and although only about 75% of the theoretical storey shear strengths, were about 15% higher than that achieved by the as-built unit EJ1. However, the retrofitted unit still showed a great deal of strength and stiffness degradation.

7.3.4 Beam Behaviour

7.3.4.1 Strains of Beam Bars Measured by Strain Gauges

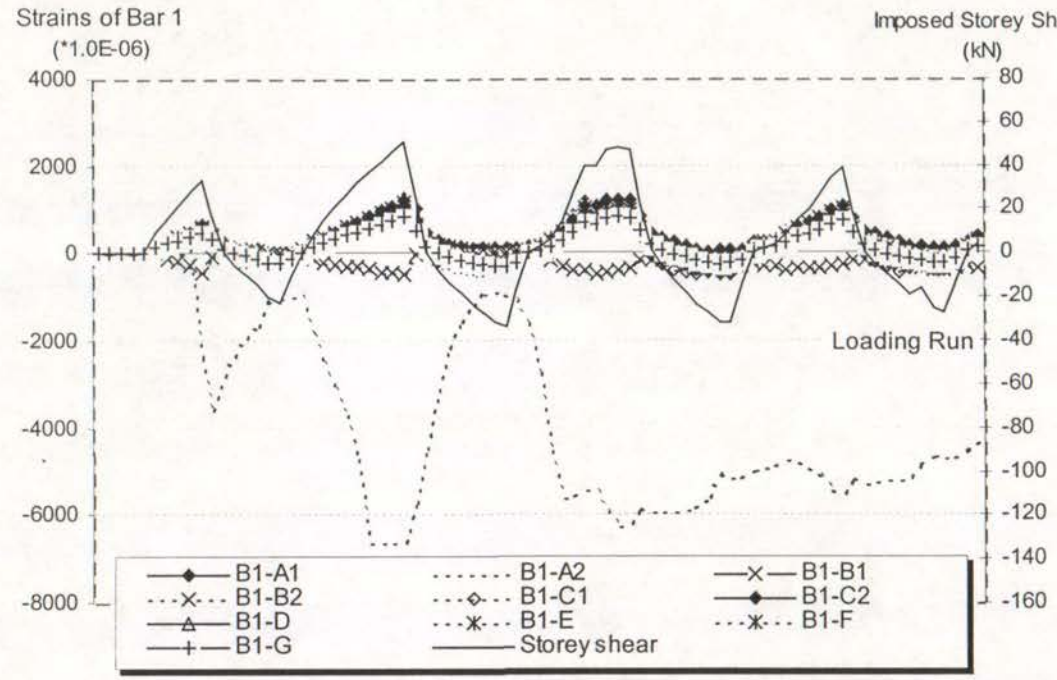

(a)

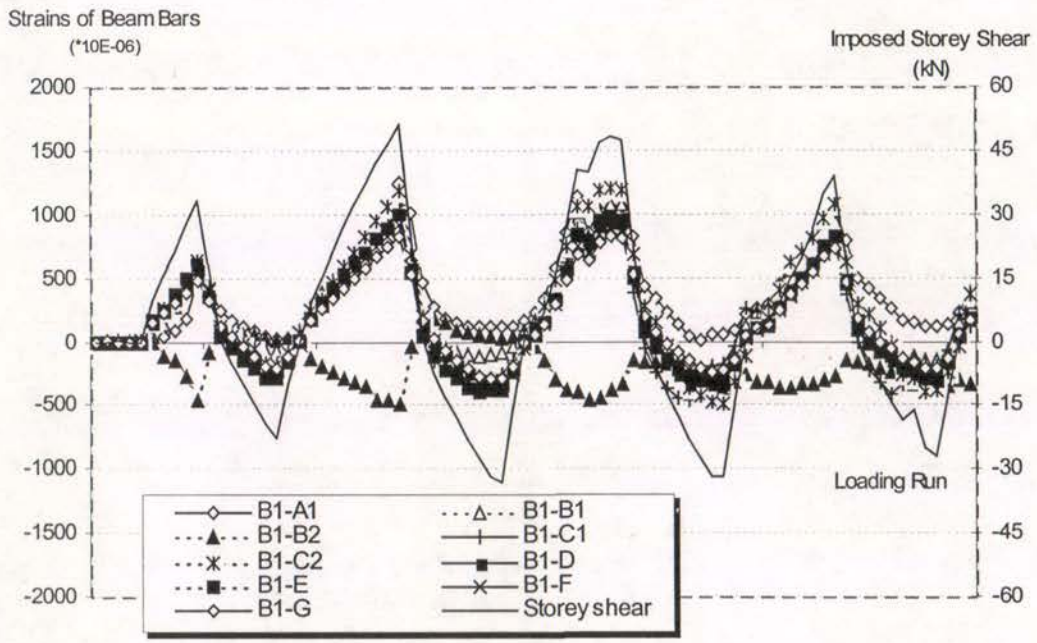

(b)

Fig.7.9 Measured Strain Variation of Beam Bars with Loading Progress

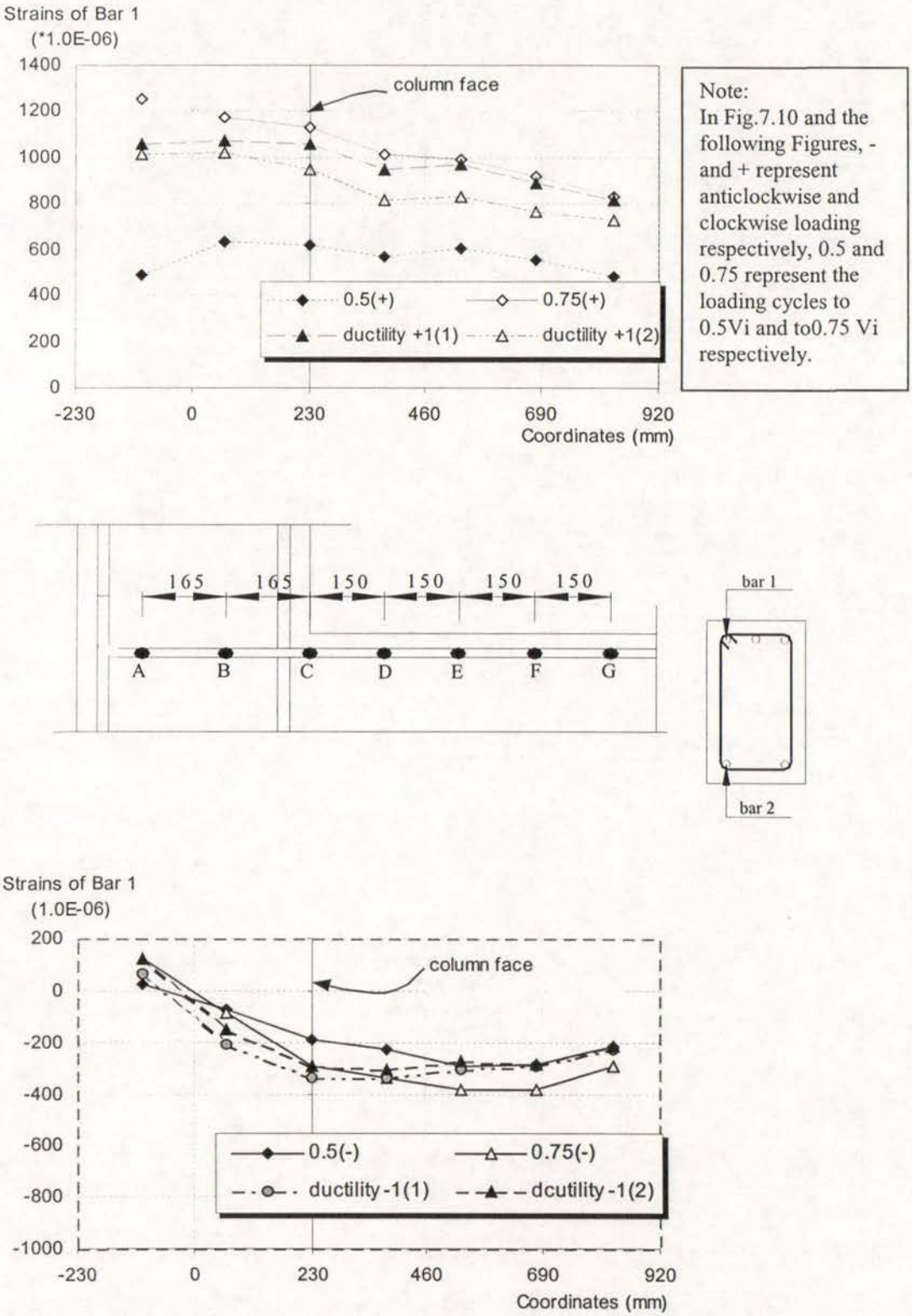

Fig.7.10 Strain Profile of Beam Bar 1 along Beam Axis

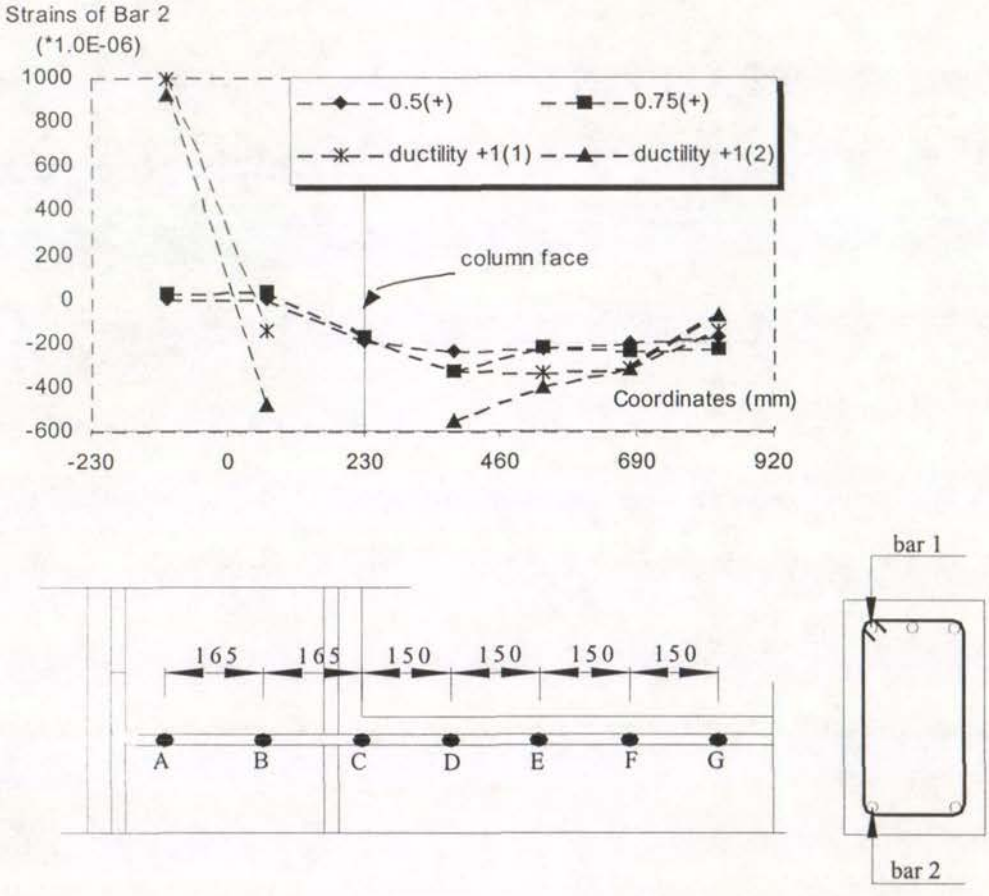

Fig. 7.11 Measured Strain Profile of Beam Bar 2

The readings from electrical resistance strain gauges were checked first to verify their reliability. For a certain strain gauge, the variation of its readings was compared with the variation of the imposed member forces, as the testing progressed. If the strain gauge readings fluctuated in the same way as that of the imposed member forces, the strain gauge was thought to behave properly. Otherwise, the strain gauge readings were not reliable.

Fig. 7.9 shows the strain variation of beam longitudinal bar 1, measured by strain gauges, until the completion of ductility 1, where strain gauges were named in the form of BN-ML, and the letters have the following meanings:

B1 and B2 mean beam bar 1 and beam bar 2 respectively; M is the gauged locations, for example, location A, or B, or C et al 9 (see Chapter 5); L is 1 or 2 if two gauges were glued at opposite surfaces of the beam bar at the same location. L = 1 means the first gauge and L = 2 means the second gauge. M is not present if only one gauge is used at one location. For example, for bar 1, B1-A1 and B1-A2 are the gauges glued oppositely to bar 1 at location A, and B2-D is the gauge glued to bar 2 at location D.

It was noted in Fig.7.9(a) that the strain gauge B1-A2 for beam bar 1 of Unit REJ1 did not perform well and the readings from this gauge were not used. All the rest strain gauges for beam bar 1 performed sensibly, see Fig.7.9(b).

Fig.7.10 and Fig.7.11 show the measured strain profiles by electrical resistance strain gauges respectively for beam bar 1 and beam bar 2. The measured beam bar strain was taken as the average value if two gauges were used at same location. For beam bar 2, the strain gauges glued at inner column face did not work properly, hence the strains of beam bar 2 at this location could not be obtained. It is seen from Fig.7.10 and Fig.7.11 that the measured tensile strains for beam bar 1 and beam bar 2 within the joint region were not less than the ones measured at inner column face throughout the testing history. Hence it could be said that complete bar slip along the beam longitudinal bars 1 and 2 must have taken place within the joint region.

Fig.7.12 compares the measured strains with the theoretical strains at inner column face for beam bar 1 when beam bar 1 was in flexural tension in the early loading cycles until the completion of loading at ductility 1. After ductility 1, some strain gauges went out of order. Fig.7.12 shows that generally the measured beam steel

strains matched well with the theoretical predictions at inner column face. At early stages, the measured steel strains were smaller than the theoretical values but became larger than the theoretical values at later stages. The theoretical values were predicted using plane section assumption. Such a comparison could not be conducted for beam bar 2 because the readings from the strain gauges on beam bar 2 at inner column face did not make sense.

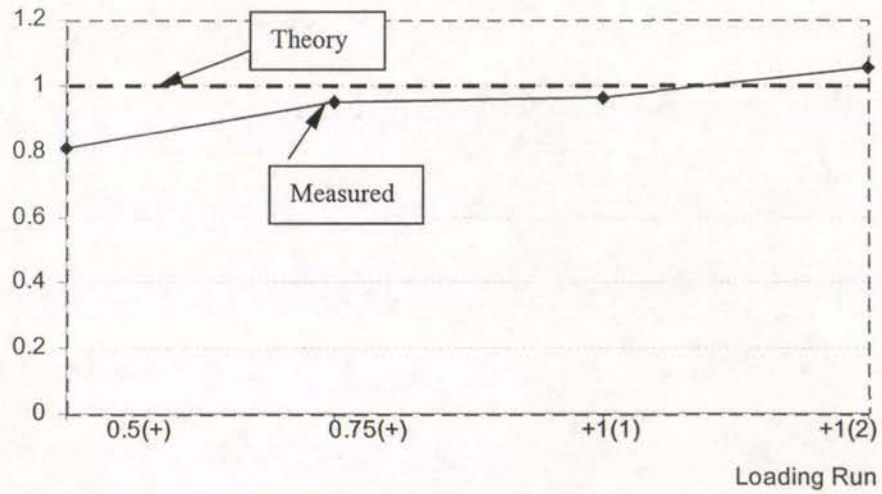

Fig.7.12 Comparison of measured strains with theoretical strains of beam bar 1 at inner column face

7.3.4.2 Beam Curvature

Fig.7.13 shows the measured beam curvature distribution along the beam for Unit REJ1. It is evident that the beam flexural deformation mainly concentrated in the fixed-end region. The curvature over beam fixed-end region was much higher than the theoretical yield curvature although the imposed beam bending moment had never reached the theoretical beam flexural strength. The theoretical beam yield curvature is 4.5E-06 for positive loading, and 4.9E-06 for negative loading.

Fig.7.14 shows the measured storey shear strengths (expressed as the percentages of the theoretical storey shear strength) versus the amplification of the beam curvatures over beam fixed-end region (expressed as the ratio of the measured beam curvatures to the correspondent theoretical values). Although the achieved force strength reduced after the loading of 75% of the theoretical strength, the amplification of the beam curvatures over the fixed-end region, relative to the theoretical predictions, increased with the loading progress, due to progressive bond degradation along the beam bars.

Fig 7.15 also shows the measured storey shear strengths versus the amplification of the beam fixed-end rotations (expressed as the ratio of the measured beam fixed-end rotations to the theoretically predicted rotations over the whole beam length). For this theoretically weak beam-strong column system, $V_{test}/V_i(\%)$ is also the stress level in the beam longitudinal bars in terms of the steel yield strength. Hence Fig.7.15 is also the relationships between the longitudinal steel stress level with the beam fixed-end rotation.

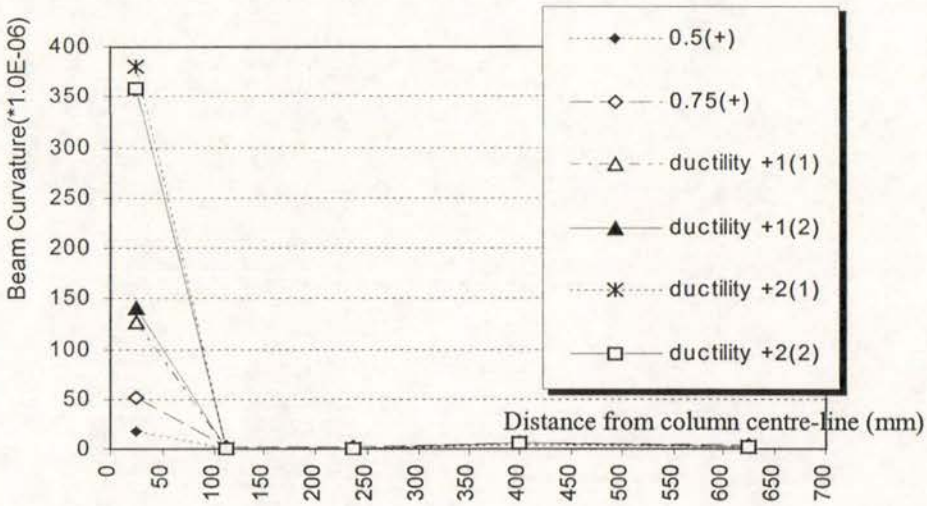

Fig.7.13 Measured Beam Curvature Profile for Unit REJ1

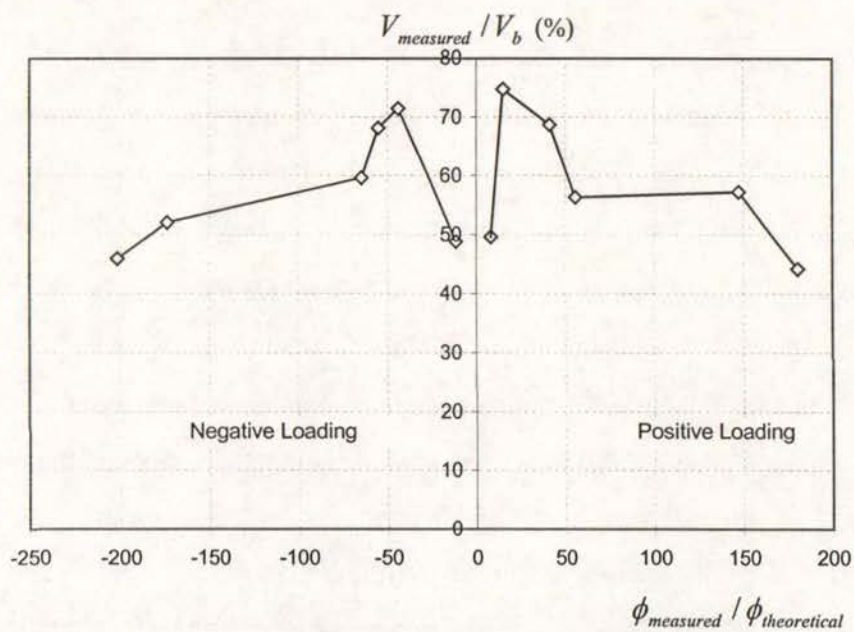

Fig.7.14 Storey Shear Strength versus Beam Curvatures over Beam Fixed-End Region

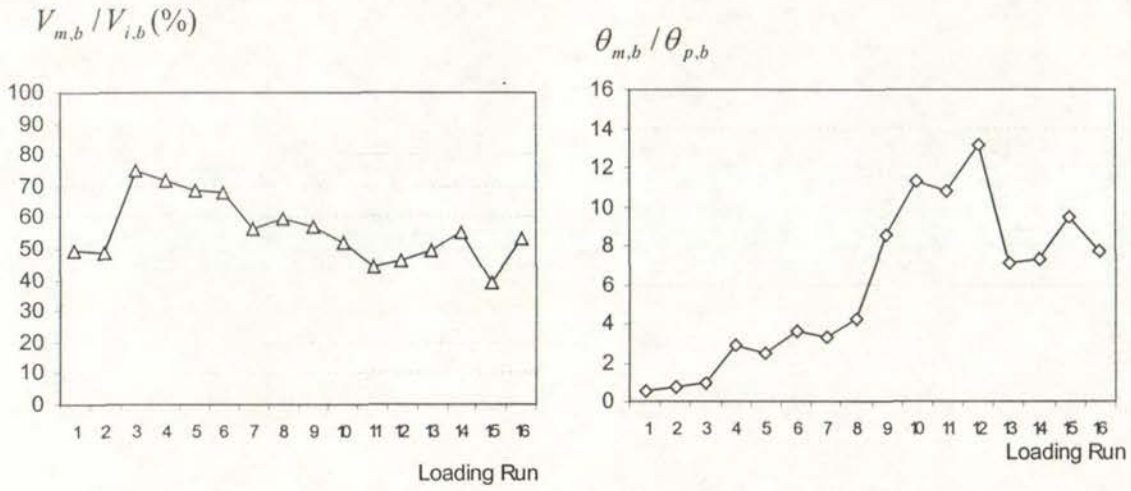

Fig.7. 15 Rotations over beam fixed-end region and storey shear strengths

7.3.5 Column Behaviour

Measured strains in the longitudinal column bars were much lower than the steel yield strain and also much lower than measured strains in the beam longitudinal bars, indicating that the column flexural performance was much better than the beam.

Measured column curvature distribution along the columns is shown in Fig.7.16. It is seen that column curvatures over fixed-end regions were much larger than column theoretical yield curvature of 4.8E-06, although the columns were expected to be in the elastic range.

Fig. 7.17 shows the measured column shear force versus the curvature amplification over column fixed-end regions. In Fig.7.17, the measured column shear force is expressed as the percentage of the column shear force strength developed at the column flexural strength, and the curvature amplification is expressed as the ratio of the measured curvature to the theoretical curvature calculated from the column shear force at the specified stage. Apparently, the measured member curvatures over fixed-end regions were much larger than the theoretical predictions, indicating that the investigation of the detailed member curvature property is not meaningful in this case. In this case, the investigation of the member's overall rotational performance is of more significance. Fig.7.18 shows the measured column shear force versus the column rotation

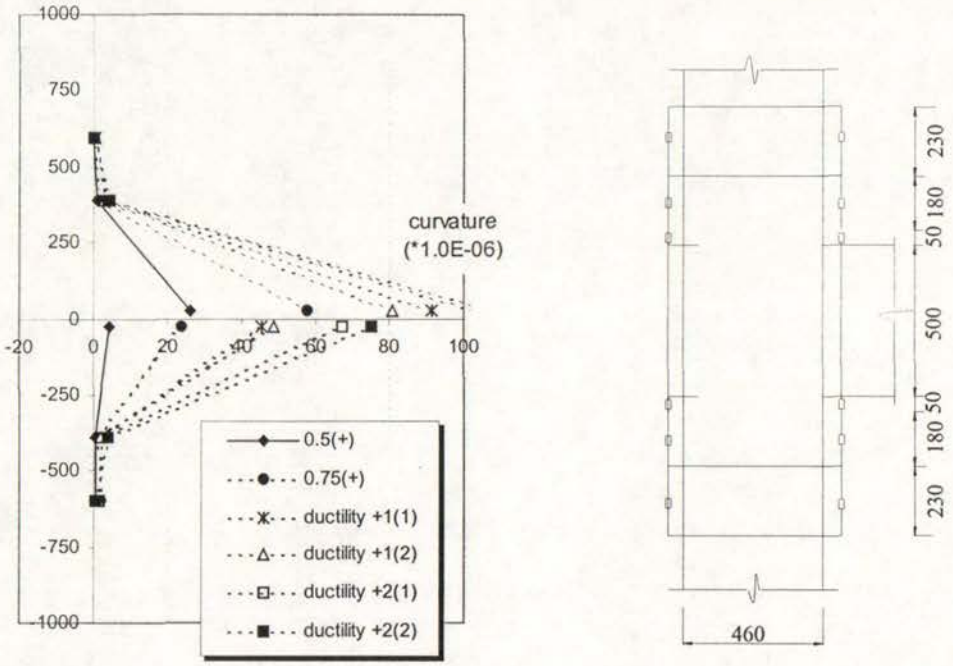

(a) Positive Loading

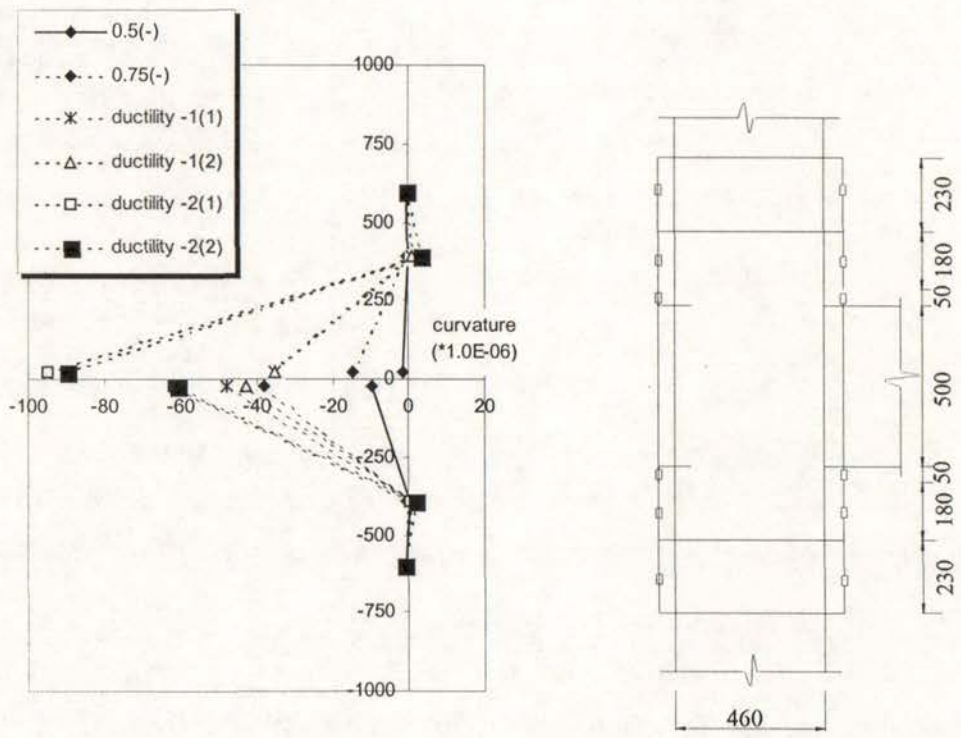

(b) Negative Loading

Fig.7.16 Column Curvature Profile of Unit REJ1

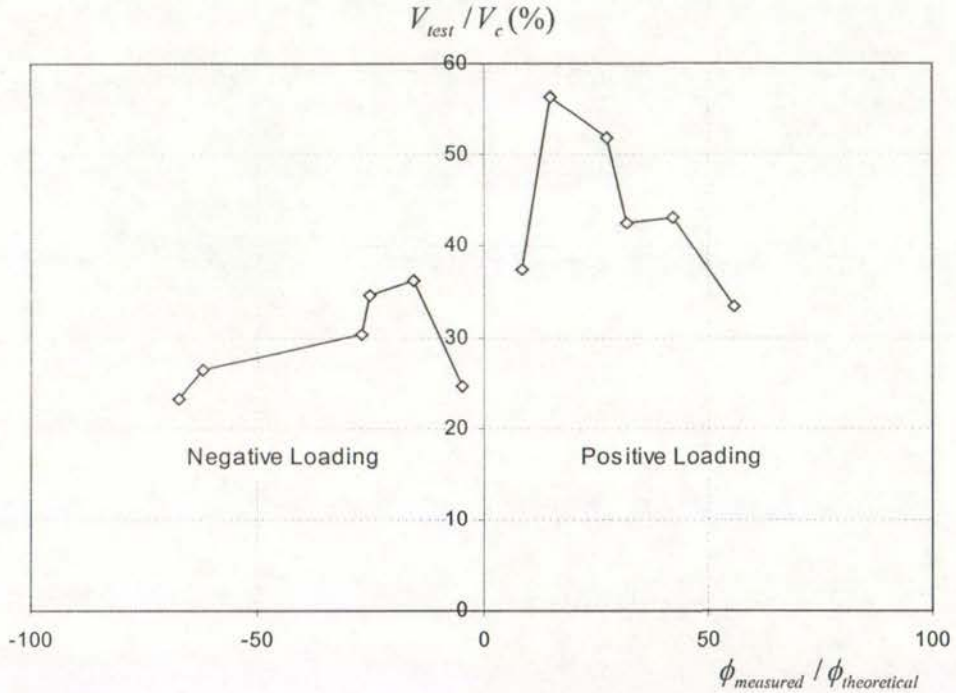

Fig.7.17 Storey shear versus curvature amplification over column fixed-end regions

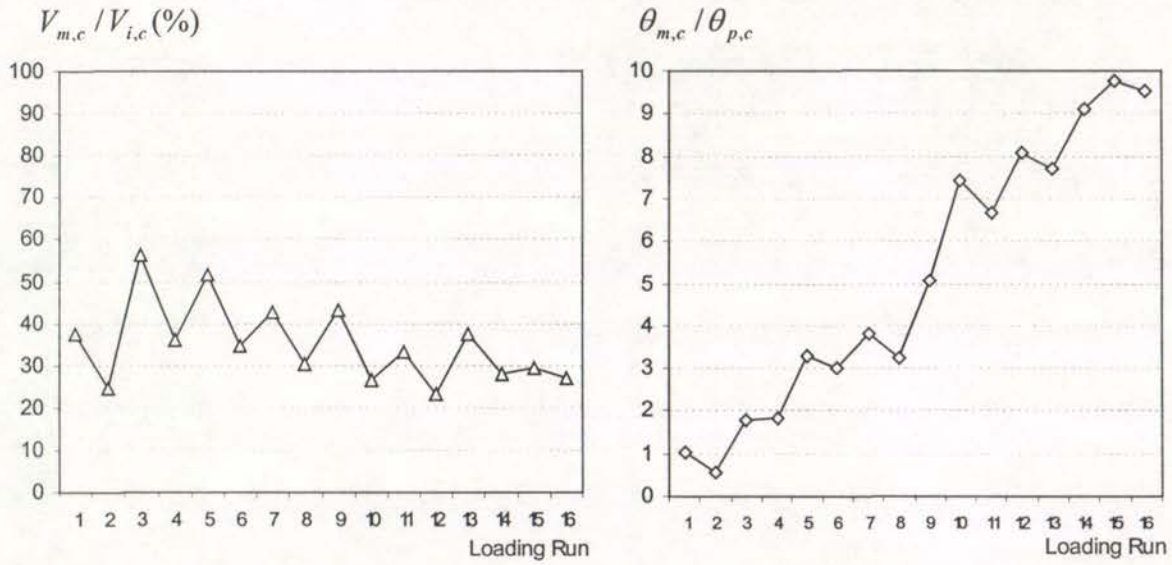

Fig.7.18 Storey shear and rotation amplification over column fixed-end regions

amplification, where the column rotation amplification is expressed as the ratio of the measured column fixed-end rotation to the theoretically predicted total column rotation. Hence Fig.7.18 illustrates the relationship between the column longitudinal steel stress level with the column fixed-end rotation.

Generally, estimated amplifications of beam rotations and column rotations are of similar magnitude although the steel stress levels were quite different. Whether or not the amplification of member rotations is dependent on the developed stress level needs to be further studied.

7.3.6 Joint Behaviour

7.3.6.1 Joint Shear Stress

The measured maximum nominal horizontal joint shear stress for Unit REJ1 was 1.37MPa or $0.23\sqrt{f_c'}$ Mpa, based on the measured member forces and plane section theory. In comparison, the estimated maximum nominal horizontal joint shear stress for anti-clockwise loading direction was lower, being 0.9 MPa, or $0.15\sqrt{f_c'}$ MPa. The joint shear force at the development of the joint diagonal cracking was $0.3\sqrt{f_c'}$ MPa in the case of zero axial column load if expressed in terms of the nominal horizontal joint shear stress. Evidently, the attained maximum nominal horizontal joint shear stresses by Unit REJ1 was low enough to prevent the joint shear failure.

7.3.6.2 Measured Strains in Joint Shear Reinforcement and Fibre-Glass Jacketing

The strains in three joint hoops were measured by electrical resistance strain gauges, one set of the joint hoop was located at the centre of the joint core and the other two sets were located at the beam faces. The measured joint hoop strains were contrasted to the strains measured for column transverse reinforcement adjacent to the joint core in Fig.7.19, where the positions of the five sets of column transverse reinforcement were also illustrated in Fig.7.19.

For well-designed exterior beam-column joint subassemblages, the beam bar hooks are bent into the joint cores and the member forces will be transferred across the joint core by a concrete diagonal strut. Hence the joint horizontal hoops at the joint core centre will be subjected to higher tensile stresses due to Poisson's effect as for axially loaded columns in compression, compared to those close to beam faces [P13]. However,

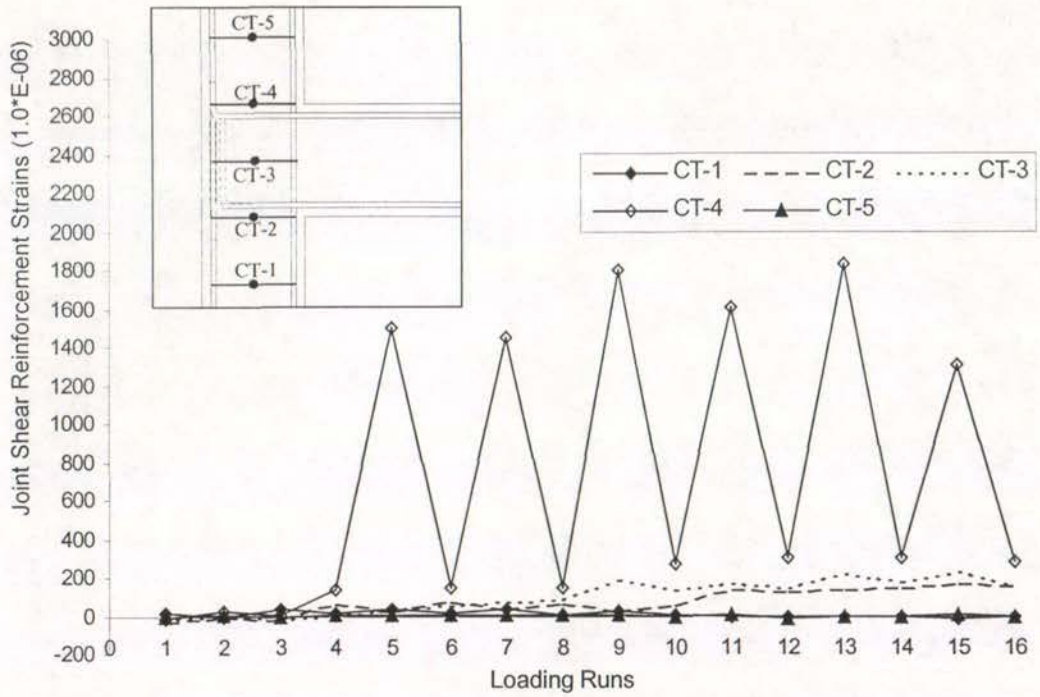

Fig.7.19 Joint Shear Reinforcement and Column Stirrup Strains of Unit REJ1

Fig.7.19 shows different evidence, that is, the strain measured in the joint hoop CT-4 of Unit REJ1, which was located at the beam face, was much larger than the measured strains in CT-3, which was at the centre of the joint core. This was because bending out configuration of the beam bars as was the case of Unit REJ1 required the actuation of an alternative force path as postulated in Chapter 4, and hence the joint hoops at beam flexural tensile face will be highly stressed. Severe bond degradation as was the case for Unit REJ1 resulted in a greatly reduced joint shear force assigned to truss action. Hence the joint shear reinforcement provided at the centre of the joint core would make no difference in the shear performance of the as-built exterior beam-column joint components.

Fig.7.19 also shows clearly that CT-4 was subjected to a much higher tensile stress compared to column transverse reinforcement CT-1 and CT-5. Apparently the cause for the joint hoop at beam flexural tensile face to be highly stressed was not because of high column shear resistance demand, but was due to the requirement for control of concrete tensile cracking along the beam bar hook and the actuation of the alternative force path to transmit the member forces across the joint core.

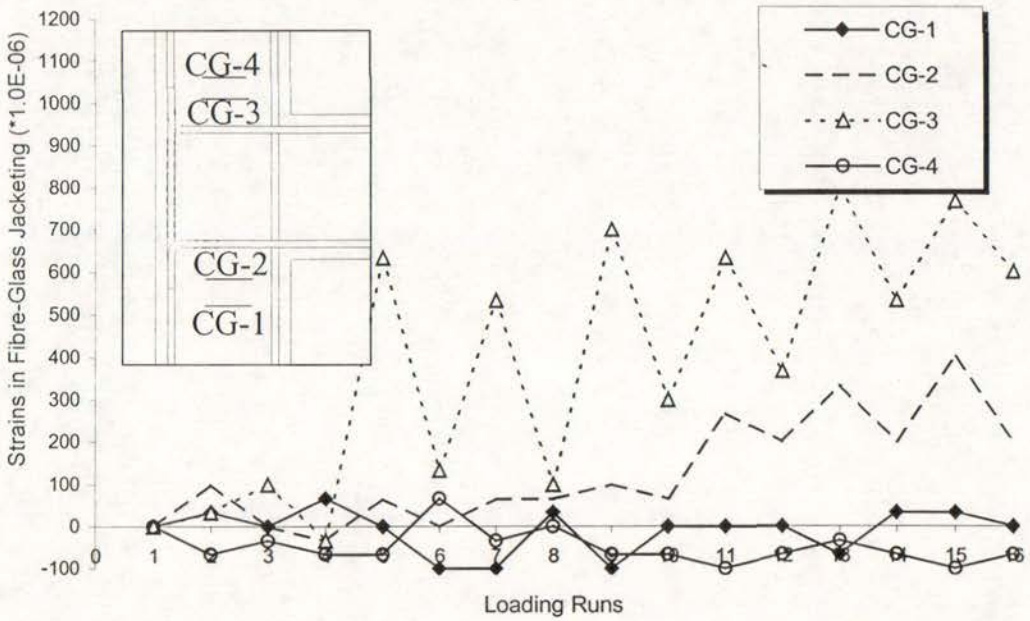

Fig.7.20 Measured Strains in Fibre-Glass Jacketing by Clip Gages for Unit REJ1

Fig.7.20 shows the measured strains in fibre-glass jacketing by clip gages, where positive strains represent tensile strains and negative strains represent compressive strains, similar to the definition of steel strains measured by electrical resistance strain gauges. Apparently, the fibre-glass jacketing was more stressed adjacent to the joint core, as seen from the measurement of clip gages 2 and 3, than that far away from the joint core as seen from the measurements of clip gauges 1 and 4. Severe bond degradation caused the beam steel tension force to be mainly transmitted within the bend, hence the concrete tension cracking associated with the resistance to the beam steel tension force started from the beginning of the beam bar bend. The fibre-glass jacketing started to be stressed only after column concrete cracking within the confined column area. As a result, the fibre-glass jacket was more stressed in tension adjacent to the beam faces.

7.3.6.3 Joint Shear Distortion and Expansion

Whereas in the case of test on Unit EJ1 the measured maximum joint shear distortion was 5.38×10^{-3}, the measured maximum joint shear distortion for Unit REJ1 was 1.63×10^{-3}, which was much smaller, although the maximum horizontal nominal joint shear stress for Unit REJ1 was about 36% higher than that with Unit EJ1. Better joint shear performance of Unit REJ1 was much better than that of Unit EJ1, this occurred as a result of the actuation of a stronger concrete strut mechanism for Unit REJ1. Therefore in the case of the beam longitudinal bars being bent away from the joint core, the external jacketing in the column areas above and below the joint core can actuate an alternative concrete strut mechanism to transmit the member forces across the joint core as postulated in Section 4.4.2.

The influence of the used steel type on the joint shear behaviour also can be identified if the maximum joint shear distortion of Unit REJ1 was contrasted to that of Unit O7. The maximum joint shear distortion measured for Unit O7 was 35×10^{-3}, which was about 22 times the measured maximum joint shear distortion measured for Unit REJ1, although the two tests achieved similar storey shear strengths, being about 75% of the theoretical storey shear strengths. Severe bond degradation and slip along the beam longitudinal reinforcement within and adjacent to the joint core, although greatly increased the structural flexibility by causing a big beam fixed-end rotation, resulted in much improved joint integrity.

7.3.7 Displacement Components

Fig.7.21 shows the estimated horizontal displacement components, where the horizontal displacement components were expressed as percentages of the storey displacement at the peaks of the selected loading cycles.

Fig.7.21 shows that, similar to the test of Unit EJ1, beam displacement component generally had been very large throughout the whole test, being about 85% of the storey displacement. As far as the beam deformation is concerned, the beam fixed-end rotation increased gradually with the loading while the beam curvature contribution decreased gradually. Evidently, the poor stiffness performance demonstrated by Unit REJ1 was due to big beam fixed-end rotation resulting from severe bond degradation along the beam bars within and adjacent to the joint core.

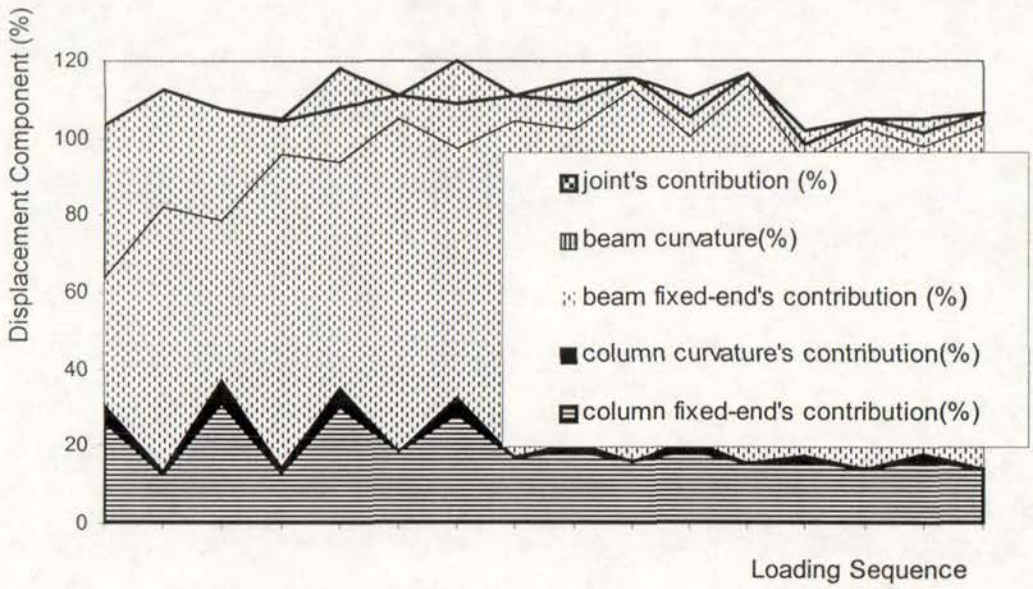

Fig.7.21 Displacement Components Measured for Unit REJ1

When compared with the test observation for Unit O7 where the contribution of joint shear distortion to the total storey displacements reached up to 66% for positive loading cycle and 68% for the negative loading cycle, the contribution of joint shear distortion estimated for Unit REJ1 was much smaller, being about 9.6% of the storey displacement although both tests achieved similar storey shear strength in terms of the percentages of the theoretical storey shear strength of the unit. Unit O7 was identical to Unit REJ1 except that Unit O7 was reinforced by deformed bars and Unit REJ1 was retrofitted by fibre-glass jacketing in the column areas above and below the joint core. The much smaller joint displacement component for Unit REJ1 was because of two reasons. One reason was that severe bond degradation along the beam main bars within the joint core of Unit REJ1 caused much less beam steel tension force transmitted into the joint core by bond, hence the joint shear deformation reduced significantly. The other reason was that retrofitting in the column areas adjacent to the joint core using fibre-glass jacketing actuated the postulated robust concrete strut mechanism, and concrete strut mechanism has much higher stiffness than truss mechanism with deformed bars. Hence the fibre-glass jacketing technique is a very effective way to improve the overall performance of as-built exterior beam-column

joint components with the beam bar hooks bent away from the joint core when plain round longitudinal reinforcement is used.

In a word, the use of plain round bars improved the joint shear performance but it increased the possibility of concrete tension cracking along the beam bar hook, hence increased the demand for retrofitting the column areas above and below the joint core using external jacketing in order to actuate the postulated alternative force path. If the alternative joint shear force path could be actuated, it would be a very stiff concrete strut. In this case, the critical part of the exterior beam-column subassemblage would be shifted from the joint shear performance to the beam fixed-end rotation.

7.3.8 Summary

The damaged as-built exterior beam-column joint unit was retrofitted by wrapping the column areas immediately above and below the joint core using fibre-glass jacketing, and it became Unit REJ1. Unit REJ1 was tested subjected to simulated seismic loading with zero axial column load, as for test on Unit EJ1. This test was to investigate the possibility of actuating the postulated alternative force path in Section 4.4.2 when the plain round beam longitudinal bars were bent away from the joint core in the exterior columns.

1. Test on Unit REJ1 demonstrated that fibre-glass jacketing in the column areas adjacent to the joint core significantly improved the general seismic performance of as-built exterior beam-column joint assemblies where the plain round beam longitudinal bars are bent away from the joint core. The fibre-glass jacketing in the column areas adjacent to the joint core controlled the concrete tension cracking along the beam bar hook, actuated the postulated concrete strut mechanism which could transmit the member forces across the joint core. As a result, the seismic performance of the test unit was governed by beam flexural behaviour, rather than by the premature concrete tension cracking along the beam bar hooks as for Unit EJ1.

2. The attained storey shear strength of the retrofitted unit REJ1 was 135% of the measured storey shear strength for as-built unit EJ1, but it was still 25% less than the theoretical storey shear strength of the unit, although the seismic performance of the unit was dominated by the beam flexure. Bond degradation along the beam

longitudinal bars caused that the theoretical beam flexural strength estimated using ordinary flexure theory could not be attained.

3. The estimated initial structural stiffness for Unit REJ1 at loading of 75% of the theoretical storey shear strength of the unit was about 40% of the theoretical prediction, which was based on an assumed effective beam and column moment inertia of 50% of the gross sectional values. The stiffness estimated at the loading of 50% of the theoretical storey shear strength was about 2.4 times that estimated for as-built unit EJ1. Apparently, the enhancement of the attained stiffness resulting from wrapping the column areas adjacent to the joint core was more pronounced than that of the attained force strength.

4. External column jacketing adjacent to the joint core activated the postulated joint shear force path, which was a robust concrete strut mechanism. Therefore although the maximum joint horizontal shear input for Unit REJ1 was larger than that for as-built unit EJ1, due to the enhanced available storey shear strength, the joint shear performance was at least as good as that observed for Unit EJ1.

5. As far as the individual reinforced concrete beams and columns with plain round longitudinal reinforcement are concerned, the seismic performance is governed by flexure, rather than by shear. In this case, the theoretical flexural strength of the member can not be attained, and the initial stiffness attained by the member, which can be estimated by taking the member fixed-end rotation only, is much lower than that estimated theoretically.

6. Comparative study of the test results of Units EJ1, REJ1 and Unit O7 revealed the following findings:

(1). The most critical part of as-built exterior beam-column joint EJ1 with the plain round beam bar hooks bent out of the joint core was the failure associated with concrete tension cracking orientated by the beam bar hook if sufficient column transverse reinforcement is not available adjacent to the joint core. Under such a circumstance, external column jacketing adjacent to the joint core as employed for test of REJ1 is a very efficient way to improve the overall seismic performance. Such a retrofit technique can control the concrete tension cracking orientated by the beam bar hook and mobilise the postulated steeper concrete strut mechanism to transmit the

member forces across the joint core. As a result, the overall performance of Unit REJ1 was no longer dominated by the concrete tension cracking in the column as was the case for test of EJ1, but it was dominated by the big beam fixed-end rotation.

(2). The most critical part of as-built exterior beam-column joint deformation components with typical reinforcing details of pre-1970s construction became the joint shear failure in the case of using deformed bars for longitudinal reinforcing bars, as was the case of test of Hakuto's O7.

7.4 TEST OF UNIT EJ2

7.4.1 Introduction

As-built full-scale exterior beam-column joint unit EJ2 was otherwise identical to Unit EJ1 except that Unit EJ2 had the beam bar hooks bent into the joint core. As for Unit EJ1, Unit EJ2 was also tested under simulated seismic loading with zero axial column load. This test aimed at investigating the influence of the beam bar hook details in exterior column on the seismic performance of existing reinforced concrete exterior beam-column joint components containing plain round longitudinal bars and other reinforcing details typical of pre-1970 existing reinforced concrete moment resisting frame structures in New Zealand. In addition, test on Unit EJ2 was identical to Hakuto's test on Unit O6 [H1] but Hakuto used deformed longitudinal reinforcement. Comparative study of test results of Units EJ2 and Hakuto's Unit O6 is conducted to identify the effect of the plain round bars used on the seismic performance of existing reinforced concrete frame structures.

7.4.2 Crack Development and Failure Mode

Fig. 7.22 shows the crack development observed for Unit EJ2.

In loading run 1, which was the peak of clockwise $0.5V_i$, flexural cracks initiated in the beam and columns as expected. Also observed in the loading run 1 was the development of the vertical crack running along the outer layer of the column longitudinal bars in the upper column adjacent to the joint core, and this occurred due to column bar buckling resulting from inadequate column transverse reinforcement adjacent to the joint core and bond degradation along the column longitudinal bars.

In the loading run 3 at the peak of clockwise $0.75V_i$ where the maximum storey shear strength was attained, the existing vertical crack extended vertically from the upper column into the joint core due to the progress of column bar buckling and the opening action of the beam bar hooks. The development of the existing vertical crack into joint diagonal tension cracks was also observed at this stage. The development of the beam and column flexural cracks was mainly limited to the beam and column interfaces due to severe bond degradation and slip along the longitudinal reinforcement within and adjacent to the joint core. The column flexural crack development was observed to be

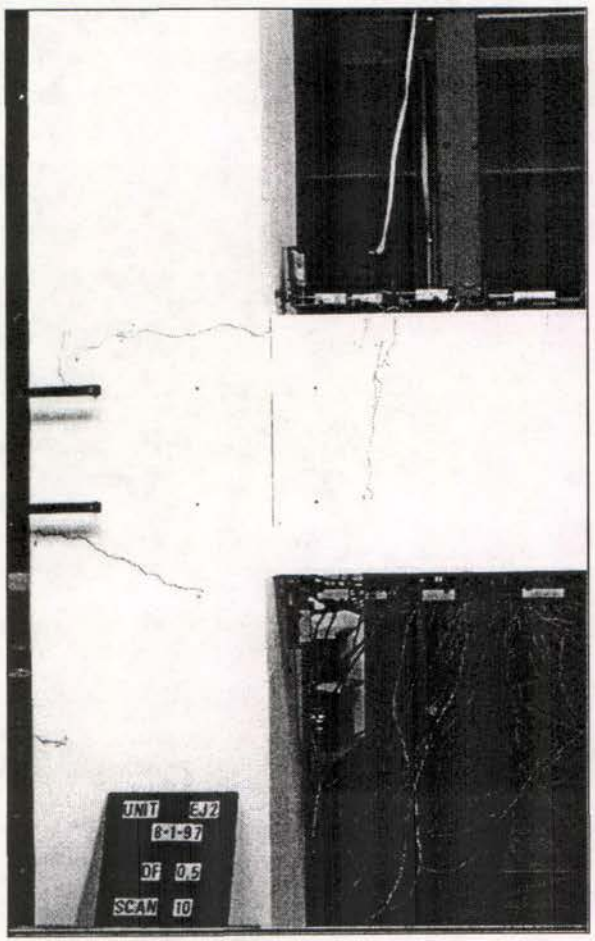

(a) Loading at 0.5Vi

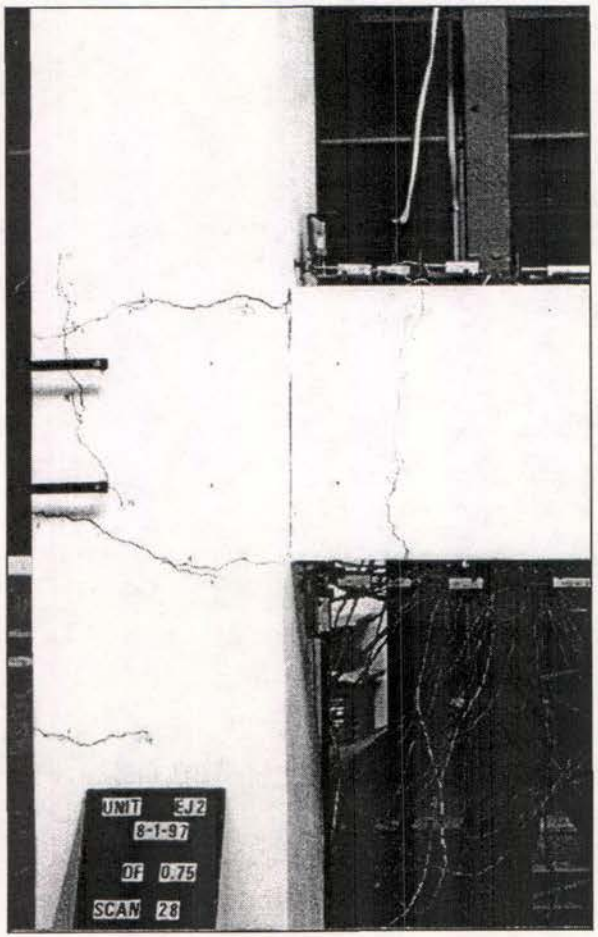

(b) Loading at 0.75Vi

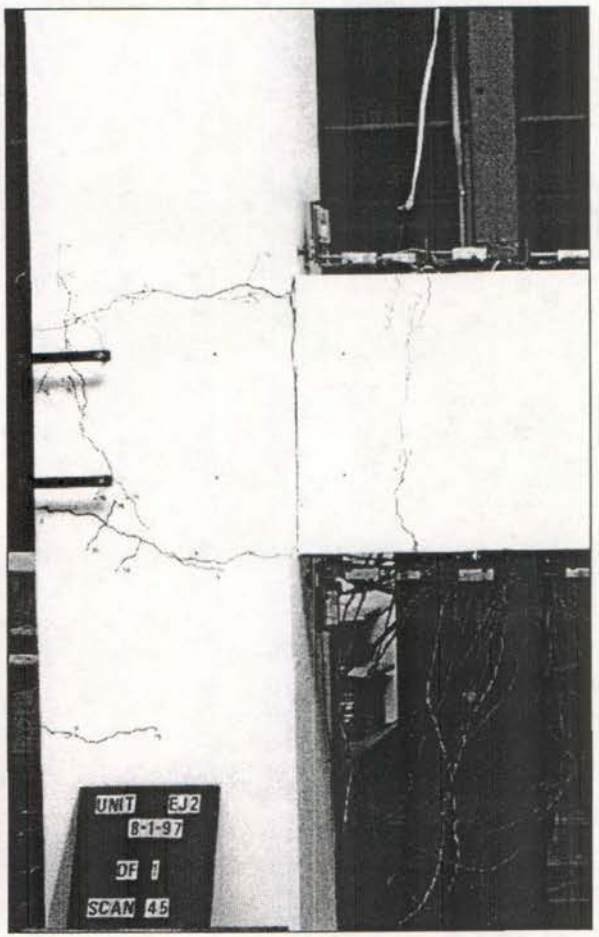

(c) End of Ductility 1

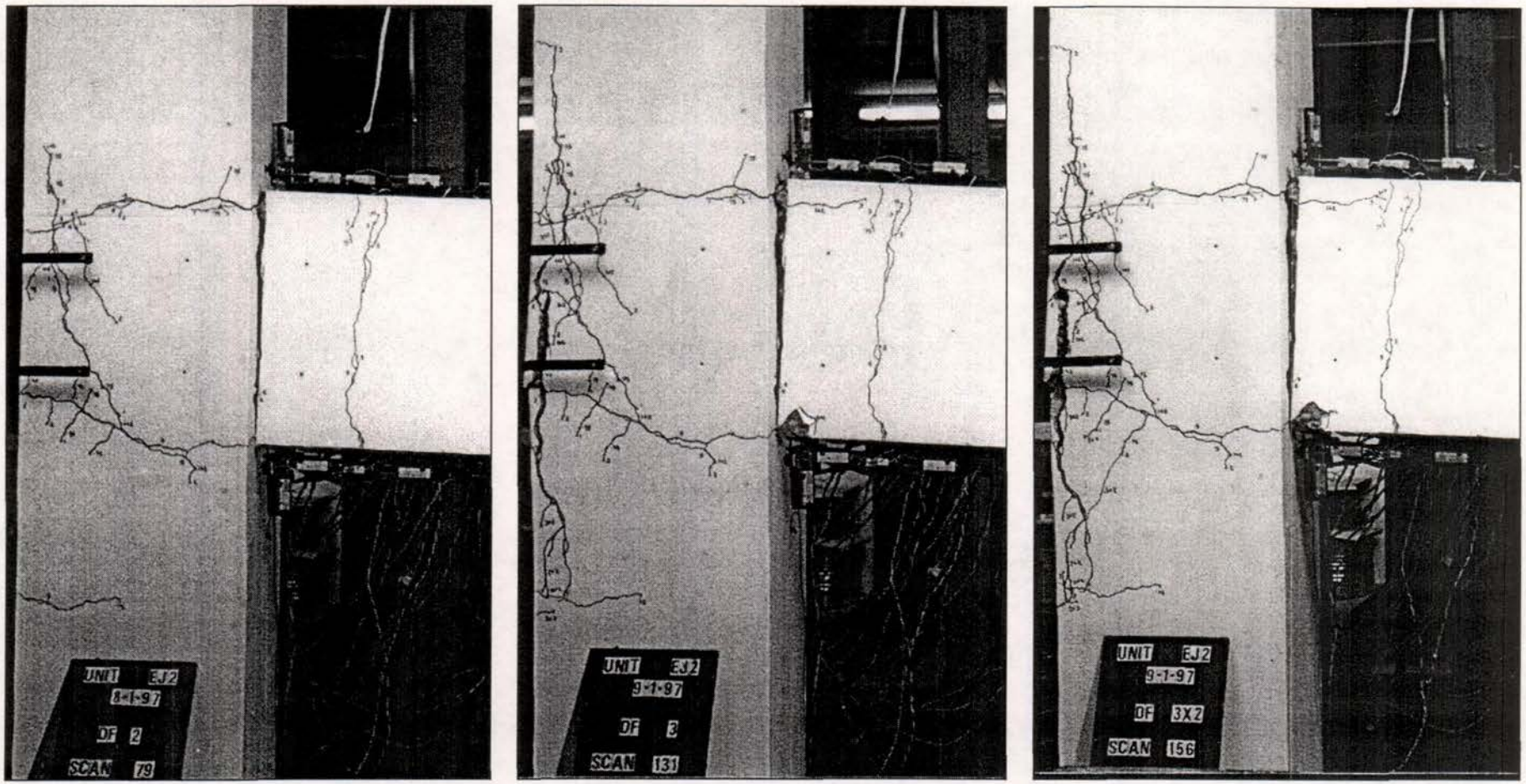

(d) End of Loadng at First Dcutility 2 (e) End of Laoding at Ductility 2 (f) Final Look

Fig.7.22 Crack Development and Final Appearance of Unit EJ2

not so apparent as that for the beam, indicating that bond degradation was more severe along the beam main bars than that along the column main bars as expected for a weak beam-strong column system.

Observed crack development during anti-clockwise loading was similar to that during clockwise loading, and the maximum storey shear strength of the unit was attained at anti-clockwise loading peak of $0.75V_i$.

During subsequent loading cycles after the loading cycle at $0.75V_i$, the attained storey shear strength degraded gradually, and the prominent crack development was in the major beam flexural crack at column face and in the damage resulting from interaction between the column bar buckling and the opening action of the beam bar hooks. Progressive bond degradation and slip along the beam bars within the joint core not only had caused the development of the major beam flexural crack at column face but also had caused the increase in the beam steel force needed to be transferred at the bend. Higher beam steel force required to be transmitted at the bend, together with outer joint concrete cover spalling resulting from progressive column bar buckling, enhanced the opening action of the beam bar hooks. Hence the degrading beam flexural performance and the damage caused by the column bar buckling and the opening action of the beam bar hooks governed the strength development of the unit and became the final failure triggers of Unit EJ2.

Throughout the whole test history of Unit EJ2, no diagonal concrete tension cracks were observed in the beam and columns, similar to the tests on Units EJ1 and REJ1. This indicates once again that the seismic performance of concrete members reinforced by plain round longitudinal bars is more likely to be dominated by flexure, rather than by shear.

Apparently, the observed test evidence for Unit EJ2 was significantly different from that for Hakuto's Unit O6, which was identical to Unit EJ2 except that Hakuto's Unit O6 used deformed reinforcing bars. Whereas in the case of Hakuto's test on Unit O6 the final failure was due to the shear failure in the beam and in the joint, the joint core of Unit EJ2 only suffered minor concrete cracking, and the performance of its beam was totally governed by flexure.

Of particular interest is that the observed joint crack orientation for Unit EJ2 was very different from that for retrofitted Unit REJ1. The observed joint shear cracks of Units EJ1 and REJ1 were about 45° to the horizontal axis and initiated from the midway of the beam bar hook, whereas the joint diagonal tension cracks observed of Unit EJ2 were approximately corner to corner joint diagonal cracks. This led to the conclusion that the actuated joint concrete strut mechanisms are of different orientations for different beam bar hook configurations in the exterior columns.

7.4.3 Load-versus-Displacement Response Measured for Unit EJ2

Fig.7.23 shows the measured storey shear versus storey displacement and drift hysteresis loops for Unit EJ2. Also shown in Fig.7.23 is the theoretical storey shear strength of the unit, V_i , at the attainment of the beam flexural strength for both clockwise and anti-clockwise loading directions. Fig. 7.23 demonstrates that the detail of the beam bar hooks bent into the joint core in the exterior columns greatly improved the seismic behaviour of exterior beam-column joint subassemblages, when compared with the similar test unit EJ1 with the beam bar hooks bent away from the joint core in the exterior columns.

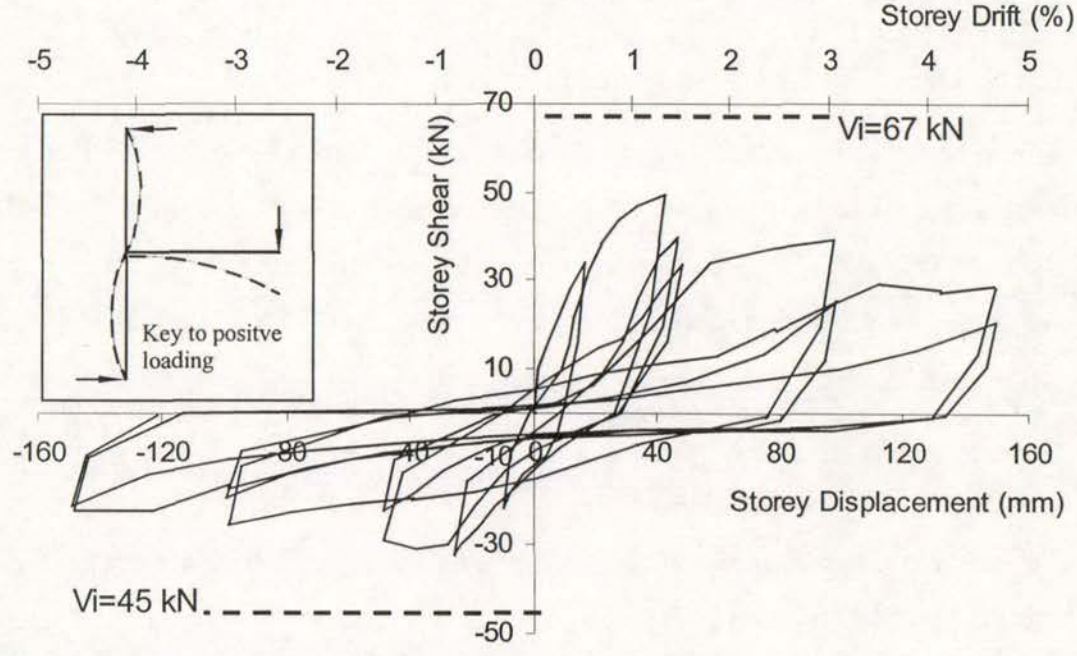

Fig. 7.23 Storey Shear versus Storey Displacement and Storey Drift Hysteresis Loops Measured of Unit EJ2

The maximum storey shear strength attained by Unit EJ2, which occurred at a storey drift of approximately 1.3% in the loading cycle of $0.75V_i$, was only 75% of the theoretical storey shear strength for both loading directions. The achieved storey shear strength by Unit EJ2 was higher than that by Unit EJ1, indicating that the bending configuration of the beam bars in the exterior columns will have significant effect on the available force strength. The achieved storey shear strength by Unit EJ2, if expressed as the percentages of the theoretical storey shear strength, was comparable to that of Unit REJ1, which was retrofitted by wrapping the column areas immediately adjacent to the joint core. Hence, for as-built exterior beam-column joint units, the inadequate anchorage configuration of the beam bar hooks bent away from the joint cores in the exterior columns will lead to a lower force strength attainment of the unit if the column transverse reinforcement adjacent to the joint core is insufficient. But the inadequate anchorage configuration of the beam bar hooks bent out of the joint cores in exterior column will not impair the available structural strength property of exterior beam-column joint components if sufficient column transverse reinforcement is available adjacent to the joint core. The force strength property observed for Unit EJ2 was also contrasted to that for Hakuto's Unit O6, which was otherwise identical to Unit EJ2 but reinforced by deformed longitudinal reinforcement. Hakuto's Unit O6 attained the unit's theoretical storey shear strength. The lower load strength attainment of Unit EJ2 in comparison with Hakuto's Unit O6 was not only because of severe bond degradation along the beam longitudinal reinforcement but also because of premature concrete tension cracking along the beam bar hooks. Severe bond degradation along the beam longitudinal reinforcement resulting from the use of plain round longitudinal bars caused the attained beam flexural strength to be lower than its theoretical prediction, as explained before. Premature concrete tension cracking along the beam bar hooks was associated with the interaction of the column bar buckling and the opening action of the beam bar hooks and it was facilitated by the use of plain round beam longitudinal bars. Consequently, the attained storey shear strength by Unit EJ2 was lower than that by Hakuto's Unit O6.

The first yield displacement was determined using the method described in Section 5.3.2 for the test of Unit EJ2, and it was equivalent to a storey drift of 1.5%. It is surprised to notice that the first yield displacement determined for Unit EJ2 was 3.6

times the displacement at first yield measured from Hakuto's test on Unit O6 [H1]. In Chapter 6, it was found that the use of the plain round longitudinal reinforcement caused an increase in the measured displacement at first yield by 50% for as-built interior beam-column joint units. Hence the adverse influence of the used steel type on the structural stiffness property is more significant for as-built exterior beam-column joint units, compared to as-built interior beam-column joint units. Also of interest is that the measured initial stiffness for Unit EJ2 was only 57% of the average initial stiffness of 2.1 kN/mm measured for Unit REJ1 at loading cycle of 0.75 V_i. This demonstrated that, if the alternative force path across the joint core can be achieved, namely sufficient column transverse reinforcement is available adjacent to the joint core, the bending out configuration of the plain round beam bars in the exterior columns can result in at least similar, if not better, strength and stiffness performance to that with the beam bar hooks bent into the joint core.

Significant pinching of the loops is evident in Fig. 7.23, similar to the test evidence of Unit EJ1, indicating very poor energy dissipating capacity of Unit EJ2. Pinching of the hysteresis loops is a typical feature of beam-column joint components reinforced by plain round longitudinal reinforcement because of the formation of a major beam flexural crack at the column face as a consequence of severe bond degradation along the plain round beam longitudinal reinforcement.

Fig. 7.23 also shows significant strength degradation after the maximum force strength was attained for Unit EJ2. Strength degradation was also observed for the second loading cycle at the same deformation level, compared to the first loading cycle. This was mainly due to the progressive failure of bond mechanism along the beam longitudinal bars within and adjacent to the joint core and the progressive failure associated with interaction of column bar buckling and the opening action of the beam bar hooks.

In summary, the test on Unit EJ2 attained a maximum storey shear that was approximately 25 % less than the theoretical storey shear strengths at a storey drift of approximately 1.3 %. The measured hysteresis loops demonstrated significant pinching with cyclic loading. Configuration of the plain round beam bar hooks bent into the joint cores in exterior columns increased the available force strengths. The utilisation of plain round longitudinal reinforcement greatly improved joint shear

performance, but caused the attained member flexural strengths and the structural stiffness to reduce great deal, and the reduction in the available structural stiffness was especially significant, compared to that in the available force strength. However, the inadequate anchorage detail of the plain round beam bar hooks bent away from the joint cores will not impair the available force strength and stiffness properties if sufficient column transverse reinforcement is provided adjacent to the joint core.

7.4.4 Measured Strains of Longitudinal Reinforcement

Fig.7.24 and Fig.7.25 show the measured strain profiles by electrical resistance strain gauges for beam bar 1 and beam bar 2 respectively. Evidently, significant bond degradation and bar slip must have taken place within the joint core and adjacent to the joint core in the beam along the beam flexural tension bars (see Fig.7.24 (a) and Fig.7.25 (b)). Measured steel stresses in the flexural beam tension bars were nearly the same from point B, which was 65 mm away from joint centre-line, to point E, which is 300 mm from the column inner face in the beam. Fig.7.26 compares the measured steel strains with the theoretical strains for beam bars 1 and 2 at inner column face when the beam bars were in flexural tension in the early loading cycles until the completion of loading at ductility 1. For beam bar 1, the measured strains matched with the theoretical strain better than that for beam bar 2, and beam bar 2 tended to be more subjected to bond slip. However, the measured strains presented very big differences from the theoretical values, based on plane section theory. The more severe the bond degradation along the member longitudinal bars is, the bigger the measured steel tensile strains are relative to the theoretical predictions.

Measured steel strains along the column longitudinal bars were small, and they disagreed with the theoretical prediction significantly, giving a signal that caution needs to be taken in using these measured steel strains.

7.4.5 Member Curvatures

Measured member curvatures were not expected to agree with the theoretical predictions as demonstrated by Units 1 and 2 as well as Units REJ1.

Fig.7.27 and Fig. 7.28 show the progress of the fixed-end rotation of beam and columns, and the steel stress level in the member flexural tension bars (or the imposed member force level) for Unit EJ2. The member fixed- end rotation is expressed as the

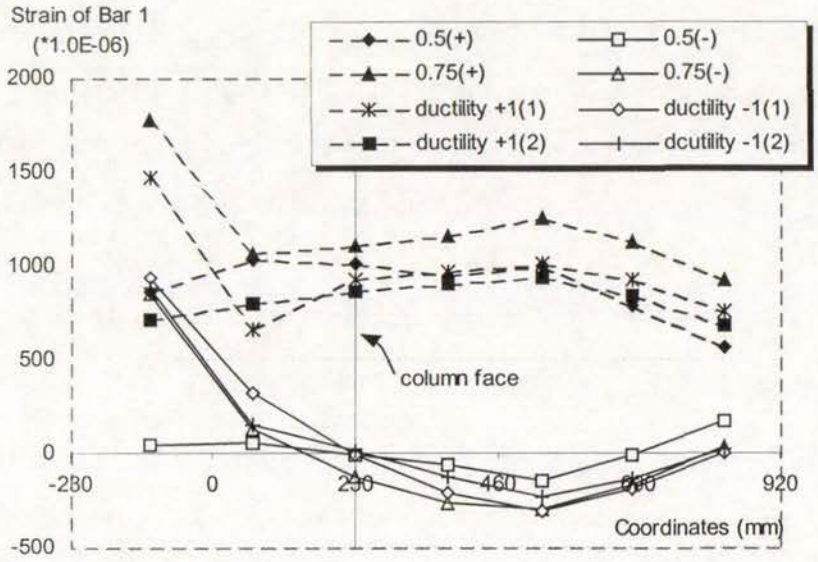

Fig.7.24 Strain Profiles of Beam Bar 1 Measured by Electrical Strain Gauges

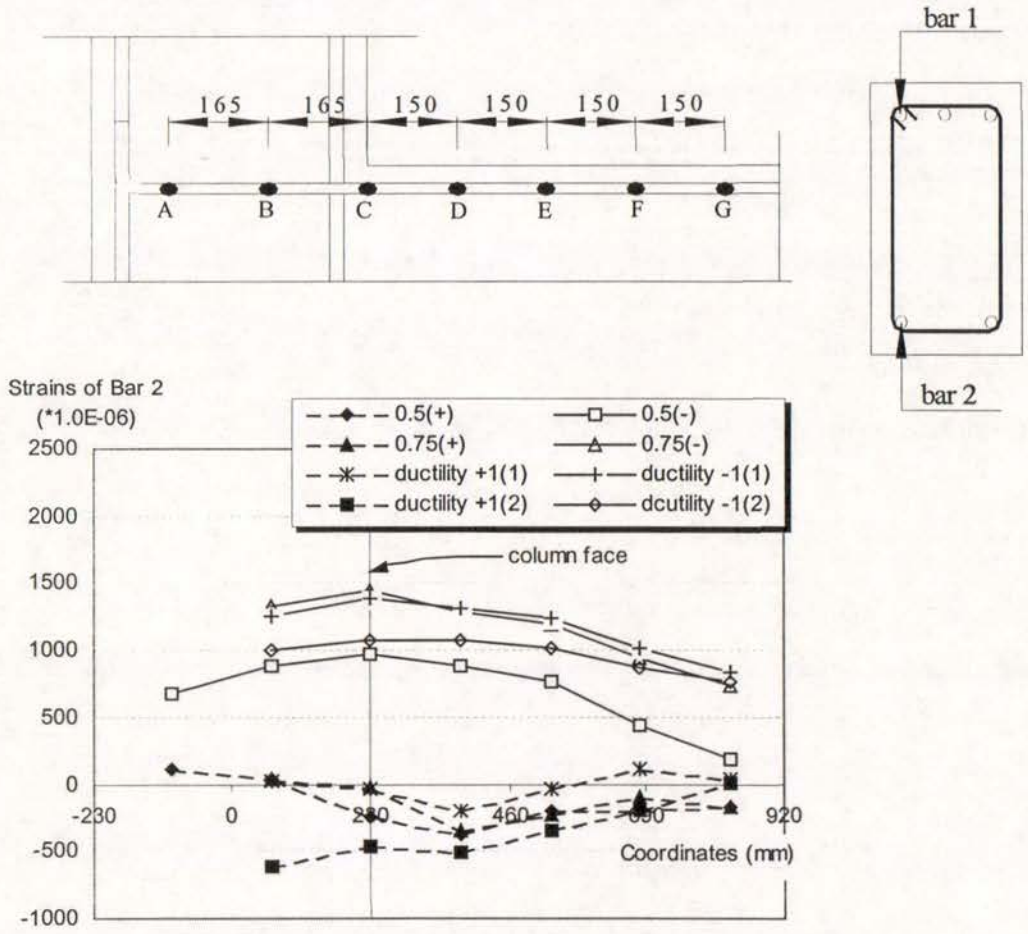

Fig.7.25 Strain Profiles of Beam Bar 2 Measured by Electrical Strain Gauges

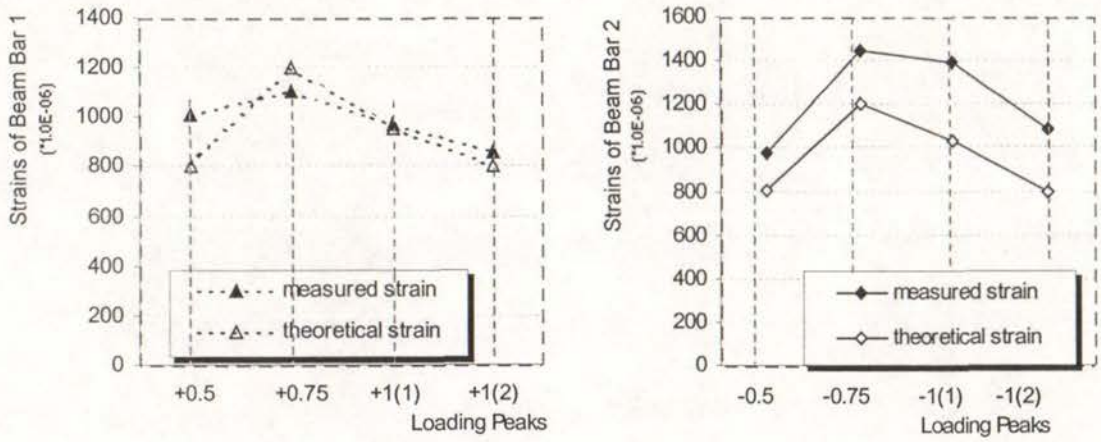

(a) Bar 1 (b) Bar 2

Fig.7.26 Comparison of measured and theoretical steel strains at column face

ratio of the measured member fixed-end rotations to the theoretically predicted member total rotations, referred to as rotation amplification θ_m / θ_t. The imposed beam shear force is expressed as the percentage of the imposed beam shear $V_{b,m}$ to the theoretical beam shear force strength, $V_{b,i}$, which was obtained based on the beam theoretical flexural strength. Similarly, the imposed column shear force level is expressed as $V_{cm} / V_{ct}(\%)$, where V_{cm} and V_{ct} are the measured column shear and the column shear force strength at developing the column theoretical flexural strength, respectively.

It is evident from Figs.7.27, 7.28 and 7.29 that amplification of the member fixed-end rotation increases nearly proportionally with the loading cycles, and the higher the imposed force level on the member is, the more rapid the increase in the amplification of the member fixed-end rotation is. The determination of the stiffness degradation in modelling the member hysteretic response needs to consider this fact.

7.4.6 Joint Behaviour

7.4.6.1 Joint Shear Stress

The measured maximum nominal horizontal joint shear stress for Unit EJ2, obtained based on the measured member forces and plane section theory, occurred when the joint core of Unit EJ2 developed the diagonal tension cracking at the loading peaks of

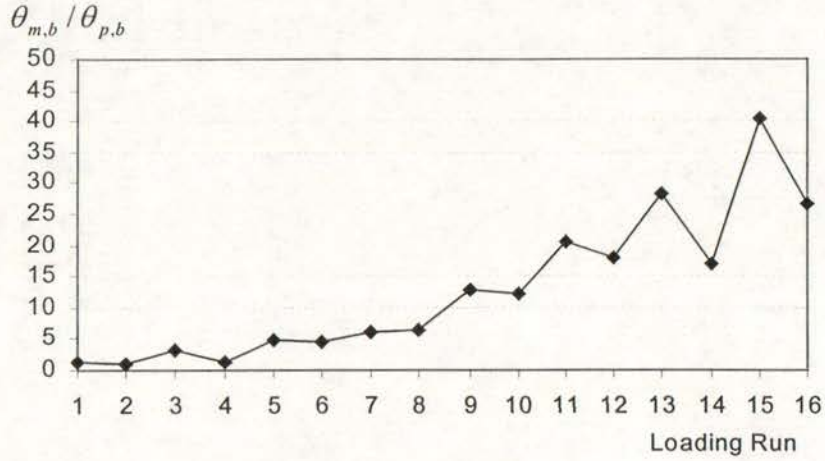

(a) Variation of rotation over beam fixed-end region

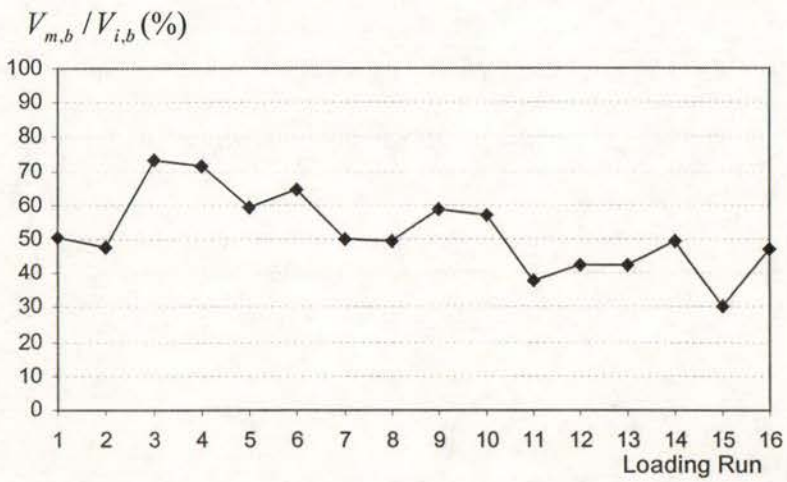

(b) Variation of imposed beam shear, expressed as the percentage of the beam shear strength at developing the beam flexural strength

Fig. 7.27 Rotation over beam fixed-end region and storey shears versus loading runs

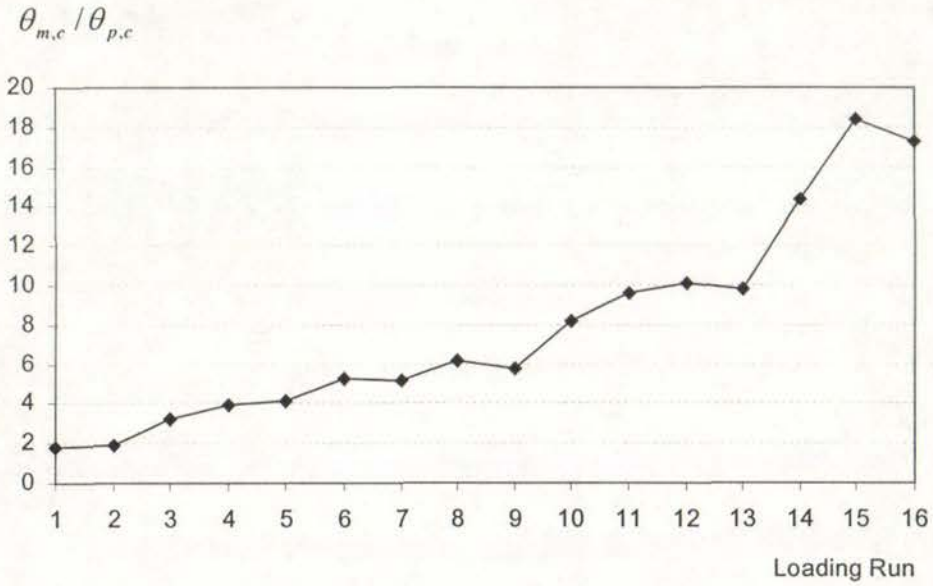

(a) Variation of rotation over column fixed-end regions

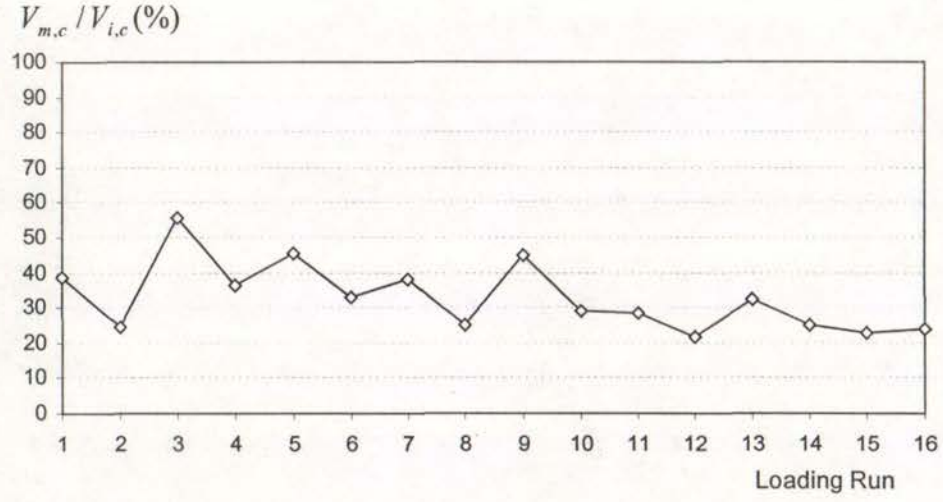

(b) Variation of imposed storey shear, expressed as the percentage of the column shear strength at developing the column flexural strength

Fig. 7.28 Rotation over column fixed-end region and storey shears versus loading runs

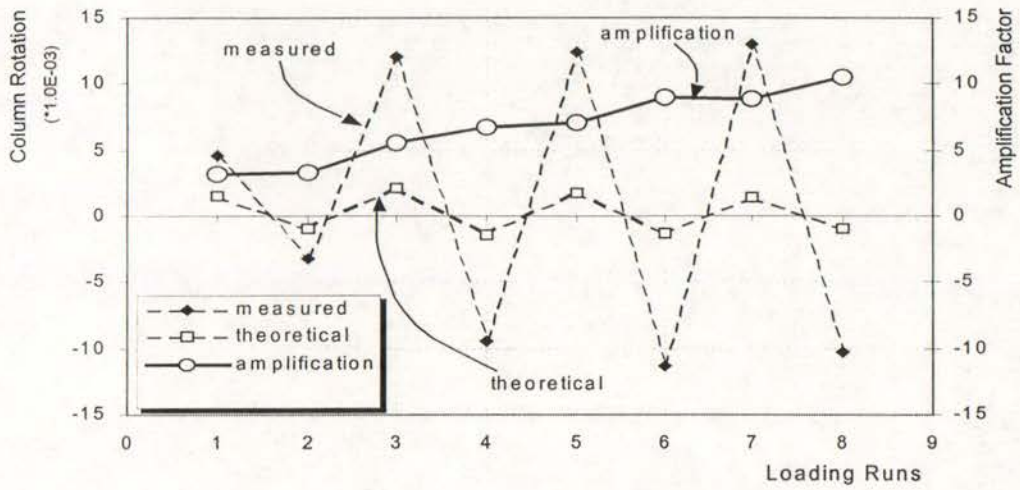

Fig. 7.29 Measured and theoretical column fixed-end rotation and the amplification

$0.75V_i$, and it was 1.37MPa or $0.23\sqrt{f_c'}$ MPa for the clockwise loading, and 0.9 MPa, or $0.15\sqrt{f_c'}$ MPa for anti-clockwise loading. Evidently, the attained maximum nominal horizontal joint shear stress was well below the theoretical joint shear capacity at diagonal tension cracking of $0.3\sqrt{f_c'}$ MPa in terms of nominal joint shear stress. This complied with the test evidence that the joint core of Unit EJ2 was not extensively cracked. Neither test of Unit EJ1 nor test of Unit EJ2 was dominated by the joint shear failure.

The nominal horizontal joint shear stress of Unit EJ2 at developing the joint diagonal tension cracking is compared to that of Hakuto's Unit O6, which was identical to Unit EJ2 except the use of deformed reinforcing bars. For Hakuto's Unit O6, the nominal horizontal joint shear stress at which the joint diagonal crack initiated was about $0.31\sqrt{f_c'}$ MPa, and this was higher than the estimated nominal horizontal joint shear stress at which the joint diagonal crack initiated for Unit EJ2. Apparently, the use of plain round bars for longitudinal reinforcement of existing exterior beam-column joints enhanced the local concrete tensile stress due to the concentration of steel force transfer on the bar bend, and increased the discrepancy between the actual local concrete tensile stresses and the estimated nominal horizontal joint shear stress, compared to the case with deformed longitudinal bars. Hence, when plain round longitudinal reinforcement is used, the estimated nominal horizontal joint shear stress

will be lower. However, when plain round bars are used for longitudinal reinforcement, the attained member flexural strength is lower than the theoretical value, then the maximum nominal horizontal joint shear stress will be low. Usually, the joint shear behaviour of existing exterior beam-column joints would not hamper the performance of the structure in this case.

7.4.6.2 Joint Shear Distortion

Fig. 7.30 illustrates the variations of the joint shear distortion, joint displacement component and storey shear with the loading estimated for Unit EJ2. The maximum joint shear distortion was only approximately 0.63 %. Gradual increases in the joint shear distortion and joint displacement components were observed with the loading progress after the joint diagonal crack occurred at the loading of clockwise $0.75V_i$, but the joint shear distortion generally was very small.

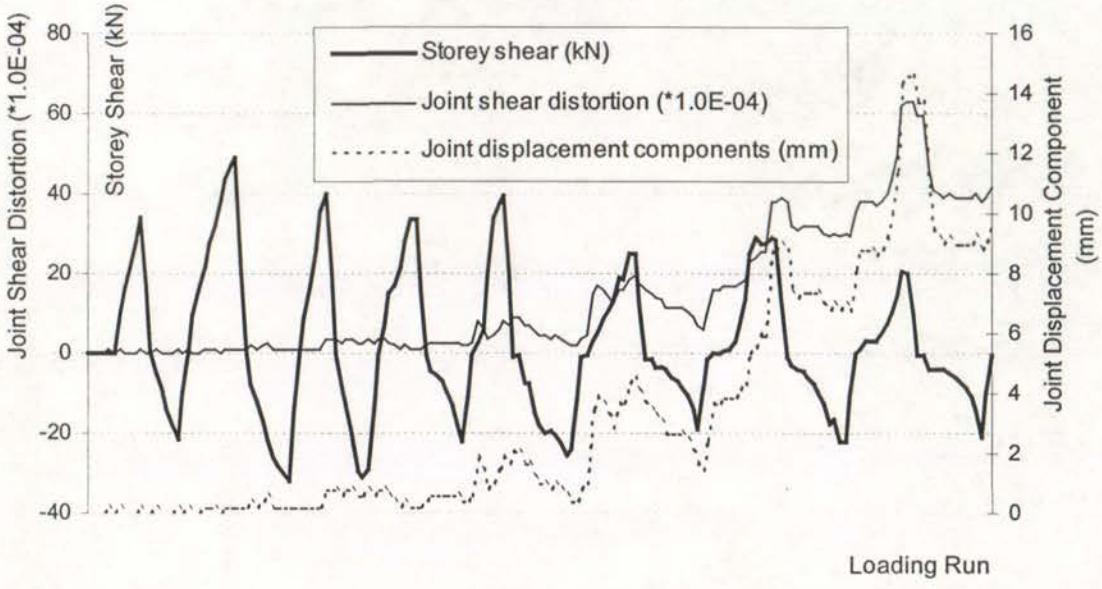

Fig.7.30 Joint shear distortion, joint displacement component and storey shear of EJ2

The maximum joint shear distortion reached by test of Unit EJ2 was comparable to the maximum joint shear distortion of 0.52% measured for Unit EJ1. Evidently the joint cores of Units EJ2 and EJ1 were of sound integrity throughout the whole testing histories due to severe bond degradation along the beam bars within the joint core resulting from the use of plain round longitudinal reinforcing bars. Whereas in the case of Hakuto's test on Unit O6 the maximum joint shear distortion was 1.5%, the

maximum joint shear distortion observed for Unit EJ2 was only about 50% of that amount with Unit O6, indicating that the use of plain round longitudinal reinforcement led to much less cracked joint cores.

7.4.6.3 Joint Hoop Strains

The measured strains in three joint hoops, CT3, CT2 and CT-4, were measured by electrical strain gauges for Unit EJ2. CT-3 was located at the centre of the joint core and CT2 and CT4 were located at the beam faces. Two sets of column transverse reinforcement adjacent to the joint core of Unit EJ2 were also measured by electrical resistance strain gauges. Fig.7.31 shows the measured strains in joint hoops and two sets of column transverse reinforcement.

Evidently, the joint hoop at the centre of the joint core of CT-3 was subjected to higher tensile strain than the other joint hoops located close to the beam faces of CT-2

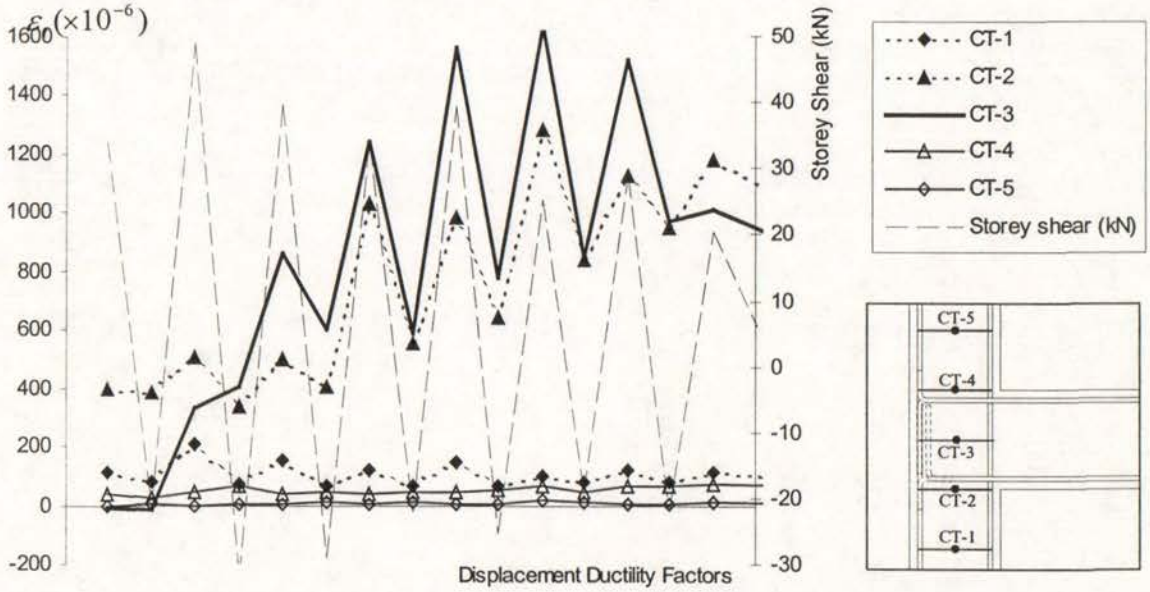

Fig.7.31 Joint Hoop Strains and Storey Shears Measured for Unit EJ2

and CT-4. This evidence is similar to the evidence observed for exterior beam-column joint components with the beam bars bent into the joint core [P13, H1]. When the member forces are transferred across the joint core by the way of joint diagonal concrete strut, the diagonal strut acts as a column axially loaded in compression with loading heads at both ends. In this case, the lateral expansion of the column will

reached the biggest value at the mid-height of the column. However this evidence disagreed with the observed evidence for Unit EJ1 where the joint hoops at the beam faces were more stressed in tension compared to the joint hoop at the centre of the joint core. Only difference between the test of Unit EJ1 and test of Unit EJ2 was the bending configuration of the beam bar hook. Hence the following conclusions can be reached:

When the beam bars of exterior beam-column joint components are bent into the joint core, the joint hoops at the centre of the joint core contributed more to the joint shear resistance, compared to the joint hoops located away from the joint core centre. However, when the beam bars of exterior beam-column joint components are not bent into the joint core, the force path to transmit the member forces across the joint core is totally different from the ordinary postulated force path, and an alternative force path is required to be actuated. In this case, the overall performance of the exterior beam-column joint units is more dependent on the joint hoops adjacent to the beam face as well as column stirrups adjacent to the joint core, rather than the joint hoop at the centre of the joint core.

Therefore in assessing the joint shear performance of exterior beam-column joint components with the beam bar hooks bent away from the joint core, the information on the amount of joint horizontal shear reinforcement is absolutely irrelevant.

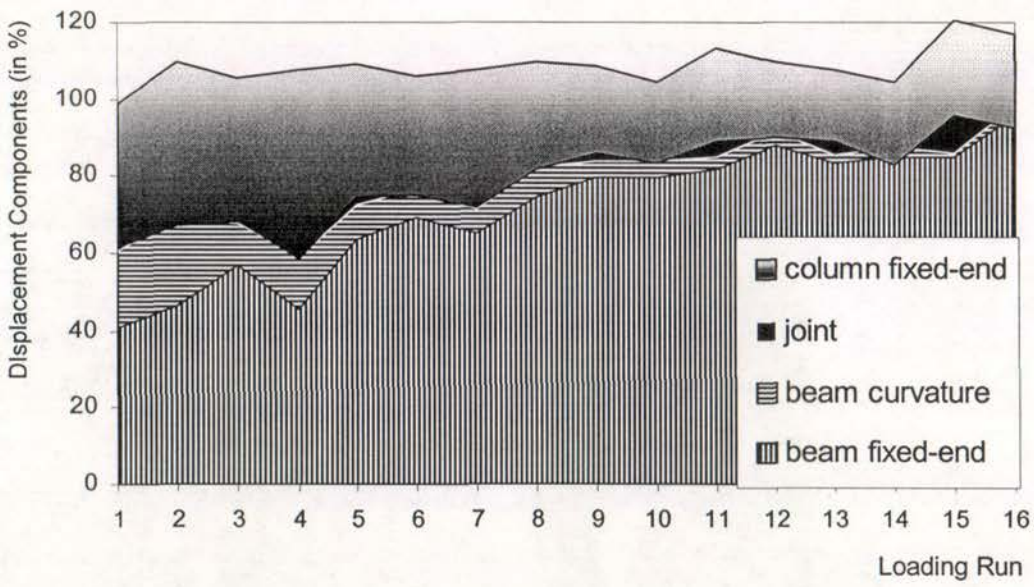

Fig. 7.32 Displacement Components Estimated for Unit EJ2

7.4.7 Displacement Components

Fig.7.32 shows the displacement components estimated for Unit EJ2. Contribution to the total storey displacement by beam fixed-end rotation increased rapidly with the loading progress, and reached up to 80% of the total storey displacement. Contribution of the column fixed-end rotation to the total storey displacement, although was high at the beginning of the loading, decreased gradually with the loading progress, indicating the damage concentration on the beam due to the formation of a weak beam-strength column failure mechanism during the testing as predicted theoretically.

In general, the contributions of the beam curvatures and the joint shear distortions to the storey displacement were very small throughout the whole testing history.

7.4.8 Summary

A full-scale one-way exterior beam-column joint unit EJ2, which was reinforced by plain round bars and had the beam bar hooks bent into the joint core, was tested under simulated seismic loading with zero axial column load in order to investigate the influence of the beam bar hook details on the overall performance of existing reinforced concrete frame structures. Unit EJ2 had small amount of transverse reinforcement in the beam and columns and contained only limited joint shear reinforcement. Unit EJ2 was identical to as-built exterior beam-column joint Unit EJ1 except the arrangement of the beam bar hooks, and it was also identical to Hakuto's test Unit O6 except that Hakuto's Unit O6 used deformed longitudinal reinforcement.

1. The test showed that the overall performance of similar exterior beam-column joint components EJ2 was unsatisfactory in terms of the attainment and maintenance of the structural strength and stiffness properties. Seismic behaviour observed for Unit EJ2 was dominated by the beam flexural behaviour and the premature concrete tension cracking along the beam bar hooks. Premature concrete tension cracking along the beam bar hooks was associated with the interaction of column bar buckling adjacent to the joint core and the opening action of the beam bar hooks, due to inadequate joint horizontal shear reinforcement and severe bond degradation along the longitudinal reinforcement. Severe bond degradation along the longitudinal reinforcement not only caused the degrading beam flexural behaviour, but also facilitated the column bar buckling and the opening action of the beam bar hooks,

hence leading to the concrete tension cracking failure along the outer layer of the column bars adjacent to and within the joint core.

2. The storey shear strength was attained at storey drift of 1.5% by Unit EJ2, and it was about 25% less than the theoretical storey shear strength. This was partially because of severe bond degradation along the longitudinal bars of the beam for this weak beam-strong column system. Also observed was significant strength degradation for Unit EJ2, and this was due to the development of bond degradation along the longitudinal beam bars as the loading progressed.

3. The initial stiffness attained of Unit EJ2 was 1.2 kN/mm, and this was equal to a storey drift of 1.5% at first yield. The adverse effect of the used steel type on the structural stiffness property is more significant for as-built exterior beam-column joint components than that for interior beam-column joint components.

4. The seismic performance of individual beam and columns was dominated by flexure only, as revealed by test on Unit REJ1. The joint core was observed to be of good integrity.

5. The test on Unit EJ2 demonstrated that the joint horizontal shear reinforcement is more needed for preventing the failure associated with the column bar buckling and the opening action of the beam bar hook than that for providing joint shear capacity.

6. Comparative study of the test results of Units EJ1 and EJ2 revealed that (1). The beam bar hook configuration in exterior column has an important influence on the available force strength property of exterior beam-column joint components when the columns contained small amount of transverse reinforcement adjacent to the joint core. The configuration of the beam bar hooks bent into the joint core as for Unit EJ2 led to about 25% increase in the available storey shear strength of the unit, compared to that of Unit EJ1 which had the beam bar hooks bent away from the joint core. (2). The overall seismic performance of existing exterior beam-column joint components is dependent on the amount of joint horizontal shear reinforcement at the centre of the joint core if the beam bar hooks are bent into the joint cores, but it is dependent on the column transverse reinforcement immediately above and below the joint cores if the beam bar hooks are NOT bent into the joint cores.

7. Comparative study of the test results of Units EJ1 and REJ1 showed that the strength and stiffness properties of as-built exterior beam-column joint units with the beam bar hooks bent away from the joint cores can be as good as that with the beam bar hooks bent into the joint core, should extensive column transverse reinforcement be available adjacent to the joint core. Evidently, external wrapping of the column parts adjacent to the joint core of as-built exterior beam-column joint components could upgrade the as-built reinforced concrete frame structures to similar performance to that with the beam bar hooks bent into the joint cores.

8. Comparative study of the test results of Unit EJ2 and Hakuto's Unit O6 identifies that the use of plain round longitudinal reinforcement for Unit EJ2, although leading to much better integrity of the joint core due to the occurrence of severe bond degradation along the beam longitudinal bars within the joint core for Unit EJ2, caused significant reduction in the available force strength and structural stiffness of the unit, especially in the available structural stiffness. Compared with the case with deformed longitudinal reinforcement, exterior beam-column joints reinforced by plain round longitudinal reinforcement need more column transverse reinforcement adjacent to and within the joint core for preventing column bar buckling and controlling the opening action of the beam bars in tension.

7.5 TEST OF UNIT EJ3

7.5.1 General

As-built full-scale exterior beam-column joint unit EJ3 was identical to as-built exterior beam-column joint Unit EJ1, and it was tested under simulated seismic loading with the presence of a constant compressive axial column load of $0.25 A_g f_c^{'}$ in order to investigate the influence of compressive axial column load on the seismic performance of as-built exterior beam-column joint assemblies designed to out-dated seismic codes when the beam bar hooks are bent away from the joint core.

7.5.2 Crack Development and Damage

The crack development and the final appearance of Unit EJ3 are shown in Fig.7.33. Flexural cracks were only observed to develop in the beam, not in the columns, throughout the whole testing histories, indicating the formation of the predicted weak beam-strong column failure mechanism. The beam flexural cracking was characterised by being sparsely spaced and having one major beam flexural crack adjacent to the joint core. This was due to severe bond degradation and bar slip along the beam longitudinal bars within and adjacent to the joint core. At the later stages of clockwise loading at displacement ductility of 2, a vertical crack along the outer layer of the column main bars was observed in the lower left corner of the joint core, but it was not so pronounced. The development of the vertical crack along the outer layer of the column bars occurred due to column bar buckling and the outward pushing action of the bottom beam bars, which were in compression. The final failure trigger of the test on Unit EJ3 was the degrading beam flexural performance.

Evidently the test evidence of Unit EJ3 was very different from that of Unit EJ1. Test specimens EJ1 and EJ3 were identical, but one unit was tested with zero axial column load while the other unit was tested with the existence of constant column compressive axial load of $0.25 A_g f_c^{'}$. For test on Unit EJ1, the interaction of column bar buckling and the opening action of the beam bar hooks, which occurred due to inadequate column transverse reinforcement adjacent to the joint core and severe bond degradation along the longitudinal reinforcement, initiated the final failure of the unit.

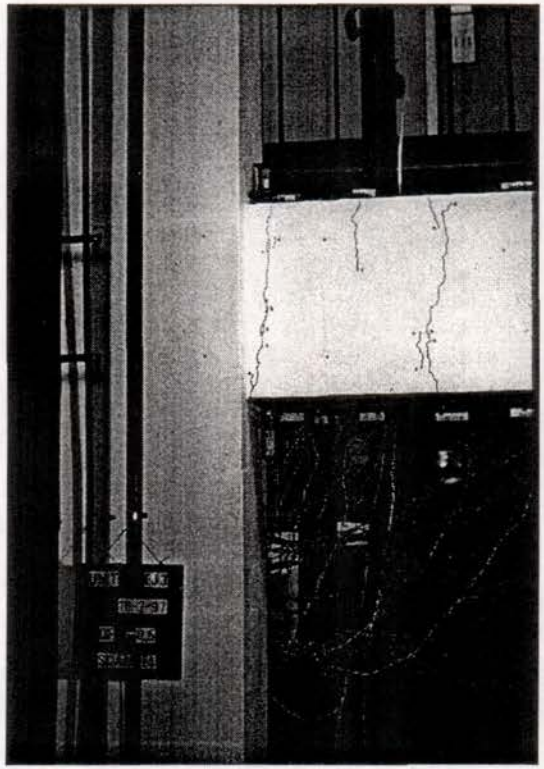

(a) Loading at 0.5Vi

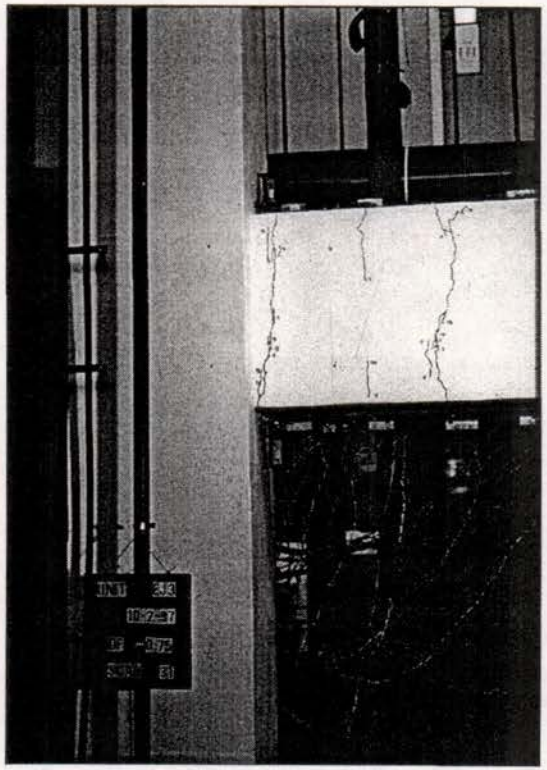

(b) Loading at 0.75Vi

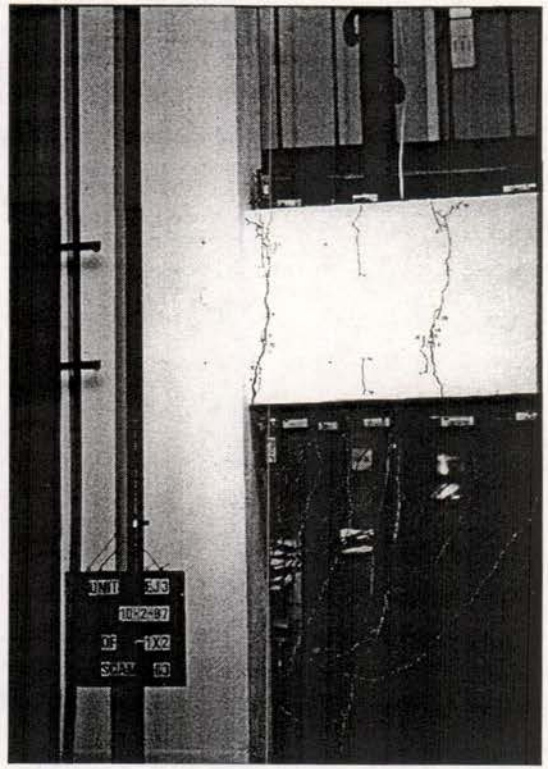

(c) End of Ductility 1

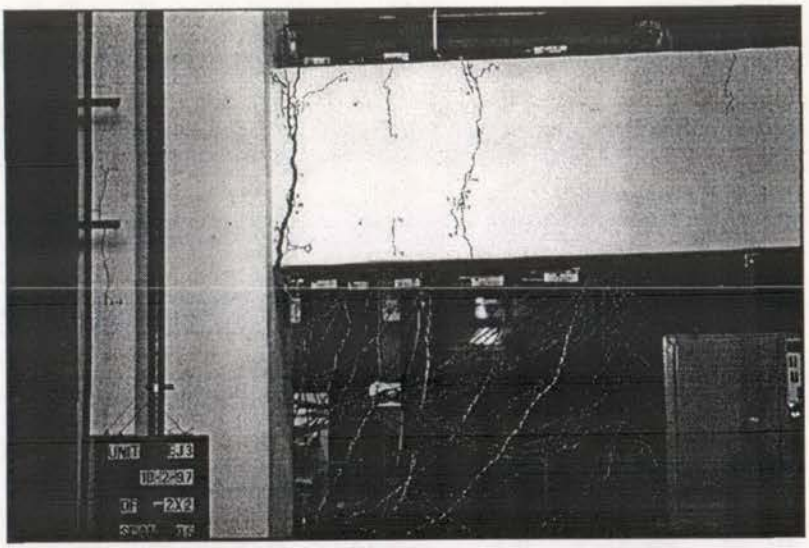

(d) End of Loading at ductility 2

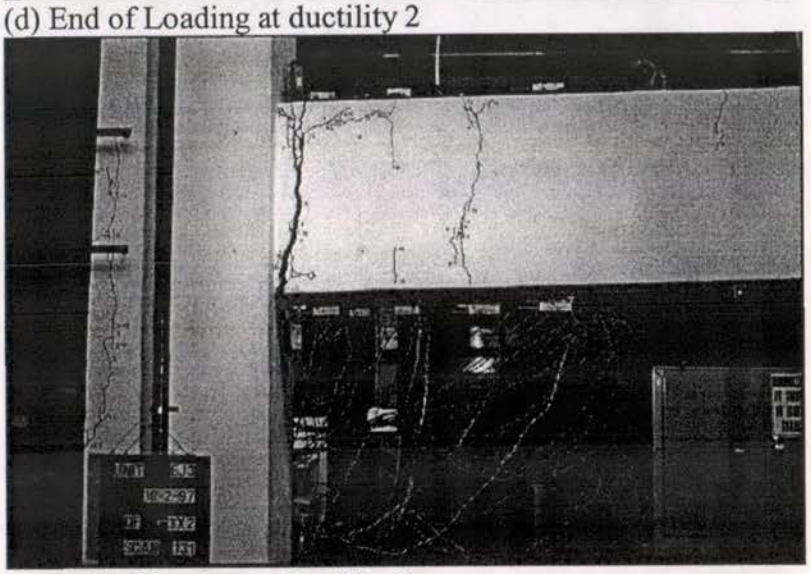

(e) End of loading at ductility 3

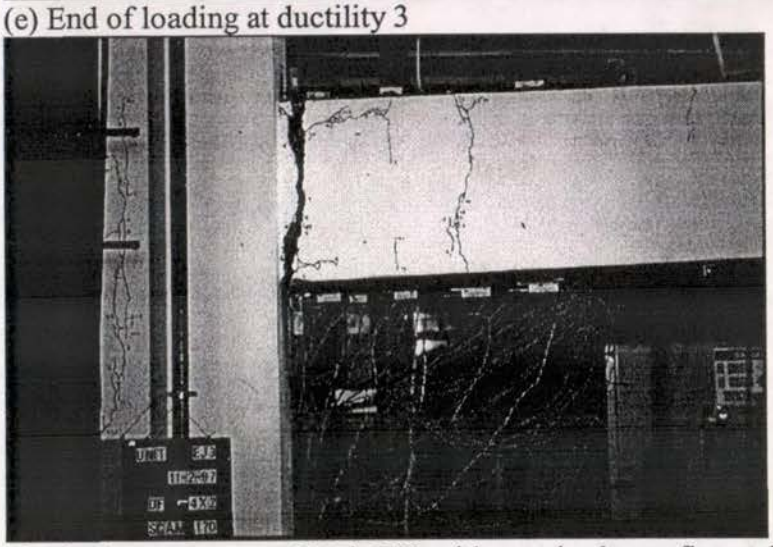

(f) Final appearance of Unit EJ3 with a major beam flexural crack at column face

Fig. 7.33 Crack development and final appearance of Unit EJ3

Existence of constant compressive axial column load of 0.25 $A_g f_c^{'}$ for test on Unit EJ3 enhanced the force transfer from the beam tension steel to the joint core concrete by bond within the joint region, resulted in a smaller proportion of the beam steel tension force to be transferred at the bend, consequently leading to much relieved opening action of the beam bar hooks. As a result, the development of concrete tension cracking orientated by the bending configuration of the beam longitudinal reinforcing bars in exterior columns was totally prevented for the test on Unit EJ3.

In addition, the axial column compressive load of 0.25 $A_g f_c^{'}$ also prevented the development of the column flexural cracks for test of Unit EJ3, and greatly improved the bond condition along the column longitudinal reinforcement.

Throughout the whole testing history of EJ3, no shear cracks were observed in the beam, columns and the joint core although the theoretical considerations conducted previously indicated a possibly very inadequate beam shear performance as seen in Table 4.8.

7.5.3 Observed Load versus Displacement Hysteresis Response

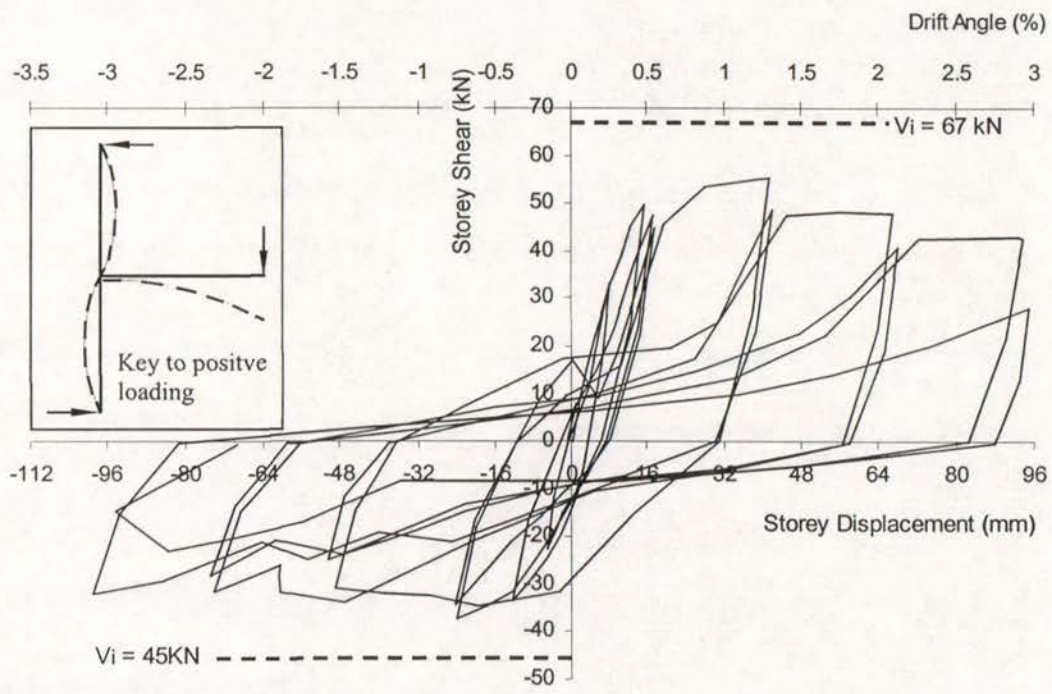

Fig. 7.34 Storey Shear versus Storey Displacement and Storey Drift Hysteresis Loops Measured for Unit EJ3

Fig.7.34 shows the storey (horizontal) shear versus storey (horizontal) displacement and storey drift hysteresis loops measured for Unit EJ3. Also shown in Fig.7.34 is the theoretical storey shear strengths of the unit, V_i, at the attainment of beam flexural strengths for both loading directions.

Fig.7.34 illustrates that the existence of constant compressive axial column load of $0.25 A_g f_c^{'}$ for test on Unit EJ3 resulted in a much improved general seismic performance, compared to the test observations of Unit EJ1.

The displacement at first yield, which was measured using the method described previously, was equal to a storey drift of 0.66% and 0.51% respectively for clockwise loading and anti-clockwise loading. Alternatively, the measured initial stiffness was 3.19 kN/mm and 2.75 kN/mm for clockwise and anti-clockwise loading respectively. Compared to the measured initial stiffness of 1.7 kN/m for Unit EJ1 in the loading of clockwise loading at $0.5 V_i$, the measured initial stiffness for test on Unit EJ3 was about 1.88 times that observed for test on Unit EJ1. Significantly improved structural stiffness property observed for test of Unit EJ3 was due to much reduced beam and column fixed-end rotations. Existence of constant compressive axial column load of $0.25 A_g f_c^{'}$ for test on Unit EJ3 greatly reduced the induced tensile strains in column longitudinal bars and enhanced the force transfer from the beam tension steel to the surrounding concrete by bond within the joint core. As a result, the measured maximum beam and column fixed-end rotations for Unit EJ3 were respectively only 70% and 40% of the measured maximum beam and column fixed-end rotations for Unit EJ2, although the attained force strength by Unit EJ2 was only about 88% that by Unit EJ3.

During clockwise loading, the storey shear force strength was attained by Unit EJ3 at a storey drift of 1.3% in the loading to displacement ductility of 2, and it was about 12% less than the corresponding theoretical storey shear strength of the unit at the attainment of the beam negative flexural strength. However, the attained storey shear strength by Unit EJ3 was about 1.6 times the storey shear force strength attained by Unit EJ1. During anti-clockwise loading, the storey shear force strength was attained by Unit EJ3 at a storey drift of 0.6% in the loading to displacement ductility of 1, and

it was about 15 % less than the corresponding theoretical storey shear strength of the unit at the attainment of the beam positive flexural strength. But this was about 1.5 times the storey shear force strength attained by Unit EJ1. Significant strength enhancement observed for EJ3 compared to test on Unit EJ1 was because the existence of constant compressive axial column load of $0.25\,A_g f_c^{'}$ for test of Unit EJ3, suppressed the opening action of the beam bar hooks, leading to entire prevention of premature concrete tension cracking failure along the beam bar hooks. As a result, the weakest part of the test unit EJ3 was shifted from the premature concrete tension cracking oriented by the beam bar hook configuration as for test on Unit EJ1 to the degrading beam flexural performance.

Observed pinching of the hysteresis loops for the test on Unit EJ3 although still significant was much less pronounced when compared to that observed for similar exterior beam-column joint units but tested with zero axial column load, for example, Unit EJ2. Pinching of the hysteresis loops observed for test on Unit EJ2 occurred due to the major flexural cracks at beam and column interface. The existence of the compressive axial column load for test on Unit EJ3 improved the bond condition along the beam longitudinal reinforcement within the joint core, and produced a less pronounced beam flexural crack at column face, consequently leading to less pinched hysteresis loops for test of Unit EJ3.

In summary, the existence of compressive axial column load for the test on Unit EJ3 enhanced the available storey shear force strength and stiffness and improved the structural energy dissipating capacity. Test on Unit EJ3 reached the maximum storey shear that was approximately 15% less than the theoretical storey shear strengths at storey drift of approximately 1.3% for clockwise loading but at storey drift of 0.6% for anti-clockwise loading. Softening with cyclic loading and pinching of the hysteresis loops observed for test on Unit EJ3 were not so significant as that observed for similar tests but tested with zero axial column load. Existence of compressive axial column load for test on Unit EJ3 also enhanced the force capacity associated with the opening of the beam bar hooks in tension, shifting the weakest link of the unit to be the beam flexural behaviour. However, the plain round longitudinal bars used meant that the concrete members could not attain their theoretical flexural strengths and the non-linear deformation did not spread over an area called "plastic hinge region" as for the

deformed bar case, but was limited to a major flexural crack at beam and column interface.

7.5.4 Strains in Longitudinal Reinforcement of Beam and Columns

Figs.7.35 and 7.36 show the measured strain profiles by electrical resistance strain gauges along beam bar 1 and beam bar 2 respectively. Compared with the measured steel strain profile along the beam longitudinal bars of Unit EJ2 (see Figs.7.22 and 7.23), bond degradation and bar slip along the beam longitudinal bars of Unit EJ3 were apparently improved within the joint region from inner column face to the joint centre-line.

Fig.7.37 compares the measured steel strains with the theoretical strains for beam bars 1 and 2 at inner column face when the beam bars were in flexural tension in the early loading cycles until the completion of loading at ductility 1. The imposed steel stress levels on the beam longitudinal bars were expressed as the percentages of the theoretical beam shear strength, namely, $V_{m,b}/V_{i,b}(\%)$, where $V_{m,b}$ and $V_{i,b}$ are respectively the imposed steel stress levels on the beam longitudinal bars and the theoretical beam shear strength calculated based on the beam flexural strength. Similarly, the imposed steel stress levels on the column longitudinal bars were expressed as $V_{m,c}/V_{i,c}(\%)$, where $V_{m,c}$ and $V_{i,c}$ are respectively the imposed steel stress levels on the column longitudinal bars and the theoretical column shear strength calculated based on the column flexural strength.

For beam bar 1, the measured strains showed better correlation with the theoretical strain than that for beam bar 2, because beam bar 2 tended to be more subjected to bond slip. Generally, the measured steel tensile strains were higher than the theoretical predictions based on plane section assumption. As the bond degradation along the member longitudinal bars progressed, the discrepancies between the measured steel tensile strains and the theoretical predictions tended to increase.

Measured column steel strains were generally small and they matched with the theoretical predictions well.

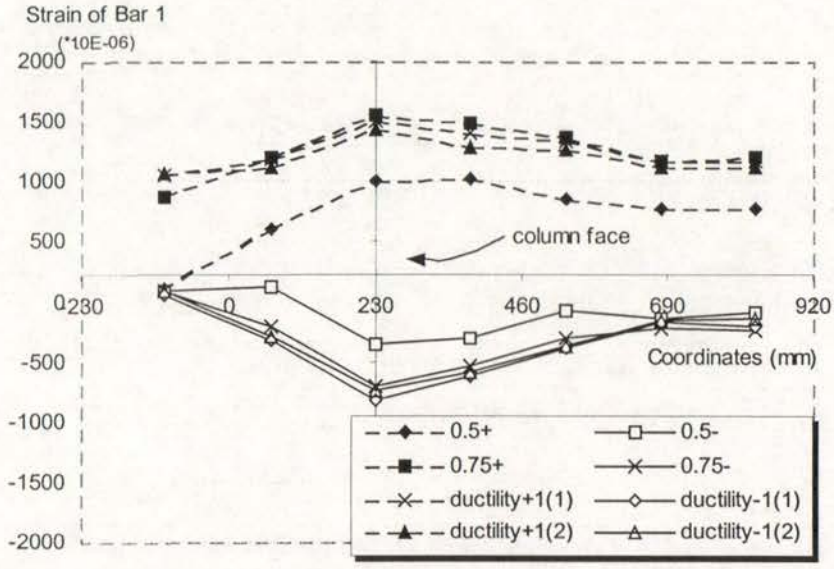

Fig.7.35 Strain Profiles of Beam Bar 1 Measured by Electrical Strain Gauges

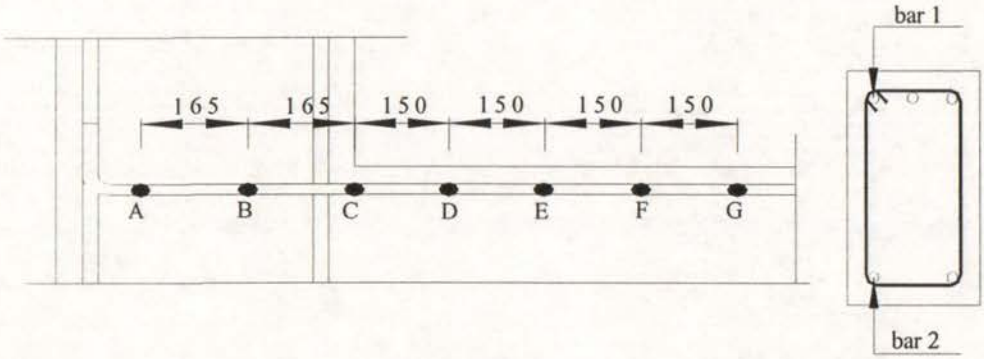

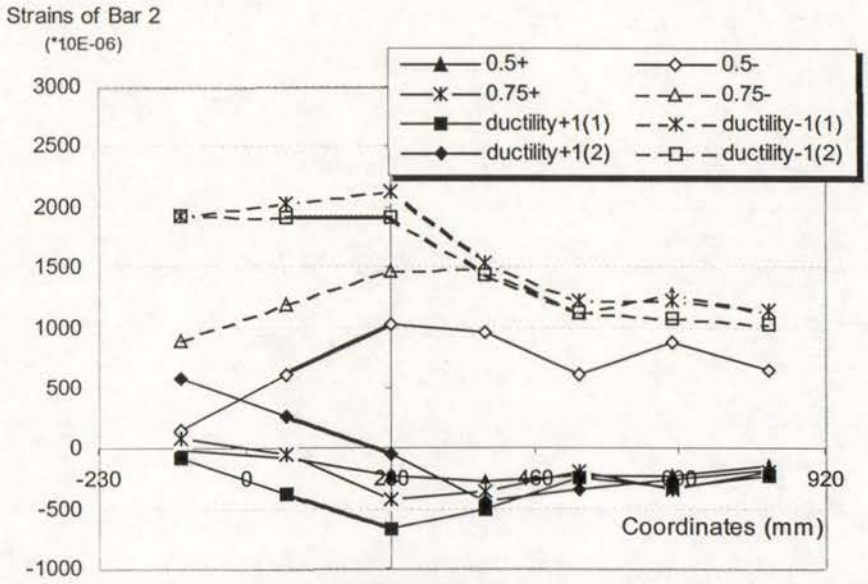

Fig.7.36 Strain Profiles of Beam Bar 2 Measured by Electrical Strain Gauges

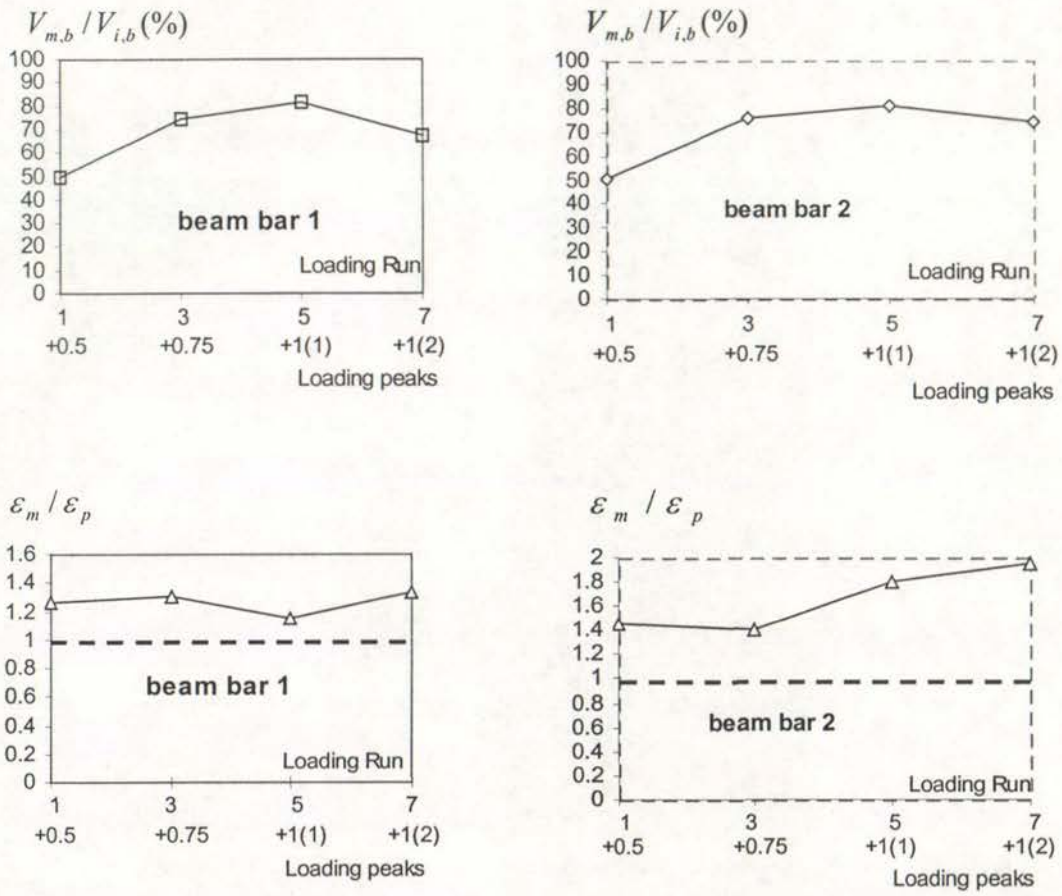

(a) Beam Bar 1 (b) Beam Bar 2

Fig.7.37 Comparison of measured and theoretical beam bar strains at column face

7.5.5 Member Curvature Property

The investigation of linear members reinforced by plain round bars should only consider the member fixed-end regions because the total member deformations were mainly attributed to the rotations over the member fixed-end regions. Fig.7.38 and Fig.7.39 show the rotation angles over the fixed-end regions and the correspondent shear forces for beam and columns, respectively. In figs.7.38 and 7.39, the member rotations over the fixed-end regions were expressed in terms of the ratios of the measured fixed-end rotations to the theoretically predicted rotations over the whole member length, and the imposed member force strengths were expressed in terms of the percentages of the imposed member force to the member force strength obtained based on its flexural strength.

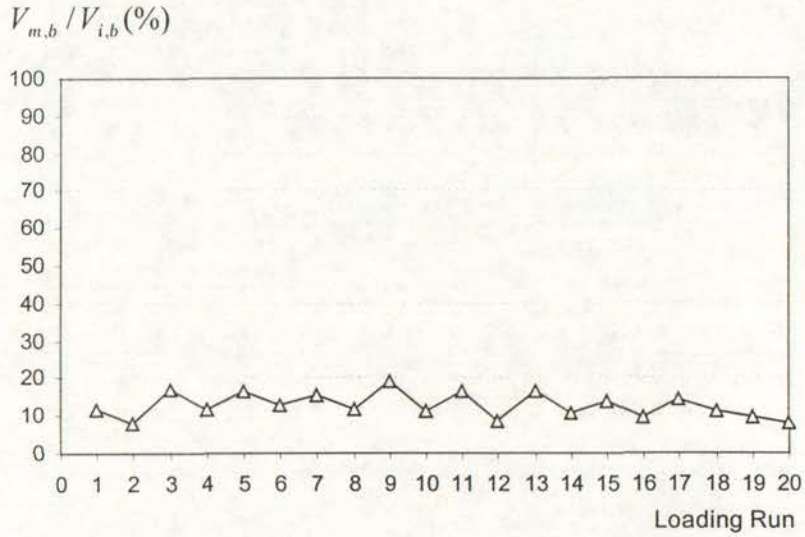

(a) Variation of Imposed Beam Shear Level

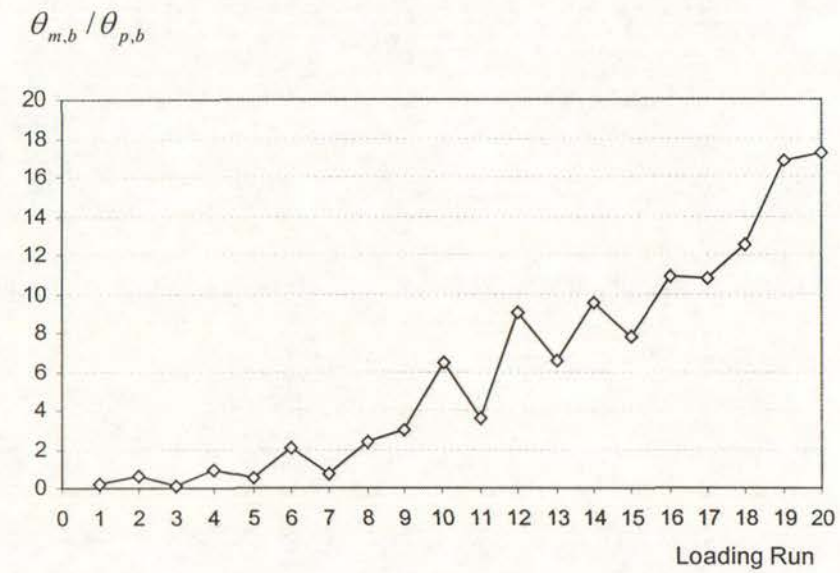

(b) Variation of beam fixed-end rotations

Fig.7. 36 Amplification of Beam Fixed-End Rotation and Beam Shear

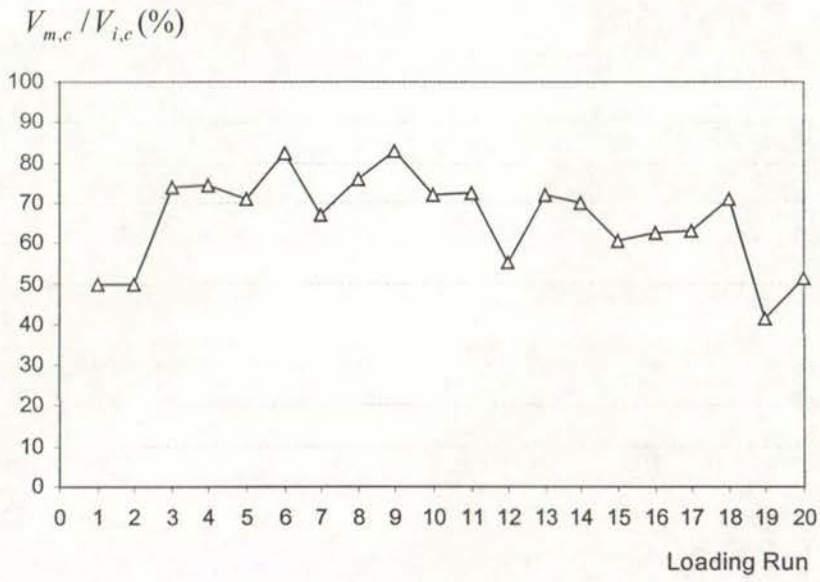

(a) Variation of Imposed Column Shear Level

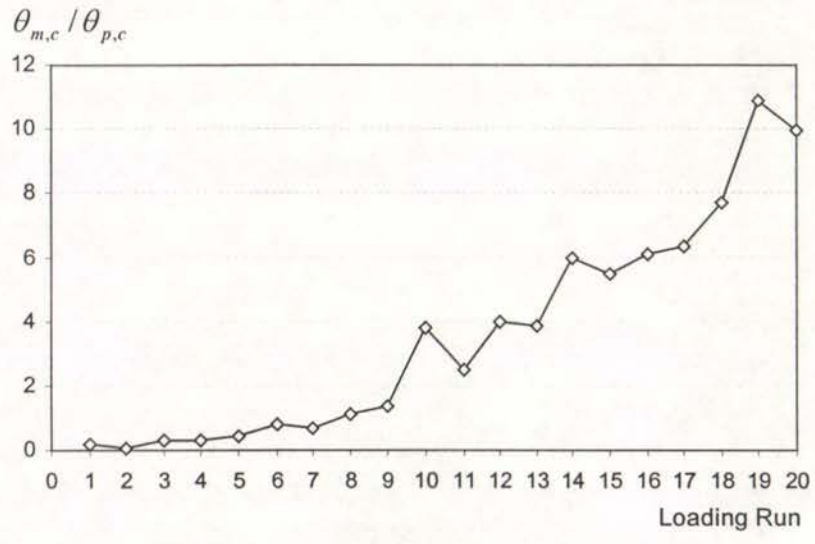

(b)Variation of column fixed-end rotations

Fig.7. 37 Amplification of Column Fixed-End Rotations and Storey Shears

In figs. 7.38 and 7.39, the imposed member shear force had never reached its theoretical force strength, where the member theoretical force strength was obtained according to the member's flexural strength. Equally, the tensile longitudinal reinforcement should have been theoretically in elastic range. The measured member fixed-end rotation was much bigger than the theoretically predicted member total rotation, which was estimated for the same force level. Discrepancies between the measured member fixed-end rotation and the theoretically predicted member total rotation increased as the loading progressed even the attained force strength reduced, indicating that the attained stiffness degraded as the loading cycles progressed. Progressive bond degradation along the member longitudinal bars not only caused the structural stiffness to degrade rapidly, but also resulted in the degradation of member flexural strength due to the violation of plane section assumption. The stiffness degradation was observed to be much quicker than the strength degradation, so the final performance of the tested structure would be governed by the structural displacement criteria.

Evidently, the analysis of the structure should allow for the stiffness and strength degradation according to the loading cycle.

7.5.6 Joint Behaviour

7.5.6.1 Joint Shear Stress

The estimated maximum nominal horizontal joint shear stress for Unit EJ3 during clockwise loading occurred at storey drift of 1.3% at displacement ductility of 2, and it was 1.6 MPa, or $0.27\sqrt{f_c'}$ MPa. In comparison, the estimated maximum nominal horizontal joint shear stress for anti-clockwise loading direction occurred at a storey drift of 0.6% at displacement ductility of 1, and it was lower, being 1.04 MPa, or $0.17\sqrt{f_c'}$ MPa. Evidently, the attained joint shear stress level of Unit EJ3 in both loading directions was well below the joint shear stress level of $0.78\sqrt{f_c'}$ MPa, which corresponds to the joint shear force strength at the stage of concrete diagonal tension cracking of the joint core, estimated using Mohr's circle for stress and assuming the concrete diagonal tension strength of $0.3\sqrt{f_c'}$ MPa.

7.5.6.2 Joint Hoop Strains

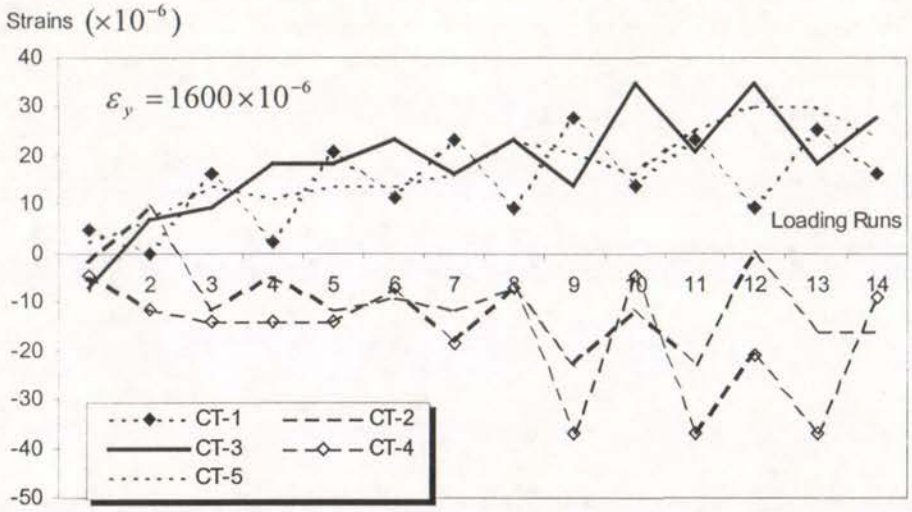

Fig. 7.39 Measured strains in joint hoops and column transverse reinforcement

Fig. 7.39 shows the joint hoop strains measured for Unit EJ3 using electrical resistance strain gauges.

Whereas in the case of test on Unit EJ1 the measured maximum strain in joint hoop CT-4 was well beyond the steel yield strain, the measured joint hoop strain in CT-4 for test of Unit EJ3 was very low, and it was less than 2.5% of the steel yield strain. Unit EJ1 and Unit EJ3 were identical but Unit EJ1 was tested with zero axial column load, and Unit EJ3 was tested with the existence of constant compressive axial column load $0.25A_g f_c'$. Such test evidence suggested that the alternative joint shear mechanism as proposed in Chapter 4 was not actuated and the force transfer across the joint core in this case was mainly by a much enlarged diagonal joint concrete strut. Due to the presence of column axial compressive load, the beam tensile steel force was transferred by bond to the surrounding concrete within the column flexural compression zone.

7.5.6.3 Joint Shear Distortion and Joint Expansion

Compared to the test of EJ1 where the induced maximum joint shear distortion was 0.52%, the maximum joint shear distortion measured for test of EJ3 of 0.66×10^{-4} was much smaller. Actually, the measured maximum joint shear distortion of 0.66×10^{-4} for test of EJ3 only corresponded to one digital reading, so the shear deformation of the joint core of Unit EJ3 could be said to be Nil. This occurred due to the complete prevention of concrete cracking in the joint core resulting from the

enhancement of the joint concrete strut mechanism by the compressive axial column load. Unlike joint truss mechanism, joint concrete strut mechanism is very stiff.

7.5.7 Displacement Components

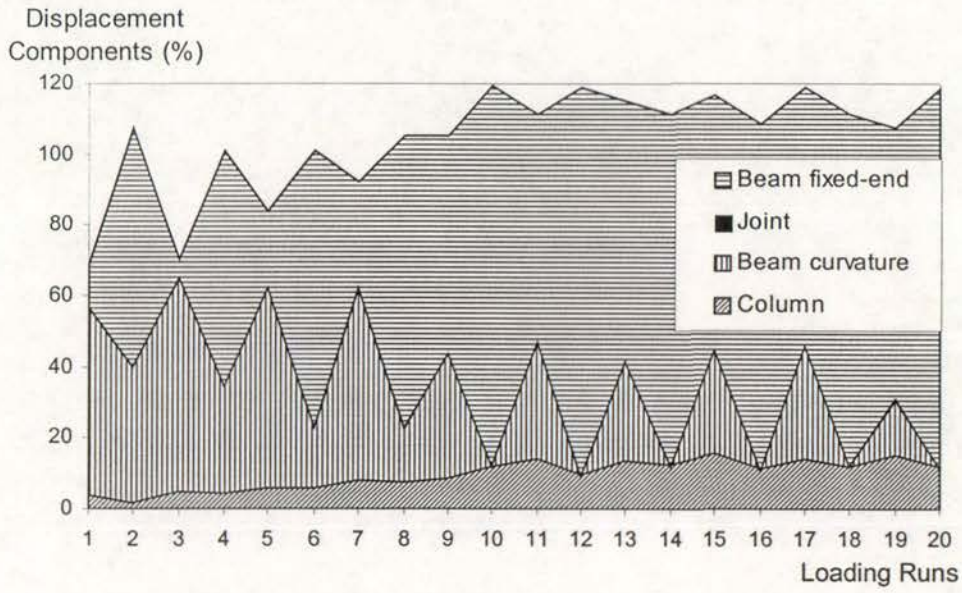

Fig. 7.40 Displacement Components Measured for Test of Unit EJ3

Fig. 7.40 shows the measured contributions of beam flexural deformations to the storey displacements, expressed as percentages of the measured storey horizontal displacement.

Fig.7.40 shows that the contribution of beam deformation to the storey deflection was significantly larger than the column displacement contribution. Especially the contribution of beam fixed-end rotation increased as the loading progressed, and evidently the beam fixed-end rotation was the major contribution to the storey displacement. This suggested that the seismic performance of the tested exterior beam-column joint component be governed by the degrading beam flexural behaviour.

7.5.8 Summary

An as-built full-scale exterior beam-column joint unit EJ3 was constructed. Unit EJ3 was characterised by plain round beam longitudinal reinforcing bars being bent away from the joint core in the exterior column, the members having inadequate amount of transverse reinforcement, and the joint core having very limited shear reinforcement. Unit EJ3 was identical to as-built test Unit EJ1 but tested under simulated seismic

loading with the presence of a constant compressive axial column load of $0.25 A_g f_c^{'}$. Test on Unit EJ3 was to investigate the effect of axial column load on the seismic behaviour of as-built exterior beam-column joint components. Theoretical considerations showed that transverse reinforcement in the members of Unit EJ3 was very inadequate, especially in the beam, according to the requirement of shear force capacity and the requirement for preventing longitudinal bar buckling and confining the compressed concrete.

1. Simulated seismic loading test on Unit EJ3 showed that the overall seismic performance of Unit EJ3 was dominated by the beam flexural behaviour only, the degradation of the beam flexural performance with the loading was mainly limited in the major beam flexural crack at column face. Compressive axial column load enhanced the force transfer by bond from the beam tension steel to the surrounding concrete prior to the bend, and reduced the beam steel tension force needed to be transferred at the bend. In addition, the presence of compressive axial column load for test of EJ3 actuated the stiff corner to corner joint diagonal concrete strut due to enlarged column flexural compression zone, hence led to perfect joint core integrity. As a result, premature concrete tension cracking resulting from the interaction between the column bar buckling and the opening action of the beam bar hooks as occurred for test on Unit EJ1 was entirely prevented for test on Unit EJ3, and the most critical area was shifted to the major beam flexural crack at column face for test of Unit EJ3, which was associated with severe bond degradation along the beam longitudinal reinforcement adjacent to the joint core.

2. The presence of constant compressive axial column load of $0.25 A_g f_c^{'}$ greatly improved the force strength and stiffness performance of the test unit. The attained storey shear strength by Unit EJ3 was approximately 12% less than the theoretical storey shear strength for both clockwise and anti-clockwise loading. The storey shear strength of the unit was attained by unit EJ3 at storey drift of approximately 1.3% for clockwise loading but at storey drift of 0.6% for anti-clockwise loading. The attained displacement at first yield was equal to a storey drift of 0.66% and 0.51% respectively for clockwise loading and anti-clockwise loading.

3. Results of test on Unit EJ3 were contrasted to the results of test on Unit EJ1. Such a contrast revealed that the presence of compressive axial column load of $0.25 A_g f_c^{'}$ for test of EJ3 caused the measured initial stiffness to be about 1.8 times the measured initial stiffness for Unit EJ1 and the attained storey shear strength to increase by about 33% of the theoretical storey shear strength. In addition, the presence of compressive axial column load of $0.25 A_g f_c^{'}$ for test of EJ3 also greatly improved energy dissipating capacity of the system.

7.6 TEST OF UNIT EJ4

7.6.1 General

As-built full-scale exterior beam-column joint unit EJ4 was identical to the as-built full-scale exterior beam-column joint unit EJ2, and Unit EJ4 was tested under simulated seismic loading with a constant compressive axial column load of $0.23 A_g f_c^{'}$ present, in order to investigate the influence of compressive axial column load on the seismic performance of exterior beam-column joint components when the test units had the reinforcing details typical of pre-1970s reinforced concrete frame structures.

7.6.2 Crack Development and Damage

The appearance of Unit EJ4 at the end of testing is shown in Fig.7.41.

The observed damage throughout the whole testing for test on Unit EJ4 was the flexural cracks developed in the beam and a vertical crack developed along the outer layer of column bars in the upper left corner of the joint core which occurred in the loading at anticlockwise displacement ductility of 3 for test of Unit EJ4. The beam flexural cracking was mainly in the beam flexural crack adjacent to the joint core, referred to as the major beam flexural crack. This occurred due to the occurrence of severe bond degradation and bar slip along the beam longitudinal bars adjacent to and within the joint core. The development of the vertical crack along the outer layer of the column longitudinal reinforcement occurred because of column bar buckling, which was associated with severe bond degradation along the outer layer of the column bars. However, the development of this vertical crack was much less apparent compared to that of the major beam flexural crack at column face. No damage was observed to the columns for test on Unit EJ4. Apparently the predicted weak beam-strong column failure mechanism formed, and the final failure trigger for test on Unit EJ4 was due to the beam flexural behaviour, which degraded with the loading owing to severe bond degradation along the beam longitudinal bars adjacent to the joint core.

Throughout the whole testing of EJ4, no shear cracks developed in the members and the joint although theoretical consideration previously conducted showed potentially very inadequate beam shear performance as seen in Table 4.8. Hence the method for

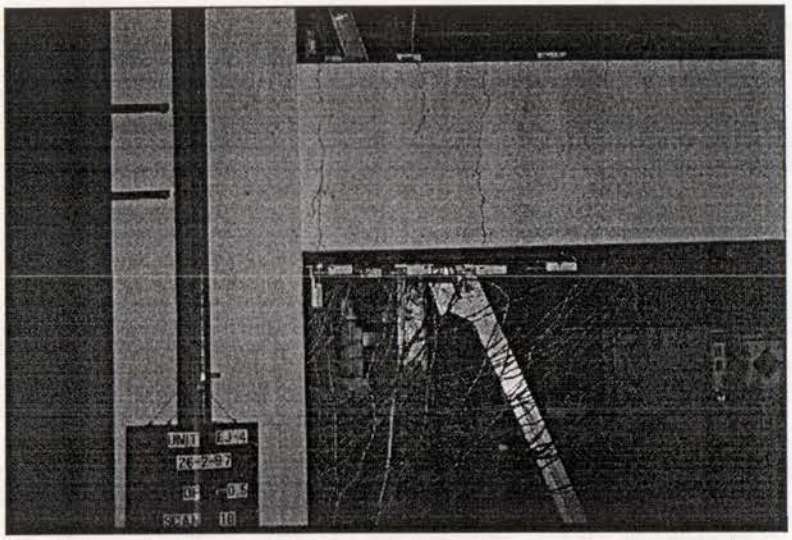

(a) Loading at 0.5Vi

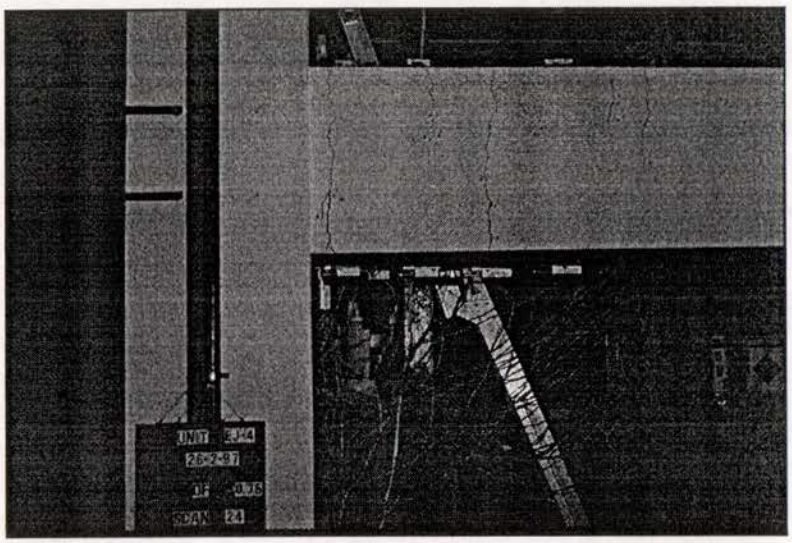

(b) Loading at 0.75Vi

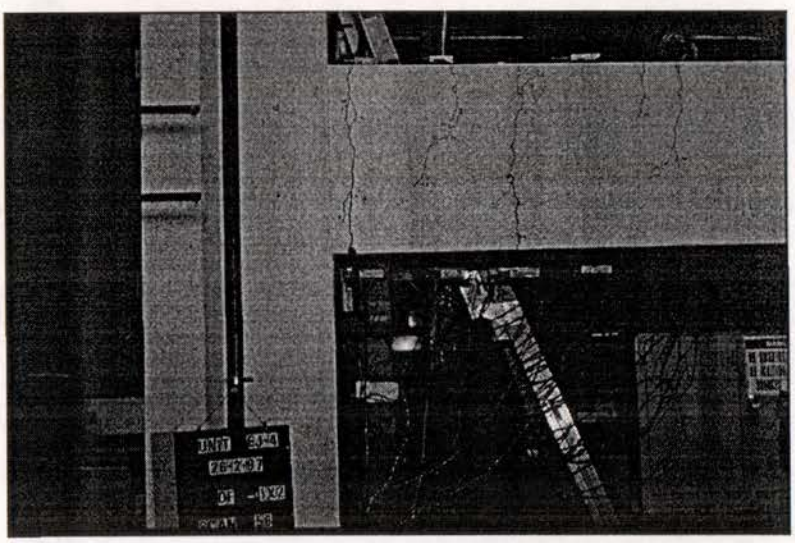

(c) End of loading at ductility 1

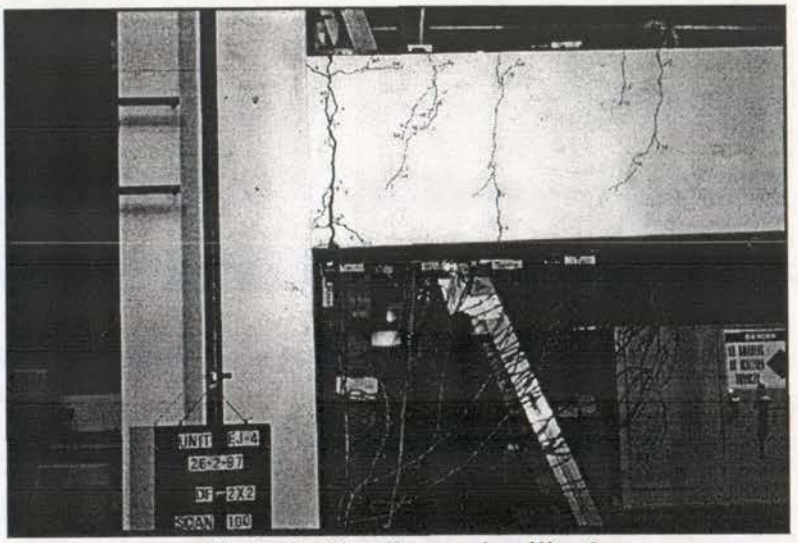

(d) End of loading at ductility 2

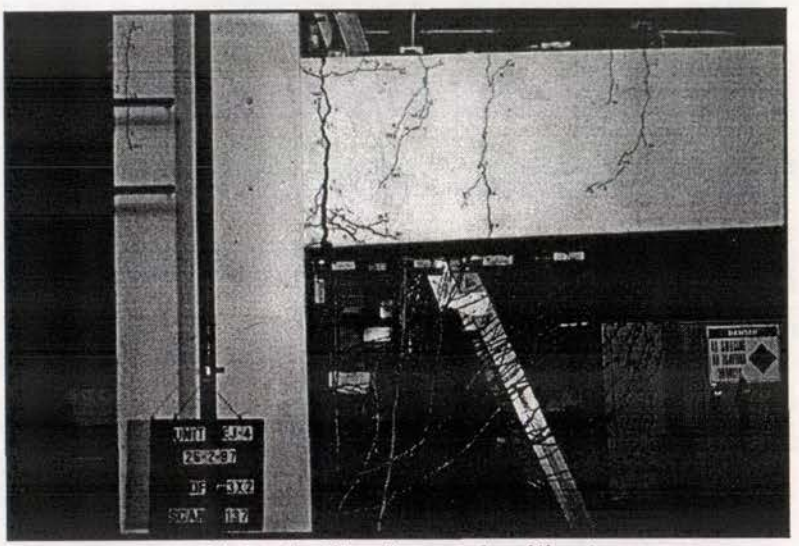

(e) End of loading at ductility 3

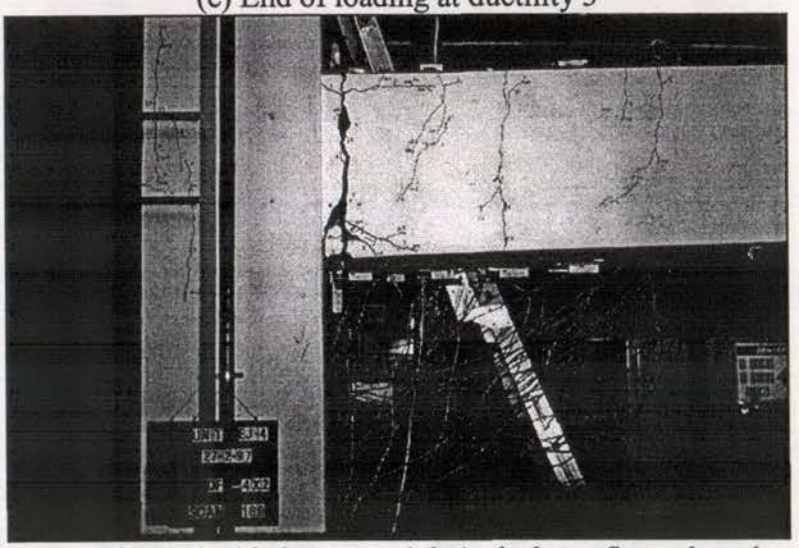

(f) Final appearance of Unit 4 with damage mainly in the beam flexural crack at column face

Fig.7.41 Crack development and final appearance of Unit EJ4

estimating the shear resisting capacity of linear concrete members reinforced by deformed bars can not be used to estimate the shear resisting capacity of linear concrete members reinforced by plain round bars.

The test evidence observed for test on Unit EJ4 was obviously very different from that for test on Unit EJ2. The prominent damage development observed for test on Unit EJ2 was the damage resulting from the interaction between the column bar buckling and the opening action of the beam bar hooks due to inadequate column transverse reinforcement adjacent to and within the joint core. The difference in the observed evidence of tests of EJ2 and EJ4 was apparently attributed to the compressive axial column load. The imposed axial column load during seismic loading was zero for test of EJ2 and $0.23 A_g f_c^{'}$ for test of EJ4. The existence of constant compression axial column load $0.23 A_g f_c^{'}$ for test of EJ4 enhanced the force transfer by bond within the joint region from the beam tension steel to the joint core concrete, hence greatly reduced the amount of the beam steel tension force needed to be transferred at the bend by bearing force, leading to much reduced possibility of the failure associated with the beam bar opening action.

7.6.3 Hysteretic Response of Test on EJ4

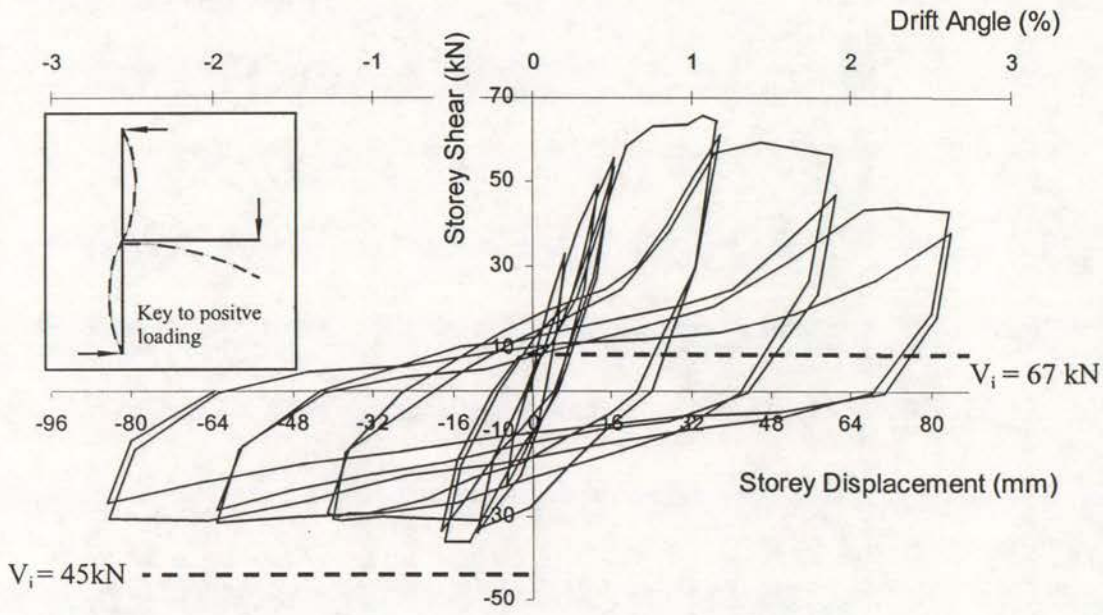

Fig. 7.42 Storey Shear Force versus Horizontal Storey Displacement Loops of EJ4

Fig.7.42 shows the measured storey shear versus storey displacement and drift hysteresis loops for Unit EJ4. Also shown in Fig.7.42 is the theoretical strength of the unit in terms of the storey shear, V_i, at the attainment of beam flexural strength for both clockwise and anti-clockwise loading directions.

The general seismic performance of test on Unit EJ4 was greatly improved, compared with test on Unit EJ2. The evident improvement in the seismic performance demonstrated by the test onf EJ4 was mainly because the premature concrete tension cracking along the beam bar hooks in tension was entirely suppressed due to the compressive axial column load of $0.23 A_g f_c^{'}$. Also, the seismic performance demonstrated by test of EJ4 was better when compared with that by test on Unit EJ3, and this was attributed to the more adequate configuration of the beam longitudinal bars in the exterior columns of Unit EJ4.

In Fig.7.42, the theoretical storey shear strength determined at the attainment of negative beam flexural strength was attained by test on Unit EJ4 during clockwise loading and it occurred at a storey drift of 1.1%, which was equal to a displacement ductility factor μ_Δ of 2. The attained storey shear strength by test on Unit EJ4 for anti-clockwise loading was about 16% less than the theoretical storey shear strength determined at the attainment of positive beam flexural strength and it occurred at a storey drift of 0.6%, which was equal to a displacement ductility factor μ_Δ of 1. Compared to test on Unit EJ2 where the attained storey shear strength was only about 75% of the theoretical storey shear strength for both loading directions, the attained storey shear force strength observed for test on Unit EJ4 increased by 9% to 25%. Compressive axial column load present for test on Unit EJ4 not only mobilised an enlarged joint concrete strut mechanism to transfer the member forces across the joint core, but also reduced the beam steel tension force needed to be transmitted at the beam bar bend, hence relieving the opening action of the beam longitudinal bars and preventing the concrete tension cracking along the beam bar hooks, in comparison with test of EJ2. When compared to test on Unit EJ3 where the available storey shear strength was about 90% of the theoretical storey shear strength, the increase in the attained storey shear strength by test of EJ4 was negligible. Unit EJ3 and Unit EJ4 were identical except the difference in beam bar hook arrangements and both units were tested with a constant compressive axial column load of 1800 kN present. This

suggests that the beam bar hook details have no notable influence on the structural force strength performance of as-built exterior beam-column joint components if the concrete tension cracking failure associated with the interaction between column bar buckling and the opening action of the beam bar hooks can be prevented.

The measured displacement at first yield for test of Unit EJ4 using the method described in Section 5.3.2 was equivalent to a storey drift of 0.53% at first yield. The initial stiffness thus was 3.3 kN/mm on average for test on Unit EJ4. It is surprised to find that the measured initial stiffness for test on Unit EJ4 was 2.75 times the measured initial stiffness of 1.2 kN/mm for Unit EJ2. Significant improvement in the observed initial stiffness for test on Unit EJ4 was attributed to much reduced bond degradation along the beam longitudinal bars within the joint core owing to the presence of compressive axial column load. When compared to test of Unit EJ3 where the measured initial stiffness was 3.0 kN/mm, the improvement in the stiffness performance of test of EJ4 was very insignificant. Hence if the premature concrete tension cracking along the beam bar hooks in tension can be totally prevented, the beam bar hook configuration in the exterior columns will not influence the structural stiffness performance.

Some pinching of the storey shear force versus storey displacement hysteresis loops was observed in Fig.7.42 for test of EJ4 and the pinching was observed to progress with the loading progress. The low stiffness at the beginning of each load run is due to displacement across the major open beam flexural crack at inner column face in the flexural compression zone of the beam, which was caused by tension in the previous loading run. Increase in the stiffness occurred mainly after the major beam flexural crack closed and the flexural compression started to be transmitted across the major beam flexural crack. Strength degradation was also observed for test on Unit EJ4, and it was of similar significance to test on Unit EJ3. However, the strength degradation observed for test on Unit EJ4 was much less significant than that for test on Unit EJ2. Progress of bond degradation along the beam longitudinal reinforcement adjacent to and within the joint core caused the attained beam flexural strength to reduce with the loading progress, leading to the observed strength degradation. Compressive axial column load for test on Unit EJ4 greatly enhanced the bond mechanism to transfer the beam steel tension force to the surrounding concrete, leading to much improved

energy dissipating capacity of the test unit, compared to test on Unit EJ2. Also compressive axial column load totally prevented the premature concrete tension cracking along the bema bar hooks in tension for test on Unit EJ4, consequently, the effect of the beam bar hook configuration in exterior column became insignificant on the structural energy dissipating capacities, as demonstrated by tests on Units EJ3 and EJ4.

In summary, test on Unit EJ4 demonstrated that the existence of compressive axial column load for test on Unit EJ3 enhanced the available storey shear force strength and stiffness, especially the structural stiffness, and also improved the structural energy dissipating capacity, compared to test on Unit EJ2. Test on Unit EJ4 reached the theoretical storey shear strength of the unit at storey drift of approximately 1.1% for clockwise loading but it reached the storey shear strength which was about 15% less than the theoretical storey shear strengths at storey drift of 0.6% for anti-clockwise loading. The attainment of the available storey shear strength observed for test on Unit EJ4 was at similar drift level to test on Unit EJ3. Softening with cyclic loading and pinching of the hysteresis loops observed for test on Unit EJ4 were of similar significance to test on Unit EJ3 and were not so significant as that observed for test of Unit EJ2. Compressive axial column load of 0.23 $A_g f_c^{'}$ to 0.25 $A_g f_c^{'}$ present for tests on Units EJ3 and Unit EJ4 caused the influence of the beam bar hook details on the structural strength performance, stiffness performance and the energy dissipating capacity to be very insignificant.

7.6.4 Strains in Member Longitudinal Reinforcement

Fig.7.43 shows the measured strain profiles by electrical resistance strain gauges along beam bar 1 and beam bar 2 respectively. Compared with the measured steel strain profile along the beam longitudinal bars of Unit EJ2 (see Figs.7.24 and 7.25), bond degradation and bar slip along the beam longitudinal bars of Unit EJ4 were apparently improved within the joint region and the strains of beam flexural tensile reinforcement gradually decreased within the joint region relative to the steel strain at inner column face. When compared to the observed strain profile of beam tension bars of Unit EJ3 (Fig.7.35 and Fig.7.36), it was found that units EJ3 and EJ4 had generally similar bond condition along the beam longitudinal bars within the joint region.

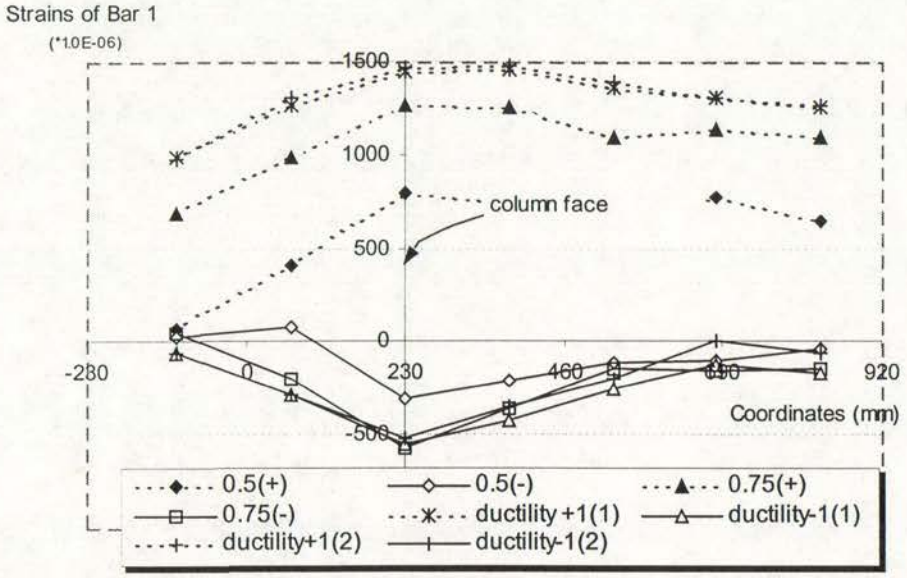

(a) Beam Bar 1

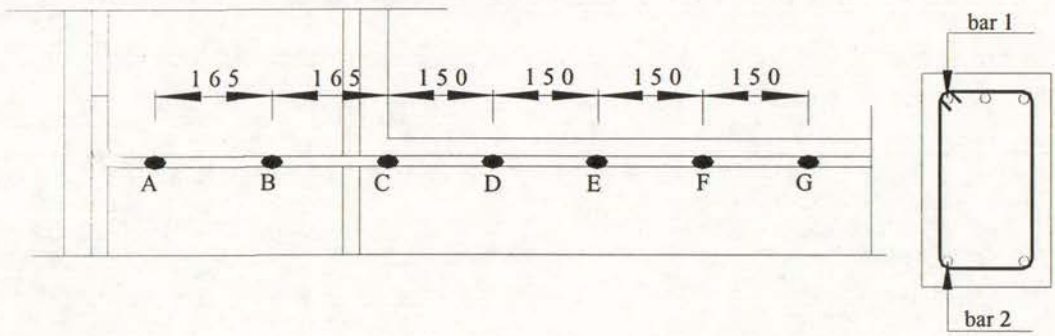

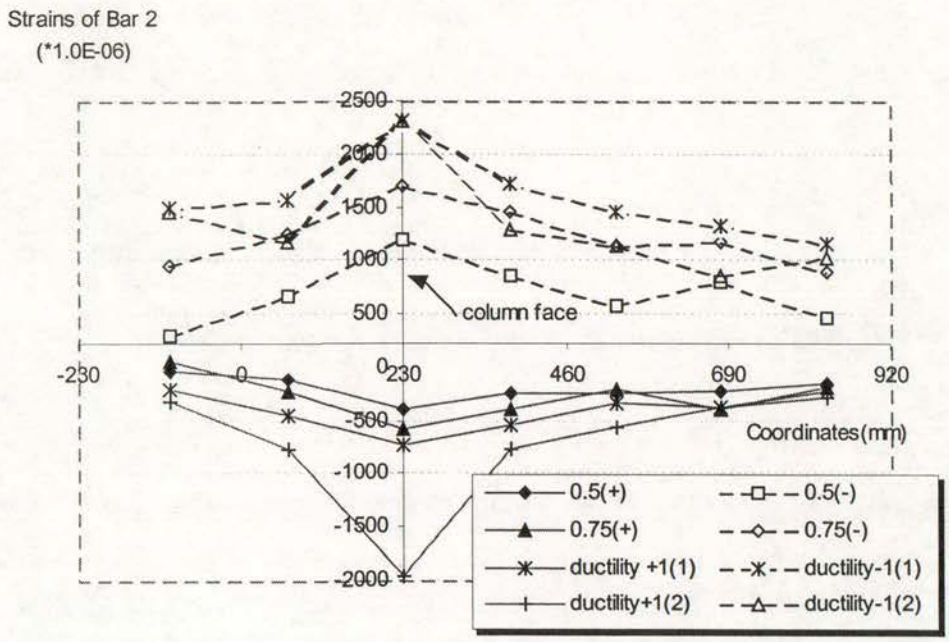

(b) Beam Bar 2

Fig.7.43 Strain Profiles of Beam Bar 1 and Beam Bar 2 of Unit EJ4

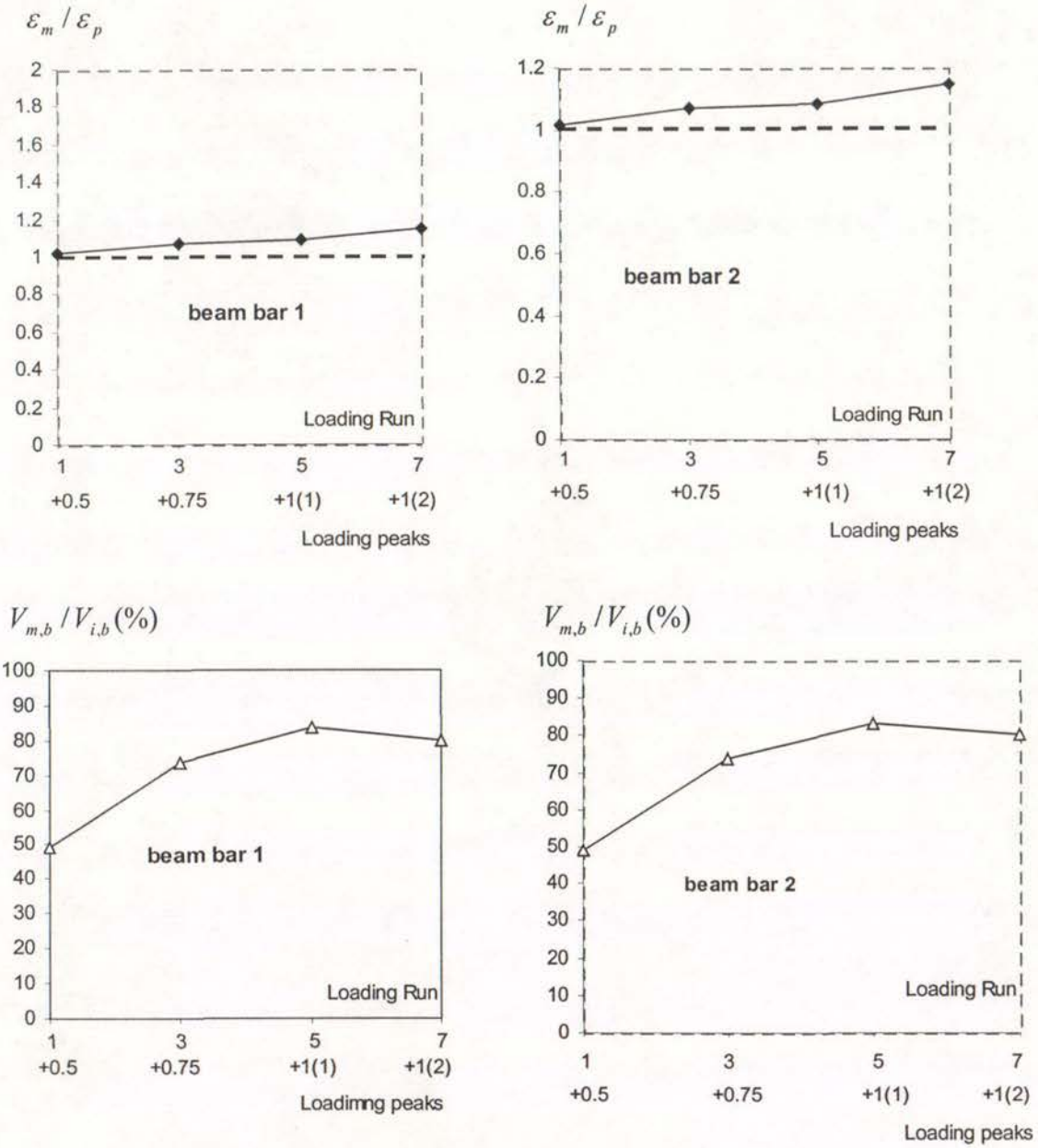

Beam Bar 1 (b) Beam Bar 2

Fig.7.44 Comparison of measured and theoretical beam bar strains at column face

Fig.7.44 compares the measured steel strains with the theoretically predicted strains of beam flexural tension bars at inner column face for Unit EJ4. The theoretical predictions were based on the measured beam shear forces and ordinary flexure theory established on the basis of plane-section assumption based. The measured tension strains for beam flexural tension bars at column inner face were higher than the theoretical predictions and the discrepancies increased generally with the loading progress due to the progressive bond deterioration along the member longitudinal bars. The measured tension strains can vary from 105% to 200% the theoretical predictions.

7.6.5 Member Curvature Property

Only the rotation angles over the linear member's fixed-end regions are of concern for Unit EJ4. Fig.7.45 and Fig.7.46 show the rotation angles over the fixed-end regions and the imposed force strengths for beam and column, respectively. Again in figs.7.45 and 7.46, the member rotations over the fixed-end regions were expressed in terms of the ratios of the measured rotations over the member fixed-end regions to the theoretically predicted rotations over the whole member length, referred to as amplifications of member rotations. The imposed member force strengths were expressed in terms of the percentages of the imposed member force to the member force strength obtained based on its own flexural strengths because the bond degradation along the member longitudinal bars are related to the stress level of the flexural tensile reinforcement.

It is seen from Fig.7.45 that amplification of the beam fixed-end rotation increased nearly proportionally with the loading cycles. This trend is similar to the test observation for Unit EJ3 but the magnitudes of the discrepancies between the measured member fixed-end rotation and the theoretically predicted total beam rotation were smaller than those for test on Unit EJ3. Whereas in the case of Unit EJ3 the measured beam fixed-end rotation reached up to 18 times the theoretically predicted beam total rotation, the measured beam fixed-end rotation was about 9 times the theoretically predicted total beam rotation for test on Unit EJ4. This was as a consequence of easier force disposition across the joint region when the beam bar hooks were bent into the joint core. Unlike the test observations for Unit EJ3 which

had the measured column fixed-end rotation to be equivalent to 11 times the theoretically predicted total column flexural deflection at most, the observed column fixed-end rotation for Unit EJ4 was never significant. Such a difference was due to the used measurement technique. A steel plate was glued to the beam face and this plate became a reference point for the potentiometer mounted over column fixed-end region. As a consequence, the concrete cracking over beam fixed end region could significantly influence the readings from this linear potentiometer. Unreliability of the readings of linear potentiometers for measuring column fixed-end rotations could be also detected by the obtained displacement components for Unit EJ4 (see Fig.7.48). In fact, the column flexural deformation for Units EJ3 and EJ4 should be of similar magnitudes.

7.6.6 Joint Behaviour

7.6.6.1 Joint Shear Stress

The estimated maximum nominal horizontal joint shear stresses for Unit EJ4, based on the measured member forces and the plane section assumption, were of similar magnitude to those of Unit EJ3 in both clockwise and anti-clockwise loading direction, and were 1.8 MPa, or $0.3\sqrt{f_c'}$ MPa in clockwise loading direction and 1.04 MPa, or $0.17\sqrt{f_c'}$ MPa in anti-clockwise loading direction respectively. The maximum nominal horizontal joint shear stresses estimated for Unit EJ4 evidently were well below the joint shear capacity at the stage of diagonal tension cracking of the joint cores, which was $0.78\sqrt{f_c'}$ MPa, estimated using Mohr's circle for stress and assuming the concrete diagonal tension strength of $0.3\sqrt{f_c'}$ MPa [H1], if expressed in terms of nominal horizontal joint shear stress. The joint core of Unit EJ4 was of excellent integrity till the end of testing of EJ4.

7.6.6.2 Joint Shear Distortion and Joint Expansion

The maximum joint shear distortion measured for EJ4 was very small, being 0.0063%, which was of similar magnitude to Unit EJ3. Hence the joint core of Unit EJ4 was in excellent condition. In contrast, Unit EJ2, which was identical to Unit EJ4, had a maximum joint shear distortion of 0.52%. The significant improvement of the joint shear performance demonstrated by the test of Unit

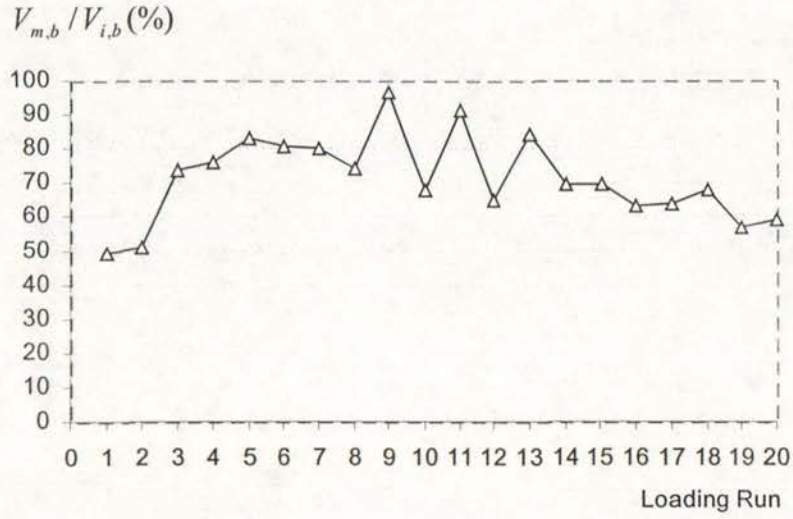

(a) Variation of Imposed Beam Shear Level

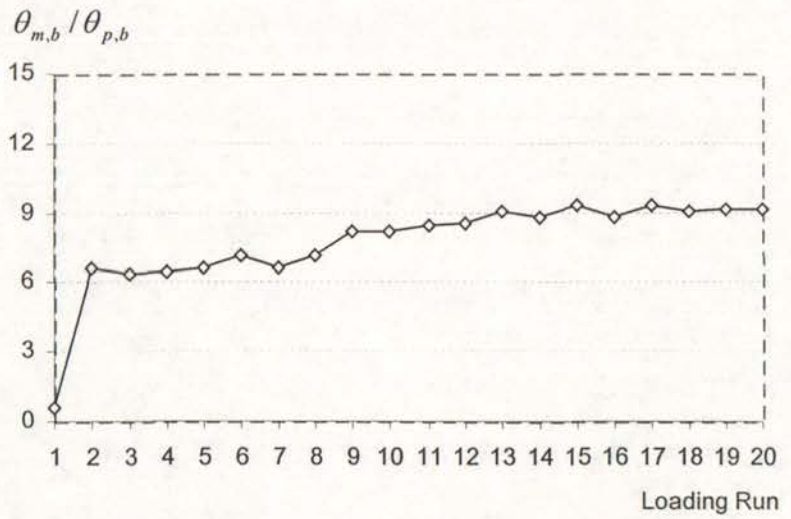

(a) Variation of beam fixed-end rotations

Fig.7. 45 Amplification of Beam Fixed-End Rotation and Beam Shear

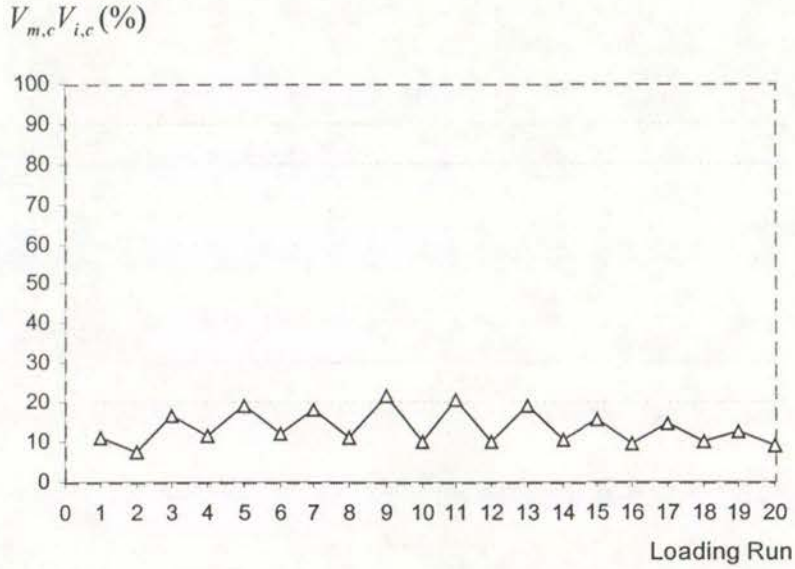

(a) Variation of Imposed Column Shear Level

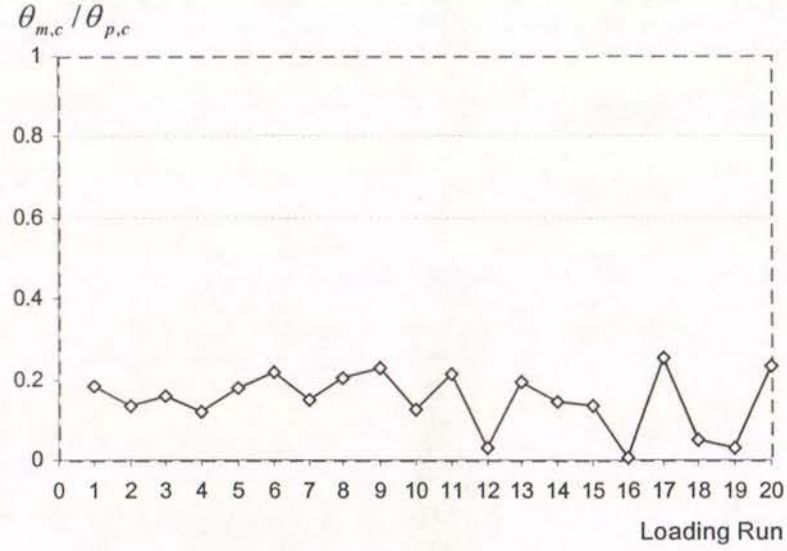

(b) Variation of column fixed-end rotations

Fig.7.46 Amplification of Column Fixed-End Rotation and Column Shear

EJ4 was due to the total prevention of the concrete tension cracking along the hooks of the beam bars in tension as a result of the enhancement of the joint corner to corner concrete strut mechanism by the compressive axial column load, similar to the test of Unit EJ3.

Apparently, the contribution of the joint shear deformation to storey deflection can be neglected should the compressive axial column load be greater than $0.2 A_g f_c^{'}$ for exterior beam-column joint components.

7.5.6.3 *Joint Hoop Strains*

Fig.7.47 shows the measured strains in the joint hoops and the column transverse reinforcement adjacent to the joint core for test on Unit EJ4. All the measured strains were very small, and none of them was larger than 35×10^{-6}. Whereas in the case of thetest on Unit EJ2 the joint hoop strains in the mid-depth of the joint core were up to the steel yield level of 1600×10^{-6}, the joint hoops of Unit EJ4 were not significantly strained. This was because the enhanced diagonal concrete strut mechanism in the joint can transmit the member forces across the joint core without the expense of big joint lateral expansion.

Although the joint hoop strains were generally low, it still can be seen that the joint hoop strain at the joint mid-height was the largest when the beam bars are bent into the joint core. Hence different bending configurations of the beam bars in exterior column will actuate different joint shear mechanisms.

7.6.7 Displacement Components

Fig. 7.48 shows the measured displacement components for test of EJ4, where the contribution to storey displacement of the joint displacement was within 0.15 mm and it was ignored here. The contribution of column deformation to storey deflection considered here only came from the column deformation within the fixed-end region.

Fig.7.48 clearly shows that the major contribution to storey deflection was from the beam deformation, which consisted of 80% to 99% of the total storey displacement. Contribution of column deformation to storey displacement was relatively small because the columns were basically only in the early elastic range throughout the

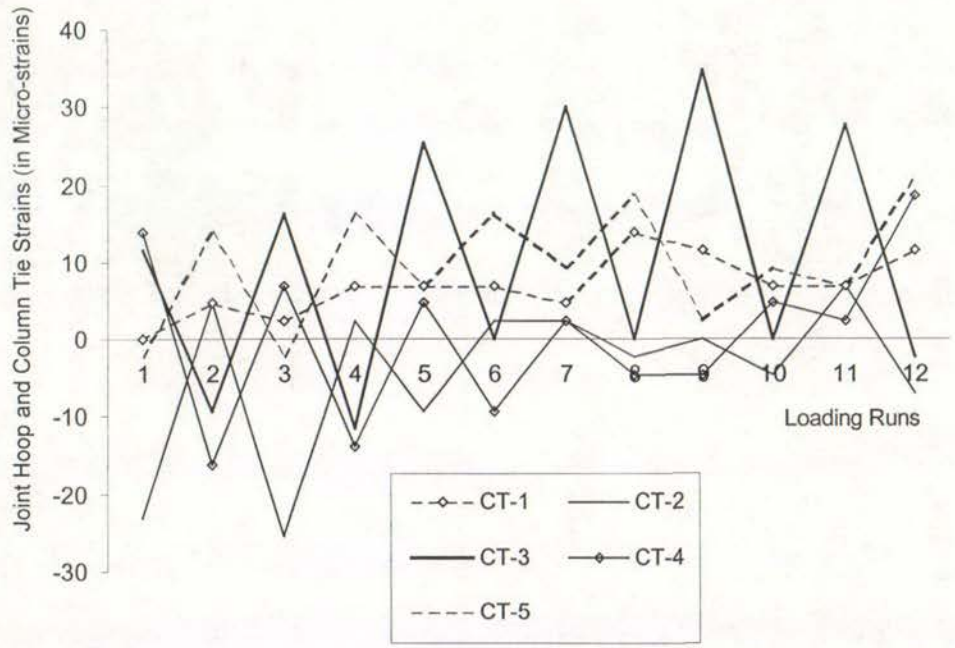

Fig.7.47 Strains Measured for Joint Hoops and Column Transverse Reinforcement

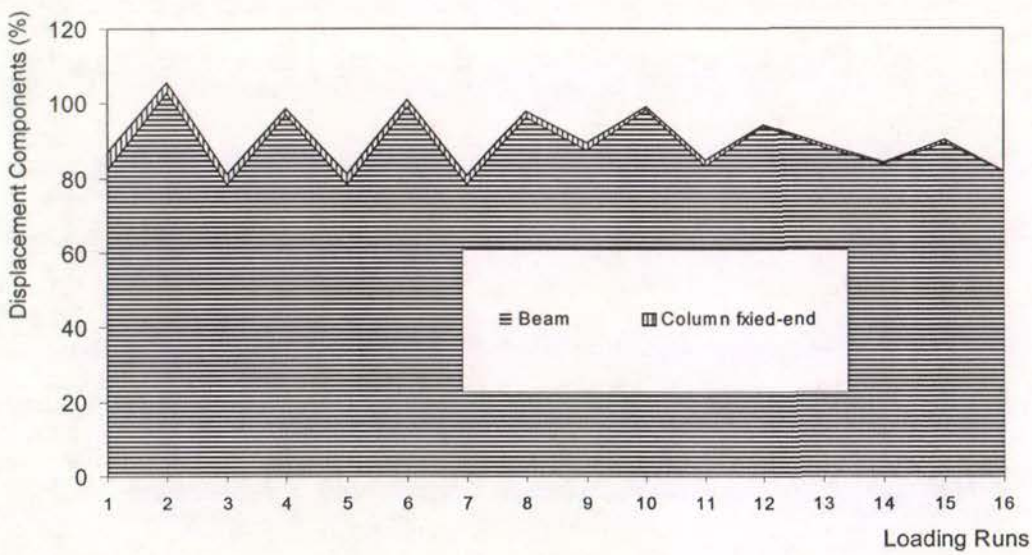

Fig. 7.48 Displacement Components Measured for Test of Unit EJ4

whole testing history. Evidently, the damage to the test unit EJ4 was limited to the beam.

In Fig.7.48, the contribution of column deformation to storey deflection was generally very small and it was observed to fluctuate in the same way as that of the beam deformation. The estimated total storey displacements obtained by summing up the contributions of beam and column deformations were significantly different from the measured storey displacements. This was because the measurements associated with the linear potentiometers over column fixed-end regions gave unreliable readings.

7.6.8 Summary

A full-scale exterior beam-column joint unit EJ4 was fabricated and tested under simulated seismic loading with the presence of a constant compressive axial column load of $0.23 A_g f_c^{'}$ in order to investigate the effect of axial column load on the seismic behaviour of exterior beam-column joint components. Test Unit EJ4 was identical to test unit EJ2, and the beam and columns had inadequate amount of transverse reinforcement and the joint core had very limited shear reinforcement as was common in existing reinforced concrete frame structures. The plain round beam longitudinal reinforcing bars were bent into the joint core in the exterior column as is current practice. Unit EJ3 and Unit EJ4 were identical except the arrangement of the beam bar hooks, and both units were tested with constant axial column load of 1800 kN present. Theoretical considerations showed that transverse reinforcement in the members could be very inadequate for Unit EJ4, especially in the beam, according to the requirement of shear resisting capacity and the requirement for preventing longitudinal bar buckling and confining the compressed concrete.

1. The test on Unit EJ4 showed that the overall performance of the test unit was again dominated by flexure only. The presence of a constant compressive axial column load of $0.23 A_g f_c^{'}$ for test of EJ4 greatly improved the seismic performance of otherwise similar reinforced concrete moment resisting frame structures when compared to the test on Unit EJ2, and the influence of the beam bar hook details on the overall seismic behaviour of the as-built exterior beam-column joint assemblies was found to be very small when compared to the test on Unit EJ3.

2. Compressive axial column load for test on Unit EJ4 enhanced the force transfer by bond from the beam tension steel to the surrounding concrete prior to the bend, and greatly reduced the beam steel tension force needed to be transferred at the bend. Consequently, the premature concrete tension cracking failure along the beam bar hook, which was associated with the interaction between the column bar buckling and the opening action of the beam bar hooks as occurred for the test on Unit EJ2, was entirely prevented during the test on Unit EJ4. The final failure of Unit EJ4 was initiated by the degrading beam flexural behaviour as for Unit EJ3.

The storey shear strengths were attained by the test on Unit EJ4 at a storey drift of 1.1% during clockwise loading but at a storey drift of 0.6% during anti-clockwise loading. The attained storey shear strength during clockwise loading was equal to the theoretical storey shear strength determined at the attainment of negative beam flexural strength, and the attained storey shear strength during anti-clockwise loading was about 16% less than the theoretical storey shear strength determined at the attainment of positive beam flexural strength.

The measured displacement at first yield for test of Unit EJ4 was equivalent to a storey drift of 0.53%.

3. Results of test on Unit EJ4 were contrasted to the results of test on Unit EJ2. Such a contrast revealed that the presence of compressive axial column load of $0.23\,A_g f_c^{'}$ for the test of EJ4 caused the measured initial stiffness to be 2.75 times the measured initial stiffness for test on Unit EJ2 and the attained storey shear strength by Unit EJ4 to increase by about 15% of the theoretical storey shear strength. Furthermore, compressive axial column load of $0.23\,A_g f_c^{'}$ for test of EJ4 also greatly improved energy dissipating capacity of the system due to significant improvement of beam flexural stiffness.

4. The results of the test on Unit EJ4 were also contrasted to the results of the test on Unit EJ3. The presence of the compressive axial column load of 1800 kN for the tests on Unit EJ3 and Unit EJ4 caused the effects of the different arrangements of the beam bar hooks in exterior column on the stiffness and strength attainment and maintenance as well as the energy dissipating capacity of the unit to be very small.

CHAPTER 8

CONCLUSIONS AND DISCUSSIONS

This simulated seismic load test series involved six as-built reinforced concrete beam-column joints and one retrofitted as-built exterior beam-column joint. The simulated seismic load tests on as-built beam-column joints were conducted as part of an investigation of the behaviour of existing reinforced concrete structures designed to pre-1970s codes when subjected to severe earthquake forces. The test on the retrofitted as-built exterior beam-column joint was conducted to investigate the possible retrofit technique for existing reinforced concrete building structures. Two of the as-built test units were identical full-scale interior beam-column joints, the other four as-built test units were identical full-scale exterior beam-column joints except the arrangement of the beam bar hooks in exterior column. The longitudinal and transverse reinforcement was from plain round bars. The as-built reinforced concrete beam-column joint test units were replicas of parts of the moment resisting frame of an existing building in Christchurch that was constructed in the 1950s. The as-built exterior beam-column joint with the beam bar hooks bent away from the joint core, Unit EJ1, was retrofitted after damaged by wrapping the column areas above and below the joint core using fibre-glass material, and tested again.

8.1 CONCLUSIONS FROM TESTS ON INTERIOR BEAM-COLUMN JOINT UNITS

For the tests on two identical interior beam-column joint units 1 and 2, Unit 1 was tested with zero axial column load, and Unit 2 with a constant axial column load of $0.12A_g f_c^{'}$, where $f_c^{'}$= concrete cylinder compressive strength and A_g= the gross column section area. The tests on these two as-built interior beam-column joints led to the following conclusions:

1. The measured stiffness of the Units was very low, being about 30% of the theoretical stiffness at first yield. Also, the storey shear strengths reached by Units 1 and 2 at a storey drift of 2% were 85% and 77%, respectively, of the theoretical strengths based

on the flexural strength of the members. Column bar buckling was found to be the cause of the eventual failure of both test units.

2. It was found that the compressive axial column load enhanced the column bar buckling and the joint shear failure, causing the attained strength expressed as the percentage of the theoretical strength to be reduced. The compressive axial column load did not improve the structural stiffness behaviour at all.

3. Comparative study of the test results of Unit 1, in which the axial column load was zero, with the results of test on an identical beam-column joint unit reinforced by deformed longitudinal reinforcement indicates that the utilisation of plain round longitudinal reinforcement results in lower structural stiffness and a lower strength attainment as a percentage of the theoretical strength. The utilisation of plain round longitudinal reinforcement enhances the joint shear capacity associated with the joint concrete diagonal strut, owing to severe bar slip. Therefore, the use of information on structural behaviour obtained from tests where deformed bars were used for longitudinal reinforcement could be misleading when estimating the probable seismic performance of existing reinforced concrete structures which are reinforced by plain round longitudinal reinforcement and have small amount of transverse reinforcement in members.

8.2 CONCLUSIONS FROM TESTS ON EXTERIOR BEAM-COLUMN JOINT UNITS

1. The results of simulated seismic loading tests on Units EJ1 and EJ2, which were conducted with zero axial column load present, showed very poor strength and stiffness behaviour, and the final failure of the as-built units was dominated by premature concrete tension cracking along the beam bar hooks, which was initiated by the interaction between the column bar buckling and the opening action of the beam bar hooks, irrespective of the beam bar hook details. The different beam bar hook details in exterior column were found to have significant influences on the structural strength and stiffness performance when the axial column compressive load was low. The different beam bar hook details were also found to enhance the need for column transverse reinforcement at different locations.

The attained storey shear strength by the as-built exterior beam-column joint unit EJ1, which had the beam bar hooks bent away from the joint core, was only 55% of the theoretical storey shear strength of the unit and it occurred at a storey drift of about 2%. In contrast, the attained storey shear strength by the as-built exterior beam-column joint unit EJ2, which had the beam bar hooks bent into the joint core, was about 75% of the theoretical storey shear strength of the unit and it occurred at a storey drift of about 1.5%. The observed improvement in the available storey shear force strength due to more adequate beam bar hook configuration for Unit EJ2 was as high as 20% of the theoretical storey shear strength when the axial column load was very low.

2. When contrasted to the results from Hakuto's tests on Units O6 and O7, it was found that the use of plain round longitudinal reinforcement totally suppressed the shear failure in the beam and the joint core which had occurred for Hakuto's tests on Units O6 and O7, but it resulted in significant reductions in the available storey force strength and stiffness, especially in the available stiffness. The use of plain round longitudinal reinforcement, although leading to much improved shear performance in the beam and the joint core, enhanced column bar buckling and the opening action of the beam bar hooks in tension, thus initiating the premature failure of concrete tension cracking along

the beam bar hooks. The storey shear strengths attained by Hakuto's Unit O7 and Unit O6 were respectively 75% and 100% of the theoretical storey shear strengths. The reduction in the attained storey shear strength due to the use of plain round longitudinal reinforcement was 20 to 25% of the theoretical storey shear strength of the units. The displacement measured at first yield by Hakuto's Unit O6 was about 28% the measured displacement at first yield for Unit EJ2, and this suggests that the use of plain round longitudinal reinforcement caused much more significant decrease in the attained initial stiffness of the unit, compared to the adverse effect on the attained storey shear force strength of the unit.

3. The simulated seismic loading tests on Units EJ3 and EJ4, which were conducted with the axial column compressive load of 0.23 to $0.25 A_g f_c^{'}$ present, showed that the presence of compressive axial column load of about $0.25 A_g f_c^{'}$ resulted in much improved seismic performance of the as-built test units, in terms of the attained force strength, structural stiffness and the energy dissipating capacity. Due to the presence of compressive axial column load of about $0.25 A_g f_c^{'}$, the force transfer by bond from the beam tension steel to the surrounding concrete was enhanced prior to the bend. As a result, the beam steel tension force needed to be transferred at the bend was reduced, and premature concrete tension cracking failure along the beam bar hook was entirely prevented and the seismic performance of the test units was dominated by the beam flexural behaviour.

The attained force strengths by tests on Units EJ3 and Unit EJ4 were of similar magnitude in terms of their theoretical storey shear strengths and they occurred at similar storey drift levels. The storey shear force strengths were attained by Unit EJ3 and Unit EJ4 at a storey drift of about 1.1 to 1.5% for clockwise loading direction but at a storey drift of about 0.6% for anti-clockwise loading, and they were approximately 10 to 12% less than the theoretical storey shear strengths. The initial stiffnesses measured for Unit EJ3 and Unit EJ4 were also similar, and they were equivalent to a storey drift of about 0.6% at first yield.

4. In comparison with the tests on the identical units but with zero axial column load, namely, the tests on Unit EJ1 and Unit EJ2, the presence of compressive axial column load of 0.23 to $0.25 A_g f_c^{'}$ not only caused the measured initial stiffness to increase by 88% and the available storey shear strength to increase by about 20 to 33% of the theoretical storey shear strengths, but also greatly improved the energy dissipating capacity of the system by reducing softening and pinching of the hysteresis loops.

5. For the retrofitted as-built exterior beam-column joint Unit REJ1, the simulated seismic load test was conducted with zero axial column load. The test on Unit REJ1 showed that fibre-glass jacketing in the column areas above and below the joint core controlled the premature concrete tension cracking failure associated with the interaction of column bar buckling and the opening action of the beam bar hooks, and actuated the alternative joint force path, which was a steeper concrete strut compared to corner to corner joint diagonal concrete strut. Consequently the attained force strength and stiffness were greatly enhanced, and the energy dissipating capacities of the system was enhanced as well. The final failure trigger became the degrading beam flexural behaviour. However, the attained force strength and stiffness by the retrofiited unit REJ1 were still low, and this was due to severe bond degradation along the plain round beam longitudinal bars.

6. The adverse effects on the attained force strength and stiffness properties due to the utilisation of the plain round longitudinal reinforcement were more severe for the as-built exterior beam-column joints, compared to the cases for the as-built interior beam-column joints.

8.3 DISCUSSIONS AND SUGGESTIONS

1. As described before, the seismic performance of the tests on Unit REJ1 and Units EJ3 and EJ4 was dominated by the beam flexural behaviour. According to capacity design principles, the reinforced concrete components would demonstrate satisfactory performance, in terms of the attained force strength and ductility capacity, if the non-linear seismic performance was dominated by the beam flexural behaviour. However, for the existing reinforced concrete components reinforced by plain round longitudinal bars, severe bond degradation along the member longitudinal bars meant that the theoretical member flexural strength could not be attained and the non-linear deformation was only limited to a major flexural crack at beam-column interface, rather than in a bigger plastic hinge region. This was demonstrated by tests on Unit REJ1, and Units EJ3 and EJ4. As a result, the seismic performance of the tested as-built and the retrofitted units was very poor in terms of the attained force strength and the attained structural stiffness. Hence, the real concern is the degradation of beam flexural behaviour, rather than the shear behaviour as was the case with deformed bars. Severe bond degradation along the plain round longitudinal bars used for linear concrete members not only led to low attainment of the member flexural strengths and the initial stiffnesses, but also led to significant degradation of the force strength and the stiffness as the loading progresses.

2. External wrapping of the as-built lap-spliced reinforced concrete columns tested at the University of Canterbury has demonstrated to be able to enhance the bond mechanism along the plain round column longitudinal bars. It is suggested that external wrapping, say fibre-glass wrapping, be applied to the beam area adjacent to the joint core of the existing exterior beam-column joint components where possible when plain round longitudinal bars are used. Such a retrofit is expected to improve the bond mechanism along the beam longitudinal bars adjacent to the joint core, leading to the increases in the attained beam flexural strength and the beam flexural stiffness. As a result, the degradation of the beam flexural behaviour could be greatly reduced and the overall seismic performance of similar weak beam-strong column systems greatly improved.

Fatigue behaviour of the retrofitted members in such a way apparently needs to be studied.

3. The flexible performance of the units in the elastic range (approximately 2% storey drift at first yield) suggests that the interaction of such frames with masonry infills should not be ignored. Many frame buildings designed to pre-1970s seismic codes have masonry infills which are not separated from the frames. In addition, the flexible performance of the test units also suggests that P-Δ effects of similar existing reinforced concrete frame buildings should be allowed for.

4. Observed concentration of member flexural deformation on the major flexural crack at beam-column interfaces suggests that the structural dynamic analysis could alternatively use a flexural spring at the end of member, rather than a concept of plastic hinge region. In this case, a flexural spring describes the moment capacities and flexural rotation hysteretic behaviour. This is simply because the ordinary determination of the plastic hinge length can not be used and the total rotation over the fixed-end region, which is much smaller than plastic hinge region, can be a better indicator for member flexural deformation.

Therefore, adequate modelling of the member's fixed-end rotation behaviour becomes very important and suitable models, which can distinguish the differences in terms of deformation response between the well design reinforced concrete member and existing reinforced members containing plain round longitudinal bars apparently are needed. One important consideration in this aspect is the distinction between rotational capacity and ductility capacity of the members is important, because concrete members reinforced by plain round bars, although leading to large member rotation capacity, do not perform in a ductile manner.

5. Tests on four full-scale one-way as-built exterior beam-column joint units showed that (1). the seismic performance of the as-built exterior beam-column joint components reinforced by plain round longitudinal bars would be governed by the premature concrete tension cracking failure along the plain round beam bar hooks, irrespective of the beam bar hook details, when the axial column compressive load is very low. (2). the seismic

performance of the as-built exterior beam-column joint components reinforced by plain round longitudinal bars would be governed by the degrading beam flexural behaviour and the effect of the beam bar hook details would be very small, when the axial column compressive load is high, at least, $0.23 A_g f_c^{'}$.(3). No shear failure in the beam and the joint core was detected, indicating that the shear performance of concrete linear members and the joint cores would not hamper the seismic performance of the tested components. Hence, as far as the seismic assessment of existing reinforced concrete frame structures are concerned, the attainment and maintenance of the force strengths of the critical failure mechanisms, premature concrete tension cracking failure along the plain round beam bar hooks and the degrading beam flexure, need to be investigated. This is seen in Chapter 8.

6. Simulated seismic load tests in this project demonstrated that the storey drift, rather than the displacement ductility based on the measured yield displacement, should be used as the indicator of the imposed displacement level when the plain round longitudinal bars are used. Hence, the information on member local behaviour should be associated with the storey drift index.

REFERENCES

[A1] Aoyama, H., "A method for the Evaluation of the seismic Capacity of Existing Reinforced Concrete Buildings in Japan", *Bulletin of the New Zealand National Society for Earthquake Engineering*, Vol.14, No.3, Sept. 1981, pp105-130

[A2] Aoyama, H., "Outline of Earthquake Provisions in the Recently Revised Japanese Building Code", *Bulletin of the New Zealand National Society for Earthquake Engineering*, Vol.14, No.2, June 1981

[A3] ATC, " A Handbook for Seismic Evaluation of Existing Buildings ATC-22", *Applied Technology Council*, Redwood City, California, ATC21, 1989, 169pp

[A4] ATC, "Rapid Visual Screening of Buildings for Potential Seismic Hazards: A Handbook, *Applied Technology Council,* Redwood City, California, ATC21,1988

[A5] ATC, "Evaluating the Seismic Resistance of Existing Buildings ATC-14" *Applied Technology Council*, Redwood City, California, 1987,370pp

[A6] Aycardi, L. E., Mander, J. B., and Reinhorn, A. M., "Seismic Resistance of Reinforced Concrete Frame Structures Designed Only for Gravity Loads: Part II - Experimental Performance of Subassemblages", *Technical Report NCEER-92-0028,* December 1, 1992

[A7] Alcocer, S.M., and Jirsa, J.O., "Strength of Reinforced Concrete Frame Connections Rehabilitated by Jacketing" Structural Journal of American Concrete Institute, Vol.90, No.3, May 1993

[B1] Brunsdon, D. R and Priestly, M.J.N., "Assessment of Seismic Performance Characteristics of Reinforced Concrete Buildings Constructed Between 1936 and 1975", *Bulletin of the New Zealand National Society for Earthquake Engineering*, Vol. 17, No.3, Sept. 1984, pp.163—181

[B2] Benuska, L., "Loma Prieta Earthquake Reconnaissance Report", *Earthquake Spectra, EERI, Supplement to* Vol.6, No.1, 1990, pp 151-187

[B3] Beres, A., White, R.N., and Gergely,P., "Seismic Behaviour of Reinforced Concrete Frame Structures With Non-ductile Details: Part I - Summary of Experimental Findings of Full-Scale Beam-Column Joint Tests", *Technical Report NCEER-92-0024,* September 30, 1992

[B4] Beres, A., White, R.N., and Gergely,P., "Detailed Experimental Results of Interior and Exterior Beam-Column Joint Tests Related to Lightly Reinforced Concrete Frame Buildings", *Technical Report 92-7, Cornell University, Ithaca, NY*, 1992

[B5] Bracci, J.M., Reinhorn, A. M., and Mander, J. B., "Seismic Resistance of Reinforced Concrete Frame Structures Designed Only for Gravity Loads: Part I - Design and Properties of a One-Third Scale Model Structure", *Technical Report NCEER-92-0027,* December 1, 1992

[B6] Bracci, J.M., Reinhorn, A. M., and Mander, J. B., "Seismic Resistance of Reinforced Concrete Frame Structures Designed Only for Gravity Loads: Part III - Experimental Performance and Analytical Study of a Structural Model", *Technical Report NCEER-92-0029,* December 1, 1992

[C1] Collins, M.P., and Mitchell, D., "*Prestressed Concrete Structures*", Response Republications, Canada, 1997

[C2] Cheung, P. C., Seismic Design of Reinforced Concrete Beam-Column Joints with Floor Slab, *Research Report 91-4, Department of Civil Engineering, University of Canterbury*, Oct. 1991

[C3] Clough, R.W., Benuska,K.L, Wilson,E.L.,"Inelstic Earthquake Response of Tall Building", *Proceedings of Third World Conference on Earthquake Engineering*, New Zealand, Vol. Section II, pp68-89(1965)

[C4] Carr, A. "*RUAUMOKO - Inelastic Dynamic Analysis*", Department of Civil Engineering, University of Canterbury, 1996

[C5] Crisafulli, F. J. et al, "Seismic Behaviour of Reinforced Concrete Structures with Masonry Infills", *Doctoral Thesis, Department of Civil Engineering, University of Canterbury*, 1997

[C6] Chapman, H.E., "Seismic Retrofitting of Highway Bridges", *Bulletin of the New Zealand National Society for Earthquake Engineering*, Vol.24, No.2, June 1991, pp186-201

[C7] Clough, R.W., Benuska, K.L., and Lin, T.Y., "FHA Study of Seismic Design Criteria for High Rise Buildings, HUDTS-3", Aug., 1966, *Federal Housing Administration, Washington, D.C.*

[D1] Dekker, D. R. and Park, R., " The Repair and Strengthenening of Reinforced Concrete Bridge Piers", *Research Report 92-1, Department of Civil Engineering, University of Canterbury,* March 1992.

[D2]. Dowell, R. K., Seible, F. and Wilson, E. L., " Pivot Hysteresis Model for Reinforced Concrete Members", *ACI Structural Journal*, Vol.95, No.5, Sept-Oct. 1998 pp607-617

[E1] El - Attar, A. G., White, R. N., and Gergely, P., " Behaviour of Gravity Load Designed Reinforced Concrete Buildings Subjected to Earthquakes", *ACI Structural Journal*, Vol.94, No.2, March-April 1997, pp133-145

[F1] Fenwick, R.C. and Megget, L.M., "Elongation and Load Deflection Characteristics of Reinforced Concrete Members Containing Plastic Hinges", *Bulletin of the New Zealand National Society for Earthquake Engineering*, Vo.26, No.1, March 1993, pp28-41

[F2] Filippou, F.C., D'Ambrisi, A. and Issa,A., "Effects of Reinforcement Slip on hysteretic Behaviour of Reinforced Concrete Frame Members", *ACI Structural Journal*, Vol.96, No.3, May-June 1999, pp327-335

[G1] Giberson, M.F., "The Response of Nonlinear Multi-story Structures subjected to Earthquake Excitation", *Earthquake Engineering Research Laboratory, California Institute of Technology Pasadena, California, EERL Report* (1967).

[G2] Giberson, M.F., "Two Nonlinear Beams with Definitions of Ductility", *Journal of the Structural Division, Proceedings of the American Society of Civil Engineers*, Vol. 95, No.ST2, Feb. 1969, pp137-157.

[H1] Hakuto, S., Park, R. and Tanaka, H., "Retrofitting of Reinforced Concrete Moment Resisting Frames", *Research Report 95-4, Department of Civil Engineering, University of Canterbury,* August 1995

[H2] Hakuto, S., Park, R. and Tanaka, H., "Behaviour of As-Built and Retrofitted Beam-Column Joints of a 1950s Designed Reinforced Concrete Building Frame", *Proceedings of Technical Conference of New Zealand Concrete Society*, Taupo, New Zealand, March 1995

[H3] Hakuto, S., Park, R. and Tanaka, H., "Seismic Performance of Existing Reinforced Concrete Building Frames", *Proceedings of Technical Conference of New Zealand Concrete Society*, Taupo, New Zealand, March 1995

[H4] Hill, G., "Guild to Instrumentation, Transducers, and Data Loggers", *Department of Civil Engineering, University of Canterbury*, December 1995

[H5] Hakuto, S., Park, R. and Tanaka, H., "Effect of deterioration of Bond of Beam Bars Passing Through Interior Beam-Column Joints on Flexural Strength and Ductility", *ACI Structural Journal*, Vol.96, No.5, September-October 1999, pp858-864

[H6] Hwang, S. J. and Lee, H. J., "Analytical Model for Predicting Shear Strength of Exterior Reinforced Concrete Beam-Column Joints for Seismic Resistance", *ACI Structural Journal*, Vol.946, No.5, September-October 1999, pp846-857

[J1] Jury, R. D., " A Decade of Progress Since the Edgecumbe Earthquake-Buildings", *Bulletin of the New Zealand National Society for Earthquake Engineering*, Vol.30, No.2, June 1997, pp174-176

[J2] Jara, M., Hernandez, C., Garcia, R. and Robles, F., " The Mexico Earthquake of September 19, 1985. Typical Cases of Repair and Strengthening of Concrete Buildings", *Earthquake Spectra*, Vol. 5, No.1, California, USA, Feb.1989

[K1]. Kunnath, Sashi K., Reinhorn Andrei M. and Park, Young J., "Analytical Modeling of Inelastic Seismic Response of R/C Structures", *Journal of Structural Engineering, ASCE*, Vol. 116, No.4 April 1990, pp996-1017

[K2]. Kabeyasawa, T., Shiohara, H., Otani, S., and Aoyama, H., "Analysis of the Full-Scale Seven-Story reinforced Concrete Test Structure", *Journal of the Faculty of Engineering, the University of Tokyo (B)*, Vol. XXXVII-I, March 1983, pp431-478

[K3]. Kitayama, K., Otani,S., and Aoyama, H., "Earthquake Resistant Design Criteria for Reinforced Concrete Interior Beam-Column Joints", *Proceedings of Pacific Conference on Earthquake Engineering*, 1987, Wairakei, Vol. 1, pp315-326

[L1] Liu, A. and Park, R., " Seismic Load Tests on Two Interior Beam-Column Joints Reinforced by Plain Round Bars Designed to Pre-1970s Seismic Codes", *Bulletin of the New Zealand National Society for Earthquake Engineering*, Vol.31, No.3, Sept. 1998.

[L2] Lees, J.M. and Burgoyne, C. J., "Experimental Study of Influence of Bond on Flexural Behaviour of Concrete Beams Pretensioned with Aramid Fiber Reinforced Plastics", *ACI Structural Journal*, Vol.96, No.3, May-June 1999, pp377-385

[L3] Lees, J.M. and Burgoyne, C. J., "Rigid Body Analysis of Concrete Beams Pre-Tensioned with Partially Bonded AFRP Tendons", Proceedings of the Third International Symposium on Non-Metallic (FRP) Reinforcement for Concrete Structures, Japan Concrete Institute, Japan, Oct. 1997, pp759-766

[M1] Maffei, J., Seismic Evaluation & Retrofit Technology for Bridges, *Transfund New Zealand Research Report*, No.78, 1997

[M2] Maffei, J., Seismic Testing & Behaviour of A 1936-Designed Reinforced Concrete Bridge, *Transfund New Zealand Research Report*, No.78, 1997

[M3] Moehle, J.P., "Preliminary Report on the Seismological and Engineering Aspects of the January 17,1994 Northridge Earthquake", *Report UCB/EERC-94-01, Earthquake Engineering Research Center, University of California at Berkeley*, 1994

[M4] Mahin, S.A. and Bertero, V.V., "An Evaluation of Inelastic Seismic Design Spectra", *American Society of Civil Engineering*, Vol.107, No.ST9, Sept. 1981, pp1777-1795

[M5] Marti, P., "How To Treat Shear in Structural Concrete", *ACI Structural Journal*, Vol.96, No.3, May-June 1999, pp408-414

[M6] Moehle, J.P., Nicoletti, J.P., Lehman, D.E., "Review of Seismic Research Results on Existing Buildings", *Report No. SSC 94-03, Seismic Safety Commission, State of California,* Fall 1994.

[M7] Magenes and Calvi, "In-Plane Seismic Response of Brick Masonry Walls", Earthquake Engineering and Structural Dynamics, Vol. ?, No.?, pp? Year ? 1997

[N1] NZS3101: 1995, "The Design of Concrete Structures, NZS3101: 1995", *Standards New Zealand,* Wellington, 1995

[N2] Norena F, Castaneda C and Iglesias J "The Mexico Earthquake of September 19, 1985, Evaluation of the Seismic Capacity of Buildings in Mexico City" *Earthquake Spectra,* Vol.5, No.1 California, USA, February 1989

[N3] *"A draft document of Guidelines for the Seismic Assessment of pre-1975 Reinforced Concrete Structures and Structural Steel Buildings"*, prepared by a study group of the

New Zealand National Society for Earthquake Engineering for the Building Industry Authority, April 1994.

[N4] "*The Assessment and Improvement of the Structural Performance of earthquake Risk Buildings, Draft for General Release*", New Zealand National Society for Earthquake Engineering, June 1996, pp122

[O1] Ohkubo, M., "*A Note for the Seminar on the Method for Evaluating Seismic Performance of Existing Reinforced Concrete Buildings*", Kyushu Institute of Design, 1990

[O2] Otani, S. and Sozen, M.A.,"Behaviour of Multistory Reinforced Concrete Frames during Earthquakes", *Structural Research Series No.392, University of Illinois, Urbana, Illinois* (1972)

[O3] Otani, Shunsuke, "Nonlinear Dynamic Analysis of Reinforced Concrete Structures", *Canadian Journal of Civil Engineering*, Vol.7, No.2, pp333-344 (1980).

[O4] Otani, Shunsuke, "Hysteresis Models of Reinforced Concrete for Earthquake Response Analysis", *Journal of the Faculty of Engineering, The University of Tokyo (B)*, Vol. XXXVI, No.2, pp407 - 441 (1981).

[P1] Park, R. and Paulay, T., *Reinforced Concrete Structures*, John Wiley & Sons, New York, 1975, p769

[P2] Park, R "Review of Code Developments in New Zealand", *Bulletin of New Zealand National Society for Earthquake Engineering*, Vol 104, No.3, 1981

[P3] Park, R., "Seismic Assessment and Retrofit of Concrete Structures-United States and New Zealand Developments", *Proceedings of Technical Conference of New Zealand Concrete Society, Wairakei*, 1992, pp18-25

[P4] Priestley, M.J.N, and Calvi, G.M., "Towards a Capacity Design Assessment Procedure for Reinforced Concrete Frames", *Earthquake Spectra*, Vol.7, No.3, 1991, pp413-437

[P5] Priestley, M.J.N., " Displacement Based Seismic Assessment of Existing Reinforced Concrete Buildings", *Proceedings of Pacific Conference on Earthquake Engineering, Vol.2, Melbourne,* 1995, pp 225-244

[P6] Park, R., "A Static Force-Based Procedure for the Seismic Assessment of Existing Reinforced Concrete Moment Resisting Frames", *Bulletin of the New Zealand National Society for Earthquake Engineering*, Vol.30, No.3, 1997, pp213-226

[P7] Park,R, I J Billings, G C Clifton, J Cousins, A Filiatrault, D N Jennings, LCP Jones, N D Perin, S L Rooney, J Sinclair, D D Spurr, H Tanaka and G Walker (1995) " The Hyogo-ken Nanbu Earthquake(The Great Hanshin Earthquake) of 17 January 1995. Report of the NZNSEE Reconnaissance Team, *Bulletin of the New Zealand National Society for Earthquake Engineering,* Vol.28, No.1, 1995, pp1- 98

[P8] Park, R., "Evaluation of Ductility of Structures and Structural Assemblages from the Laboratory Testing", *Bulletin of the New Zealand National Society for Earthquake Engineering*, Vol.22, No.3, Sept. 1989, pp 155-166

[P9] Priestley, M.J.N., Seible, F., and Calvi, G. M., " *Seismic Design and Retrofit of Bridges*", John Wiley & Sons, Inc., New York, 1996, p686

[P10] Paulay, T., Equilibrium Criteria for Reinforced Concrete Beam-Column Joints, *ACI Structural Journal*, Nov.-Dec. 1989 P635-643

[P11] Paulay,T., and Priestley, M.J.N., *Seismic Design of Reinforced Concrete and Masonry Buildings*, John Wiley & Sons, Inc., New York, 1992

[P12] Priestley, M.J.N., Seible, F., and Calvi, G.M., *Seismic Design and Retrofit of Bridges*, John Wiley & Sons, Inc. USA, 1996

[P13] Paulay, T. and Scarpas, A., "The Behaviour of Exterior Beam-Column Joints", *Bulletin of the New Zealand National Society for Earthquake Engineering*, Vol.14, No.3, Sept. 1981, pp131-144

[P14] Park, R., Gaerty, L. and Stevenson, E. C., " Tests on an Interior Reinforced Concrete Beam-Column Joint", *Bulletin of the New Zealand National Society for Earthquake Engineering*, Vol.14, No.2, June 1981, pp81-92

[P15] Pessiki, S.P., Conley, C.H., Gergely, P., and White, R.N., " Seismic Behaviour of Lightly-Reinforced Concrete Column and Beam-Column joint Details", *Technical Report NCEER-90-0014,* August 2, 1990

[P16]. Pantazopoulou, S.J., Moehle, J.P., and Shahrooz, B.M., " Simple Analytical Model for T-Beams in Flexure", *Journal of Structural Engineering, ASCE,* Vol.114, No.7, July 1988, pp1507-1523

[P17] Priestley, M.J.N., and Kowalsky, M.J., "Aspects of Drift and Ductility Capacity of Rectangular Cantilever Structural Walls" *Bulletin of the New Zealand National Society for Earthquake Engineering*, Vol 31, No.2, 1998, p73-85

[P18] Priestley, M.J.N., "Brief Comments on Elastic Flexibility of Reinforced Concrete Frames and Significance to Seismic Design", *Bulletin of the New Zealand National Society for Earthquake Engineering*, Vol.31, No.4, 1998, p246-259

[P19] Park, R., "Ductility Evaluation from Laboratory and Analytical Testing", State –of- art Report in Special Theme Session SG on Ductility Evaluation and Design of Concrete Structures and Elements, *Proceedings of the 9th WCEE*, Tokyo/Kyoto, 1988, Vol. VIII, pp 605-615

[P20] Paulay, T., "Displacement Compatibility Considerations in the Seismic Design of Buildings", *Department of Civil Engineering, University of Canterbury*, Oct. 1998

[P21] Prietley, M.J.N and Calvi, G.M., "Concepts and Procedures for Direct Displacement-Based Design and Assessment", *Proceedings of the International Workshop on Seismic Design Methodologies for the Next Generation of Codes,* Belkema, Rotterdam, 1997, pp 171-181

[P22] Prietley, M.J.N. " Displacement-Based Seismic Assessment of reinforced Concrete Buildings", *Journal of Earthquake Engineering,* Vol.1, No.1, 1997, pp157-192

[P23] Priestley, M J N, Seible F and Chai Y H., " Design Guildlines for Assessment, Retrofit and Repair of Bridges for Seismic Performance" Report SSRP92-01, University of California, San Diego, 1992.

[P24] Priestley, M.J.N. and Seible, F., "Design of Seismic Retrofit Measures for Concrete Bridges", Seismic Assessment and Retrofit of Concrete Broidges, Report SSRP 91-03, University of California, San Diego, 1990, pp196-234

[P25] Priestley, M.J.N, Fyfe, E., and Seible, F.,"Column Retrofit Using Fiberglass-Epoxy Jackets", First Annual Seismic Research Workshop, California Department of Transportation, Sacamento, Dec.1991, pp 217-224

[R1] Rodriguez, M. and Park, R., "Repair and Strengthening of Reinforced Concrete Buildings for Earthquake Resistance", *Earthquake Spectra*, Vol. 7, No.3, 1991, pp439-459

[R2] Rodriguez, M. and Park, R., "Seismic Load Tests of Reinforced Concrete columns Strengthened by Jacketing", *Structural Journal of the American Concrete Institute*, Vol. 91, No.2, 1994, pp150-159

[R3] Rodriguez, M. and Park, R., "Seismic Load Tests of Reinforced Concrete Columns Strengthened by Jacketing", *Proceedings of the annual Technical Conference of the New Zealand Concrete Society*, Wairakei, Sept. 1990, pp72 - 83.

[S1] SANZ(1976), *Code of Practice for General Structural Design and Design Loadings for Buildings NZS 4203:1976*, Standards Association of New Zealand, Wellington

[S2] SANZ(1982), *Code of Practice for the Design of Concrete Structures NZS 3101 Part 1:1982, and Commentary on the Design of Concrete Structures NZS 3101 Part 2:1982*, Standards Association of New Zealand, Wellington

[S3] SNZ(1992), *Code of Practice for General Structural Design and Design Loadings for Buildings NZS 4203:1992, Volumn 1 Code of Practice and Volumn 2 Commentary,* Standards Association of New Zealand, Wellington

[S4] SNZ(1995), *Part 1 The Design of Concrete Structures and Part2 Commentary on the Design of Concrete Structures*, Concrete Structures Standard, NZS 3101:1995, Standards Association of New Zealand, Wellington

[S5] Sugano, S., "Seismic Capacity Evaluation of Existing Reinforced Concrete Buildings in Japan", *A Seminar Note at University of Canterbury*, April 1995

[S6] Satyarno, I., "Adaptive Pushover Analysis for the Seismic Assessment of Older Reinforced Concrete Buildings", Doctoral Thesis, Department of Civil Engineering, University of Canterbury, 2000

[S7] Shibata, A., and M.A. Sozen, "Substitute Structure Method for Seismic Design in Reinforced Concrete", *Journal of Mechanics Division, ASCE*, Vol. 102, No.ST1, 1976, pp1-18

[S8] Shiohara, Hitoshi "A New Model for Joint Shear Failure of Reinforced Concrete Interior Beam-Column Joints", *Journal of the School of Engineering, The University of Tokyo*, Vol. XLV (1998), pp15-40

[S9] Stoppenhagen, D.R.,and Jirsa, J.O., "Seismic Repair of a reinforced Concrete Frame using Encased Columns", University of Texas at Austin, PMFSEL, 1987 May, Report No.87-1

[S10] Stewart, W.G. "The Seismic Design of Plywood Sheathed Shear Walls", Ph.D Thesis, *Department of Civil Engineering, University of Canterbury, Christchurch, NZ*, 1987, pp395

[T1] Takeda, T. Sozen, M.A. and Nielsen, N.N., "Reinforced Concrete Response to Simulated Earthquakes", *J. Struct. Engrg. Div., ASCE*, V.96, No.12, 1970, pp2257-2573

[W1] Wallace, J., " Behaviour of Beam Lap Splices under Seismic Loading, Master of Engineering Thesis, *Department of Civil Engineering, University of Canterbury*, 1996

APPENDIX ONE:

SEISMIC ASSESSMENT OF TEST UNITS

1. FLEXURAL STRENGTH CALCULATION OF BEAMS AND COLUMNS

Calculation Rules:

- Equilibrium equation using New Zealand Code Approach NZS3101:1995 was

$$\alpha_1 f_c' \, a \, b + A_s' \, f_s' = A_s \, f_y + N^* \qquad (1.1)$$

where: N^* is the applied axial load, N^* is positive if in compression and negative if in tension, see Fig.A-1; a is the depth of equivalent rectangular concrete compressive zone, a = β c, and c is the depth of concrete compressive zone in calculating the strains using plane section assumption; A_s' and f_s' are the flexural compressive steel area and the compressive steel stress in flexural compression steel respectively; A_s and f_y are the flexural tension steel area and the steel tension stress in flexural tension steel; b is the width of the member.

- β is 0.85 if $f_c' \leq 30$ MPa, however, if $f_c' > 30$ MPa, $\beta = 0.85 - 0.008 \, (f_c' - 30)$

but $\beta \geq 0.65$ has to be satisfied.

- $\alpha_1 = 0.85$ for $f_c' \leq 55$ MPa, and $\alpha_1 = 0.85 - 0.004(f_c' - 55)$ for $f_c' > 55$MPa, but α_1 must be not less than 0.75.
- Compressive flexural steel strain is found by using plane section theory and assuming the extreme concrete compressive strain is 0.003 as follows:

$$\varepsilon_s' = \frac{c - d'}{c} 0.003 \qquad (1.2)$$

$$f_s' = \varepsilon_s' E_s = 600 \, \frac{c - d'}{c} \qquad (1.3)$$

- Flexural strength can be found using the following equation:

$$M_b = A_s \, f_y (d - d') + \alpha_1 \, f_c' \, a \, b \, (d' - a/2) \qquad (1.4)$$

$$M_c = A_s \, f_y (d - \frac{h}{2}) + A_s' \, f_s' (d - \frac{h}{2}) + \alpha_1 \, f_c' \, a \, b \, (\frac{h}{2} - \frac{a}{2}) \qquad (1.5)$$

The diagrams for beam and column flexural strength calculation are illustrated in Fig. A-1.

The dimensions and reinforcing amounts used in beam and column strength calculation is listed in Table 1.1(a) and Table 1.1(b) for the interior beam column joint units and the exterior beam-column joint units respectively. It is noted that the two interior beam column joint units had the same dimensions and the same amount of reinforcing bars, and the four

exterior beam-column joint units had the same dimensions and the same amount of reinforcing bars except the beam bar hook details in exterior columns.

Table 1.1(a) Dimensions and Reinforcing Detail Parameters of Units 1 and 2

	For beam positive bending	For beam negative bending	For column bending
As (mm^2)	905	1809.6	1357
As'(mm^2)	1809.6	905	1357
p (%)	0.656	1.31	1.13
p' (%)	1.31	0.656	1.13
d (mm)	460	460	260
d'(mm)	40	40	40
b (mm)	300	300	460
$E_s(MPa)$	$2\times10^5 MPa$		

Table 1.1(b) Dimensions and Reinforcing Detail Parameters of Units EJ1 through EJ4

	For beam positive bending	For beam negative bending	For column bending
As (mm^2)	905	1357	905
As'(mm^2)	1357	905	905
p (%)	0.656	0.983	0.468
p' (%)	0.983	0.656	0.468
d (mm)	460	460	420
d'(mm)	40	40	40
b (mm)	300	300	460
$E_s(MPa)$	$2\times10^5 MPa$		

Table 1.2 Parameters $f_c^{'}$, f_y, f_{yt} N^*, α_1 and β for all units

Unit	$f_c^{'}$ (MPa)	f_y (MPa)	f_{yt} (MPa)	N^* (N)	α_1	β
Unit 1	43.8	321	318	0.0	0.85	0.74
Unit 2	48.9	321	318	800,000	0.85	0.70
Unit EJ1	34.0	321	318	0.0	0.85	0.82
Unit EJ2	29.2	321	318	0.0	0.85	0.85
Unit EJ3	34.0	321	318	1,800,000	0.85	0.82
Unit EJ4	36.5	321	318	1,800,000	0.85	0.80

To simplify the calculation of the member flexural strength, the parameters f_c', f_y, N^*, α_1 and β are summarised in Table 1.2 for all units, and the calculated member flexural strengths is summarised in Table 1.3 for all the units.

Table1.3 Member Flexural Strength of Test Units

Unit	Beam Negative Bending	Beam Positive Bending	Column
Unit 1	c = 53.6 mm a = 39 mm	c = 39 mm a = 29 mm	c = 38 mm a = 28 mm
	$M_b^- = 250$ kN-m	$M_b^+ = 129$ kN-m	$M_c = 108$ kN-m
Unit 2	c = 51.8 mm a = 36 mm	c = 38 mm a = 27 mm	c = 67 mm a = 47 mm
	$M_b^- = 251$ kN-m	$M_b^+ = 129$ kN-m	$M_c = 198$ kN-m
Unit EJ1	c = 48.2 mm a = 40 mm	c = 40.2 mm a = 33 mm	c = 34.5 mm a = 28.3 mm
	$M_b^- = 190$ kN-m	$M_b^+ = 129$ kN-m	$M_c = 120$ kN-m
Unit EJ2	c = 56.7 mm a = 43 mm	c = 41.4 mm a = 35.2 mm	c = 36.1 mm a = 30.6 mm
	$M_b^- = 189$ kN-m	$M_b^+ = 128$ kN-m	$M_c = 119$ kN-m
Unit EJ3	c = 48.2 mm a = 40 mm	c = 40.2 mm a = 33 mm	c = 154.8 mm a = 127 mm $f_s' = 600\frac{c-40}{c} > 321$ $f_s' = 321$MPa
	$M_b^- = 190$ kN-m	$M_b^+ = 129$ kN-m	$M_c = 392$ kN-m
Unit EJ4	c = 47.3 mm a = 37.8 mm	c = 39.8 mm a = 31.8 mm	c = 148.3 mm a = 118.7 mm $f_s' = 600\frac{c-40}{c} > 321$ $f_s' = 321$MPa
	$M_b^- = 190$ kN-m	$M_b^+ = 129$ kN-m	$M_c = 400.0$ kN-m

The ratio of the sum of column moment capacity to the sum of beam moment capacity, calculated at the centre-line of the joint core, is listed in Table 1.4 for all test units.

Table 1.4 Ratio of Column Flexural Strength to Beam Flexural Strength at a Joint

Units	Unit 1	Unit 2	Unit EJ1	Unit EJ2	Unit EJ3	Unit EJ4
$\sum M_c / \sum M_b$	0.63	1.16	2.07 (+) 1.40 (-)	2.07 (+) 1.40 (-)	6.76 (+) 4.59 (-)	6.90 (+) 4.68 (-)

(+) means that the value is associated with the positive beam bending direction and (-) means that the value is associated with the beam negative bending direction.

From Table 1.4, it is clear that Unit 1 would develop plastic hinges in columns, but Unit 2 would develop plastic hinges in beams. For all the four exterior beam-column joint units EJ1 through EJ4, the beam would develop plastic hinge.

2. CALCULATION OF MEMBER YIELD CURVATURES

(1). Depth of Concrete Compressive Zone at First Yield:

- **For Beams and Columns without Axial Load**

Members should be still in the elastic range at first yield stage. In this case, the depth of the concrete compressive zone can be found by assuming a triangular distribution of concrete compressive stress. Under this assumption, k can be found as follows for the member with zero axial load [P1]:

$$k = [(\rho + \rho')^2 n^2 + 2(\rho + \frac{\rho' d'}{d})n]^{\frac{1}{2}} - (\rho + \rho')n \qquad (1.6)$$

where k is the coefficient of the concrete compressive zone, kd is the depth of the concrete compressive zone, and n is the ratio of steel elastic modulus to concrete elastic modulus.

$E_s = 2 \times 10^5 MPa$ for all units, and $E_c = 3320\sqrt{f_c'} + 6900(MPa)$ = 28872, 30116, 26259, 24840, 26259 and 20958 MPa, according to NZS3101:1995, for Units 1, 2, EJ1, EJ2, EJ3 and EJ4 respectively. When ACI equation $E_c = 4730\sqrt{f_c'}(MPa)$ is used, E_c = 31303, 33076, 27580, 25560, 27580 and 28576 MPa, for Units 1, 2, EJ1, EJ2, EJ3 and EJ4 respectively. Using the second set of concrete elastic modulus, the ratio of steel elastic modulus to concrete elastic modulus is calculated and listed in Table 1.5.

Table 1.5 Ratio of Steel Elastic Modulus to Concrete Elastic Modulus

Unit	Unit 1	Unit 2	Unit EJ1	Unit EJ2	Unit EJ3	Unit EJ4
$n = E_s / E_c$	6.4	6.0	7.3	7.8	7.3	7.0

- **For Columns with Compressive Axial Load**

Say the compressive axial load is N^*, assuming that concrete compressive stress be in elastic range, so use the following equation to find k at the first yield stage (see Fig.A-2),

$$A_s f_y + N^* = A_s' \varepsilon_s' E_s + \frac{1}{2} kd \varepsilon_c E_c b \qquad (1.7)$$

$$\varepsilon_s' = (kd - d')/(d - kd)\varepsilon_y \qquad (1.8)$$

$$\varepsilon_c = kd/(d - kd) \times \varepsilon_y \qquad (1.9)$$

(2). Member Curvature and Moment Capacity at First Yield

$$\Phi_y = \frac{f_y}{E_s d(1-k)} \qquad (1.10)$$

$$M_y = A_s f_y (\mathrm{d}-\frac{1}{3} kd) + A_s^{'} f_s^{'} (\frac{1}{3} kd - d^{'}) \quad \text{if } N^*=0.0 \qquad (1.11)$$

$$M_y = A_s f_y (\mathrm{d} - \frac{1}{2}h) + A_s^{'} \times f_s^{'} (\mathrm{d} - \frac{1}{2}h)$$

$$+ \frac{1}{2} kd\ f_c \mathrm{b} (\frac{1}{2}h - \frac{1}{3} kd) \quad \text{if } N^* \neq 0.0 \qquad (1.11)'$$

Calculated member curvatures at first yield using the method described above are summarised in Table 1.6 for all the units.

Calculation of yield curvatures of columns with axial load, such as, for Unit 2, Units EJ3 and EJ4, are described in detail below, because of its complexity.

Table 1.6 Member Curvatures at First Yield

Unit	Beam Negative Bending		Beam Positive Bending		Column	
	k	Φ_y ($\times 10^{-6}$)	k	Φ_y ($\times 10^{-6}$)	k	Φ_y ($\times 10^{-6}$)
Unit 1	0.311	5.0	0.213	4.4	0.288	8.6
Unit 2	0.304	5.0	0.209	4.4	0.43	10.7
Unit EJ1	0.288	4.9	0.23	4.5	0.21	4.8
Unit EJ2	0.30	5.0	0.24	4.6	0.22	4.9
Unit EJ3	0.29	4.9	0.23	4.5	0.52	7.9
Unit EJ4	0.28	4.9	0.23	4.5	0.50	7.7

(3). Detailed Calculation of Yield Curvature of Columns with Axial Load

The calculation of yield curvature of columns with axial load, such as the columns for Unit 2, Units EJ3 and EJ4 is described in detail as follows due to the complexity caused by the presence of column axial load.

- Column Yield Curvature of Unit 2

f_y=321MPa, $A_s = A_s^{'}$=1357 mm^2, $f_c^{'}$= 48.9MPa, b = 460mm, d = 300-40 = 260 (mm)

$\rho = \rho^{'}$ = 0.0113, E_c=4730 $\sqrt{f_c^{'}}$ MPa =33076 MPa, E_s = 200000 MPa, n = 6

Substituting the parameters above into Eqs.(1.7), (1.8) and (1.9) leads to

$$1357\times321 + 800000 = 1357\times\frac{260k-40}{260(1-k)}\times\varepsilon_y E_s + 0.5k\times\frac{260k}{1-k}\varepsilon_y E_c\times460$$

This gives k = 0.43

Check, $f_c = \frac{k}{1-k} f_y/n$ = 40.35 MPa < $f_c^{'}$=43.8 MPa, Approximately "ok"

Φ_y = 10.7E-06

- Column Yield Curvature of Unit EJ3

Substituting the relevant parameters of Unit EJ3 in Table 1.1(b), Table 1.2 and Table 1.5 into equations 1.7, 1.8 and 1.9 leads to

$$905\times321 + 1800000 = 905\times\frac{42k-4}{42(1-k)}\times\varepsilon_y E_s + 0.5k\times\frac{420k}{1-k}\varepsilon_y E_c\times460$$

This gives k = 0.48, $f_c = \frac{k}{1-k} f_y/n$ = 40.87 MPa > $f_c^{'}$=34MPa, so concrete is in non-linear state and linear concrete stress distribution is obviously not true. Hence using the following equation [C1]:

$$A_s^{'} f_s^{'} + \alpha_1 f_c^{'} \beta\, c\, b = A_s f_y + N^{*} \qquad (1.12)$$

where: $\varepsilon_s^{'} = (c - d^{'})/(d-c)\varepsilon_y$

$f_s^{'} = \frac{c-40}{420-c} f_y$, α_1 and β are listed for different concrete stress states in Reference C1, using trial method to find the "c".

For concrete of $f_c^{'}$, $\varepsilon_c^{'}$=0.00215 (Concrete Peak Strain)

(1). Try $\varepsilon_t/\varepsilon_c^{'}$=0.75, α_1=0.762, β=0.691

so: $A_s^{'} f_s^{'} + \alpha_1 f_c^{'} \beta\, c\, b = 905\frac{c-40}{420-c}\times321 + 0.691\times0.762\times34\times c\times460$=2090505

905(c-40) 321+8235.112 c(420-c) =2090505(420-c)

c^2 -709.3c+108061 =0, c =221.6 mm

Check: $\varepsilon_s = \frac{d-c}{c}\varepsilon_t$=$1.44368\times10^{-3}$, so below yield, try again

(2) Try $\varepsilon_t/\varepsilon_c^{'}$=1, α_1=0.884 β=0.728

so: $A_s^{'} f_s^{'} + \alpha_1 f_c^{'} \beta\, c\, b = 905\frac{c-40}{420-c}\times321 + 0.884\times0.728\times34\times c\times460$=2090505

c^2 -656.7c+88414 =0, so c=189 mm

Check: $\varepsilon_s = \frac{d-c}{c}\varepsilon_t = 2.6266\times10^{-3}$, so much bigger than first yield strain. Use interpolation method to find a good c,

$$c = 221.6 + \frac{189-221.6}{2.6266\times10^{-3} - 1.44368\times10^{-3}}(1.605\text{-}1.44368)\times10^{-3} = 217 \text{ mm}$$

In that case, $f_s^{'}$=280 MPa, $\alpha_1 = 0.762 + \frac{0.884-0.762}{189-221.6}(217\text{-}221.6) = 0.779$

$$\beta = 0.691 + \frac{0.728-0.691}{189-221.6}(217\text{-}221.6) = 0.696$$

$$\Phi_{yc}^{+} = \Phi_{yc}^{-} = \varepsilon_y/(\text{d-c}) = \frac{1.605\times10^{-3}}{420-217} = 7.91\times10^{-6}$$

$$M_{yc}^{+} = M_{yc}^{-} = 905\times321\times(230\text{-}40) + A_s^{'} f_s^{'}(230\text{-}40) + \alpha_1 f_c^{'} \beta c b (230 - 0.5\beta c)$$

= 387609107 N-mm = 388 kN-m

- Column Yield Curvature of Unit EJ4

f_y=321MPa, $A_s = A_s^{'}$ = 905 mm^2, $f_c^{'}$=36.5 MPa, b= 460mm, d=460-40 =420 (mm)

$\rho = \rho^{'}$ = 0.468%, E_c = 4730 $\sqrt{f_c^{'}}$ MPa =28576 MPa, E_s = 200000 MPa, n = 7

Substituting the parameters above into Eqs.(1.7), (1.8) and (1.9) leads to :

$$905\times321 + 1800000 = 905\times\frac{42k-4}{42(1-k)}\times\varepsilon_y E_s + 0.5k\times\frac{420k}{1-k}\varepsilon_y E_c \times 460$$

This gives k = 0.473

Check: $f_c = \frac{k}{1-k} f_y/n$ = 41MPa > $f_c^{'}$=34MPa, so concrete is in non-linear state and Equation (1.12) should be sued, similar to that for Unit EJ3.

Using trial method to find the "c".

For concrete of $f_c^{'}$= 36.5 MPa, $\varepsilon_c^{'}$=0.00215 (Concrete Peak Strain), use the values associated with $f_c^{'}$= 34 MPa due to unavailable data for $f_c^{'}$= 36.5 MPa in Reference C1.

(1). Try $\varepsilon_t/\varepsilon_c^{'}$=0.75, α_1=0.762, β=0.691

so: $A_s^{'} f_s^{'} + \alpha_1 f_c^{'} \beta c b = 905\frac{c-40}{420-c}\times321 + 0.691\times0.762\times36.5\times c\times460 = 2090505$

c^2 -689.5c+100658.6 =0 so c =210 mm

Check: $\varepsilon_s = \frac{d-c}{c}\varepsilon_t = 1.6125\times10^{-3}$, and it is close to steel yield strain of $\varepsilon_y = 1.605\times10^{-3}$.

$$f_s^{'} = \frac{c-40}{420-c} f_y = 260 \text{ MPa}$$

$$\Phi_{yc}^{+} = \Phi_{yc}^{-} = \varepsilon_y / (\text{d-c}) = \frac{1.605 \times 10^{-3}}{420-210} = 7.66 \times 10^{-6}$$

$$M_{yc}^{+} = M_{yc}^{-} = 905 \times 321 \times (230\text{-}40) + A_s^{'} f_s^{'} (230\text{-}40) + \alpha_1 f_c^{'} \beta c b (230 - 0.5 \beta c)$$

$$= 392205015 \text{ N-mm} = 392 \text{ kN-m}$$

3. CALCULATION OF MEMBER ULTIMATE CURVATURE OF TEST UNITS

Member ultimate curvatures are calculated using the measured material strengths and assuming that the ultimate concrete compressive strain is 0.004. Similar to the flexural strength calculation, find the distance form the extreme compression fibre to the neutral axis, c, which satisfies the equilibrium equation (1.1).

$$\alpha_1 f_c^{'} \text{ a b} + A_s^{'} f_s^{'} = A_s f_y + N^{*} \qquad (1.1)$$

The previous equations 1.2 and 1.3, in the case of using the ultimate concrete compressive strain of 0.004, become:

$$\varepsilon_s^{'} = \frac{c-d^{'}}{c} 0.004 \qquad (1.2)'$$

$$f_s^{'} = 800 \frac{c-40}{c} \qquad (1.3)'$$

$$\Phi_u = \frac{0.004}{c} \qquad (1.13)$$

The calculated member ultimate curvature is listed in Tables 1.7 for tests on Units 1, 2, EJ1 through EJ4.

Table 1.7 Calculated Member Ultimate Curvature

Unit	Beam Negative Bending		Beam Positive Bending		Column	
	c (mm)	$\Phi_u (\times 10^{-5})$	c (mm)	$\Phi_u (\times 10^{-5})$	c (mm)	$\Phi_u (\times 10^{-5})$
Unit 1	50	8.0	39	10.3	37.8	10.6
Unit 2	50	8.0	37	10.8	62.8	6.4
Unit EJ1	46.7	8.6	40.2	9.9	35.3	11.3
Unit EJ2	48.6	8.2	41	9.8	36.7	10.9
Unit EJ3	46.2	8.7	40	10	165.1	2.4
Unit EJ4	46	8.7	40	10	157.7	2.5

Table 1.8 Calculated Member Curvature Ductility Factor μ_Φ

Unit	Part of the unit	Bending direction	$\Phi_y (\times 1.0E\text{-}06)$	$\Phi_u (\times 1.0E\text{-}06)$	μ_Φ
Unit 1	Beams	Negative bending	5.0	80	16
		Positive Bending	4.4	103	23
	Columns		8.6	106	12
Unit 2	Beams	Negative bending	5.0	80	16
		Positive bending	4.4	108	25
	Columns		10.7	64	6
Unit EJ1	Beam	Negative bending	4.9	86	18
		Positive bending	4.5	99	22
	Columns		4.8	113	24
Unit EJ2	Beam	Negative Bending	5.0	82	16
		Positive Bending	4.6	98	21
	Columns		4.9	109	22
Unit EJ3	Beam	Negative Bending	4.9	87	18
		Positive Bending	4.5	100	22
	Columns		7.9	24	3
Unit EJ4	Beam	Negative Bending	4.9	87	18
		Positive Bending	4.5	100	22
	Columns		7.7	25	3

4. Member Curvature Ductility Factor

Based on the calculated member curvature at first yield (Table 1.6) and at ultimate stage (Table 1.7), the curvature ductility factors of members are computed and listed in Table 1.8 for all the test units.

5. THE IMPOSED SHEAR FORCES ON THE MEMBERS:

5.1 Storey Shear Strength and Imposed Column Shear Forces

The storey shear strength, V_c of each unit is developed at the attainment of the theoretical flexural strengths of the critical members. For all the six tests, except the test on Unit 1, the theoretical storey shear force strength of the unit is dominated by the flexural strengths of the beams (beam).

V_c is calculated as follows:

For interior beam-column joint units,

$$V_c = \frac{M_b^+ + M_b^-}{(1905-150)} \times \frac{1905}{3200} \text{ (N)}$$ for weak beam-strong column systems, such as, Unit 2

$$V_c = \frac{M_c}{1600-250} \text{ (N)}$$ for weak column-strong beam systems, such as, Unit 1

For exterior beam-column joint units, the storey shear force strength of the unit is dominated by the beam flexural strength,

$$V_c^+ = \frac{M_b^+}{1905-230} \times 1905/3200 \text{ (N)}$$ for positive beam bending

$$V_c^- = \frac{M_b^-}{1905-230} \times 1905/3200 \text{ (N)}$$ for negative beam bending

Note that the flexural moment capacity has a unit N-mm in above equations.

The theoretical storey shear force strength is summarised in Table 1.9 for all the units.

Table 1.9 Storey Shear Force Strength of Test Units

Unit	Unit 1	Unit 2	Unit EJ1		Unit EJ2		Unit EJ3		Unit EJ4	
			+	-	+	-	+	-	+	-
V_c (kN)	80	128	46	67	46	67	46	67	46	67
$v_{n,c}$ (MPa)	$0.10\sqrt{f_c'}$	$0.15\sqrt{f_c'}$	$0.06\sqrt{f_c'}$		$0.06\sqrt{f_c'}$		$0.06\sqrt{f_c'}$		$0.06\sqrt{f_c'}$	

The imposed shear forces on members should be calculated at the development of the theoretical storey shear strength of the unit. Therefore, the imposed column shear force is actually the storey shear strengths of the unit, V_c.

The maximum nominal column shear stress at the theoretical flexural strength of the unit is given by

$$v_{n,c} = \frac{V_c}{b_c d_c} \qquad (1.14)$$

Hence the nominal column shear stress at the theoretical flexural strength of the unit is $0.10\sqrt{f_c'}$, $0.15\sqrt{f_c'}$, $0.06\sqrt{f_c'}$, $0.064\sqrt{f_c'}$, $0.06\sqrt{f_c'}$ and $0.06\sqrt{f_c'}$ MPa for Units 1, 2, EJ1 to EJ4 respectively.

5.2 Imposed Beam Shear Force

The imposed beam shear force should be calculated according to the storey shear force strength of the unit.

For a weak beam-strong column system, the maximum imposed beam shear forces are usually obtained at the development of beam negative flexural strength because beam negative flexural strengths are larger than beam positive flexural strengths. For a weak column-strong beam system, the imposed beam shear forces are obtained at the development of the system's storey shear force strength using force equilibrium condition.

$V_b = V_c \times 3200/3810 = 67$ kN for Unit 1

$V_b = M_b^-$ (kN-mm) /(1905-$\frac{1}{2}h_b$)(mm) =143 kN for Unit 2

$V_b = M_b^-$ (kN-mm) /(1905-$\frac{1}{2}h_b$)(mm) =113 kN for Unit EJ1 through EJ4

The imposed beam shear forces for all test units are listed in Table 1.10.

Table 1.10 Imposed Beam Shear Force (kN)

Unit	Unit 1	Unit 2	Unit EJ1	Unit EJ2	Unit EJ3	Unit EJ4
V_b (kN)	67	143	113	113	113	113
$v_{n,b}$ (MPa)	$0.073\sqrt{f_c'}$	$0.15\sqrt{f_c'}$	$0.14\sqrt{f_c'}$	$0.15\sqrt{f_c'}$	$0.14\sqrt{f_c'}$	$0.14\sqrt{f_c'}$

The maximum nominal beam shear stress at the theoretical flexural strength of the units is given by

$$v_{n,b} = \frac{V_b}{b_w d} \qquad (1.15)$$

Hence the nominal beam shear stress at the theoretical flexural strength of the units is $0.073\sqrt{f_c'}$, $0.15\sqrt{f_c'}$, $0.14\sqrt{f_c'}$, $0.15\sqrt{f_c'}$, $0.14\sqrt{f_c'}$ and $0.14\sqrt{f_c'}$ MPa for Units 1, 2, EJ1 to EJ4 respectively.

5.3 Imposed Maximum Horizontal Joint Shear Force

The imposed horizontal joint shear force is

$$V_{jh} = T_1 + T_2 - V_c \quad \text{for interior beam-column joints} \qquad (1.16)$$

$$V_{jh} = T_b - V_c \quad \text{for exterior beam-column joint} \qquad (1.17)$$

where: T_1 and T_2 are the tensile forces in tension reinforcement of the left and right beams respectively for interior beam-column joints, when the storey shear strength is developed; T_b is the tensile forces in beam tension reinforcement for exterior beam-column joints, when the storey shear strength is developed.

For Unit 1, which was a weak column-strong beam system, the imposed horizontal joint shear force is estimated by assuming that the two beams share equally the imposed bending moment because the beams still in the elastic range. In elastic range, the beam steel tension stress, f_s, can be found by getting k using equation 1.6. With the known k and the known external bending moment, using equation 1.11 can give the correspondent beam steel tension stress. Beam steel tension forces, T_1 and T_2 then can be calculated based on beam steel tension stress.

Typically, external bending moment is 118 kN-m for the beams of Unit 1, the k is found to be k = 0.311 for beam negative bending of Unit 1 and k= 0.213 for beam positive bending of Unit 1. As a result, $\varepsilon_s = 7.88\times10^{-4}$ and ε_s=1.52E-03 for beam negative bending and positive bending respectively.

Therefore, $V_{jh} = T_1 + T_2 - V_c$ = 483 kN for Unit 1

For the rest five tests, including tests on Unit 2, Unit EJ1 through Unit EJ4, the storey shear force strength of the unit is governed by the beam flexural strength, so the beam steel tension forces are the steel forces at yield level.

$V_{jh} = (A_s + A_s')f_y - V_c = 6\times452\times321 - 128000$ (N) =744kN for Unit 2

$V_{jh} = A_s f_y - V_c = 1357\times321 - 67500$ (N) = 368 kN for Units EJ1 through EJ4

Table 1.11 Imposed horizontal joint shear force (kN)

Unit	Unit 1	Unit 2	Unit EJ1	Unit EJ2	Unit EJ3	Unit EJ4
V_{jh} (kN)	483	744	368	368	368	368
v_{jh} (MPa)	$0.5\sqrt{f_c'}$	$0.8\sqrt{f_c'}$	$0.3\sqrt{f_c'}$	$0.3\sqrt{f_c'}$	$0.3\sqrt{f_c'}$	$0.3\sqrt{f_c'}$

Similarly, the nominal horizontal joint shear stress at the development of the flexural strengths of the test units can be calculated using

$$v_{jh} = \frac{V_{jh}}{b_j h_c} \tag{1.18}$$

It gives $0.5\sqrt{f_c'}$, $0.8\sqrt{f_c'}$, $0.3\sqrt{f_c'}$, $0.3\sqrt{f_c'}$, $0.3\sqrt{f_c'}$ and $0.3\sqrt{f_c'}$ MPa for Units 1, 2 EJ1 to EJ4 respectively. Alternatively, the nominal horizontal joint shear stress at the development of the flexural strengths of the test units is $0.08 f_c'$, $0.11 f_c'$, $0.05 f_c'$, $0.06 f_c'$, $0.05 f_c'$, $0.05 f_c'$ MPa for Unit 1, Unit 2, Unit EJ1, Unit EJ2, Unit EJ3 and Unit EJ4 respectively.

The imposed joint horizontal shear forces and the nominal horizontal joint shear stress are summarised in Table 1.11 for all test units.

6. ESTIMATION OF SHEAR CAPACITY OF MEMBERS AND BEAM-COLUMN JOINTS

Estimation of the shear capacity was carried out using both the NZS3101 Method and the current seismic assessment procedures recommended by Park. Measured material strengths and a strength reduction factor of unity are used here.

6.1 NZS3101: 1995 Method

The probable shear force strengths of the plastic hinge regions are calculated using NZS3101: 1995 design provisions for structures designed for ductility. The shear strengths of other regions are calculated using the non-seismic design provisions of NZS3101: 1995. It is noted that NZS3101 does not have a method for calculating the shear strength of existing beam-column joints.

(1). Beam Shear Force Capacity

According to NZS3101:1995, the beam shear force capacity is calculated as follows:

$$V_{pb} = v_c b_w d + \frac{A_v f_{yt} d}{s} = \underline{k}\sqrt{f_c'} b_w d + \frac{A_v f_{yt} d}{s} \tag{1.19}$$

where: v_c =nominal shear stress carried by the concrete mechanism, f_c' = probable concrete compressive strength, b_w = width of beam web, d= effective depth of beam, A_v =area of transverse shear reinforcement, $\rho_w = A_s / b_w d$ and A_s is area of tension reinforcement.

In the non-seismic provisions of NZS3101: 1995,

$$v_c = (0.07+10\rho w)\sqrt{fc'} \quad (fc' \text{ is in unit of MPa}) \qquad (1.20)$$

In plastic hinge regions,

$$v_c = 0.0 \qquad (1.21)$$

For the beams of Unit 1, non-seismic provision is applied because the beams were not expected to form plastic hinges. For other test units, including Unit 2 and Units EJ1 through EJ4, v_c is taken as zero in calculating the beam shear force capacity. The calculated beam shear force capacity for Unit 1, Unit 2, Unit EJ1 through EJ4 using the method of NZS3101: 1995 are respectively 146 kN, 22 kN, 22 kN, 22 kN, 22kN and 22 kN.

(2). Column Shear Force Capacity

According to NZS3101:1995, the column shear capacities are calculated as follows:

$$V_{pc} = v_c b_w d + \frac{A_v f_{yt} d}{s} = V_{pc,c} + V_{pc,s} \qquad (1.22)$$

$$v_c = (1+\frac{3N^*}{A_g f_c'}) v_b \qquad (1.23)$$

where: A_g = column gross sectional area, ρ_w = column tensile reinforcement ratio, b_w = column width, d= effective depth of column section, A_v = area of transverse reinforcement, f_{yt} = yield strength of transverse reinforcement.

In non-seismic provisions of NZS3101:1995,

$$v_b = \underline{k}\sqrt{f_c'} = (0.07+10\rho_w)\sqrt{f_c'} \qquad (1.24)$$

In plastic hinge regions where the axial load is less than $0.1 f_c'$,

$$v_c = 0.0 \qquad (1.25)$$

Hence,

$V_{pc,c} = 0.0$ for Unit 1

$= (1+\frac{3N^*}{A_g f_c'})(0.07+10\rho_w)\sqrt{f_c'}\ b_w d = 209$ kN for Unit 2

$$V_{pc,c} = (1+\frac{3N^*}{A_g f_c^{'}})(0.07+10\rho_w)\sqrt{f_c^{'}}\ b_w \mathrm{d}$$

= 132 kN for Unit EJ1

= 122 kN for Unit EJ2

= 230kN for Unit EJ3

= 232 kN for Unit EJ4

The contribution of column transverse reinforcement to the total column shear force capacities is:

$$V_{pc,s} = \frac{A_v f_{yt} d}{s} = 56.6\times 2\times 318\times 260/230 = 41 \text{ kN}$$ for Units 1 and 2

$$V_{pc,s} = \frac{A_v f_{yt} d}{s} = 56.6\times 318\times 420/305 = 25 \text{ kN}$$ for Units EJ1 to EJ4

Column shear force strength is the sum of the contribution of concrete to the shear strength and the contribution of column transverse reinforcement to the shear strength.

6.2 Method Proposed by Park in Reference P6

Detailed description of the method proposed by Park for estimating the shear force strength of members and beam-column joints can be seen in Chapter 2. For the members where plastic hinges were expected, the member shear strength will be estimated by taking into account of the imposed member curvature ductility. Generally, the method proposed by Park in Reference P6 will give less conservative estimations of the shear force capacity of the members and beam-column joints in existing reinforced concrete structures.

(1). Beam Shear Force Capacity

The beam shear capacities are estimated as follows, according to the method proposed by Park [P6]:

$$V_{pb} = V_{b,c} + V_{b,s} \qquad (1.26)$$

in which: $V_{b,c} = \underline{k}\sqrt{f_c^{'}}\ b_w d$, $V_{b,s} = A_v f_{yt} d / s$

For the beams of Unit 1 where plastic hinges were not expected, $\underline{k}$ is taken as 0.2 (see Chapter 2). For the beams of Unit 2 and Units EJ1 through EJ4 where plastic hinges were expected, $\underline{k}$ is found according to the imposed ductility factor of the members (see Table 1.12 for all units).

Using the values of parameters summarised in Table 1.1(a) and Table 1.1(b) and the coefficient k in *Table 1.12*, the beam shear force capacity is estimated for all the units (see Table 1.12).

Table 1.12 Coefficient k for Estimating Beam Shear Force Capacity

Units	Unit 1	Unit 2	Unit EJ1	Unit EJ2	Unit EJ3	Unit EJ4
$f_c^{'}$ (MPa)	43.8	48.9	34	29.2	34	36.5
k	0.2	0.05	0.05	0.05	0.05	0.05
V_{pb} (kN)	204	70	62	59	62	63

(2). Column Shear Force Capacity

Using the proposed method for estimating the column shear force capacities by Priestley, rather than the method by Park, the column shear force capacities are estimated as follows (see Chapter 2):

Table 1.13 Estimation of Column Shear Force Capacity Using Method in P6

Units	Unit 1	Unit 2	Unit EJ1	Unit EJ2	Unit EJ3	Unit EJ4
$f_c^{'}$ (MPa)	43.8	48.9	34	29.2	34	36.5
N^* (kN)	0.0	800	0.0	0.0	1800	1800
a (mm)	28	47	28	31	127	119
tanα	NA	NA	NA	NA	0.104	0.107
k	0.1	0.29	0.29	0.29	0.29	0.29
$V_{c,c}$ (kN)	73	224	286	265	286.2	296.9
V_n (kN)	0	72	0	0	187.2	192.6
$V_{c,s}$ (kN)	61	61	38.8	38.8	38.8	38.8
V_{pc} (kN)	134	358	325	304	512	528

$$V_{pc} = V_{c,c} + V_{c,s} + V_n \qquad (1.27)$$

in which, $V_{c,c} = v_c \; 0.8 \; A_g = k\sqrt{f_c^{'}} \; 0.8 \; A_g$ (1.28)

$$V_{c,s} = \frac{A_v f_{yt} d^{"}}{s}(\cot 30°) \qquad (1.29)$$

$$V_n = \mathrm{N}^{*} \tan \alpha \qquad (1.30)$$

$\tan\alpha = (h_c - a)/l_c$

where: a is the equivalent depth of the rectangular compressive concrete block at ultimate state.

Detailed calculation of column shear force capacity is listed in *Table 1.13* for all the units, based on the expected curvature ductility imposed as listed in *Table 1.8.*

(3). Horizontal Shear Force Capacity of Beam-Column Joints

The maximum horizontal shear capacity of beam-column joints is calculated using only the current seismic assessment procedures proposed by Park. NZS3101: 1995 gives no indication for estimating the shear force capacities of existing beam-column joint cores.

For both interior and exterior beam-column joints, the probable horizontal shear force capacity is obtained by the following equation [P6].

$$V_{Pjh} = v_c \; b_j \; h_j + V_{Pjh,S} \qquad (1.31)$$

where: $v_c = \underline{k} \sqrt{f_c^{'}} \sqrt{1 + \frac{N^{*}}{A_g \underline{k} \sqrt{f_c^{'}}}}$ and $\underline{k}$ is the coefficient associated with the imposed ductility factor, b_j and h_j are the effective joint width and depth respectively, and they are determined based on NZS3101: 1995.

According to NZS3101:1995, h_j is taken as h_c, which is the overall depth of column in the direction of the horizontal joint shear to be considered, b_j is taken as:

I. where $b_c > b_w$: either $b_j = b_c$, or $b_j = b_w + 0.5 h_c$, whichever is the smaller;

II. where $b_c < b_w$: either $b_j = b_w$ or $b_j = b_c + 0.5 h_c$, whichever is the smaller.

As a result, b_j = 450 mm and h_j = 300 mm for two interior beam-column joints, but b_j = 460 mm and h_j = 460 mm for the four exterior beam-column joint units.

$V_{Pjh,S}$ = contribution of horizontal joint shear reinforcement, and it is zero for two interior beam-column joints and $V_{Pjh,S}$ =56.6×318 =18 kN for the four exterior beam-column joint units. Detailed calculation is seen in Table 1.14.

Table 1.14. Estimated Horizontal Joint Shear Capacity

Unit	Unit 1	Unit 2	Unit EJ1	Unit EJ2	Unit EJ3	Unit EJ4
N^* (kN)	0.0	800.0	0.0	0.0	1800.0	1800.0
$f_c^{'}$ (MPa)	43.8	48.9	34	29.2	34	36.5
k	0.3	0.3	0.1	0.3	0.1	0.3
v_c	1.99	4.07	0.583	1.621	2.302	4.325
V_{Pjh} (kN)	268	550	141	361	505	933

The estimated shear force capacity of beams, columns and beam-column joints, for all the units, is listed in Table 1.15. The investigation of the amount of transverse reinforcement for resisting the shear force is seen in Chapter 4.

Table 1.15 Shear Force Capacity of Beams, Columns and Beam-Column Joints (kN)

Part of Units	Unit 1	Unit 2	Unit EJ1	Unit EJ2	Unit EJ3	Unit EJ4
Beams, V_{pb} (kN)	146 (204)	22 (70)	22 (62)	22 (59)	22 (62)	22 (63)
Columns, V_{pc} (kN)	41 (134)	250 (358)	157 (325)	147 (304)	255 (512)	257 (528)
Beam-Column Joints, V_{Pjh} (kN)	(268)	(550)	(141)	(361)	(505)	(933)

Note: Values without bracket are given by NZS3101: 1995, and the values with brackets are given by the method proposed by Park [P6].

7. Requirement of Transverse Reinforcement Quantities for Anti-buckling

For all the tests, the axial load ratios on the columns are low. In this case ($N^* < 0.3 A_g f_c^{'}$), the transverse reinforcement is more required for preventing buckling of longitudinal bars than that for confining the compressed concrete. Hence, apart from the investigation of the amount of transverse reinforcement according to the shear requirement as conducted before, the amount of transverse reinforcement is also investigated according to the requirement for preventing bar buckling using NZS3101: 1995. The procedure proposed in Reference P6 does not have a method in this regard.

7.1 Beams

- **Code Specification on Spacing Limit of Beam Transverse Reinforcement**

According to NZS3101: 1995, centre-to-centre spacing of stirrups or ties along the beam members shall not exceed the smaller of the least lateral dimension of the cross section or 16 times longitudinal bar diameter; centre-to-centre spacing of stirrups or ties in potential plastic hinge regions shall not exceed either d/4 or 6 times the diameter of any longitudinal compression bar to be restrained in the outer layers.

For Unit 1 where beams were not expected to form plastic hinges, b_w =300 mm< $16d_b$ =384 mm. Hence, s =300 mm governs.

For Unit 2 and Unit EJ1 through EJ4, beams were expected to develop plastic hinges, d/4 = 460/4 =115 mm < 6 d_b =144 mm. Hence, s = 115 mm governs.

- **Code Specification on Size Limit of Beam Transverse Reinforcement**

According to NZS3101: 1995, the diameter of the stirrup-ties in beams shall not be less than 5 mm. In addition, the area of one leg of a stirrup-tie placed in potential plastic hinge regions in the direction of potential buckling of the longitudinal bar shall not be less than:

$$A_{te} = \frac{\sum A_b f_y}{96 f_{yt}} \frac{s}{d_b} \qquad (1.32)$$

where $\sum A_b$ is the sum of the area of the longitudinal bars reliant on the tie.

For Unit 1 where beams were not expected to form plastic hinges, A_{te} = Area of D5 =19.6(mm^2). Area of per set shall not be less than 40 mm^2 for Unit 1.

For Unit 2 and Units EJ1 through EJ4, beams were expected to develop plastic hinges, the limit on area of one leg of a stirrup-tie shall be calculated by Equation 1.32.

$$A_{te} = \frac{\sum A_b f_y}{96 f_{yt}} \frac{s}{d_b}$$

$$= \frac{2D24 \times 321}{96 \times 318} \times \frac{115}{24} = 45.5 \text{ (mm}^2\text{)} \qquad \text{for Unit 2}$$

$$= \frac{1.5D24 \times 321}{96 \times 318} \times \frac{115}{24} = 34.2 \text{ (mm}^2\text{)} \qquad \text{for Units EJ1 to EJ4}$$

Area of per set shall not be less than 91 mm^2 for Unit 2 and 68 mm^2 for Units EJ1 to EJ4.

7.2 Columns

- **Code Specification on Spacing Limit of Column Transverse Reinforcement**

According to NZS3101: 1995, centre-to-centre spacing of stirrups or ties along the column members shall not exceed the smaller of 1/3 of the least lateral dimension of the cross section or 10 times longitudinal bar diameter; centre-to-centre spacing of stirrups or ties in potential plastic hinge regions shall not exceed either 1/4 of the least lateral dimension of the cross section or 6 times the diameter of any longitudinal compression bar to be restrained.

For Unit 1 where columns were expected to develop plastic hinges, $b_c/4 = 75$ mm $< 6d_b = 144$ mm. Hence, s =75 mm governs.

For Unit 2 and Unit EJ1 through EJ4, columns were not expected to develop plastic hinges,

$b_c/3 = 100$ mm $< 10d_b = 240$ mm, so s = 100 mm governs for Unit 2

$b_c/3 = 153$ mm $< 10d_b = 240$ mm, so s = 153 mm governs for Unit EJ1 to EJ4

- **Code Specification on Size Limit of Column Transverse Reinforcement**

According to NZS3101: 1995, the diameter of the stirrup-ties in columns shall not be less than 10 mm for the column longitudinal bars with diameter 20 mm to 32 mm. The area of one leg of a stirrup-tie, when governed by the requirement for anti-buckling, shall not be less than:

$$A_{te} = \frac{\sum A_b f_y}{135 f_{yt}} \frac{s}{d_b} \qquad (1.33)$$

In potential plastic hinge regions of columns, the area of one leg of a stirrup-tie, when governed by the requirement for anti-buckling, shall not be less than:

$$A_{te} \quad \frac{\sum A_b f_y}{96 f_{yt}} \frac{s}{d_b} \qquad (1.32)$$

where $\sum A_b$ is the sum of the area of the longitudinal bars reliant on the tie.

For Unit 1 where columns were expected to develop plastic hinges, the limit on area of one leg of a stirrup-tie is calculated using Equation 1.32.

$$A_{te} = \frac{\sum A_b f_y}{96 f_{yt}} \frac{s}{d_b} = \frac{D24 \times 321}{96 \times 318} \times \frac{75}{24} = 14.9 (\text{mm}^2) \qquad \text{for Unit 1}$$

For Unit 2 and Unit EJ1 through EJ4, columns were not expected to develop plastic hinges, the limit on area of one leg of a stirrup-tie shall be calculated by Equation 1.33.

$$A_{te} = \frac{\sum A_b f_y}{135 f_{yt}} \frac{s}{d_b} = \frac{D24 \times 321}{135 \times 318} \times \frac{100}{24} = 14.1 \ (\text{mm}^2) \quad \text{for Unit 2}$$

$$= \frac{D24 \times 321}{135 \times 318} \times \frac{153}{24} = 21.5 \ (\text{mm}^2) \quad \text{for Units EJ1 to EJ4}$$

In this case, area of per set shall not be less than 60 mm^2 for Unit 1, and shall not be less than 57 mm^2 for Unit 2, and shall not be less than 43 mm^2 for Units EJ1 to EJ4.

7.3 Beam-Column Joints

NZS3101: 1995 also has specification to limit the spacing and size of column transverse reinforcement within beam-column joints.

According to Clause 11.4.4.5 of NZS3101: 1995, the spacing of sets of column ties or hoops within a joint shall not exceed 10 times the column bar diameter or 200 mm, whichever is less.

$10d_b = 10*24 = 240$ mm for all the units

Hence, so s = 200 mm governs.

- Area Limit

According to Clause 11.4.4.5 of NZS3101: 1995, the quantities of horizontal joint reinforcement shall conform to that required by Eq.1.34.

The area of one leg of horizontal joint reinforcement shall not be less than:

$$A_{te} = \frac{\sum A_b f_y}{96 f_{yt}} \frac{s}{d_b} = \frac{452 \times 321}{96 \times 318} \frac{200}{24} = 39.6 \text{ (mm}^2\text{)}$$ for all the units

Hence, area of per set of horizontal transverse reinforcement within the joints shall not be less than 79 mm^2

Summary of the results obtained from this theoretical consideration is seen in Chapter 4 of the thesis.

8. Development of the Longitudinal Reinforcement within Joints

NZS3101: 1995 has the specifications on the maximum diameter of beam bars passing through the joints. Note that NZS3101: 1995 specifies the use of deformed longitudinal reinforcement.

According to NZS3101: 1995, the maximum diameter of beam bars passing through the interior joints should satisfy the following requirement by equation 1.34:

$$\frac{d_b}{h_c} \leq 3.3\alpha_f \frac{\sqrt{f_c'}}{\alpha_o f_y} \qquad (1.34)$$

where, α_f =1.0 for one-way frames and α_o is 1.0 when the plastic hinges are not expected in the beams, and α_o =1.25 when plastic hinges are expected to develop at column faces.

This gives $\frac{d_b}{h_c} \leq 14.7$ for Unit 1 and $\frac{d_b}{h_c} \leq 17.4$ for Unit 2.

NZS3101: 1995 also has the specifications on the maximum diameter of deformed column bars passing through the joints. According to NZS3101: 1995, when columns are designed to develop plastic hinges in the end regions, equation 1.34 needs to be satisfied; but when columns are not intended to develop plastic hinges in the end regions, the maximum diameter of column bars may exceed that given by equation 1.34 by 25%.

$$\frac{d_b}{h_b} \leq 3.2\frac{\sqrt{f_c'}}{f_y} \qquad (1.35)$$

For Unit 1, columns are expected to develop plastic hinges, $\frac{d_b}{h_b} \leq 15.1$, and for Unit 2 and Units EJ1 to EJ4, columns are not expected to develop plastic hinges, $\frac{d_b}{h_b} \leq 11.5$, 13.8, 14.9, 13.8, 13.3 respectively.